

1-1-2010

Investigations of factors affecting pine and cottonwood pyrolysis oil aging

Caitlin Durnin Naske

Follow this and additional works at: <https://scholarsjunction.msstate.edu/td>

Recommended Citation

Naske, Caitlin Durnin, "Investigations of factors affecting pine and cottonwood pyrolysis oil aging" (2010).
Theses and Dissertations. 2868.
<https://scholarsjunction.msstate.edu/td/2868>

This Graduate Thesis - Open Access is brought to you for free and open access by the Theses and Dissertations at Scholars Junction. It has been accepted for inclusion in Theses and Dissertations by an authorized administrator of Scholars Junction. For more information, please contact scholcomm@msstate.libanswers.com.

INVESTIGATIONS OF FACTORS AFFECTING PINE AND COTTONWOOD
PYROLYSIS OIL AGING

By

Caitlin Durnin Naske

A Thesis
Submitted to the Faculty of
Mississippi State University
in Partial Fulfillment of the Requirements
for the Degree of Masters of Science
in Chemical Engineering
in the Swalm School of Chemical Engineering

Mississippi State, Mississippi

December 2010

Copyright 2010

By

Caitlin Durnin Naske

INVESTIGATIONS OF FACTORS AFFECTING PINE AND COTTONWOOD
PYROLYSIS OIL AGING

By

Caitlin Durnin Naske

Approved:

Keisha B. Walters
Assistant Professor of Chemical
Engineering
(Director of Masters)

Priscilla J. Hill
Associate Professor of Chemical
Engineering
(Committee Member)

Adrienne R. Minerick
Associate Professor of Chemical
Engineering
(Committee Member)

Bill Elmore
Associate Professor of Chemical
Engineering
(Committee Member)

Rafael Hernandez
Associate Professor of Chemical
Engineering
(Graduate Coordinator)

Sarah A. Rajala
Dean of the Bagley College of
Engineering

Name: Caitlin Durnin Naske

Date of Degree: December 10, 2010

Institution: Mississippi State University

Major Field: Chemical Engineering

Major Professor: Dr. Keisha B. Walters

Title of Study: INVESTIGATIONS OF FACTORS AFFECTING PINE AND
COTTONWOOD PYROLYSIS OIL AGING

Pages in Study: 388

Candidate for Degree of Masters of Science

Studies of aging processes were conducted on pyrolysis oils produced from pine and cottonwood biomass (clear wood, whole tree, bark and needles/leaves). Accelerated aging at 80 °C for up to 504 h was employed to investigate the short and long-term effects of feedstock, phase separation, char particulates, and solvent addition on pyrolysis oil properties. Feedstock containing forestry residue was found to increase water content of neat pyrolysis oil and the collection method (total vs. fractionated) affects all of the properties with the largest impact on viscosity and as produced molecular weight. Post-condensation liquid filtration did not prevent aging-related water content or molecular weight increases during aging but did retard aging reactions in pine clear wood and pine bark pyrolysis oils. Methanol addition retarded the aging reactions in pine needle fractionated pyrolysis oil; at 15 wt% phase separation was prevented and molecular weight increased 11 % after 504 h of aging.

DEDICATION

I'd like to dedicate this thesis to my husband, Dan Naske, who has always encouraged, supported and inspired me to achieve my utmost potential and to my parents, John and Carolyn Durnin, for all of their love and support throughout my academic years.

ACKNOWLEDGEMENTS

I'd like to thank everyone who as assisted my research efforts within the past two years. Most of all I would like to thank my advisor, Dr. Keisha Walters, who has been a wonderful advisor, teacher and mentor during this process. I'd also like to thank the members of my committee, Dr. P. Hill, Dr. A. Minerick and Dr. B. Elmore, for their time and input regarding my research project and thesis. This project was funded through the Sustainable Energy Research Center at Mississippi State University under U.S. Department of Energy award DE-FG3606GO86025. Also, all tree harvesting, biomass preparation and pyrolysis oil production was done by Brian Mitchell of Forestry Products in addition to Dr. Steele for access to the Forestry Products laboratory. Collaboration with Dr. Jose Rodriguez (water content, calorimetry, etc.) and Bill Holmes (GC-MS) proved to be very helpful.

A special thanks to the undergraduate research students who made it possible to collect the large data set needed for all of the studies, especially Sarah Crosby, Andrew McMaster, Jason Speed, Zach Wynne, and Philip Polk.

TABLE OF CONTENTS

	Page
DEDICATION	ii
ACKNOWLEDGEMENTS	iii
LIST OF TABLES	xi
LIST OF FIGURES	xv
CHAPTER	
I. INTRODUCTION	1
1.1 Drive for Alternative Fuel.....	1
1.2 Biomass.....	3
1.3 What is Pyrolysis?.....	5
1.4 Reactors.....	7
1.5 Composition.....	9
1.6 Barriers to Direct Application.....	12
1.7 Corrosion.....	12
1.8 Aging.....	13
1.9 Phase Separation.....	15
1.10 Char & Filtration.....	16
1.11 Upgrading.....	18
1.12 Solvent Addition.....	19
1.13 Toxicity.....	21
1.14 Economics.....	22
1.15 References.....	23
II. COMPARISON OF PHYSICAL AND CHEMICAL PROPERTIES OF COTTONWOOD AND PINE BIOMASS, PYROLYSIS OIL AND CHAR.....	29
2.1 Abstract.....	29
2.2 Introduction.....	29
2.3 Methods and Materials.....	35
2.4 Results and Discussion.....	37
2.4.1 Biomass.....	37

2.4.2	Pyrolysis.....	38
2.4.3	Elemental Analysis	39
2.4.4	Biomass and Char Comparison Using DRIFTS	41
2.4.5	Solids Removed by Crude Filtration.....	46
2.4.6	pH.....	47
2.4.7	Density	49
2.4.8	Water Content.....	50
2.4.9	Rheology.....	53
2.4.10	ATR-FTIR Spectra- need to insert the spectra for the pyrolysis oil and compare	55
2.4.10.1	Cottonwood Pyrolysis Oil.....	55
2.4.10.2	Pine Pyrolysis Oil	58
2.4.10.3	Cottonwood vs. Pine Pyrolysis Oil	60
2.5	Conclusions.....	62
2.6	References.....	63
III.	STATISTICAL ANALYSIS OF THE EFFECT OF FEEDSTOCK ON ACCELERATED AGING ON PINE AND COTTONWOOD PYROLYSIS OIL PROPERTIES.....	65
3.1	Abstract.....	65
3.2	Introduction.....	65
3.3	Statistical Method	66
3.4	Results and Discussion	67
3.4.1	Phase Separation.....	67
3.4.2	Statistical Analysis: 2 ^k Factorial Method.....	69
3.4.3	Comparison of Pyrolysis Oil Properties During Aging	71
3.5	Conclusions.....	75
3.6	References.....	76
IV.	EVOLUTION OF PHASE SEPARATION DURING ACCELERATED AGING IN PINE PYROLYSIS OIL	77
4.1	Abstract.....	77
4.2	Introduction.....	78
4.3	Methods and Materials.....	83
4.4	Results and Discussion	87
4.4.2	Phase Separation.....	88
4.4.3	pH measurement	89
4.4.4	Water Content.....	89
4.4.5	Calorimetric Analysis	90
4.4.6	Viscosity	91
4.4.7	Pendant Drop	93
4.4.8	GPC.....	95
4.4.9	GC/MS	97
4.4.10	ATR-FTIR Spectroscopy	100

4.4.11	Proposed Reactions/ Phase Separation Mechanisms	103
4.5	Conclusions.....	106
4.6	References.....	107
V.	POST CONENSATION FILTRATION OF PINE AND COTTONWOOD PYROLYSIS OIL AND THE IMPACT ON ACCELERATED AGING REACTIONS	110
5.1	Abstract.....	110
5.2	Introduction.....	112
5.3	Methods and Materials.....	116
5.4	Results and Discussion Part I.....	123
5.4.1	Water Content	123
5.4.2	pH Measurements	124
5.4.3	Particle Size Analysis	125
5.4.4	FTIR Characterization of Filtered Particles.....	127
5.4.5	Rheology	129
5.4.6	Molecular Weight Determination	130
5.4.7	Gas Chromatography/Mass Spectroscopy (GC/MS).....	130
5.4.8	FTIR Spectroscopy	133
5.4.9	Postulated Aging Reactions	136
5.4.10	Conclusions.....	139
5.5	Results and Discussion Part II	139
5.5.1	Filtering Pyrolysis oil.....	139
5.5.2	Filtration.....	140
5.5.3	Visual Observation of Phase Separation.....	141
5.5.4	pH.....	143
5.5.5	Water Content	145
5.5.6	Viscosity	149
5.5.7	GPC.....	153
5.5.8	ATR Analysis.....	157
5.5.9	Quantitative IR Analysis: Peak Height Ratio	162
5.5.10	GC-MS.....	168
5.5.11	Proposed Reactions.....	174
5.6	Conclusions.....	175
5.7	References.....	177
VI.	EFFECTS OF METHANOL ADDITION TO FRACTIONATED AND TOTAL PINE NEEDLE PYROLYSIS OIL DURING ACCELERATED AGING.....	180
6.1	Abstract.....	180
6.2	Introduction.....	180
6.3	Methods and Materials.....	186
6.4	Results and Discussion	189
6.4.1	Aging.....	189

6.4.2	pH.....	190
6.4.3	Density.....	191
6.4.4	Water Content.....	192
6.4.5	Rheology.....	193
6.4.6	Gel Permeation Chromatography (GPC).....	196
6.4.7	ATR-FTIR: Qualitative Analysis of PNT vs. PNF.....	201
6.4.8	Pyrolysis oil ATR-FTIR: Qualitative and Quantitative Analysis during aging.....	203
6.4.9	ATR-FTIR of Top Crust Phase.....	211
6.4.10	GC-MS data.....	216
6.4.11	Proposed Reactions.....	220
6.4.12	Conclusions.....	220
6.4.13	References.....	222
VII.	RHEOLOGICAL EFFECTS OF CHAR, SAND, AND SILICA ADDITION TO COTTONWOOD PYROLYSIS OIL.....	225
7.1	Abstract.....	225
7.2	Introduction.....	225
7.3	Methods and Materials.....	228
7.4	Results and Discussion.....	230
7.4.1	Particle Analysis.....	230
7.4.2	Particle Addition.....	232
7.4.3	Rheology: Cottonwood Whole Tree Total [CWTT].....	233
7.4.4	Rheology: Cottonwood Bark Total [CBT].....	240
7.4.5	ATR-FTIR Spectroscopy.....	245
7.5	Conclusions.....	247
7.6	References.....	248
VIII.	CONCLUSIONS AND RECOMMENDATIONS.....	250
8.1	Conclusions.....	250
8.1.1	General.....	250
8.1.2	Filtration.....	251
8.1.3	Methanol Addition.....	252
8.1.4	Solids Addition.....	253
8.2	Recommendations.....	253
8.2.1	General.....	253
8.2.2	Filtration.....	253
8.2.3	Methanol Addition.....	254
8.2.4	Solids Addition.....	254
A	PYROLYSIS OIL PROCEDURES.....	255
A.1	Working with Pyrolysis Oil General.....	256
A.2	Accelerated Aging of Pyrolysis Oil.....	257

A.3	Filtration Methods for Pyrolysis Oil	258
A.3.1	Filters Tested	258
A.3.2	Results From Filtration Testing	258
A.3.3	Volumes After Crude Filtration	259
A.3.4	Vacuum Filtration	260
A.3.5	Centrifuge Filter Preparation	262
A.3.6	Centrifugation	262
A.3.7	Cleaning Inside the Centrifuge	263
A.3.8	Centrifuge Filter Separation	263
A.3.9	Pyrolysis Oil Centrifuge Test Tube Cleaning	264
A.4	pH Adjustment of Pyrolysis Oil	265
A.5	pH Measurements	265
A.5.2	SevenEasy pH Meter:	266
1.5.3	SevenEasy Setup	266
1.5.4	SevenEasy Calibration	267
A.5.5	Accument Basic pH Meter	268
A.5.6	Pyrolysis Oil pH Measurement	269
A.6	Pyrolysis Oil Water Content	270
A.6.1	Procedure for Water Content (Aquametry Apparatus II & ASTM E 203-01)	270
A.6.2	Notes	271
A.6.3	Calculations	271
A.7	Pyrolysis Oil Viscosity Determination by Rheology	272
A.7.2	Instrument Startup and Calibrations	272
A.7.2.1	Monthly Calibrations	274
A.7.2.2	Daily Calibrations	274
A.7.2.3	Instrument Inertia	275
A.7.2.4	Geometry Inertia	275
A.7.2.5	Bearing Friction Correction	275
A.7.2.6	Rotational Mapping	276
A.7.2.7	Zero the Geometry Gap	277
A.7.3	Software	277
A.7.4	Pyrolysis Oil Sample Application	279
A.7.5	Data Collection	280
A.7.6	Saving Data and Data Analysis	280
A.7.7	Cleaning	281
A.7.8	Instrument Shutdown	281
A.7.9	Troubleshooting	282
A.7.9.1	Oscillations in the Data	282
A.7.9.2	Decrease in Viscosity When Shear Rate is Increased	282
A.8	PolySEL Pyrolysis Oil GPC	282
A.8.1	Sample Preparation	282
A.8.2	GPC Instrumentation	284
A.8.3	Data Collection	285
A.8.4	Exporting Data in Star/Importing Data in Breeze	286

A.8.5	GPC Calibration.....	288
A.8.6	Data Analysis.....	291
A.8.7	Routine Maintenance.....	293
A.9	FTIR- Transmission, ATR and DRIFT.....	293
A.9.1	FTIR Maintenance.....	293
A.9.1.1	Clearing air line.....	293
A.9.1.2	Instrument Alignment.....	294
A.9.1.3	KBr Crystal Cleaning Procedure.....	296
A.9.2	FTIR: Transmission.....	296
A.9.2.1	Pyrolysis Oil Sample Preparation.....	296
A.9.2.2	Data Collection.....	297
A.9.3	Attenuate Total Reflectance (ATR).....	299
A.9.3.1	ATR: Filling the Liquid Nitrogen MCT Detector Dewar.....	299
A.9.3.2	ATR: Start-up.....	299
A.9.3.3	Collecting Data.....	300
A.9.4	Diffused Reflectance Infrared Fourier Transform (DRIFT) Spectroscopy:.....	302
B	PRELIMINARY INVESTIGATION OF COTTONWOOD PYROLYSIS OIL.....	304
B.1	Methods and Materials.....	305
B.2	Results and Discussion.....	306
B.2.1	Elemental Analysis.....	306
B.2.2	pH and Acid Value.....	306
B.2.3	Water Content.....	307
B.2.4	Viscosity.....	309
B.2.5	FTIR Spectroscopy.....	310
B.2.6	Gel Permeation Chromatography.....	311
B.2.7	GC-MS.....	312
C	KOH ADDITION TO PINE PYROLYSIS OIL.....	315
C.1	Materials and Methods.....	316
C.2	Results and Discussion.....	316
C.2.1	Physical Observations.....	316
C.2.2	pH Adjustment.....	317
C.2.3	Aging.....	317
C.2.4	pH Measurements.....	318
C.2.5	Water Content.....	319
C.2.6	Transmission FTIR.....	320
C.3	Conclusions.....	325
C.4	References.....	326
D	CONTROLLED POLYMERIZATION OF PINE PYROLYSIS OIL.....	327

D.1	Materials and Methods.....	328
D.1.1	Controlled Polymerization #1	328
D.1.1.1	Sample number, catalyst.....	328
D.1.1.2	Conditions.....	328
D.1.2	Controlled Polymerization #2	329
D.1.2.1	Sample number, catalyst.....	329
D.1.2.2	Conditions (Samples 1-6)	329
D.2	Results and Discussion	330
D.2.1	Pyrolysis Oil Controlled Polymerization #1	330
D.2.2	Pyrolysis Oil Controlled Polymerization #2	332
D.2.2.1	Physical Observations.....	332
D.2.2.2	FTIR and DRIFT.....	332
D.2.2.3	Calorimetry	338
D.2.2.4	Gel Permeation Chromatography	339
D.3	References.....	341
E	XRF DATA FOR PINE AND COTTONWOOD BIOMASS AND CHAR	342
E.1	Method.....	343
E.2	Results and Discussion	343
F	INVESTIGATION INTO THE EFFECT OF PYROLYSIS OIL CONTACT WITH POLYMER MATERIALS	345
F.1	Abstract.....	346
F.2	Introduction.....	347
F.3	Experimental Set-up.....	349
F.3.1	Polymer Materials.....	349
F.3.2	Bio-oil Treatment.....	351
F.3.3	Tension testing.....	352
F.3.4	Scanning Electron Microscopy (SEM).....	353
F.3.5	X-ray Photon Spectroscopy (XPS)	353
F.4	Results and Discussion	354
F.4.1	Bio-oil- pH.....	354
F.4.2	Bio-oil Treatment.....	354
F.4.3	Tensile Testing: PP	356
F.4.4	Tensile Testing: PVC.....	360
F.4.5	SEM: PP.....	364
F.4.6	SEM: PVC	367
F.4.7	XPS Analysis: PP.....	369
F.4.8	XPS Analysis: PVC	378
F.5	Conclusions.....	384
F.6	Future Work.....	385
F.7	References.....	387

LIST OF TABLES

TABLE		Page
1.1	The tabulated overview of MIM content, water content for various pyrolysis oils from various published papers.....	11
2.1	Cottonwood biomass composition of whole tree on a dry basis.....	37
2.2	Pine biomass composition of whole tree on a dry basis.....	38
2.3	Yields for pyrolysis oil and char produced from cottonwood tree biomass, as a whole tree and individual tree components.....	39
2.4	Yields for pyrolysis oil and char as produced from pine tree biomass, as a whole tree and individual tree components.....	39
2.5	Elemental analysis results (C, H, N only) showing the atomic percentages of carbon (C), hydrogen (H), nitrogen (N) and remainder (R) for cottonwood biomass: clear wood, whole tree, leaves, and bark.....	40
2.6	Elemental analysis results (C, H, N only) for cottonwood pyrolysis oil collected from different feedstock and condenser combinations (as indicated by the numbers in parentheses). Percentages of carbon (C), hydrogen (H), nitrogen (N), and the remainder (R) are shown.....	41
3.1	Identification of phase separation in neat and aged (80 °C for 24 or 504 hours) cottonwood pyrolysis oil samples.....	68
3.2	Identification of phase separation in neat and aged (80 °C for 24 or 504 hours) pine pyrolysis oil samples.....	69
3.3	Statistical P-test comparison for neat (unaged) pyrolysis oil based on tree species and forestry residue content.....	70
3.4	Statistical P-test comparison for neat (unaged) pyrolysis oil based on oil tpe/fraction, total and fractionated.....	71
3.5	Statistical P-test comparison for pyrolysis oil aged for 24 h based on tree species and forestry residue content.....	72

3.6	Statistical P-test comparison for pyrolysis oil aged for 504 hours based on tree species and forestry residue content.....	73
3.7	Aging of Pine Pyrolysis oil for 24 and 504 hours	74
3.8	Aging of Cottonwood Pyrolysis oil for 24 and 504 hours	74
4.1	Comparison of pH, water content, viscosity, and weight average molecular weight (Mw) for two batches of PWTF pyrolysis oil over the duration of an aging study at 80 °C.....	88
4.2	GPC data overview including number average (Mn), weight average (Mw), and size average (Mz) molecular weights and polydispersity index (PDI) for PWTF pyrolysis oil combined phase after aging at 80 °C up to 504 hours.....	97
4.3	GPC data overview including number average (Mn), weight average (Mw), and size average (Mz) molecular weights and polydispersity index (PDI) for PWTF pyrolysis oil top and bottom phases after aging at 80 °C up to 504 hours.....	97
5.1	Functional group identifications for the major FTIR peaks in Figure 5.	128
5.2	Percent solids removed by each filtration step: two vacuum filtrations (VF) followed by centrifugal filtration (CF). Note the PBF and CCWF oils were not subjected to the second vacuum filtrations.....	140
5.3	Phase separation observations for pine-derived pyrolysis oils.....	142
5.4	Phase separation observations for cottonwood-derived pyrolysis oils.....	142
7.1	Calculated weight and volume percentages for sand, char, fumed silica, and silica packing that were added to cottonwood whole tree total [CWTT] and cottonwood whole tree total [CBT] pyrolysis oils.....	233
7.2	Average viscosities (as measured between 100-1000 1/s for both increasing and decreasing shear) of cottonwood whole tree total [CWTT] pyrolysis oil with added char, sand, silica packing, and fumed silica.	235
7.3	Average viscosity overview for cottonwood bark total [CBT] pyrolysis oil shear increasing (0.1 to 1000 1/s) and shear decreasing (1000 to 0.1 1/s) with char, sand, silica packing and fumed silica added.	241
A.1	The different filtration methods available including pore size.	258

A.2	Volumes (mL) of the cottonwood and pine pyrolysis oils after crude filtration.....	260
A.3	Rheometer Calibration Schedule.....	274
A.4	Polystyrene standard data including weight average, number average and point average molecular weights and polydispersiy (PDI).....	288
B.1	Elemental composition of neat cottonwood clear wood total pyrolysis oil.....	306
B.2	Top five target compounds identified in the quantitative GC/MS data analysis for cottonwood clear wood pyrolysis oil aged at 80°C for 0 and 7 days.....	313
B.3	Top five target compounds identified in the quantitative GC/MS data analysis for cottonwood clear wood pyrolysis oil aged at 80°C for 0 and 7 days.....	313
C.1	The weights of pine clear wood fractionated pyrolysis oil and KOH added.	317
C.2	Initial and final weights and calculated % change in weight for PCWF pyrolysis oil controls and aged samples at 80 °C for 7 and 14 days.	318
F.1	Calculated mechanical properties for the control polypropylene specimens including the average, standard deviation and 95% CI.	358
F.2	Tensile test results from the collected data the bio-oil treated polypropylene specimens.	359
F.3	Comparison of the mechanical properties of the control and bio-oil treated polypropylene.....	359
F.4	Tensile test results from the collected data the control polyvinyl chloride specimens	361
F.5	Tensile test results from the collected data the bio-oil treated polyvinyl chloride specimens.	362
F.6	Comparison of the mechanical properties of the control and bio-oil treated polyvinyl chloride.....	363
F.7	The peak fitting results for the high resolution XPS data of the control PP C 1 s peak.....	374

F.8	The peak fitting results for the high resolution XPS data of the bio-oil treated PP C 1 s peak.....	375
F.9	The potential minerals responsible for the Si peak in the bio-oil treated PP specimens ^{23,24}	376
F.10	Peak fitting results for the high resolution XPS data of the control PVC C 1 s peak.....	382
F.11	The peak fitting results for the high resolution XPS data of the bio-oil treated PVC C 1 s peak.....	383

LIST OF FIGURES

FIGURE	Page
1.1 Energy sources (left) and energy demand sectors (right) [EIA 2008].	2
2.1 DRIFTS spectra collected for cottonwood biomass whole tree (a), bark (b), leaves (c), and clear wood (d).	43
2.2 DRIFTS spectra collected for pine biomass whole tree (a), needles (b), bark (c), and clear wood (d).	44
2.3 DRIFTS spectra collected for cottonwood char whole tree (a), leaves (b), bark (c) and clear wood (d).	45
2.4 DRIFTS spectra collected for pine char whole tree (a), needles (b), bark (c) and clear wood (d).	46
2.5 Images of cottonwood solids removed by crude filtration, cleaned and dried: clear wood (a), whole tree (b), bark (c), and leaves (d).	47
2.6 Images of pine solids removed by crude filtration, cleaned and dried: pine heart wood (a), whole tree (b), and bark (c).	47
2.7 pH measurements for pyrolysis oil and pyrolysis oil fractions produced from cottonwood (left) and pine (right) biomass. Error bars represent 95% confidence intervals.	49
2.8 Calculated densities for neat (non-aged) pyrolysis oil and pyrolysis oil fractions produced from cottonwood (left) and pine (right) biomass. Error bars represent 95% confidence intervals.	50
2.9 Measured water content for pine-derived pyrolysis oil, as determined by Karl Fischer titration. Average values are shown as data labels on each column and error bars represent 95% confidence intervals.	51
2.10 Water content for cottonwood-derived pyrolysis oils, as determined by Karl Fischer titration. Average values are shown as data labels on each column and error bars represent 95% confidence intervals.	52

2.11	Rheology traces for pine bark fractionated (PNF), pine whole tree total (PWTT), pine clear wood fractionated (PCWF), pine needle total (PNT) and pine clear wood water condensate (PCW-WC).....	53
2.12	Average viscosity measurements (as determined by rheology) for neat (non-aged) cottonwood (left) and pine (right) pyrolysis oil comparing bark, clear wood, leaves/needles and whole tree oil including total, fractionated and condensate produced from cottonwood. Error bars represent 95 % confidence intervals.....	55
2.13	Cottonwood clear wood fractionated (a) and total (b) pyrolysis oil and water condensate top bottom (c) and water condensate top phase (d) ATR spectra (common scale, ATR corrected).....	57
2.14	Cottonwood whole tree fractionated (a) and total top (c) and bottom (b) phases pyrolysis oil and water condensate (d) ATR spectra.....	57
2.15	Cottonwood bark fractionated (a) and total (c) pyrolysis oil and water condensate (b) ATR spectra.....	58
2.16	Cottonwood leaves fractionated (a) and total (b) pyrolysis oils and water condensate (c) ATR spectra.....	58
2.17	Pine clear wood total (a) and fractionated(c) pyrolysis oil and water condensate (b) ATR spectra.....	59
2.18	Pine whole tree total (a) and fractionated (b) pyrolysis oil and water condensate (c) ATR spectra.....	59
2.19	Pine bark water condensate (a) and fractionated (b) and total (c) pyrolysis oil ATR spectra.....	60
2.20	Pine needles fractionated (a) and total bottom (b) and top (c) and water condensate bottom (d) and top (e) ATR spectra.....	60
2.21	Pine fractionated pyrolysis oils derived from whole tree (a), needles (b), bark (c), and clear wood (d).....	61
2.22	Cottonwood fractionated pyrolysis oils derived from clear wood (a), leaves top (c) and bottom (b) phases , bark (d) and whole tree (e).....	62
4.1	Photographs displaying phase separation in PWTF pyrolysis oil aged at 80 °C for 504 hours at 5 °C (a) and as it begins to warm to room temperature (b and c).....	88
4.2	pH measurements for the PWTF pyrolysis oil samples aged at 80 °C for up to 504 h.....	89

4.3	Water content for PWTF-94 pyrolysis oil aged at 80 °C for up to 24 h (left) and 168 to 504 h (right) for combined, top and bottom phases (with 95% CI error bars).	90
4.4	Calorimetry data (Calorie/gram) for combined and separate phases of PWTF-94 pyrolysis oil aged at 80 °C for up to 504 h. A 95% CI error bar is presented for the 6 h sample.	91
4.5	Average viscosities for PWTF pyrolysis oil aged at 80 °C for up to 504 h. Error bars represent 95% CI.	92
4.6	Rheology data (collected at 40 °C; 10-1000 1/s) for PWTF-94 pyrolysis oil aged at 80 °C for up to 504 h.	93
4.7	Pendant drop images for PWTF pyrolysis oil aged at 80 °C for 6 h and 12 h [top L-R] and 24 h, 336 h (1 week)* and 504 h (3 weeks)* [bottom L-R]. (* Droplets of the top phase only.)	94
4.8	Interfacial tensions (IFT) measured using the pendant drop method for PWTF oil samples as a function of aging time at 80 °C.	95
4.9	Measured weight average molecular weight (Mw) as a function of aging time (at 80 °C) up to 504 h for combined, top and bottom phases. All data points include 95 % confidence interval error bars.	96
4.10	GC-MS Ion Chromatogram for PWTF-94 neat (a), 336 h bottom (b) and top (c) phases and 504 h bottom (d) and top (e) phases.	98
4.11	GC-MS determined percent change in concentrations, based on the control, for the top and bottom phases of PWTF-94 pyrolysis oil after aging at 80 °C for 336 and 504 h along with chemical structures.	99
4.12	ATR FTIR spectra of the PWTF pyrolysis oil neat (0 hours) and aged at 80 °C for up to 504 h.	100
4.13	ATR-FTIR spectra of the top and bottom phases of PWTF pyrolysis oil aged at 80 °C for 336 and 504 h.	101
4.14	Peak height ratios calculated for five key peaks over aged up to 504 h at 80 °C.	102
4.15	Peak resolution representation for neat PWTF-94 pyrolysis oil.	103
4.16	Peak height ratios for peaks found in peak resolution.	103
4.17	Oxidation of primary alcohol to produce a carboxylic acid with an aldehyde intermediate [Carey ochem].....	104

4.18	Oxidation of secondary alcohol to produce a ketone [Carey ochem]	105
5.1	Water content data (with 95% CI error bars) as determined by Karl Fischer titration for PWTF pyrolysis oil aged at 80 °C for up to 3 weeks.....	124
5.2	Average measured pH values for unfiltered and filtered PWTF pyrolysis oil aged at 80 °C for up to 3 weeks (with 95% CI error bars).....	125
5.3	Representative optical micrographs showing particle shape, size, and distribution in unaged samples: (a) unfiltered and (b) filtered PWTF pyrolysis oil. Corresponding micrographs showing particles in aged samples (80 °C, 3 weeks) for (c) unfiltered and (d) filtered PWTF pyrolysis oil. All images are at 10X magnification. Note: light rings in the micrographs are artifacts from the microscope lens.....	126
5.4	Major axis particle size distributions for the PWTF pyrolysis oil: neat (unfiltered, unaged), filtered, and unfiltered aged at 80 °C for 3 weeks.....	127
5.5	Transmission-FTIR and DRIFTS spectra of the filtered solids before (a) and after (c) solvent washing along with spectra for PWTF pyrolysis oil (b) and pine whole tree [PWT] char (d).	128
5.6	Rheologically determined average viscosities (averaged over 100-1000 1/s) for unfiltered and filtered PWTF pyrolysis oil aged at 80 °C.....	129
5.7	Weight averaged (M_w) molecular weight for unfiltered and filtered PWTF pyrolysis oil aged at 80 °C.....	130
5.8	GC-MS ion chromatogram for the neat PWTF pyrolysis oil (bottom) and the aged unaltered PWTF pyrolysis oil at 80 °C for 3 weeks (top).....	131
5.9	GC-MS ion chromatogram for the un-aged filtered PWTF pyrolysis oil (bottom) and aged filtered PWTF pyrolysis oil at 80 °C for 3 weeks (top).	132
5.10	Major changes in GC-MS normalized peak heights (versus the controls) displayed as a function of the retention time for unfiltered (a) and filtered (b) pyrolysis oil. Peak height differentials increase over the course of the 3 week aging study for the unfiltered PWTF pyrolysis oil aged at 80 °C.	133
5.11	ATR spectra of unfiltered and filtered PWTF pyrolysis oil sample before (control) and after storage for 3 weeks at 80 °C.	134

5.12	Average peak height ratios (PHR) and 95% confidence intervals error bars for key peaks identified in unfiltered neat and aged PWTF pyrolysis oil samples (a) and filtered neat and aged PWTF pyrolysis oil samples (b).	136
5.13	Diels-Alder reaction resulting in substituted aromatic compounds [Carey, Adv Chem 2000].	137
5.14	Electrophilic aromatic substitution [Carey, Ochem]	137
5.15	Electrophilic aromatic substitution; C-acylation (top) and O-acylation (bottom) [Carey, Ochem]	138
5.16	Acid-catalyzed condensation of alcohols to form ether and water [Carey, Ochem].	138
5.17	Photos of crude filtration ('screening') (a), vacuum filtration (b) and a vacuum filter post-filtration (c).	140
5.18	pH measurements of cottonwood clear wood fractionated [CCWF] pyrolysis oil, neat and filtered, as a function of aging at 80 °C for up to 504 h (3 weeks).	143
5.19	pH measurements of pine clear wood total [PCWT, left] and pine clear wood fractionated [PCWF, right] pyrolysis oil, both neat and filtered, as a function of aging at 80 °C for up to 504 h.	144
5.20	pH measurements of pine bark fractionated [PBF] pyrolysis oil neat and filtered as a function of aging at 80 °C for up to 504 h.	145
5.21	Water content for CCWF unaltered and filtered aged up to 504 h at 80 °C.	146
5.22	Water content for PCWT unaltered and filtered aged up to 504 h at 80 °C.	147
5.23	Water content for PCWF non-filtered and filtered aged up to 504 h at 80 °C.	148
5.24	Water content of PBF pyrolysis oil, non-filtered and filtered, aged up to 504 h at 80 °C.	149
5.25	Viscosity (cP) for cottonwood clear wood fractionated [CCWF] pyrolysis oil as a function of aging time at 80 °C for up to 504 h (3 weeks).	150

5.26	Viscosity measurements for pine clear wood total [PCWT] oil as a function of aging time at 80 °C for up to 504 h.	151
5.27	Viscosity measurements for pine clear wood fractionated [PCWF] oil as a function of aging time at 80 °C for up to 504 h.	152
5.28	Viscosity measurements for pine bark fractionated [PBF] oil as a function of aging time at 80 °C for up to 504 h.	153
5.29	Weight average molecular weight for CCWF oil as a function of aging time at 80 °C for up to 504 h.	154
5.30	GPC results for PCWT oil as a function of aging time at 80 °C for up to 504 h.	155
5.31	Weight average molecular weight for PCWF oil as a function of aging time at 80 °C for up to 504 h.	156
5.32	Weight averaged molecular weight for PBF oil as a function of aging time at 80 °C for up to 504 h.	157
5.33	PBF unfiltered pyrolysis oil: neat (a) and aged at 80 °C for 12 h (b), 24 h (c), 168 h (d) and phase separated after 336 h [(e) bottom, (f) top], 504 h [(g) bottom, (h) top].	158
5.34	PBF filtered samples: unaged (a) and aged at 80 °C for 336 h [top (b), bottom (c)] and 504 h [top (d), bottom (e)] phases.	158
5.35	PCWF unfiltered pyrolysis oil samples: control (a) and aged at 80 °C for 6 h (b), 12 h (c), 24 h (d), 168 h (e), 336 h (f) and 504 h (g).	159
5.36	PCWF filtered pyrolysis oil samples: control (a) and aged at 80 °C for 24 h (b), and 504 h (c).	159
5.37	PCWF filter torn pyrolysis oil samples: control (a) and aged at 80 °C for 24 h (b) and 504 h [bottom (c), top (d)].	160
5.38	PCWT unfiltered pyrolysis oil samples: control (a) and aged at 80 °C for 6 h (b), 12 h (c), 24 h (d), 168 h (e), 336 h (f) and 504 h [bottom (g), top (h)].	160
5.39	PCWT filtered pyrolysis oil samples: control (a) and aged at 80 C for 6 h (b), 12 h (c), 24 h (d), 168 h (e), 336 h (f) and 504 h [top (g), bottom (h)] phases.	161
5.40	CCWF unfiltered neat (a), unfiltered aged for 504 h (b), filtered neat (c), filtered aged for 24 h (d) and 504 h (e).	162

5.41	Calculated PHR for CCWF pyrolysis oil neat and filtered aged for 504 hours at 80 °C.....	164
5.42	Calculated PHR for PCWT pyrolysis oil neat and filtered aged for 504 hours at 80 °C.....	165
5.43	Calculated PHR for PCWF pyrolysis oil neat and filtered aged for 504 hours at 80 °C.....	166
5.44	Calculated PHR for PCWF pyrolysis oil filter torn aged for 504 hours at 80 °C.....	166
5.45	Calculated PHR for PBF pyrolysis oil neat and filtered aged for 504 hours at 80 °C.....	168
5.46	Cumulative changes in normalized GC/MS peak heights for CCWF unfiltered and filtered samples.	169
5.47	Cumulative changes in normalized GC/MS peak heights for PCWT unfiltered samples.	170
5.48	Cumulative changes in normalized GC/MS peak heights for PCWT filtered samples.	170
5.49	Cumulative changes in normalized GC/MS peak heights for PCWF unfiltered samples.	171
5.50	Cumulative changes in normalized peak heights for PCWF filtered GC/MS data.....	172
5.51	Cumulative changes in normalized GC/MS peak heights for PBF unfiltered samples.	173
5.52	Cumulative changes in normalized GC/MS peak heights for PBF filtered samples.	173
5.53	Oxidation of alcohols [Carey].....	174
5.54	Jones Oxidation (o chem portal)	175
6.1	Photos of top crusts showing needle biomass or char particles creating highly texturized (left or smooth crust (right).	190
6.2	pH measurements for neat and 10 wt% methanol pine needle total [PNT, left] pyrolysis oil and neat and 5, 10 and 15 wt% methanol pine needle fractionated [PNF, right] pyrolysis oil aged up to 504 h at 80 °C.....	191

6.3	Calculated density for pine needle total [left] pyrolysis oil neat and 10 wt% methanol and pine needle fractionated [right] pyrolysis oil neat and 5, 10 and 15 wt% methanol aged up to 504 h at 80 °C.	192
6.4	Water content for pine needle total [left] pyrolysis oil neat and 10 wt% methanol and pine needle fractionated [right] pyrolysis oil neat and 5, 10 and 15 wt% methanol aged up to 504 h at 80 °C.	193
6.5	Viscosity for pine needle total pyrolysis oil neat and 10 wt% methanol without the solid crust [left] and including solid crust [right] aged up to 504 h at 80 °C.	194
6.6	Viscosity for pine needle fractionated pyrolysis oil neat [left] and 5, 10 and 15 wt% methanol [right] without the solid crust aged up to 504 h (3 weeks) at 80 °C. *NOTE: Y axes have difference scales*	195
6.7	Viscosity for pine needle fractionated pyrolysis oil neat [left] and 5, 10 and 15 wt% methanol [right] including the solid crust aged up to 504 h (3 weeks) at 80 °C.	196
6.8	Weight average molecular weight (MW) for PNT pyrolysis oil aged up to 504 h at 80 °C presenting the top, bottom and crust phases.	197
6.9	Weight average molecular weight (MW) for PNT 10 wt% methanol added pyrolysis oil aged up to 504 h at 80 °C presenting the top, bottom and crust phases.	197
6.10	Weight average molecular weight (MW) for pine needle fractionated pyrolysis oil aged up to 504 h 80 °C with the single-phase and phase separated data (top, bottom, and crust) shown separately.	199
6.11	Weight average molecular weight (MW) for pine needle fractionated 5 wt% methanol added pyrolysis oil aged up to 504 h at 80 °C with the single-phase and phase separated data (top, bottom, and crust) shown separately.	199
6.12	Weight average molecular weight (MW) for pine needle fractionated 10 wt% methanol added pyrolysis oil aged up to 504 h at 80 °C with the single-phase and phase separated data (top, bottom, and crust) shown separately.	200
6.13	Weight average molecular weight (MW) for pine needle fractionated 15 wt% methanol added pyrolysis oil aged up to 504 h at 80 °C with the single-phase and phase separated data (top, bottom, and crust) shown separately.	200

6.14	ATR comparison (common scale) of total (a) and fractionated (b) needle derived pyrolysis oils.	202
6.15	Peaks resolved for neat PNF carbonyl peak region.....	202
6.16	Peak fitting for the carbonyl region for neat PNW top (left) and bottom (right) phases.	203
6.17	ATR spectra collected for PNT bottom phase neat (a) and aged (b) and top phase neat (c) and aged (d) for 504 h at 80 °C.....	204
6.18	ATR spectra collected for PNT 10 wt% methanol added top phase unaged (c) and aged (d) and bottom phase un-aged (a) and aged (b) for 504 h at 80 °C.....	205
6.19	ATR spectra collected for PNF neat (a) and aged for 24 (b) and 504 (c) h at 80 °C.	206
6.20	ATR spectra collected for PNF 5 wt% methanol added unaged (a) and aged for 24 (b) and 504 h [top (d), bottom (c)] at 80 °C.....	206
6.21	ATR spectra collected for PNF 10 wt% methanol added unaged (a) and aged for 24 (b) and 504 h [top (d), bottom (c)] at 80 °C.....	207
6.22	ATR spectra collected for PNF 15 wt% methanol added unaged (a) and aged for 24 (b) and 504 h (c) at 80 °C.....	207
6.23	PHR for peak 1018 cm ⁻¹ (left) and 1268 cm ⁻¹ (right) comparing PNW top and bottom phases for unaltered and 10 wt% methanol added samples during aging up to 504 h at 80 °C.	209
6.24	PHR for peak 1643 cm ⁻¹ (left), 1594 cm ⁻¹ (center) and 1513 cm ⁻¹ (right) comparing PNW top and bottom phases for unaltered and 10 wt% methanol samples during aging up to 504 h at 80 °C.....	209
6.25	Ratios of peak heights from peak fitting #3/#2	210
6.26	PHR for peak 1018 cm ⁻¹ comparing PNF unaltered, 5, 10 and 15 wt% methanol added samples during aging up to 504 h at 80 °C.....	211
6.27	Peak fitting for PNF 15 wt% methanol added control (left) and aged for 504 h (right).....	211
6.28	ATR spectra for PNT pyrolysis unaltered top crust after 24 (a) and 504 (b) hours and 10 wt% methanol after 504 h (c).....	212

6.29	ATR spectra of unaltered PNF pyrolysis oil crust phase after aging for 24 (c, e) and 504 hours (d) and 5 wt% MeOH added crust phase after aging for 24 (b) and 504 (a) h.	213
6.30	ATR spectra of pine needles fractionated pyrolysis oil 10 wt% MeOH added crust phase after aging for 24 (c, e) and 504 hours (d) and 15 wt% MeOH added crust phase after aging for 24 (b) and 504 (a) h.	213
6.31	DRIFT spectra for the crust solids for unaltered pine needle pyrolysis oil aged for 24 h (d) and 504 (c) h and 10 wt% MeOH added pyrolysis oil samples aged for 24 h (a) and 504 h (b) at 80 °C.....	215
6.32	DRIFT spectra for the crust solids for PNF unaltered aged for 504 h (a), and 10 wt% methanol added aged for 24 h (b) and 5 wt% methanol added aged for 504 h (c).....	215
6.33	DRIFT spectra for the pine needle char (a) and pine needle biomass (b).	216
6.34	GC-MS analysis of ion 91 for unaltered and 10 wt% added PNT during aging	217
6.35	GC-MS analysis of ion 90 for unaltered and 10 wt% added PNT during aging	217
6.36	Changes in normalized heights from control samples for PNT unaltered and 10 wt% methanol added samples aged at 80 °C for 24 and 504 h.	218
6.37	Changes in normalized heights from control samples for PNF unaltered and 5 wt% methanol added samples aged at 80 °C for 24 and 504 h.	219
6.38	Changes in normalized heights from control samples for 10 and 15 wt% methanol added samples aged at 80 °C for 24 and 504 hours.....	220
7.1	Particle size distributions for CWTT char showing the major (left) and minor (right) axes.	231
7.2	Particle size distributions for CBT char showing the major (left) and minor (right) axes.	231
7.3	Particle size distributions for sand showing the major (left) and minor (right) axes.....	232
7.4	Step-shear rheology data for cottonwood whole tree total [CWTT] pyrolysis oil. Neat (as produced) and char added (3.98, 3.07, and 1.29 %v/v) samples were tested from 0.1 to 1000 1/s [left] and then from 1000 to 0.1 1/s [right].	237

7.5	Rheology from 0.1 to 1000 1/s [left] and 1000 to 0.1 1/s [right] for cottonwood whole tree total [CWTT] pyrolysis oil neat and with 4.76, 2.43, and 1.16 v/v% of added sand.	238
7.6	Rheology from 0.1 to 1000 1/s [left] and 1000 to 0.1 1/s [right] for cottonwood whole tree total [CWTT] pyrolysis oil neat and 3.89, 0.51 and 1.13 v/v% of fumed silica added.	239
7.7	Rheology from 0.1 to 1000 1/s [left] and 1000 to 0.1 1/s [right] for cottonwood whole tree total [CWTT] pyrolysis oil neat and 5.49, 2.24 and 0.96 % by volume of silica packing added.	239
7.8	Rheology from 0.1 to 1000 1/s [left] and 1000 to 0.1 1/s [right] for cottonwood bark total [CBT] pyrolysis oil neat and 4.28, 1.72 and 0.92 % by volume of char added.	243
7.9	Rheology from 0.1 to 1000 1/s [left] and 1000 to 0.1 1/s [right] for cottonwood bark total [CBT] pyrolysis oil neat and 3.4, 1.63 and 0.83 % by volume of sand added.	243
7.10	Rheology from 0.1 to 1000 1/s [left] and 1000 to 0.1 1/s [right] for cottonwood bark total [CBT] pyrolysis oil neat and 3.2, 1.77 and 0.69 % by volume of fumed silica added.	244
7.11	Rheology from 0.1 to 1000 1/s [left] and 1000 to 0.1 1/s [right] for cottonwood bark total [CBT] pyrolysis oil neat and 2.76, 1.64 and 0.92 % by volume of silica packing added.	244
7.12	ATR-FTIR spectra of cottonwood whole tree total [CWTT] pyrolysis oil: neat (a), sand (b, 4.76 % v/v), char (c, 3.98 % v/v), silica packing (d, 5.49 % v/v), and fumed silica (e, 3.89 % v/v).	246
7.13	ATR-FTIR spectra of cottonwood bark total [CBT] pyrolysis oil: neat (a), sand (b, 3.4 % v/v), char (c, 4.28 % v/v), silica packing (d, 2.76 % v/v), and fumed silica (e, 3.2 % v/v).	246
A.1	pH meter set-ups SevenEasy (left)[seveeasy manual] and Accument Basic (right) [accument basic manual].....	266
A.2	The keypad representation of the SevenEasy pH meter.....	266
A.3	The SevenEasy pH slope display.	268
A.4	The keypad representation of the Accument Basic pH meter.	268
A.5	AR 1500 ex rheometer (TA Instruments)	272

B.1	pH and acid value for cottonwood clear wood pyrolysis oil neat and aged up to 7 days at 80 °C.....	307
B.2	Water Content for cottonwood clear wood pyrolysis oil neat and aged up to 7 days at 80 °C.	308
B.3	Water Content for cottonwood clear wood pyrolysis oil neat and aged up to 7 days at 80 °C comparing the top and bottom phase with the mixed oil.....	309
B.4	Viscosity measurements for CCWT oil neat and aged for 7 days at 80 °C.....	310
B.5	Transmission FTIR spectra collected for CCWT oil neat and aged at 80 °C up to 7 days.	310
B.6	Weight averaged molecular weight <MW> of cottonwood clear wood pyrolysis oil was found to increase during aging at 80 °C.....	311
B.7	GPC traces displaying the progression during aging and the formation of the bi-modal distribution.....	312
C.1	Measured pH of neat and pH adjusted pyrolysis oils stored at 5 °C and aged at 80 °C for 7 and 14 days.	319
C.2	Water Content for neat and pH adjusted pyrolysis oils stored at 5 °C and aged at 80 °C for 7 and 14 days.	320
C.3	Transmission spectral comparison of unaged control (~pH2) and pH adjusted PCWF pyrolysis oil samples.....	321
C.4	PCWF pyrolysis oil neat aged at 80 °C for 7 and 14 days.....	322
C.5	PCWF pyrolysis oil pH adjusted to 5 and aged at 80 °C for 7 and 14 days.....	323
C.6	PCWF pyrolysis oil pH adjusted to 7 and aged at 80 °C for 7 and 14 days.....	324
C.7	PCWF pyrolysis oil adjusted to pH 9 and aged at 80 °C for 7 and 14 days.....	324
D.1	FTIR spectral comparison of neat pine clear wood fractionated [PCWF] pyrolysis oil (a) and PCWF polymerized pyrolysis oil with p-toluic acid catalyst (b) and AlCl ₃ catalyst (c).....	331

D.2	Spectral comparison in the fingerprint region of neat pine clear wood fractionated [PCWF] pyrolysis oil (a) and PCWF polymerized pyrolysis oil with p-toluic acid catalyst (b) and AlCl ₃ catalyst (c).	332
D.3	FTIR transmission spectrum of neat Pine Clear Wood Fractionated [PCWF] (a) compared to the DRIFT spectra of the “polymerized” pyrolysis oil samples of PCWF without catalyst (b-d) and with stannous octanoate catalyst (e, f).....	333
D.4	Fingerprint region of the FTIR transmission spectrum of neat Pine Clear Wood Fractionated [PCWF] (a) compared to the DRIFT spectra of the “polymerized” pyrolysis oil samples of PCWF without catalyst (b-d) and with stannous octanoate catalyst (e, f).....	334
D.5	FTIR spectral comparison of neat pine clear wood fractionated [PCWF] (a) and polymerized samples 7 (b), 8 (c), and 9 (d) of PCWF at ~21 °C (room temperature) and stannous octanoate catalyst.	335
D.6	The Fingerprint region of neat pine clear wood fractionated [PCWF] (a) and polymerized samples 7 (b), 8 (c), and 9 (d) of PCWF at ~21 °C (room temperature) and stannous octanoate catalyst.	336
D.7	Spectral comparison of neat pine clear wood fractionated [PCWF] (b) to the polymerized samples 10 (d), 11 (a), and 12 (c) of PCWF at 5 °C with the addition of stannous octanoate catalyst.	337
D.8	FTIR spectrum of the collected condensate during the controlled polymerization run #2 by a liquid nitrogen vacuum trap.	338
D.9	Calorimetry data for polymerized pyrolysis oil	339
D.10	Molecular weight for soluble portions of polymerized pyrolysis oils.....	340
E.1	XRF data for cottonwood biomass (left) and char (right) showing SiO ₂ , Na ₂ O, CaO, K ₂ O, MgO and P ₂ O ₅ atomic percentages.	344
E.2	XRF data for pine biomass (left) and char (right) showing SiO ₂ , Na ₂ O, CaO, K ₂ O, MgO and P ₂ O ₅ atomic percentages.....	344
F.1	Table 2 from Hu, 2006 displaying the tensile strength and breaking extension ration of PP after thermal degradation of 0, 10, and 20 days ²⁰	349
F.2	The visual appearance of neat PVC (top) and PP (bottom)	351
F.3	Measured pH values of the control bio-oil and the bio-oil PP and PVC were stored in.	354

F.4	Visual comparison of neat PP (left) to bio-oil treated PP (right).....	355
F.5	Measured initial and final weights for the bio-oil treated PP and PVC specimens with 95% CI error bars.	356
F.6	Tensile testing specimens of the neat PP (left) and bio-oil treated PP (right).....	357
F.7	Ultimate Tensile Strength (UTS) and Tensile strength at Failure displayed for PP control and bio-oil treated averages including 95% CI error bars.	360
F.8	Tensile testing specimens of the neat PVC	361
F.9	Ultimate Tensile Strength (UTS) and Tensile strength at Failure displayed for PVC control and bio-oil treated averages including 95% CI error bars.	363
F.10	SEM images for general surfaces of PP control and PP bio-oil treated (a) PP control (x 10k), (b) PP bio-oil treated (x 10k), (c) PP control (x 500), (d) PP bio-oil treated (x 500)	365
F.11	SEM images for general surfaces on PP control and PP thermally degraded Left PP control (x 5000), Right PP thermally degraded (x 5000) [from Hu, 2006 , PP after thermal degradation of 105 days ²⁰].	366
F.12	SEM images for fracture surfaces of PP control and PP bio-oil treated (a) PP control, (x 250), (b) PP bio-oil treated (x 250), (c) PP control (x 1.5k), (d) PP bio-oil treated (x 1.5k)	367
F.13	SEM images for general surfaces on PVC control and PVC bio-oil treated (a) PVC control (x 10k), (b) PVC bio-oil treated (x 10k), (c) PVC control (x 1.5k), (d) PVC bio-oil treated (x 1.5k)	368
F.14	SEM images for fracture surfaces on PVC control and PVC bio-oil treated (a) PVC control (x 500), (b) PVC bio-oil treated (x 500), (c) PVC control (x 200), (d) PVC bio-oil treated (x 200).	369
F.15	The structures of polypropylene ¹⁶	370
F.16	Atomic percentages obtained by XPS compared for the control and bio-oil treated PP specimens.....	371
F.17	An Example of the C 1s peak fitting for a control PP specimen.....	372
F.18	An Example of the C 1s peak fitting for a bio-oil treated PP specimen.....	373

F.19	An Example of the Si 2p peak fitting for a bio-oil treated PP specimen.	376
F.20	A section of the survey scan displaying the silicon peaks.	377
F.21	A section of the survey scan displaying the Oxygen peak.	378
F.22	The structures of polyvinyl chloride ¹⁷	378
F.23	The atomic percentages obtained by XPS compared for the control and bio-oil treated specimens for PP and PVC.	379
F.24	An Example of the C 1s peak fitting for a control PVC specimen.	380
F.25	An Example of the C 1s peak fitting for a bio-oil treated PVC specimen.	381
F.26	An Example of the Si 2p peak fitting for a bio-oil treated PVC specimen.	384

CHAPTER I

INTRODUCTION

1.1 Drive for Alternative Fuel

There is currently a large dependence on fossil fuels around the world where two major factors will influence future use, global climate change and reserves and resources of fossil fuels [Schobert]. Prior to the late 1950's, the United States was energy self-sufficient; with increasing energy consumption, energy became an national import, with imported energy accounting for 26 % of total US energy consumption in 2008 [EAI 2008]. US total energy consumption in 2008 was 99.3 quadrillion BTUs (quads) of energy, and 83.436 quads (89 %) were supplied by fossil fuels [EAI 2008]. The nominal price for gasoline increased more than five times from 1978 to 2008 [EAI 2008] indicating a growing need for a low cost alternative.

Energy sources and demand sectors in the United States are presented in Figure 1.1 for 2008 where transportation accounted for 27.92 % of the total energy consumption and no one sector dominated the energy consumption significantly [EAI 2008]. Therefore all of the sectors must be considered when evaluating alternative energy sources. Also, the largest energy source in the United States in 2008 was from petroleum (37.1 %) and renewable energy was the smallest (7.3 %). The transportation sector has the highest consumption of petroleum (95 %) with only 2 % natural gas and 3 % renewable energy sources [EAI 2008].

All forms of renewable energy combined comprised 7.32 % of the total energy consumption and includes hydroelectric power (34 %), wood (28 %), biofuels (19 %), wind (7 %), geothermal (5 %), water (6 %) and solar/PV (1 %) [EAI 2008]. The biofuels category includes fuel ethanol and biodiesel [EAI 2008].

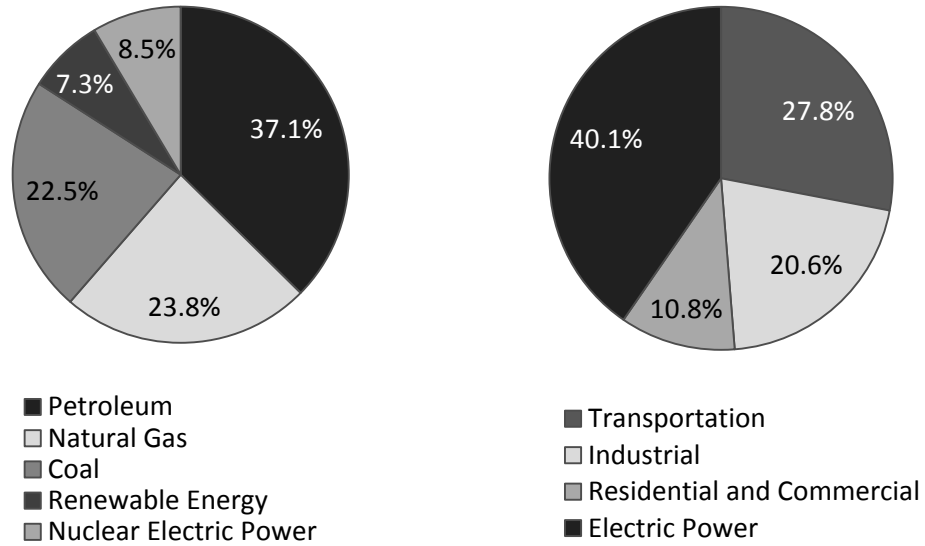


Figure 1.1 Energy sources (left) and energy demand sectors (right) [EIA 2008].

Fossil fuels including petroleum, natural gas and coal all release carbon dioxide, the most impactful greenhouse gas, upon combustion. Between 1990 and 2007 carbon dioxide emissions increased by 20 % to 6 billion metric tons [EIA]. Carbon dioxide produced by the industrial sector decreased by 8 % from 1980 to 2007 allowing transportation to surpass the industrial sector and become the largest contributor to CO₂ emissions [EIA]. Due to the high percentage of petroleum dependence in the transportation sector and the large carbon dioxide emissions there is a great need for alternative transportation fuels from renewable sources with a reduction in carbon dioxide emissions.

1.2 Biomass

Biomass was the first energy source to be used by humans and is typically forgotten or underestimated when considering renewable energy [Combarous, Schobert] and in theory should be inexhaustible given that a new plant can be grown for each one harvested [Schobert]. It is a unique as a renewable energy source as it contains fixed carbon and is considered to have the highest potential to contribute to society's future needs [Bridgewater 2007]. Vegetal biomass supplies a considerable amount of carbon worldwide and in some countries contributes up to 80 % of energy consumed [Combarous]. Biomass in forms of wood, energy crops and waste from forestry and agricultural industries presents opportunities for alternative energy sources [Bridgewater, thermal

Biomass is a unique renewable resource compared to other alternative fuels because it can provide liquid fuel to supplement or replace petroleum fuel [EERE 2010] and could be used with the existing transportation infrastructure. In addition it also has the potential to be a chemical feedstock. [EERE 2010]. Within the United States potential biomass feedstocks for this application include corn, grains, agricultural residues, energy crops, oilseeds, industrial wastes and forestry resources [EERE 2010].

The United States contains almost 2,263 million acres of land, a number that includes 369 million acres in Alaska and Hawaii. Of this acreage, 33 % is forest, 26 % grassland, pasture and range, 20 % cropland, 8 % public facilities, and 13 % miscellaneous (urban, swamps, and deserts). Approximately 50 % of this land has the potential for growing biomass and 75 % of biomass currently consumed originates in forests where a primary forest resource is logging residue. In addition, wood mill

residues, pulping liquors, and urban wood residues are secondary sources of forestry biomass [DOE, USDA].

In 2003, the Southeast US had approximately 60 million acres of privately owned forestlands and 10 million acres of publically or industrially owned land. Also, the total amount of harvested wood products in 2003 less than the annual forest growth and total forest inventory indicating that using biomass would be a sustainable source of energy [DOE, USDA].

The forest industry in Mississippi is a crucial part of the economy; timber is ranked the second highest valuable agricultural product. There were 103 saw and pulpwood mills, in addition to other wood-processing plants, statewide in 2005. Mississippi State has a reputation for lush pine forests where 36 % of the forest is loblolly-shortleaf pine forest, 27 % oak-hickory and 19 % bottomland hardwoods which incorporates oak-gum-cypress and elm-ash-cottonwood trees. In 2006 Loblolly pine (*Pinus taeda*) and sweetgum (*Liquidambar styraciflua*) were estimated at 2.9 and 2.1 billion trees respectively, the most abundant trees in Mississippi indicating approximately 47 % increase in loblolly-shortleaf pine between 1994 and 2006 [USDA, 2006]. In addition a total of 137 species were recorded with two types of cottonwood were reported, Eastern (*Populous deltoids*) and Swamp (*Populous heterophylla*) and seven types of pine tree were reported Shortleaf (*Pinus echinata*), slash (*Pinus elliottii*), spruce (*Pinus glabra*), longleaf (*Pinus palustris*), pond (*Pinus serotina*), Loblolly (*Pinus taeda*) and Virginia (*Pinus virginiana*) [USDA, 2006].

Over the past century there has been an increase in average concentration of carbon dioxide in the atmosphere as well as the Earth's average surface temperature and it is projected that it could increase by 1.5 up to 6 °C in the next hundred years along with

a substantial increase in carbon dioxide concentration [Combarous, 2008]. Biomass has been described as a clean energy source with negligible nitrogen, ash and sulfur content resulting in low NO_x and SO₂ emissions when compared to traditional petroleum fuels [Qi 2007]. Sulfur content in biomass typically ranges 0.05-0.20 wt% which translates to approximately 0.05-0.12 lb SO₂/MM BTU which falls below the maximum amount allotted [Bain 1995].

Biomass should have no net impact on the CO₂ content of the atmosphere due to the removal of CO₂ during growth via photosynthesis [Schobert 2002]. This is based on the assumption that the CO₂ consumed during growth is equal to or greater than the CO₂ produced during combustion of biomass or that by planting additional replacement plants the CO₂ can be offset. This is questionable and relies on many factors including the age and type of biomass that will be replaced, the transportation and processing of the biomass [Schobert 2002]. When grown in short rotation forests biomass and energy crops can contribute to reducing climate changes such as greenhouse gases in accordance to the Kyoto Protocol objectives [Bridgewater 2007].

1.3 What is Pyrolysis?

Gasification, combustion and pyrolysis are all methods to convert biomass to useable energy. Pyrolysis is defined as the heating of biomass in the absence of oxygen or air to produce gases, char and condensable liquids [Diebold, Bridgewater 1997]. Pyrolysis is unique in that it produces liquid fuel that can be used for transportation [Diebold, Bridgewater 1997] compared to conventional combustion and gasification of biomass that can only be applied to heating or electricity generation [Bridgewater Org GeoChem]. Pyrolysis oil also has the potential for chemical applications [Bridgewater

2007]. While the pyrolysis of many biomass types have been tested, including nut shells, straw, forestry waste, sewage sludge and olive pits, wood has been the main focus due to the consistency and comparability between tests [Bridgewater 2007] demonstrating the versatility of pyrolysis to produce oil from a variety of feedstocks.

Fast pyrolysis is defined by low vapor residence times (<1 s) [Diebold 1997], fast heating rates of 1000 °C/s [Bridgewater 2007] to regulate temperatures (450 °C- 550 °C) and results in very high yields of pyrolysis oil [Diebold 1997]. During pyrolysis biomass breaks down to form aerosols, charcoal and vapors (as the primary product) [Bridgewater 2007]. The vapor is then condensed resulting in dark brown liquid called pyrolysis oil that has approximately half the heating value of conventional petroleum oil [Bridgewater 2007]. Short residence times and high heating rates in fast pyrolysis prevent the formation of char due to rapid volatilization of low molecular weight derivatives [Diebold 1997] and are critical because the biomass particles need to be brought up to temperature while minimizing low temperatures where charcoal formation is favored [Bridgewater 2004].

Why is Pyrolysis Important?

Compared to traditional biomass fuels (e.g., black liquor, hog fuel) pyrolysis oils have the potential for high efficiency energy production; thus a large amount of funding and effort has been focused on the research and development of pyrolysis technologies to produce transportation fuels and for heat and power generation [Czernik 2004].

Pyrolysis can produce high energy density liquid fuels that could be upgraded for direct use as a fuel or a feedstock [Chen 2003] for chemicals including resins, flavorings, fertilizers or emission control agents [Bridgewater 2007]. Pyrolysis oil has been tested for heat and power applications including engines, boilers, turbines, and furnaces

[Westerhof 2007] and has been found to burn readily in preheated furnaces [Diebold, Bridgewater 1997]. Gas turbines might be operated with pyrolysis oil to produce electricity but currently the alkali content is outside the range normally recommended [Diebold, Bridgewater 1997] for existing equipment and could lead to fouling, corrosion and erosion in steam boilers and turbines [Agblevor, E&F 1996]. Diesel engines are another application for pyrolysis oil [Diebold, Bridgewater 1997] and emulsions have been tested. Blends of pyrolysis oil with ethanol or diesel fuel were successfully tested in a 2-cylinder diesel engine [Diebold, Bridgewater 1997]. A dual fuel 250 kWe engine was modified and successfully operated with full power output for 10 hours continuously using raw pyrolysis oil as the fuel [Diebold, Bridgewater 1997].

1.4 Reactors

In the past 20 years, advances in the thermal processing of biomass, especially wood, have resulted in optimization of the production of pyrolysis oils [Diebold 1997] where total yields have been reported up to 75 wt% on a dry-feed basis [Bridgewater 2007]. The proportion of the individual product streams are a function of the biomass feed, but oil (organic) yields have been reported as high as 40-65 wt% with 5-15 wt% water and 10-30 wt% (non-condensable) gases [Diebold, Bridgewater 1997]. Many reactor configurations have been designed for the production of pyrolysis oil including rotating cone and transport beds [Diebold, Bridgewater 1997], bubbling fluid beds, circulating fluid beds [Bridgewater Handbook 1999], coiled tube, tubular, ablative vortex, and ablative mill reactors [Diebold NREL 1997].

Fluidized and transported bed reactors are two designs that have become the designs of choice due to reliable and high pyrolysis oil yields [Ringer 2006]. Biomass

must be ground to particle sizes of ~2 mm to ensure rapid heat transfer [Mohan].

Currently fluidized bed systems include 400 kG/h pilot plant at DynaMotive, Canada, 250 Kg/h plant (Wellman Inc., UK) and a 20 Kg/h plant also in Canada (RTI International design [Ringer 2006]).

Bubbling fuel bed reactors require particle sizes of 2-3 mm to attain high heating rates and typically results in liquid yields of 70-75 wt%. Pilot plants include a 200 Kg/h plant at the University of Waterloo (Waterloo, Ontario Canada) and a 100 t/d plant in operation in Canada (RTI International design [Bridgewater 2007]). Circulating bed reactors have similar features, but the residence time is the same for the char and vapors and can lead to higher char content in the pyrolysis oil. The advantage of using circulating bed reactors is high throughput. Two examples of circulating bed pyrolysis reactors include the ENEL plant (Bastardo, Italy) producing 650 kg/h and a 1700 kg/h of biomass plant at Red Arrow, Wisconsin in the United States, both built by Ensyn Technologies Inc. Other reactor types, such as entrained flow, rotating cone and vacuum pyrolysis, have approximate liquid yields of 50-60, 60-70 and 35-50 wt%, respectively, on a dry feed basis [Bridgewater 2007].

Rotating cone reactors use hot sand which is circulated mechanically using a spinning cone for heat transfer. Centrifugal forces move the hot sand, vapors, char and gasses out of the reactor. Transport bed reactors the sand is heated by combustion of pyrolysis gasses or char and then the hot sand is transported by a carrier gas or gravity to the reactor, mixing with the biomass [Diebold & Bridgewater handbook 1999]

1.5 Composition

Pyrolysis liquid is fragmented portions of the biomass (50 % cellulose, 25 % hemicelluloses/ extractives and 25 % lignin) [Diebold 2000, Bridgewater 1997]; therefore, feedstock type and pyrolysis parameters, including pressure, temperature, heating rate and residence time, have a large effect on the composition and yield of pyrolysis oil product [Sensoz 2003, DeSisto 2010]. Due to the strong dependence on the reactor type, feedstock, and operating conditions, the impacts of operating conditions on the pyrolysis oil properties are feedstock and process specific [DeSisto 2010]. In addition, the composition and appearance of pyrolysis oil is dependent on the feedstock and can appear dark brown, red-brown, or dark green [Bridgewater 2007].

Pyrolysis oil is a complex, multiphase oil with upwards of 400 components [Diebold, 1997], a wide range of molecule sizes [Qi 2007], and a large amount of water (from 15 wt % up to 30-50 wt%) emulsified with the oil [Bridgewater 2003]. In comparison to traditional petroleum fuel, pyrolysis oil has high oxygen content (35 to 40 %) [Qi 2007, Diebold 2000, Milne 1997] that is present in both polar and non-polar compounds where the polar compounds allow for a significant amount of water to dissolve in the oil [Diebold 2000, Milne 1997]. Pyrolysis oil has also been described as a multiphase fluid with a network structure of oligomers and non-polar oligomeric micelles [Garcia-Perez 2006]. Large concentrations of formic and acetic acids and other carboxylic acids create a low pH [Andersson 2000] that ranges between 2.3 and 3.0 [Diebold 2000]. Other average pyrolysis oil properties include a specific gravity of 1.20, viscosity of 40-100 cP, 0.5 wt% solids [Bridgewater 1999], and a higher-heating value (HHV) of approximately 17 MJ/Kg [Bridgewater 2007] (about half of petroleum fuels [Oasmaa 2001]). Additional common properties, including water content, viscosity,

molecular weight and methanol insoluble materials (MIM), are presented in Table 1 demonstrating the variety of properties based upon different feedstocks.

Research demonstrated that 99.7 % of pyrolysis oil is composed of carbon, hydrogen and oxygen in the form of water, acids, aldehydes, alcohols, ketones, phenols, sugar, guaiacols, furans, syringols and lignin-derived phenols [Qi 2007]. Pyrolysis oils are miscible with polar solvents such as acetone, methanol, ethanol, etc. but completely immiscible in petroleum-derived fuels without the aid of surfactants [Bridgewater 2003]. In addition most of the phenolic compounds in pyrolysis oil are in the form of oligomers with molecular weights ranging 900-1500 Da [Czernik 2002]. Also, when comparing the chemical composition for fast pyrolysis oils produced from biomass as harvested (including poplar/aspens, hybrid poplar, white spruce, red maple, west hemlock and pine) glucose, xylose, propanoic acids, levoglucosan, furfural, methanol, phenol, and methylcyclopentenone were compounds found in common [Milne 1997]. Due to the complexity of pyrolysis oil, many techniques have been developed for characterization including adsorption chromatography, liquid-liquid extraction, and distillation [Andersson, 2000]. Multiple, time consuming, and difficult steps can cause these techniques to be expensive and result in incomplete analysis due to the loss of compounds during the procedures [Andersson, 2000]. These reasons, coupled with the time and temperature dependent nature of pyrolysis oil aging, makes characterization of pyrolysis oil a daunting task.

Table 1.1 The tabulated overview of MIM content, water content for various pyrolysis oils from various published papers.

Feedstock	pH	MIM (wt%)	Water (wt%)	Density (g/mL)	Viscosity (cP)	MW (Da)	Reference
Pine	2.4	0.03	17	1.24	34.7 (50 °C)	-	Oasmaa 1999
Pinus sylvestris	2.4-2.6	0.03-0.29	16-21	1.22 to 1.24	42.7-43.4 (40 °C)	-	Oasmaa 2003
Pine	2.6	0.18	11.1	1.27	58.2 (50 °C)	-	Siplia 1998
Yellow Pine	3.1	-	13	1.19	96	420	Bhattacharya 2009
Pine wood	-	0.19	16	1.19	72.5 (50 °C)	420	Ingram 2008
Pine bark	-	2.1	19.8	1.17	-	460	Ingram 2008
Pinus strobus	2.26	-	-	-	11100 (25 °C)	-	DeSisto 2010
Loblolly pine	3.08	-	16.9	1.18	65.1 (50 °C)	430	Hassan 2009
Pine	3.5	-	30	1.22	122	-	Vitolo 1999
Pine/Spruce	2.3	-	23.3	1.20	87.6 (20 °C)	-	Oasmaa 2005
Pine/Spruce	2.4	-	23.4	1.19	92.8(20 °C)	-	Oasmaa 2005
Canadian oak/Swedish pine	3.2	-	38	1.17	13.4	-	Vitolo 1999
Oak	-	0.8	22.5	1.20	49.9 (50 °C)	390	Ingram 2008
Oak	2.8	-	21.5	1.22	40.26(40 °C)	-	Shaddix 1998
Canadian oak	2.7	-	29	1.22	20.3	-	Vitolo 1999
Oak bark	-	1.83	22	1.20	-	450	Ingram 2008
Oak/Maple	2.5	-	22	1.18	59 (50 °C)	-	Oasmaa 2005
Oak/Maple	2.8	-	23.3	1.23	86.1 (50 °C)	-	Diebold 1997
Birch	2.5	0.06	18.9	1.25	35 (50 °C)	-	Oasmaa 1999
Poplar	2.8	0.045	18.9	1.20	16.2 (50 °C)	-	Oasmaa 1999
Poplar	2.8	-	20.6	-	18 cSt (40 °C)	-	Shaddix 1998
Willow	2.68	0.4	17.4	-	53.2 (40 °C)	517	Fahmi 2008
Spruce	2.4	-	23.8	1.19	17.85 (40 °C)	-	Oasmaa 2005
Hardwood	2.4	-	31.8	-	10.7 cSt (40 °C)	-	Ikura 2003
Hardwood	2.8	0.3	23.3	1.23	61.6 (50 °C)	-	Siplia 1998
Hardwood	2.5	-	24.5	1.22	43.1 (40 °C)	-	Bertoncini 2006
Hardwood	-	-	26	1.19	107 (25 °C)	-	Maggi 1994
Hardwood	-	-	27	1.20	110 (25 °C)	-	Maggi 1994
white spruce, balsam fir, larch	3	0.75	-	1.19	73.6 (50 °C)	454	Garcia-Perez 2007
Softwood bark	3	0.7	13	1.19	73.6 (50 °C)	-	Mohan
Softwood bark residue	3	2.3	13	1.19	73.6 (50 °C)	1163	Ba 2004
Softwood bark residue		0.34	5.3	1.07	40.5 (40 °C)	-	Boucher 2000
Forestry Residue	3.1-3.3	0.02-0.11	24-32	1.20-1.22	15.6-35.4 (40 °C)	-	Oasmaa 2003
Forestry Residue	2.6	0.1	27	-	30 cSt (40 °C)	-	Oasmaa 2003

1.6 Barriers to Direct Application

As produced, pyrolysis oils have multiple obstacles preventing direct implementation including instability during storage [Garcia-Perez, 2006 364-375, Ba, 2004, Qi 2007], high acidity [Garcia-Perez, 2006, 364-375] and high water content leading to corrosion, phase separation [Mohan, 2006], char containing alkali metals and low burning times [Garcia-Perez, 2006, 364-375]. Also processing difficulties include clogging nozzles, injectors or filters and/or agglomeration of components in recirculation systems [Ba 2004], deposits of waxy materials in pipes [Garcia-Perez 2006] and corrosion to gas turbine blades [Boucher 2000 II]. High concentrations of oxygen result in the storage instability also referred to as aging which leads to increased viscosity and water content as a result of condensation reactions [Oasmaa 2004, Diebold 1997] and can lead to phase separation [Oasmaa 04]. Additional changes observed during aging include increased average molecular weight, increased heating value and a decrease in volatile material such as aldehydes and ketones [Oasmaa 2004] and a breakdown in the microemulsion [Mohan, 2006]. Reactive compounds polymerize to form larger molecules resulting in changes in the physical properties [Diebold 1997]. Also, water-insoluble materials in the pyrolysis oil result in the colloidal nature and cause difficulties during storage and combustion [Ba, 2004].

1.7 Corrosion

Due to the high content of carboxylic acids [Diebold, Miilne 1997 thermochem] pyrolysis oils have low pH (2.3-3.0) [Diebold 2000] resulting in corrosion of mild steel, aluminum and nickel based materials whereas stainless steel and assorted plastics are more resistant [Darmstadt 2004]. Corrosion due to contact with pyrolysis oil has been found to worsen with elevated temperature and/or water content [Darmstadt 2004, Qiang

2008] and has been attributed to the presence of alkali metals [Agblevor 1996, Darmstadt 2004]. Ash containing alkali metals leads to fouling steam boiler tubes and hot corrosion and erosion of turbine blades [Agblevor 1996] due to condensation of alkali oxides on the blades [Boucher B&B 2000]. Ash content should be reduced to below 0.1 wt% to prevent this corrosion [Boucher B&B 2000].

A two-phase pyrolysis oil produced from softwood bark residue (balsam fir, white spruce and black spruce) was shown to corrode aluminum and copper; austenitic 316 stainless steel was shown to be corrosion resistant. The bottom phase of this pyrolysis oil was more corrosive than the top phase [Darmstadt 2004]. In a second study, aluminum, mild steel, and brass were not resistant to corrosion in rice husk pyrolysis oil and resulted in the formation of oxide deposits on those surfaces [Qiang 2008]. In contrast, stainless steel was found to be resistant such that initially corrosion causes a Cr_2O_3 film to form on the surface that prevents further corrosion [Qiang 2008]. It was also found that emulsions of pyrolysis oil with diesel fuel were able to reduce the corrosion rate compared to pyrolysis oil as produced [Qiang 2008].

Pyrolysis oil was tested in medium and slow speed diesel engines and auto-ignition was not a problem but excessive wear and corrosion in the injector loop made it difficult to maintain proper injector adjustment. This problem was attributed to the particulate content and acidity of the pyrolysis oil [Ringer 2006].

1.8 Aging

One of the major barriers to the application of pyrolysis oil is the instability during storage (aging) described as a viscosity increase at room temperature that can be accelerated by heating or retarded by cooling [Diebold, 1997]. Due to the short reactor

residence times and rapid cooling during the pyrolysis process, the condensed oils are not at thermodynamic equilibrium and so are not stable [Diebold 2000]. Over time reactive organic components react to produce large molecules changing the physical properties such as viscosity [Diebold 1997]. Chemical composition also changes during storage, moving toward thermodynamic equilibrium causing the observed changes in viscosity, molecular weight, and co-solubility of its many compounds [Diebold 2000]. Initial viscosity and aging rate varies depending on the feedstock the oil is derived from [Diebold 2000].

Multiple accelerated aging studies have been conducted comparing various temperatures and aging times [Mohan 2006]. Eucalyptus-derived pyrolysis oil viscosity doubled after a year of storage at room temperature and after 3 days at 80 °C whereas oak pyrolysis oil viscosity doubled within a day at 80 °C [Oasmaa 2000]. Pyrolysis oil stored at 20 °C for several months exhibited a viscosity increase. In contrast when stored at -14 °C the viscosity increased very slowly within the first week and after 13 months the viscosity increased less than 5 % and the water content increased from 22.7 wt% to 23.2 wt% [Oasmaa 2000].

Oak-derived pyrolysis oil demonstrated a viscosity increase after 3 months of aging at 37 °C that was determined to be equivalent to the viscosity after 4 days of aging at 60 °C or 6 hours at 90 °C and first order kinetics successfully predicted the observed viscosity increases. It was noted that the model may only be applicable for the oak pyrolysis oil due to the dependence on the high molecular weight compounds concentration and water content [Czernik, 1994]. In a separate study, the rate viscosity change for pyrolysis oils can be represented with the Arrhenius equation which indicates the involvement of chemical reactions in the aging process [Diebold 2000].

Etherification and esterification were proposed as aging mechanisms based on FTIR analyses [Czernik 1994] where hydroxyl and carbonyl components were found to react and there was a corresponding molecular weight increase during storage [Diebold 1997, Garcia-Perez 2002]. Condensation reactions were confirmed by the increase in water content during aging [Garcia-Perez 2002]. Particle growth observed is also observed and thought to be due to polymerization reactions during heating or physical agglomeration of micelles [Diebold 2000].

Preventing the aging reactions would be beneficial thus providing a liquid fuel that can be stored for long periods of time without phase separation or the formation of a thick tar [Diebold 1997].

1.9 Phase Separation

Phase separation is directly related to the storage stability barrier and can form during aging. There are two distinct types of phase separation that occur due to either a large concentration of water or high concentrations of lignin derived material [Oasmaa 2001]. A minimum of 30 wt% water will result in phase separation and feedstocks including forest residue, barks, straw, pine, eucalyptus and tropical hardwood produce multiple phase pyrolysis oil due to high levels of hydrocarbon-soluble extractives and/or alkali metals [Oasmaa 2001].

Lignin rich phase separation has been observed in the pyrolysis of forestry residue [Oasmaa 2003] and softwood bark (white spruce, balsam fir and larch) [Ba, 2004] where phase separation occurs due to significant differences in density, solubility and polarity of extractives and polar compounds [Oasmaa 2003]. Softwood bark residue pyrolysis oil was described as a colloidal system with an extractive rich top phase (16 wt%) and the

bottom phase similar to whole pyrolysis oils only with higher ash and water content [Ba, 2004].

Phase separation due to water can occur even in fresh (just produced) pyrolysis oil when the moisture content of the feedstock was too high (>15 wt%) prior to pyrolysis [Oasmaa 2001]. The addition of water to pyrolysis oil has also been shown to result in the precipitation of the heavy oil and tar [Elliot 1994]. In pine and oak derived pyrolysis oils, phase separation occurred at 25-30 and 35 wt % water, respectively [Elliot 1994]. In a second study, water a minimum of 32 wt % water was required to induce phase separation [Westerhof 2010].

Phase separation can also occurring during storage and accelerated aging. During heating of pyrolysis oils, phase separation occurs due to water formation, a by-product of aging reactions, when the total water content exceeds 30 wt and results in an aqueous phase and a heavy lignin rich phase [Oasmaa 2001]. Phase separation during aging has also been attributed to water content and the formation of large molecules by reactions such as polymerization (large molecules) and etherification and esterification (water by-product) leading to a tar like bottom phase and an acidic top phase with high water content [Mullaney 2008].

1.10 Char & Filtration

During pyrolysis, fine char particulates are entrained in the vapor resulting due to the coproduction of gasses and char [Scahill] that contains inorganic material (ash) [Hoekstra 2009] including silicates, chlorides, phosphates and sulfates that are bound to organic acids [Diebold 2000]. It has been suggested these alkali metals catalyze polymerization reactions [Ringer 2006, Diebold 2000] leading to an increase in viscosity

and visible growth in particle diameter [Diebold 2000]. Pyrolysis oil corrosion has also been attributed to alkali metals [Agblevor 1996, Darmstadt 2004] resulting in hot corrosion, fouling steam boiler tubes and erosion of turbine blades [Agblevor 1996]. It is therefore beneficial to remove the alkali metals in order to prevent corrosion and catalysis of aging reactions.

Filtration of the pyrolysis oil after condensation can remove larger char particles, but does not remove solids on the nanometer scale or particles dissolved in the pyrolysis oil and results in a high-ash sludge by-product [Diebold 2000]. Pressure filtration of condensed pyrolysis oil is difficult with the presence of gel phase formed by char-liquid interaction that results in filter saturation [Bridgewater 2007]. Even when diluted with solvents such as methanol, condensed pyrolysis oil filtration removes 20% to 50% of the total inorganic content using a 2.5- μm filter, although a second filtration was required due to the agglomeration of particles [Diebold 2000].

Cyclone filtration is the typical method in pyrolysis reactor systems [Bridgewater 2004] and remove ~90 % of large char particles such that the char remaining in the pyrolysis oil is $\leq 10 \mu\text{m}$ in diameter [Diebold 2000]. Cyclone filtration in conjunction with hot gas filtration produces a relatively char-free oil [Diebold 1997] and reduces the alkali metal content down to 10 ppm [Agblevor 1996]. Unfortunately hot gas filtration also reduces the overall yield by 10-20 % [Bridgewater 2003]. A recently developed continuous operation pilot plant with *in situ* hot gas filtration (without a cyclone) produced higher quality oil without a reduction in yield when compared to oil produced from the same reactor using only cyclone filtration [Hoekstra 2009].

Removal of char particles using hot gas filtration and a cyclone prior to condensation significantly slowed pyrolysis oil aging (as monitored by changes in

viscosity) when compared to pyrolysis oil filtered only by cyclone [Diebold 1997]. Conversely, the addition of char to pyrolysis oil has been found to accelerate the rate of the viscosity increase during storage at 45 °C over 16 days [Agblevor 1998]. In another study, char/sand particles were collected by successive wire mesh filters integrated into a fluidized bed reactor and also by external glass filters suggesting that char formation occurs in the vapor during pyrolysis [Hoekstra 2009]. The resulting pyrolysis oil, filtered by both hot gas filtration and a cyclone, was then aged at 80 °C for 24 h and showed increased molecular weights may be the result of reactions involving highly reactive compounds found in pyrolysis oil [Hoekstra 2009]. Diebold et al. found that particles had agglomerated during aging in pre-filtered pyrolysis oil and hypothesized that the entrained char particles that were not filtered just after pyrolysis may have acted as catalytic condensation sites [Diebold 2000].

1.11 Upgrading

To prevent undesired aging, physical and chemical upgrading methods have been investigated including solvent addition [Diebold 1997, Boucher 2000, Oasmaa 2004, Shaddix 1999], emulsification with diesel fuel [Bridgewater 2004], deoxygenation over zeolite catalysts, and hydrotreatment using a catalyst [Maggi 1994]. Solvent addition is used to homogenize samples, reduce the initial viscosity and retard increased viscosity during aging [Bridgewater 2007]. Hydrodeoxygenation uses solvents activated by catalysts (Ni-Mo, Co-Mo) under pressure in the presence of hydrogen or carbon monoxide and requires sophisticated technologies, complex equipment and can be expensive [Qi 2007]. Emulsions of pyrolysis oil and diesel fuel are one of the simplest

upgrading methods, requiring smallest amount of engine modification, but is also dependent on the pyrolysis oil properties [Weerachanchai 2009].

Pyrolysis oil can be emulsified in petroleum fuels with the aid of a surfactant [Bridgewater 2004]. In addition to the disadvantage of high priced surfactants, there was a significant increase in engine corrosion when tested [Bridgewater 2004]. Two stable emulsions have been developed using 5-30 % and 5-95 % pyrolysis oil in diesel oil by CANMET and University of Florence, respectively [Bridgewater 2004]. Chemical upgrading requires the full deoxygenation of the pyrolysis oil to obtain a fuel similar to traditional petroleum fuel and can be done by catalytic vapor cracking or hydrotreating. Hydrotreating is conducted at high pressure and temperature with a catalyst, resulting in the elimination of oxygen. Zeolite cracking is one example of vapor cracking. It is integrated into the pyrolysis process and the vapor is cracked with an acidic zeolite catalyst [Bridgewater 2007].

1.12 Solvent Addition

Multiple studies have investigated the addition of solvents to pyrolysis oil include methanol, acetone, ethanol, isopropanol, formic acid, and water [Diebold 97, Boucher I,II, Oasmaa 04]. Polar solvents have been shown to homogenize pyrolysis oils and reduce the initial viscosity [Diebold 1997, Oasmaa 2004], flash point and density [Oasmaa 2004] and mixing with alcohols improves the heating value [Oasmaa 2004, Weerachanchai 2009] and acidity [Weerachanchai 2009].

Solvents were added to the pyrolysis oil in concentrations up to 25 wt% before and after accelerated aging studies [Diebold 1997]. Methanol was determined to be the most effective solvent in reducing the aging effects [Diebold 97, Oasmaa 04]. Three

mechanisms were proposed for solvent addition: physical dilution, molecular dilution, or solvent reaction with the pyrolysis oil preventing the original aging reaction [Oasmaa 04].

It was demonstrated that with the addition of methanol (10 wt%) to hybrid poplar pyrolysis oil the rate of viscosity increase (aging) was reduced by almost 20 % and the methanol did not act solely by molecular dilution [Diebold 1997] In addition, methanol delayed, but did not prevent, the formation of large aromatic molecules [Diebold 1997]. A second study using pine sawdust and forestry residue derived pyrolysis oils added up to 10 wt% ethanol, methanol or isopropanol [Oasmaa 2004]. Alcohol addition decreased the viscosity and improved the homogeneity by enhancing solubility [Oasmaa 2004]. Methanol was found to be the most effective solvent by the largest decrease the initial viscosity value and only a ~ 13 % increase in viscosity after 6 hours of aging at 80 °C (3-4 months at room temperature) [Oasmaa 2004].

It is theorized that the methanol reacted with oligomers creating non-reactive oligomers and slowing the polymerization [Diebold 1997]. After aging with the addition of methanol, GC/MS analysis showed a decrease in acetic acid and an increase in methyl acetate [Diebold 1997]. In a second study, GC/MS analysis revealed that methylation occurred with the presence of methanol due to the higher concentration of methylstearate [Boucher 2000]. A third study suggested esterification and acetalization occur between pyrolysis oils and solvents due to the formation of acetal of alcohols with aldehydes, ketones, and sugars such that acetals protect the aldehyde and ketone functional groups [Oasmaa 2004].

There is still a need to better understand the mechanisms of solvent addition for the retarding of aging reactions [Qi 2007]. It was suggested that further investigation of

solvent addition to reduce the proposed reactions including polymerization by esterification, phenol/formaldehyde reactions, acetalization may prevent phase separation problems in pyrolysis oil [Qi 2007].

1.13 Toxicity

There is limited information about the toxicity of pyrolysis oil. It has been suggested that its toxicity is dependent on the composition and therefore dependant on the pyrolysis process, feedstock material and possibly age of the pyrolysis oil [Diebold 1997]. The U.S. Environmental Protection Agency classifies a material with pH less than 2 to be a hazardous [Mullaney 2001]. Although pyrolysis oil pH is typically not lower than 2, the pH can decrease during storage or aging and would then be considered to be hazardous [Mullaney 2001, Oasmaa 2001].

Unsaturated oxygenates, aldehydes and furans were shown to be the greatest acute (in descending order) toxic threat of the many components in pyrolysis oil. During aging, the toxicity generally decreases due to compounds reacting to reach thermodynamic equilibrium [Diebold 1997]. In addition, polycyclic aromatic hydrocarbons (PAHs), which are considered carcinogens [Mullaney 2001], are contained in pyrolysis oil at trace levels, which could result in environmental and health hazards when implemented as a fuel [Fabbri 2010].

Pyrolysis oil has been found to irritate the eyes (possibly irreversible damage), respiratory system, and skin [Mullaney 2001, Oasmaa 1999]. Exposure to the aerosols or smoke of pyrolysis oil is highly irritating to the respiratory tract resulting in eye irritation and damage and can lead to death with high levels of exposure over prolonged periods [Diebold 1997].

Pyrolysis oil produced above 600 °C was shown to have mutagenic effects [Oasmaa 1999]. However, pyrolysis oils were shown to have no tumorigenicity in a second study, but did have mutagenic results in a third [Diebold 1997] showing a variability in the pyrolysis oils and the potential for mutagenic effects. Also, it has been found that the chronic exposure of humans to wood smoke, a similar product, does not result in an increase in the occurrence of lung cancer [Diebold 1997]. Currently additional information needs to be collected over a wide range of pyrolysis oils to determine the overall toxicity. Toxicity remains a potential barrier for fuel applications.

1.14 Economics

Economics of pyrolysis oil production are affected by the low-grade wood chips cost (assumed to be \$18/ton) and by the plant size [Mullaney 2002]. Independent studies have shown that pyrolysis oil could be produced for \$0.13 and \$0.16 per liter, but with cogeneration the cost drops to \$0.11 per liter. At the time of that study, this price was comparable to #2 diesel fuel (\$0.2 per liter), #4 fuel oil (\$0.15 per liter), or #6 fuel oil (\$0.10 per liter) and so pyrolysis oil would be able to compete in the market [Diebold, Bridgewater 1997].

A separate study estimated that 440 US ton wet wood/day of pyrolysis oil would cost \$0.89/gal to produce or \$0.16/Mbtu (million Btu) to produce and a 110 US ton wet wood/day plant could produce pyrolysis oil at a cost of \$1.21/gal or \$0.216/Mbtu (which includes capital costs) [Mullaney 2002]. When compared to #2 fuel oil, this estimated cost for pyrolysis oil is twice as expensive to produce heat or electricity due to the pyrolysis oil have approximately half the heating value [Mullaney 2002]

1.15 References

- Adjaye, J.D.; Sharma, R.K.; Bakhshi, N.N. Characterization and stability analysis of wood-derived pyrolysis oil. *Fuel Processing Technology* 1992, 31, 241-256.
- Agblevor, F.A.; Besler, S. Inorganic Compounds in Biomass Feedstocks. 1. Effect on the Quality of Fast Pyrolysis Oils. *Energy & Fuels* 1996, 10, 293-298.
- Agblevor, F.A.; Scahill, J.; Johnson, D.K. Pyrolysis Char Catalyzed Destabilization of Biocrude Oils. *AIChE Symposium Series* 1998, 319, 94.
- Andersson, T.; Hyotylainen, T.; Riekkola, M. Analysis of phenols in pyrolysis oils by gel permeation chromatography and multidimensional liquid chromatography. *Journal of Chromatography A* 2000, 896, 343-349.
- Bain, R.L. Electricity from Biomass in the United States: Status and Future Direction. In *Proceedings, Biomass Pyrolysis Oil Properties and Combustion Meeting, Sept 26-28, Estes Park, CO*, Milne, T. A., Ed.; NREL-CP-430-7215; National Renewable Energy Laboratory: Golden, CO, 1995; 2-10.
- Biagini, E.; Barontini, F.; and Tognotti, L. Devolatilization of Biomass Fuels and Biomass Components Studied by TG/FTIR Technique. *Industrial & Engineering Chemistry Research* 2006, 45, 4486-4493.
- Ba, T.; Chaala, A.; Garcia-Perez, M.; Roy, C. Colloidal Properties of Pyrolysis oils Obtained by Vacuum Pyrolysis of Softwood Bark. Storage Stability. *Energy & Fuels* 2004, 18, 188-201.
- Ba, T.; Chaala, A. Garcia-Perez, M.; Rodrigue, D.; Roy, C. Colloidal Properties of Pyrolysis oils Obtained by Vacuum Pyrolysis of Softwood Bark. Characterization of Water-Soluble and Water-Insoluble Fractions. *Energy & Fuels* 2004, 18, 704-712.
- Biomass Multi-Year Program Plan*, Office of the Biomass Program, Energy Efficiency and Renewable Energy (EERE), US Department of Energy, March 2010.
www1.eere.energy.gov/biomass/pdfs/mypp.pdf (accessed September 23, 2010)
- Biomass as Feedstock for a Bioenergy and Bioproducts Industry: The Technical Feasibility of a billion-ton Annual Supply*. US Department of Energy (DOE) and US Department of Agriculture (USDA), April 2005.
www1.eere.energy.gov/biomass/pdfs/final_billionton_vision_report2.pdf (accessed September 23, 2010)

Boucher, M.E.; Chaalab, A.; Roy, C. Pyrolysis oils obtained by vacuum pyrolysis of softwood bark as a liquid fuel for gas turbines. Part I: Properties of pyrolysis oil and its blends with methanol and a pyrolytic aqueous phase. *Biomass & Bioenergy* 2000, 19, 351-361.

Boucher, M.E.; Chaala, A.; Roy, C. Pyrolysis oils obtained by vacuum pyrolysis of softwood bark as a liquid fuel for gas turbines. Part I: Properties of pyrolysis oil and its blends with methanol and a pyrolytic aqueous phase. *Biomass & Bioenergy* 2000, 19, 337-350.

Bridgwater, A.; Czernik, S.; Diebold, J.; Meier, D.; Oasmaa, A.; Peacocke, C.; Piskorz, J.; Radlein, D. An Introduction to Fast Pyrolysis of Biomass for Fuels and Chemicals. In *Fast Pyrolysis of Biomass: A Handbook*; CPL Press, 1999, p. 1-13.

Bridgwater, A.V.; Meier, D.; Radlein, D. An Overview of Fast Pyrolysis of Biomass. *Organic Geochemistry* 1999, 30, 1479-1493.

Bridgwater, A.V. Biomass Fast Pyrolysis. *Thermal Science* 2004, 8, 21-50.

Bridgwater, A.V. The Production of biofuels and renewable chemical by fast pyrolysis of biomass. *International Journal of Global Energy Issue* 2007, 27, 160-203.

Chaala, A.; Ba, T.; Garcia-Perez, M.; Roy, C. Colloidal Properties of Pyrolysis oils Obtained by Vacuum Pyrolysis of Softwood Bark: Aging and Thermal Stability. *Energy & Fuels* 2004, 18, 1535-1542.

Chen, G.; Andries, J.; Spliethoff, H.; Experimental Investigation of Biomass Waste (Rice Straw, Cotton Stalk, and Pine Sawdust) Pyrolysis Characteristics. *Energy Sources* 2003, 25, 331-337.

Combarrous, M.; Bonnet, J. The worlds thirst for Energy: How to Face the Challenge. In *Sustainable Energy Technologies: Options and Prospects*, Hanjalic, K.; vande Krol, R.; Lekic, A., Ed. Springer, 2008.

Czernik, S.; Johnson, D. Black, S. Stability of Wood Fast Pyrolysis Oil. *Biomass & Bioenergy* 1994, 7, 187-192.

Czernik, S. Bridgwater, A.V. Overview of Applications of Biomass Fast Pyrolysis Oil. *Energy & Fuels* 2004, 18, 590-598.

Czernik, S.; Maggi, R.; Peacocke, G.V.C. Review of Methods for Upgrading Biomass-Derived Fast Pyrolysis Oils. In *Fast Pyrolysis of Biomass: A Handbook*; Bridgwater, A., Ed.; CPL Press, Newbury; 2002; Vol. 2; p. 141-146.

Darmstadt, H.; Garcia-Perez, M.; Adnot, A.; Chaala, A.; Kretschmer, D.; Roy, C. Corrosion of Metals by Pyrolysis oil Obtained by Vacuum Pyrolysis of Softwood Bark Residues. An X-ray Photoelectron Spectroscopy and Auger Electron Spectroscopy Study. *Energy & Fuels* 2004, 18, 1291-1301.

DeSisto, W.J.; Hill, N.; Beis, S.H.; Mukkamala, S.; Joseph, J.; Baker, C.; Ong, T.; Stemmler, E.A.; Wheeler, M.C.; Frederick, B.G.; van Heiningen, A. Fast Pyrolysis of Pine Sawdust in a Fluidized-Bed Reactor. *Energy Fuels* 2010, 24, 2642–2651.

Diebold, J.P.; Bridgewater, A.V. Overview of Fast Pyrolysis of Biomass for the Production of Liquid Fuels. In *Developments in Thermochemical Biomass Conversion*; Bridgewater, A.V., Boocock, D.G.B., Ed.; Blackie Academic & Professional: New York, 1997; Vol. 1; p. 5-26.

Diebold, J.P. A Review of the Chemical and Physical Mechanisms of Storage Stability of fast Pyrolysis Pyrolysis oils. Subcontractor Report for the National Renewable Energy Laboratory NREL/SR-570-27613; National Renewable Energy Laboratory: Golden, CO, 2000.

Diebold, J.P.; Milne, T.A.; Czernik, S.; Oasmaa, A.; Bridgewater, A.V.; Cuevas, A.; Gust, S.; Huffman, D.; Piskorz, J. Proposed Specifications for Various Grades of Pyrolysis Oils. In *Developments in Thermochemical Biomass Conversion*; Bridgewater, A.V., Boocock, D.G.B., Ed.; Blackie Academic & Professional: New York, 1997; Vol. 1; p. 433-447.

Diebold, J.P.; Bridgewater, A.V. Overview of Fast Pyrolysis of Biomass for the Production of Liquid Fuels. In *Fast Pyrolysis of Biomass: A Handbook*; CPL Press: Newbury, 1999.

Diebold, J.P. A Review of the Toxicity of Biomass Pyrolysis Liquids Formed at Low Temperatures. *National Renewable Energy Laboratory*, Golden, CO, NREL/TP-430-22739, 1997.

Elliot, D.C. Analysis and Comparison of Biomass by Pyrolysis/Gasification Condensates. *Pacific Northwest Laboratory*, Richland, Washington PNL-5943, 1986.

Energy Information Administration (EIA). 2009. *Annual Energy Review 2008*. Washington, DC: US Department of Energy.

Fabbri, D.; Adamiano, A.; Torri, C. GC-MS determination of polycyclic aromatic hydrocarbons evolved from pyrolysis of biomass. *Analytical and Bioanalytical Chemistry* 2010, 397, 309-317.

Garcia-Perez, M.; Chaala, A.; Roy, C. Vacuum Pyrolysis of Sugarcane Bagasse. *Journal of Analytical and Applied Pyrolysis* 2002, 65, 111-136.

Hoekstra, E.; Hogendoorn, K.J.A.; Wang, X.; Westerhof, R.J.M.; Kersten, S.R.A.; van Swaaij, W.P.M.; Groeneveld, M.J. Fast Pyrolysis of Biomass in a Fluidized Bed Reactor: In Situ Filtering of the Vapors. *Industrial and Engineering Chemistry Research* 2009, 48, 4744-4756.

Ikura, M.; Stanciulescu, M.; Hogan, E. Emulsification of pyrolysis derived pyrolysis oil in diesel fuel. *Biomass & Bioenergy* 2003, 24, 221 – 232.

Islam, M.N.; Islam, M.N.; Beg, M.R.A.; Islam, M.R. Pyrolytic oil from fixed bed pyrolysis of municipal solid waste and its Characterization. *Renewable Energy* 2005, 30, 413–420.

Qiang, L.; Jian, Z.; XiFeng, Z. Corrosion properties of pyrolysis oil and its emulsions with diesel. *Chinese Science Bulletin* 2008, 53, 3726-3734.

Maggi, R.; Delmon, B. Characterization and Upgrading of Pyrolysis oils Produced by Rapid Thermal Processing. *Biomass & Bioenergy* 1994, 7, 245-249.

Marsman, J.H.; Wildschut, J.; Evers, P.; de Koning, S.; Heeres, H.J. Identification and classification of components on flash pyrolysis oil and hydrodeoxygenated oils by two-dimensional gas chromatography and time-of-flight mass spectroscopy. *Journal of Chromatography A* 2008, 1188, 17-25.

Milne, T.; Agblevor, F.; Davis, M., Deutch, S.; and Johnson, D. A Review of the Chemical Composition of Fast-Pyrolysis oils from Biomass. In *Developments in Thermochemical Biomass Conversion*; Bridgwater, A.V., Boocock, D.G.B.; Blackie Academic & Professional: New York, 1997; Vol. 1; p. 409-424

Mississippi's Forests, Resource Bulletin SRS-147, US Department of Agriculture (USDA) Forest Service Southern Research Station, 2006.
www.srs.fs.usda.gov/pubs/rb/rb_srs147.pdf (accessed September 24, 2010)

Mohan, D.; Pittman, C.U; Steele, P.H. Pyrolysis of Wood/Biomass for Pyrolysis oil: A Critical Review” *Energy & Fuels* 2006, 20, 848-889.

Mullaney, H. Technical, Environmental and Economic Feasibility of Pyrolysis oil in New Hampshire's North Country. New Hampshire Industrial Research Center (NHIRC) 2002.

Oasmaa, A.; Leppamaki, E.; Koponen, P.; Levander, J.; Tapola, E. Physical Characterization of Biomass-Based Pyrolysis Liquids. Application of Standard Fuel Oil Analyses. Technical Research Centre of Finland, VTT Publications 306 ESPOO 1997.

Oasmaa, A.; Peacocke, C.; A guide to physical property characterisation of biomass-derived fast pyrolysis liquids. Technical Research Centre of Finland, VTT Publication 450, ESPOO 2001.

Oasmaa, A.; Kuoppala, E.; Selin, J.; Gust, S.; Solantausta, Y. Fast Pyrolysis of Forestry Residue and Pine. 4. Improvement of the Product Quality by Solvent Addition. *Energy & Fuels* 2004, 18, 1578-1583.

Oasmaa, A.; Czernik, S. Fuel Oil Quality of Biomass Pyrolysis Oils-State of the Art for the End Users. *Energy & Fuels* 1999, 13, 914-921.

Oasmaa, A.; Kuoppala, E. Fast Pyrolysis of Forestry Residue. 3. Storage Stability of Liquid Fuel. *Energy & Fuels* 2003, 17, 1075-1084.

Oasmaa, A.; Kuoppala, E.; Solantausta, Y. Fast Pyrolysis of Forestry Residue. 2. Physicochemical Composition of Product Liquid. *Energy & Fuels* 2003, 17, 433-443.

Oasmaa, A.; Peacocke, C.; Gust, S.; Meier, D.; McLellan, R. Norms and Standards for Pyrolysis Liquids. End-User Requirements and Specifications. *Energy & Fuels* 2005, 19, 2155-2163.

Qi, Z.; Jie, C.; Tiejun, W.; Ying, X. Review of biomass pyrolysis oil properties and upgrading research. *Energy Conversion and Management* 2007, 48, 87-92.

Qiang, L.U.; Jian, Z.; XiFeng, Z. Corrosion properties of pyrolysis oil and its emulsions with Diesel”, *Chinese Science Bulletin*, 2008, 53, 3726-3734.

Ringer, M.; Putsche, V.; Scahill, J. Large Scale Pyrolysis Oil Production: A Technology Assessment and Economic Analysis. *National Renewable Energy Laboratory*, Golden, CO, NREL/TP-510-37779, 2006.

Scahill, J.W.; Diebold, J.P.; Feik, C. Removal of residual char fines from pyrolysis vapours by hot gas filtration. In *Developments in Thermochemical Biomass Conversion*; Bridgwater, A.V. Boocock D.G.B.; Blackie Academic & Professional: New York, 1997; Vol. 1; p 253-266.

Schobert, H.H. *Energy and Society: An Introduction*; Taylor & Francis: New York, 2002.

Sensoz, S. Slow pyrolysis of wood barks from *Pinus brutia* Ten. And products compositions. *Biosource Technology* 2003, 89, 307-311.

Shaddix, C.R.; Tennison, P.J.; Effects of Char Content and Simple Additive on Biomass Pyrolysis Oil Droplet Combustion. *Twenty-Seventh Symposium (International) on Combustion/The Combustion Institute* 1998, 1907-1914.

Siplia, K.; Kuoppala, E.; Fagernaes, L.; Oasmaa, A. Characterization of Biomass-base Flash Pyrolysis Oils. *Biomass & Bioenergy* 1998, 14, 103-113.

Vitolo, S.; Seggiana, M.; Frediani, P.; Ambrosinia, G.; Politia, L. Catalytic upgrading of pyrolytic oils to fuel over different zeolites. *Fuel* 1999, 78, 1147–1159.

Westerhof, R.J.M.; Kuipers, N.J.M.; Kersten, S.R.A.; Swaij, W.P.M. Controlling the Water Content of Biomass Fast Pyrolysis Oil. *Industrial and Engineering Chemistry Research* 2007, 46, 9238-9247.

CHAPTER II
COMPARISON OF PHYSICAL AND CHEMICAL PROPERTIES OF
COTTONWOOD AND PINE BIOMASS,
PYROLYSIS OIL AND CHAR

2.1 Abstract

Cottonwood and pine biomass, pyrolysis oil, and char were characterized and compared for similarities and differences that could lead to unique pyrolysis oil properties and/or aging effects. Biomass and char samples were analyzed by elemental analysis and DRIFTS. Pyrolysis oil pH, density, water content, viscosity and ATR-FTIR spectra were all collected and compared. Differences in pH, density and viscosity were observed when comparing the neat pine and cottonwood pyrolysis oils produced from various parts of the tree. In addition, when comparing pine vs. cottonwood feedstocks and comparing total pyrolysis oil, fractionated pyrolysis oil, and water condensate, the results suggested the incorporation of forestry residue (bark and/or leaves/needles) moderately affects the composition and properties of the pyrolysis oil.

2.2 Introduction

There is a growing desire to reduce petroleum fuel consumption and explore alternative energy sources, especially those that have less environmental impact [Boucher 2000]. One alternative to petroleum fuels is using biomass, a resource that has been used by mankind as an energy and food source for millennia and is estimated to contribute 10-

14 % of the world's energy [McKendry 2002]. Biomass is a general term that refers to organic material derived from plants, including trees, algae and crops [McKendry 2002].

Biomass can be characterized into four main categories: woody, aquatic, herbaceous/grasses and manures. Woody plants are typically slow growing plants consisting of tightly bound fibers and a hard external surface [McKendry 2002]. Biomass is comprised of cellulose, hemicelluloses, lignin and extractives [Czernik, 2004]. Cellulose is classified as a glucose polymer with repeating units of (1,4)-D-glucopyranose (polymer avg. molecular weight 100,000) where hemicelluloses is a polysaccharide mixture comprised of arabinose, galaturonic acids, glucose, mannose, methylglucuronic acid (polymer avg. molecular weight <30,000) [McKendry 2002]. Cellulose is typically 40-50 wt% of biomass and hemicelluloses of 20-40 wt% [McKendry 2002]. Lignin is a high molecular weight group of chemically related compounds estimated to be comprised of a three carbon chain bound to a six membered, phenyl-propane ring that can have 0 to 2 methoxyl substituents [McKendry 2002], but the specific chemical structure varies with feedstock [Oasmaa 2003]. Phenolics within hardwood lignin have two methoxy groups and softwood lignin typically only has one methoxy group. Inner bark is thought to be similar to wood lignin and outer bark is distinct from the inner bark, but the structure is unknown [Oasmaa 2003]. Extractives also vary with feedstock where softwood extractives (1-4 wt % of dry wood) consist of sterols, fatty acids, hydrocarbons, triterpenyl alcohols, triglycerides, fatty alcohols and resin acids and hardwood extractives (1-5 wt % of dry wood) are comprised of sterols and fatty acid esters [Oasmaa 2003]. Bark contains 4-5 times more extractives that contains high-molecular weight polyphenols and suberine. Needles contain 7-8 times more extractives than heart wood and have high hydroxy acid content [Oasmaa 2003]. Due to the presence of needles and

bark, forest residue is also high in extractives and ash with the actual amounts dependent on wood fraction, storage conditions, and the wood species [Oasmaa 2003].

One method to convert biomass into a fuel is thermal degradation in the absence of oxygen, or pyrolysis. Researchers in the 1980's discovered fast pyrolysis could increase the liquid yield by with high biomass heating rates and condensing the vapors quickly [Mohan 2006]. Compared to traditional fossil fuels, the use of biomass has the environmental advantage that the removal of CO₂ during the growth of the biomass offsets the CO₂ released during combustion [Mohan 2006]; therefore, pyrolyzing biomass does not contribute new CO₂ into the atmosphere [McKendry 2002]. Additional advantages include no SO_x emissions, 50% less NO_x emissions in a gas turbine as compared to diesel oil [Mohan 2006], estimated low production costs, and high thermal efficiency [Oasmaa 2003]. Considering the growing greenhouse effect and limited fossil fuel resources available, pyrolysis oil has the potential to serve as an environmentally-friendly supplement for traditional petroleum fuels in gas turbines, diesel engines, and boilers [Ba 2004].

The physical and chemical composition of pyrolysis oil is dependent on pyrolysis operating conditions [Ba 2004] and also feedstock due to partial decomposition of the biomass [Diebold 2000, Oasmaa 2003]. Pyrolysis oil is described as a dark brown, pungent smelling, free flowing, acidic liquid [Mullaney 2002] comprised of 400 or more organic compounds [Diebold 2000] including water, acids, phenols, alcohols, aldehydes, esters, ketones, sugars, furans, syngols, guaiacols [Diebold 2000], carbohydrates and lignin components [Oasmaa 2003]. These various compounds in pyrolysis oil are generally found in the following percentages: 20-25% water, 5-12% organic acids, 5-

10% non-polar hydrocarbons, 5-10% anhydrosugars and 10-25% of other oxygenated compounds 25-30% water insoluble pyrolytic lignin [Mullaney 2002].

Regardless of feedstock considerations pyrolysis oil has many barriers preventing direct application including metal corrosion, char particulates that can clog injectors or erode turbine blades, reactive components resulting in the formation of larger molecules leading to high viscosity [Oasmaa 2003], difficulties in storage, handling, transportation, and burning [Ba 2004]. Pyrolysis oil storage instability occurs at ambient or elevated temperatures and becomes a problem in preheating prior to combustion where particles grow in size within the recirculation systems due to polymerization reactions [Chaala 2004]. Alkali metals, sulfates and chlorides can accelerate oxidation within pyrolysis oil [Boucher 2000] and alkali metals—such as Na, K, Mg, P and Ca—can react with silica found in the ash resulting in a sticky, mobile liquid phase that can block airways in furnaces or boilers [McKendry 2002]. Lowering the ash content will reduce the alkali metals, improving the quality of the oil [Boucher 2000]. Certain feedstocks, including forest residue, barks, pine, straw, tropical hardwoods and eucalyptus, lead to two or more phases due to high levels of hydrocarbon-soluble extractives or alkali metals and typically the phases will not mix [Oasmaa 2001].

Water is soluble in pyrolysis oil up to 30 wt% and high molecular weight lignin compounds exist within a microemulsion [Oasmaa 2003]. When water exceeds 30 wt%, the solubility balance within the emulsion changes and the least hydrophilic lignin materials precipitate out creating a phase separation [Oasmaa 2003].

Pyrolysis oil properties are largely influenced by the type of biomass used. Biomass high in protein, such as alfalfa, grass cut for hay or bark, result in pyrolysis oil with higher nitrogen content when compared to biomass with low protein content (e.g.,

debarked wood or straw). In addition needles and bark elevated nitrogen content in forestry residue compared to clear wood mostly likely due to additional chlorophyll and proteins [Oasmaa 2003]. Generally, nitrogen is unfavorable during combustion as it can result in NO_x emissions [Diebold 2000]. Large amounts of bark and needles result in high concentrations of ash (0.1-0.2 wt %), alkali metals (400-1000 mg/kg), and nitrogen (0.1-0.4 wt %) compared to pine heart wood pyrolysis oil (50 mg/kg, 0.02-0.03 wt %, and <0.1 wt %, respectively) liquids [Oasmaa 2003]. Softwood bark contains larger amounts of lignin and extractives when compared to hardwood bark and therefore softwood bark residues are expected to have high amounts of water insoluble compounds [Ba 2004]. Also, Lignin in biomass results in phenolic compounds during pyrolysis and in softwoods tend to have one or more methoxy groups where [Diebold 2000].

Fast pyrolysis of woody biomass or forestry residue produces pyrolysis oil that are good candidates to substitute for petroleum fuels [Fratini 2006]. During lumber manufacturing and paper processes, bark is removed from center-cut wood and is therefore available as a biomass feedstock. When compared to pyrolysis oil derived from heart wood, forest residue pyrolysis oils have different properties that can be attributed to varying ratios of cellulose, hemicelluloses, lignin derived compounds and extractives [Ba 2004]. However, bark has been found to have different heat-transfer characteristics, moisture contents and typically contains higher amounts of lignin compared to heart wood [Mohan 2006]. Forestry residues (bark, shavings and sawdust) are used in North America and Europe to produce pyrolysis oil [Mohan 2006] and forest and agriculture residue biomass energy potential is estimated to be 30 EJ/yr compared to the world wide demand of 400 EJ/yr [McKendry 2002].

Forestry residue that contains substantial bark and needles leads to a lower liquid yield during pyrolysis (60-65 wt %) [Polagye] when compared to pine sawdust (68-75 wt%) [Oasmaa 2005] and have lower product quality that tends to phase separate into an extractives-rich phase (10-20%) and a second phase resembling heart wood pyrolysis oil [Polagye]. Typical properties for forest residue pyrolysis oil is 28 wt% water, has a pH of 3.0, viscosity of 15 cSt (40 °C), <0.05 wt% solids and lower heating value (LHV) 14 MJ/kg (21 MJ/kg on a dry basis) [Oasmaa 2003]. Forestry residue derived pyrolysis oil will phase separate immediately after condensation and the relative proportions of the top and bottom phases is dependent on the feedstock composition, freshness, moisture [Oasmaa 2003]. The bottom phase has similar chemical composition to that of pine pyrolysis oil with 2-6 wt% extractives, volatile acids (8-10 wt%), aldehydes and ketones (10- 15 wt%), 15-20 wt% water-insoluble (lignin derived components), 25-30 wt% water, and 30- 35 wt% sugar derivatives [Oasmaa 2003].

Bark derived pyrolysis oil is also comprised of two phases (top 16.3 wt% and bottom 83.7 wt%) that are physicochemically different and exhibit similar properties when compared to forest residue [Chaala 2004]. Softwood bark pyrolysis oils are also similar to forest residue derived oils due to higher concentrations of lignin and extractives in the bark [Ba 2004]. In addition, softwood bark contains larger amounts of lignin and extractives when compared to hardwood bark resulting in higher amounts of water-insoluble compounds [Ba 2004]. Softwood bark derived pyrolysis oil (70 wt% fir, 28 wt% white spruce, 2 wt% larch) is a good candidate for use in gas turbines with low values of Na, K and Ca (6, 2 and 13 ppm, respectively) and methanol insoluble materials (MIM) (0.34 wt%). Viscosity was reported close to gas turbine requirements at 5.3 cSt at

90 °C with 5.3 wt% water and a net heating value of (32 MJ/kg) thus requiring limited upgrading [Boucher 2000].

In the work presented here, two wood species—pine and cottonwood—are examined as biomass feedstock for pyrolysis oil. Heart wood, whole tree, bark and needle/leaf biomass is compared, along with the resultant pyrolysis oil and char, to determine how biomass composition affects the physical and chemical properties of the pyrolysis oil and subsequently its viability as a fuel.

2.3 Methods and Materials

Feedstock: Seven cottonwood and seven plantation grown Loblollypine (*Pinus taeda*) trees, all approximately 10 years old, were harvested. For each species, four trees were separated into heart wood, bark and leaf/needle biomass and three were separated into bole wood (bark, limbs and wood) and leaf/needle. All biomass was dried to 10-15% moisture content (MC) in an oven (Despatch V series VREZ-19-ZE). Heart wood and bole wood biomass was then chipped (separately) to 1-2 inch chips (Carthage Machine Inc., Model 39 chipper, 1470 rpm). Leaves/needles were added to the bole wood the total ground (Bauer Bro. Co., 25 Hp, 1465 rpm), and screened resulting in particles between 4 to 6 mm (Universal Vibrating Screener, Type S #1354). Heart wood, bark and leaf/needle biomass was also ground and screened. Prior to pyrolysis all biomass was dried to 1-2 % MC and only one bath was produced for each biomass type.

Pyrolysis: All pyrolysis oil samples were produced by the MSU Forest Products Laboratory using an auger pyrolysis reactor operated under vacuum at 400 °C, an average flow rate of 15-20 L/min, and 25 °C (± 1 °C) water condensers. Three types of samples were collected: total and fractionated oil and water condensate where the total oil

includes all of the condensers, fractionates excludes the water condensate; the product of one of the condensers with high water content. Pyrolysis oil samples were at $\sim 5^{\circ}\text{C}$ within 1 hr of production minimizing aging prior to experiments. Produced pyrolysis oils were dark in color with a pungent smell; fractionated oils were thicker, water condensates similar to water and most total oils consisted of two phases with a lower viscosity top phase (higher water content) and a more viscous bottom phase (lower water content and opaque). All cottonwood and pine samples were produced within several days each and pyrolysis oils used in this study were each taken from a 1 L production batch.

pH, Density and Water Content: pH of the pyrolysis oil was measured (Accument Basic pH meter) with a five point phosphate buffer solution (pH 2, 4, 7, 10 and 12) calibration. Density was measured by weighing known volumes of pyrolysis oil. Karl Fischer titration (Barnstead International Aquametry II Apparatus) was use to measure water content following ASTM E 203-01 with Hydranal 2 or 2E titrant and chloroform-methanol (CM) solvent. A minimum of three measurements were collected and to obtain average values and 95 % confidence intervals for pH, water content and density.

Viscosity: A TA Instruments AR 1500x rheometer and 60 mm aluminum parallel plate geometry was used in step-flow shear tests with sample volumes ranging from 500 to 1200 μm . Sample volume was maximized in all runs but varied somewhat based on sample viscosity and gap distance. A Peltier plate was used to hold the temperature at 40°C during the experiment. The system was allowed to equilibrate for 2 minutes and then viscosity data was collected over the shear rate range from 0.1 to 1000 Hz (1/s). A minimum of 10 data points were averaged over a plateau region that was observed at higher shear rates (10-1000 1/s) to obtain average viscosity values and 95% confidence intervals.

FTIR Spectroscopy: Biomass and char spectra were examined using diffuse reflectance infrared Fourier transform spectroscopy (DRIFTS) after preparation with 95% KBr powder (liquid nitrogen cooled MCT-A* detector, 4 cm⁻¹ resolution, 256 scans). Attenuated total reflectance Fourier transform infrared (ATR-FTIR) spectra were collected for neat pyrolysis oil samples on a ZnSe 60-degree ATR crystal (liquid nitrogen cooled MCT-A* detector, 4 cm⁻¹ resolution, 256 scans). All ATR spectra were ATR corrected using Thermo Electron OMNIC software.

2.4 Results and Discussion

2.4.1 Biomass

Plantation grown cottonwood trees were harvested and separated into clear wood (lumber), bark and leaf biomass. Additional trees were collected for ‘whole tree’ biomass where the clear wood, bark and leaves were dried and weight separately and recombined prior to pyrolysis; Table 2.1 presents the relative composition of each individual component (by weight) that comprised the native tree. As measured, clear wood (56.5 wt%) is the major component of the cottonwood trees and is followed by bark, stems, and leaves at 18.9, 8.5, and 3.4 wt%, respectively.

Table 2.1 Cottonwood biomass composition of whole tree on a dry basis

Component	Weight %
clear wood	56.5
bark	18.9
stems	8.5
leaves	3.4

Loblolly plantation pine trees were also harvested to collect whole tree, clear wood, bark, and needle biomass. The whole tree composition is displayed in Table 2.2 where clear wood is 65.6 wt%, stems are 17.6 wt%, and bark and needles are approximately 8.0 wt% each. Pine clear wood makes up a larger weight percent (65.6 wt%) as compared to cottonwood (56.5 wt%) and the stems have a much larger weight percent of 17.6 wt% compared to the 8.50 wt% in cottonwood. High concentrations of bark, leaves and stems can result in lower yields, phase separation and high ash content as in forestry residue and can affect aging reactions.

Table 2.2 Pine biomass composition of whole tree on a dry basis

Component	Weight %
clear wood	65.6
bark	8.8
stems	17.6
needles	8.0

2.4.2 Pyrolysis

Pyrolysis yields for both the cottonwood and pine biomass varied greatly between tree components and between pine and cottonwood. Pyrolysis oil and char yields are presented in Tables 2.3 and 2.4 for cottonwood and pine, respectively. For both feedstocks, the clear wood has the largest pyrolysis oil yield, followed by the whole tree biomass. The bark for the cottonwood biomass is the 37.6 wt% followed by leaves with 26.7 wt%. Pine needles had a larger yield of 51 wt% followed by pine bark with 40 wt%.

In addition to the pyrolysis oil yields the barks, leaves and needle char yields are much larger when compared to the clear wood and whole tree char yields.

Table 2.3 Yields for pyrolysis oil and char produced from cottonwood tree biomass, as a whole tree and individual tree components.

Biomass	Pyrolysis oil	Char
Whole Tree	49.9%	23.4%
Clear Wood	53.3%	24.7%
Bark	37.6%	33.9%
Leaves	26.7%	51.8%

Table 2.4 Yields for pyrolysis oil and char as produced from pine tree biomass, as a whole tree and individual tree components.

Biomass	Pyrolysis oil	Char
Whole Tree	56.0%	26.0%
Clear Wood	59.0%	23.0%
Bark	40.0%	40.0%
Needles	51.0%	48.0%

2.4.3 Elemental Analysis

Elemental analysis of the biomass (Table 2.5) shows the presence of nitrogen in all of the biomass samples prior to pyrolysis. Slightly higher carbon and lower oxygen contents are seen for the clear wood and whole tree biomass versus the bark and leaves biomass. (Note: The remainder percentage (R%) is assumed to be oxygen.) When comparing the elemental concentrations for pyrolysis oil (Table 2.6), the water

condensates (WC) have the lowest carbon content. Fractionated (F) pyrolysis oil samples (without the water condensate) have the highest carbon content and the total (T) pyrolysis oils have the highest oxygen content. It is also noteworthy that all of the fractionated pyrolysis oils, the cottonwood leaves whole pyrolysis oil, and cottonwood clear wood whole pyrolysis oil have some low levels of nitrogen.

Table 2.5 Elemental analysis results (C, H, N only) showing the atomic percentages of carbon (C), hydrogen (H), nitrogen (N) and remainder (R) for cottonwood biomass: clear wood, whole tree, leaves, and bark.

Sample ID	Sample Description	C%	H%	N%	R%
CWTB	Cottonwood Whole Tree	44.49	5.75	1.29	48.465
CCWB	Cottonwood Clear Wood	44.885	5.72	0.955	48.435
CBB	Cottonwood Bark	43.27	5.665	1.57	49.49
CLB	Cottonwood Leaves	41.47	5.175	2.065	51.29

Table 2.6 Elemental analysis results (C, H, N only) for cottonwood pyrolysis oil collected from different feedstock and condenser combinations (as indicated by the numbers in parentheses). Percentages of carbon (C), hydrogen (H), nitrogen (N), and the remainder (R) are shown.

Sample ID	Sample Description	Elemental Analysis			
		C%	H%	N%	R%
CCWF	Cottonwood Clear wood Fractionated	49.1	7.2	0.5	43.1
CCWT	Cottonwood Clear wood Total	36.1	7.8	0.1	56.0
CCW-WC	Cottonwood Clear wood Water Condensate	17.9	2.0	0.0	80.1
CWTF	Cottonwood Whole tree Fractionated	51.7	7.1	0.5	40.7
CWTT	Cottonwood Whole tree Total	32.5	5.2	0.0	62.3
CWT-WC	Cottonwood Whole tree Water Condensate	19.8	10.0	0.0	70.2
CBF	Cottonwood Bark Fractionated	46.4	5.1	0.4	48.0
CBT	Cottonwood Bark Total	20.3	3.7	0.0	76.0
CB-WC	Cottonwood Bark Water Condensate	8.0	0.5	0.0	91.6
CLF	Cottonwood Leaves Fractionated	33.9	8.6	1.2	56.4
CLT	Cottonwood Leaves Total	17.3	9.7	0.3	72.7
CL-WC	Cottonwood Leaves Water Condensate	10.9	7.0	0.0	82.1

2.4.4 Biomass and Char Comparison Using DRIFTS

DRIFTS spectra for the four cottonwood biomasses are presented in Figure 2.1 were the peaks indicating chemical differences between the biomass types are identified. There are three regions where the biomass spectra vary, C-H stretching ($3030-2790\text{ cm}^{-1}$), the H-C=O aldehyde peak (2728 cm^{-1}) and the carbonyl/aromatic region ($1800-1550\text{ cm}^{-1}$). In the C-H stretch region there is a small change in the bark peak and a much larger

change in the leaf peak where a broad peak appears to decrease revealing two sharp peaks at 2918 and 2849 cm^{-1} identified as asymmetrical and symmetrical stretching of methylene groups respectively [Silverstein]. All of the spectra contain aromatic combination peaks due to 6 member rings [Pretsch, Silverstein] and a peak due to the Fermi resonance of an aldehyde [Pretsch] but the aromatic combinations are less defined in the leaf biomass. The largest difference in the spectra is in the carbonyl/aromatic region where the whole tree and clear wood biomass have a dominant aromatic C=C peak at $\sim 1620 \text{ cm}^{-1}$. Bark and leaf biomass have a more dominant carbonyl peak which could be a ketone, aldehyde, carboxylic acid or ester [Silverstein, Pretsch]. These differences suggest that the whole tree is dominated by the clear wood and that the bark and leaves have similar chemical compounds. In addition, it also demonstrated that there is a compositional difference in the biomass of leaves and bark compared to clear wood.

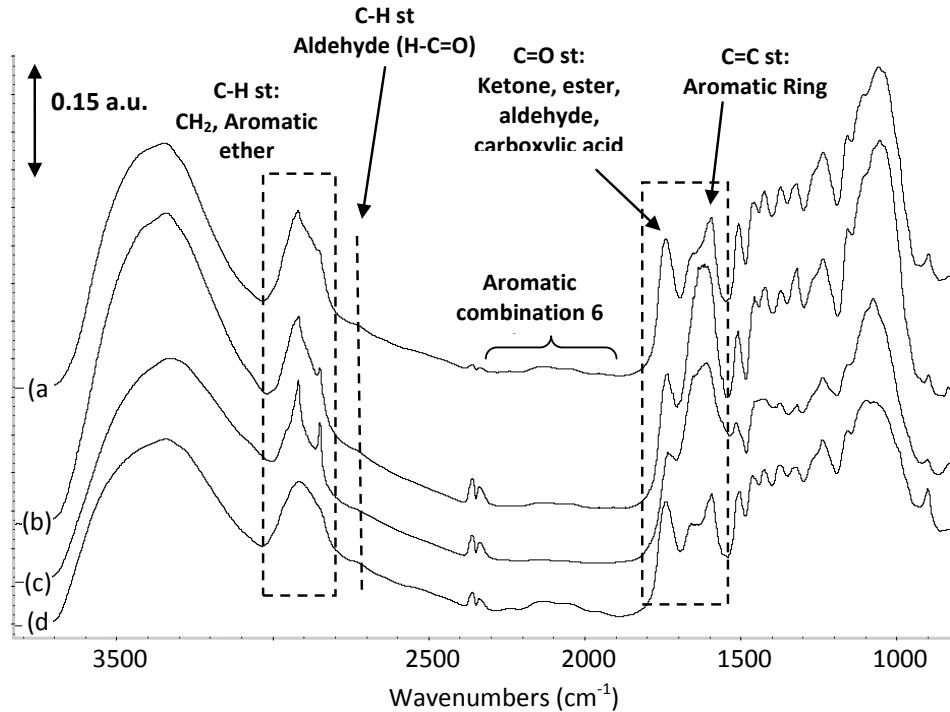


Figure 2.1 DRIFTS spectra collected for cottonwood biomass whole tree (a), bark (b), leaves (c), and clear wood (d).

Pine biomass DRIFTS spectra (Figure 2.2) were also collected and compared to find the same peaks of interest as identified in the cottonwood biomass. When compared to the cottonwood biomass the C-H stretching region remains very similar to the whole tree and clear wood spectra without strong methylene stretching. This indicates a difference in the pine and cottonwood barks and leaf/needle compositions. As in the cottonwood biomass, the aldehyde peak and aromatic combination peaks appear to be similar in all of the spectra. When examining the carbonyl/aromatic region there are also strong difference within the pine biomass spectra. The aromatic peak dominates the bark spectra but in the needle spectra there is a moderate aromatic peak and no carbonyl peak. In contrast pine clear wood has only a moderate carbonyl peak. The whole tree biomass has both peaks which indicates that both the clear wood and bark composition contribute to the composition.

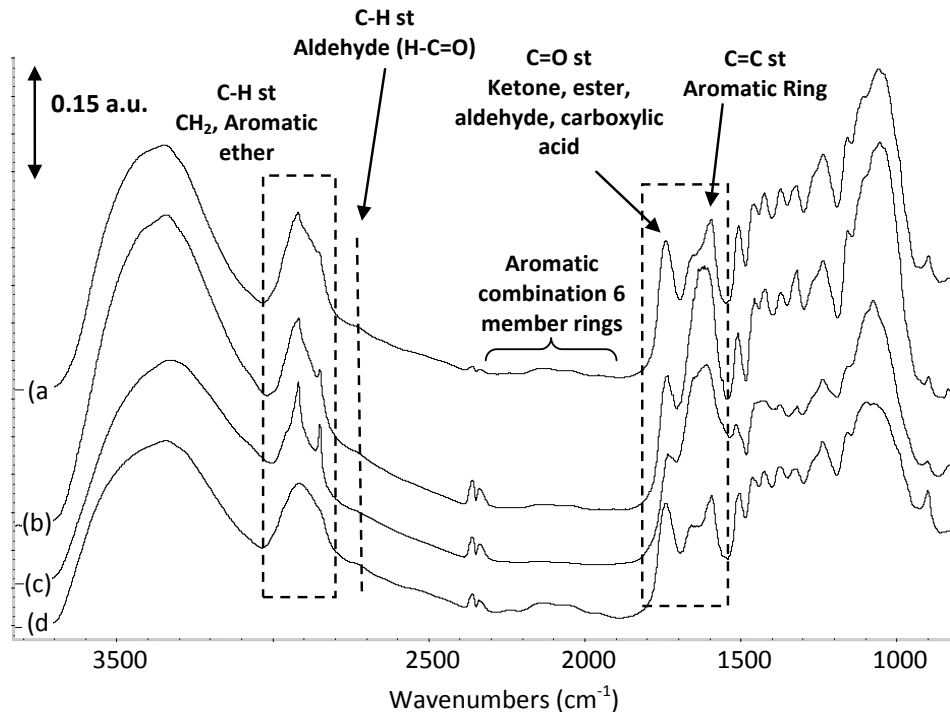


Figure 2.2 DRIFTS spectra collected for pine biomass whole tree (a), needles (b), bark (c), and clear wood (d).

DRIFT spectra for cottonwood char collected during the production of the cottonwood pyrolysis oils is presented in Figure 2.3. When compared to the biomass cottonwood char has a much different spectra with a smaller O-H stretch peak (3800-3000 cm^{-1}) which reveals smaller peaks within this regions including the C-H stretch for aromatic and cyclic compounds in addition to a peak at 3550 cm^{-1} identified as hydrogen bonded O-H stretch [Pretsch, Nakanishi, Silverstein].

Also peaks for the C-H aromatic/cyclic stretch and the O-H stretch—most likely due to free OH—are present in the hydroxyl region of the spectra and is most visible in the clear wood and whole tree spectra. Also, the carbonyl peak is nearly nonexistent. A new peak located at 1320 cm^{-1} was identified as an alkane C-H twist/wag, alkene C-H bend, or a C-O stretch in carboxylic acids [Nakanishi, Silverstein]. In addition, the leaves spectrum has a larger peak identified as a C-O or C-O-C stretch in an aromatic,

alcohol, ether or ester group and may indicate that the leaves were not completely pyrolyzed in the reactor.

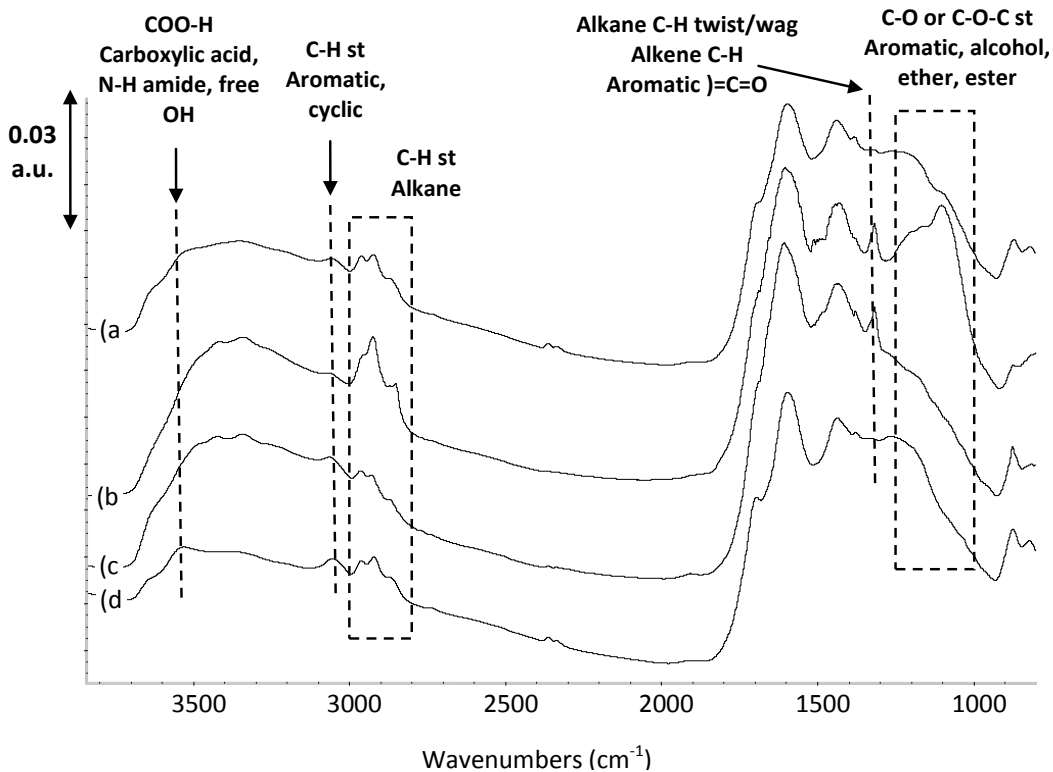


Figure 2.3 DRIFTS spectra collected for cottonwood char whole tree (a), leaves (b), bark (c) and clear wood (d).

Figure 2.4 displays the DRIFTS spectra collected for the pine char produced as a byproduct during the pine pyrolysis. The pine char has the similar peaks when compared to the cottonwood char in the hydroxyl region including the free OH peak, aromatic C-H stretch and the alkane C-H stretch. The fingerprint region has a large difference when compared to the cottonwood pyrolysis oil. The aromatic ring C=C stretch is very strong compared to the carbonyl peak and is less dominant in the clear wood char when compared to the needles, whole tree and bark.

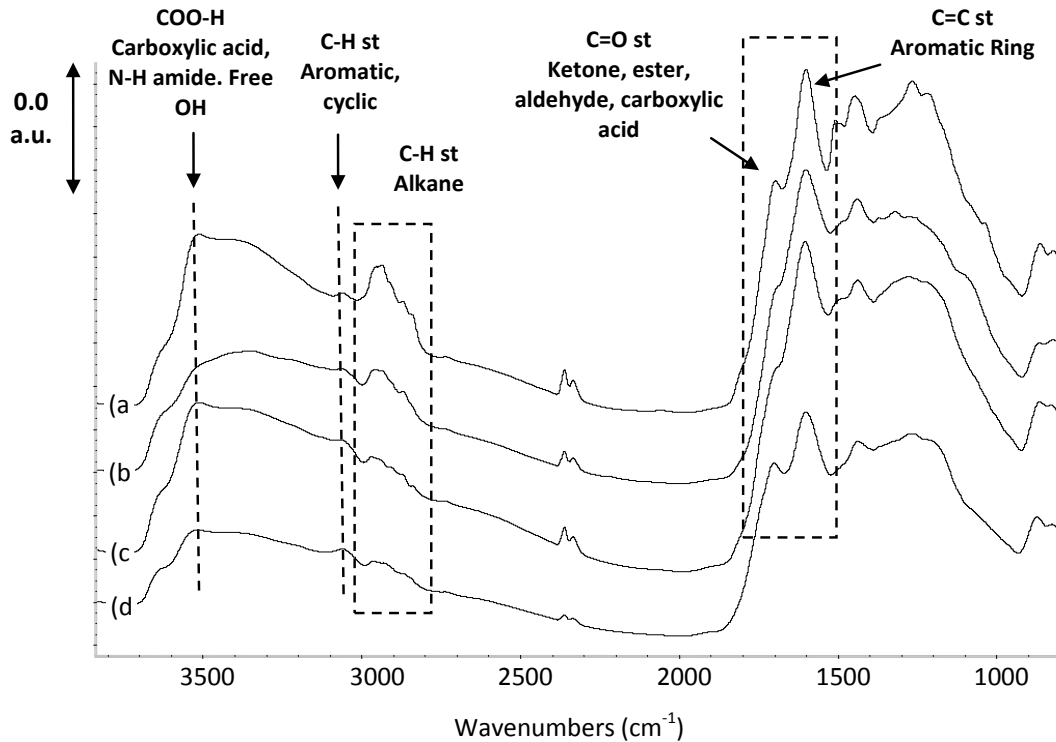


Figure 2.4 DRIFTS spectra collected for pine char whole tree (a), needles (b), bark (c) and clear wood (d).

2.4.5 Solids Removed by Crude Filtration

Solids removed by crude filtration were collected, washed and dried and images collected for the various particulates. Heart wood solids for cottonwood (Figure 2.5, a) appear to be mostly char particulates entrained during pyrolysis where cottonwood whole tree (b) and bark (c) have brown biomass like particles. Cottonwood leaves solids (d) have the most unique composition with large, flat and tan particles with appear to be unpyrolyzed leaves. In contrast the pine filtered solids (Figure 2.6) all appear to be mostly char particulates with some biomass material in the bark solids (c).

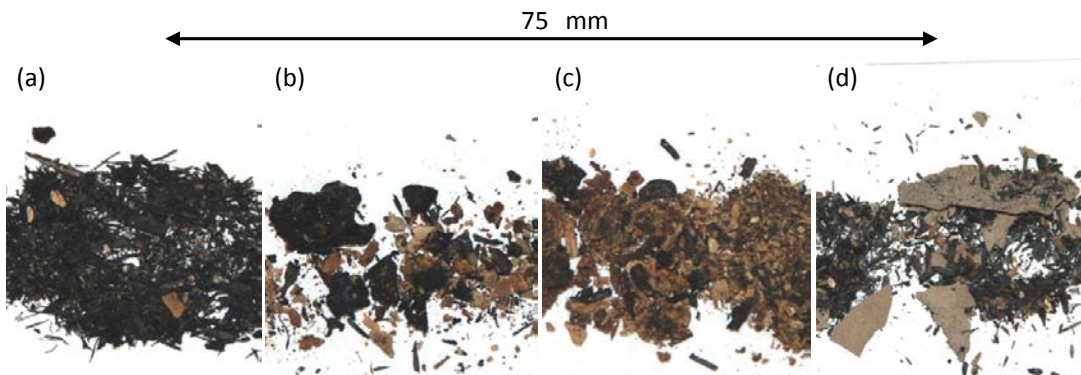


Figure 2.5 Images of cottonwood solids removed by crude filtration, cleaned and dried: clear wood (a), whole tree (b), bark (c), and leaves (d).

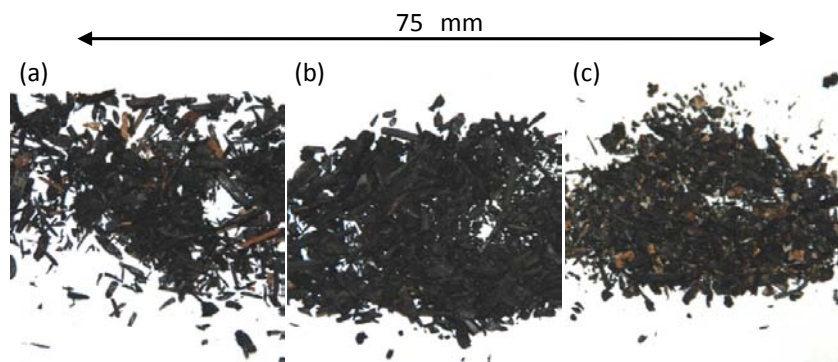


Figure 2.6 Images of pine solids removed by crude filtration, cleaned and dried: pine heart wood (a), whole tree (b), and bark (c).

2.4.6 pH

In Figure 2.7, measured average pH values for the neat cottonwood pyrolysis oil samples are displayed with 95% confidence interval error bars. Overall, all of the cottonwood pyrolysis oil and pyrolysis oil water condensate fractions are acidic with nominal pH values of 3. For the pyrolysis oil produced from clear wood and leaves, there is little to no difference between the three pyrolysis oil compositions (total, fractionated, and condensate). The condensate of the bark and whole tree (which also contains bark) pyrolysis oils showed lower pH values of 2.51 and 2.87, respectively.

For the pine whole tree there is a decrease in the pH of the water condensate from 2.97 in total and fractionated to 2.87 and for the bark the water condensate has a significantly lower pH of 2.51 compared to all of the other measurements. The whole bark pyrolysis oil also has a slight decrease in pH compared to the fractionated pyrolysis oil. It was expected that all of the water condensates would have lower pH measurements due to the large amount of organic acids thought to be present. This suggests that the bark water fraction may have a higher concentration of organic acids present which would also effect the whole tree water condensate (whole tree is comprised of clear wood, leaves and bark). Previous research have shown that bark has higher concentrations of high-molecular weight polyphenols and suberin than clear wood.¹

Pine biomass derived pyrolysis oil (Figure 2.7, right) measured pH are displayed with 95% confidence interval error bars and when compared to the cottonwood pyrolysis oil pH measurements the measurements have a larger variability ranging 2.3 to 3.3 rather than 2.5 to 3.1 in cottonwood. In addition the needle derived samples have much larger pH values and the pine bark oil samples have lower pH values compared to cottonwood pyrolysis oils. The condensates for pine clear wood and bark pyrolysis oils have a lower pH than their corresponding fractionated pyrolysis oils. Interestingly, condensates for the whole tree and needles pyrolysis oil samples have the highest pH values for the different compositions tested. In general, pyrolysis oil derived from needles has higher pH values and pyrolysis oil derived from bark has lower pH values. This provides support that the chemical composition of bark differs significantly, perhaps due to a higher concentration of organic acids, from the remainder of the tree and so the inclusion of bark in the feedstock for pyrolysis oil results in a pyrolysis oil with a lower pH.

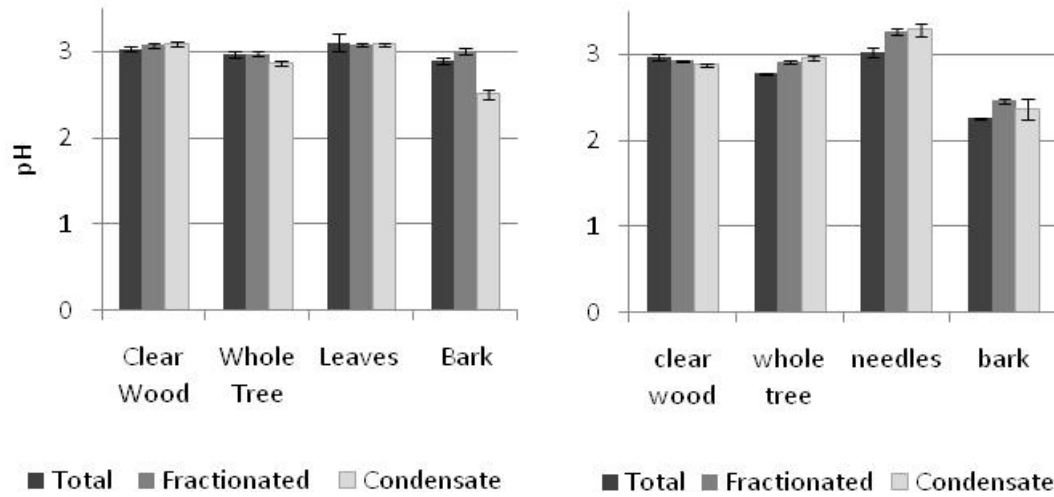


Figure 2.7 pH measurements for pyrolysis oil and pyrolysis oil fractions produced from cottonwood (left) and pine (right) biomass. Error bars represent 95% confidence intervals.

2.4.7 Density

In Figure 2.8 (left) the calculated density for the cottonwood-derived pyrolysis oil is presented with 95% confidence interval error bars. Considering the variability in these measurements, all of the measured densities are at or below 1.5 g/mL. Error bars for the whole tree pyrolysis oil compositions are larger when compared to the pyrolysis oils from other feedstocks and could indicate a greater variance in the biomass composition and subsequently the pyrolysis oil composition or perhaps simply a larger experimental error for this set of measurements. All of the data were collected by the same researcher using the same method on the same day, so there is no reason to think there is higher experimental variability with one of the data sets. Likely the variation is due to heterogeneity in the biomass/pyrolysis oil composition. With the exception of the total whole tree pyrolysis oil composition, measured pine pyrolysis oil densities range from 1.3 to 1.4 g/mL. While there does not appear to be a consistent trend in the densities of

the total and fractionated pyrolysis oils, the water condensate has a density the same or lower than the total pyrolysis oil samples for all of the cottonwood feedstocks tested.

In Figure 2.8 (right) the calculated density for the pine-derived pyrolysis oil is presented with 95% confidence intervals as error bars. The data for the bark fractionated and total pyrolysis oils are not included due to difficulty collecting the data, but will be collected for future comparison. All of the calculated densities are below 1.5 g/mL and when compared to the cottonwood pyrolysis oil densities appear to have slightly higher densities. The water condensate has the lowest density for the clear wood, whole tree and needle-derived pyrolysis oils. In addition the fractionated pyrolysis oils have densities equal to or greater than the total pyrolysis oils for the clear wood, whole tree and needle pyrolysis oils.

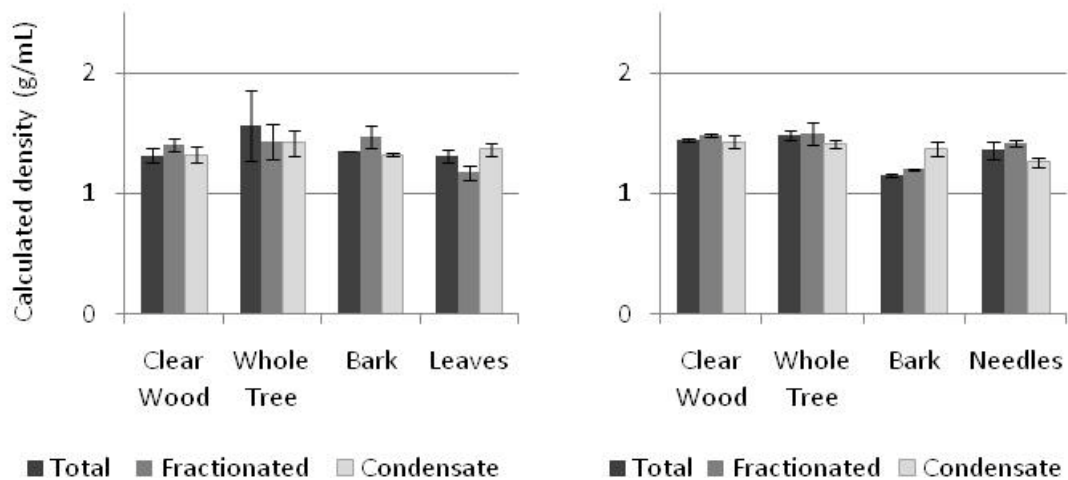


Figure 2.8 Calculated densities for neat (non-aged) pyrolysis oil and pyrolysis oil fractions produced from cottonwood (left) and pine (right) biomass. Error bars represent 95% confidence intervals.

2.4.8 Water Content

Figure 2.9 presents the water content data collected for pine-derived pyrolysis oils. As expected, water condensate had the highest water content ranging from 50-75 wt

% water. Correspondingly, the fractionated samples have the lowest water contents (18-36 wt %) and the total oil had moderate values ranging from 30 to ~50 wt % water. Water contents were also compared based on feedstock composition to determine if the presence of bark and/or leaves-needles impacted water content. Water content values for total pyrolysis oil, fractionated pyrolysis oil, and water condensate were lowest for the heart wood and highest for the bark feedstock. Total and fractionated oil samples also showed elevated water content for the whole tree versus heart wood feedstocks. Higher water contents in these pyrolysis oil samples derived from whole tree, bark and needles indicate that the inclusion of the bark and/or needles in the feedstock results in a higher water content in the final product. Compared to bark pyrolysis oils, needle-derived pyrolysis oils have lower water contents, a notable feature of which the cause is unknown.

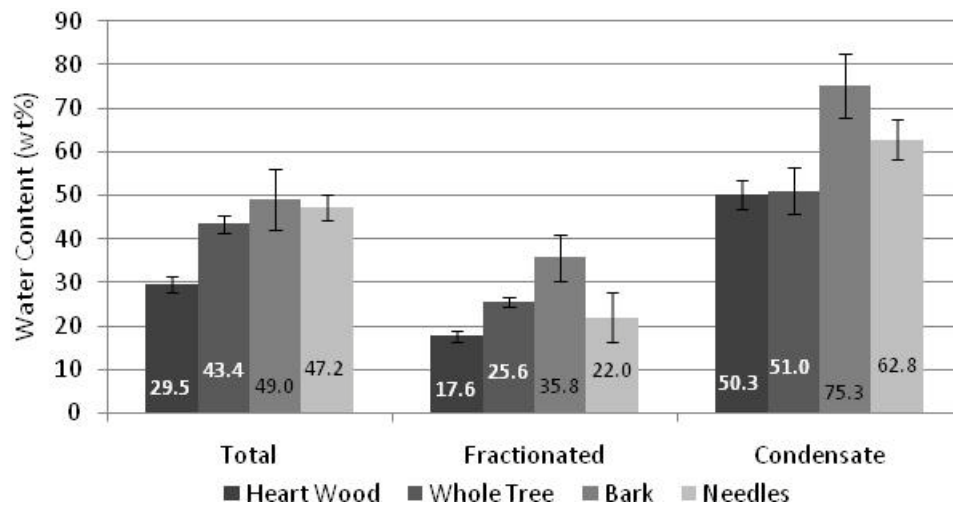


Figure 2.9 Measured water content for pine-derived pyrolysis oil, as determined by Karl Fischer titration. Average values are shown as data labels on each column and error bars represent 95% confidence intervals.

Water content data is presented for the cottonwood-derived oils and water condensate in Figure 2.10. Total pyrolysis oil and water condensate have distinct trends with increased water content as non- heart wood content is added. Leaves fractionated oil also has the largest water content but the whole tree and bark fractionated oils have slightly smaller water content when compared to the heart wood samples. Again, as expected, the cottonwood water condensate had the highest water content (48-75 wt %), followed by the total pyrolysis oil (28-60 wt %), and then the fractionated oils (17-34 wt %). In contrast to the results for pine-derived pyrolysis oil, leaves-derived cottonwood pyrolysis oil showed increased water content versus bark-derived pyrolysis oil. This strongly suggests compositional differences between the pine needles and the cottonwood leaves that result in higher water contents in pyrolysis oil produced from leaves.

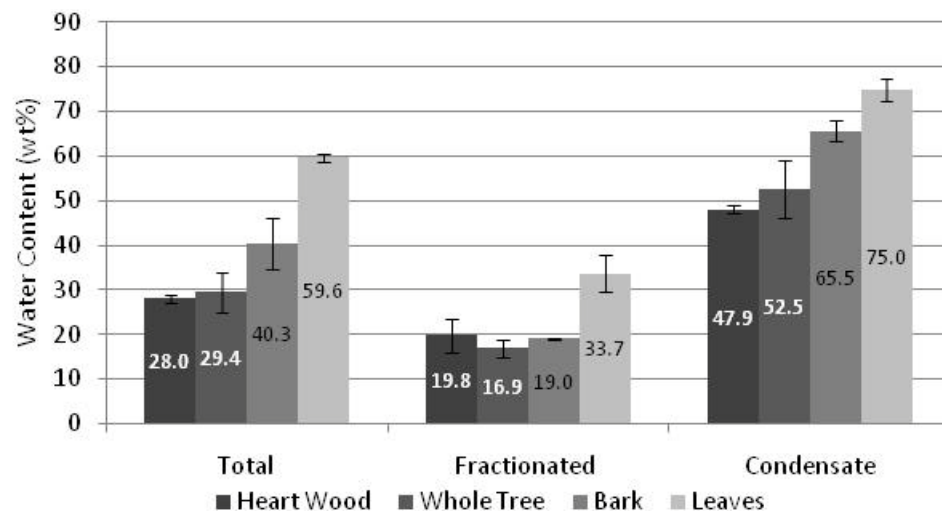


Figure 2.10 Water content for cottonwood-derived pyrolysis oils, as determined by Karl Fischer titration. Average values are shown as data labels on each column and error bars represent 95% confidence intervals.

2.4.9 Rheology

Viscosity measurements were collected by rheology where the data was averaged over the plateau region that occurred at higher shear rates (100-1000 1/s). Figure 2.11 presented several pine pyrolysis oil and water condensate rheology traces showing the large range of viscosity values and trace shapes (Newtonian and nonNewtonian). The plateau region is located to the right of the dashed line.

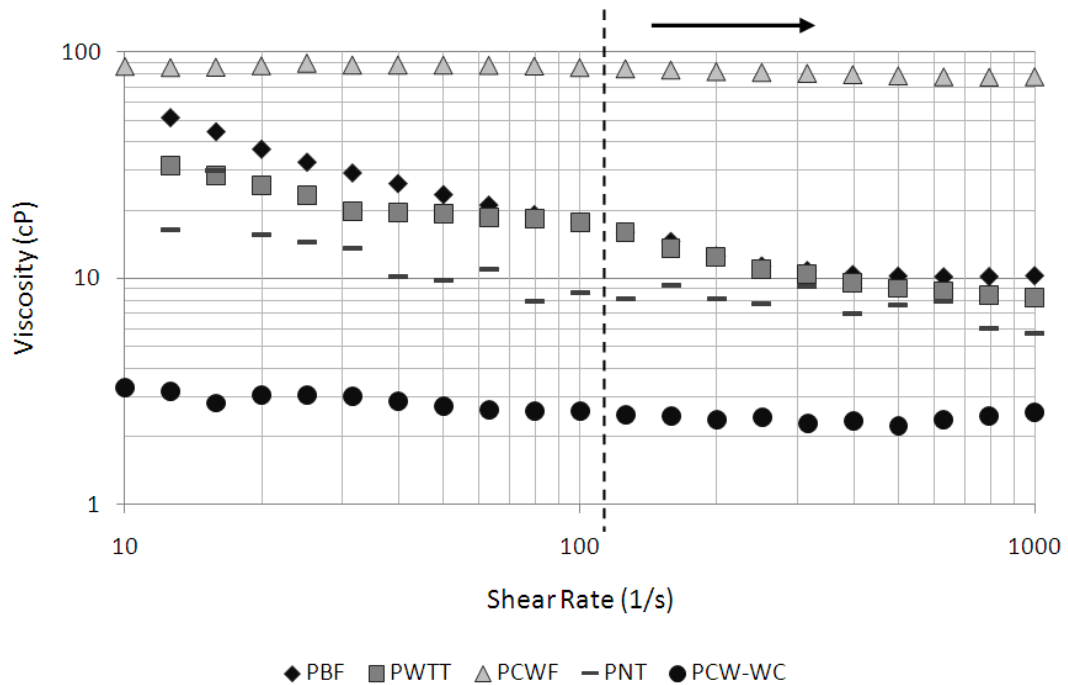


Figure 2.11 Rheology traces for pine bark fractionated (PNF), pine whole tree total (PWTT), pine clear wood fractionated (PCWF), pine needle total (PNT) and pine clear wood water condensate (PCW-WC).

Viscosity measurements for the non-aged pyrolysis oil compositions (total, fractionated, and water condensate) derived from cottonwood clear wood, whole tree, bark, and leaves are presented in Figure 2.12. Comparing the 95 % confidence interval error bars, the error in the viscosity measurements are reasonable considering the large

amount of particles present in the pyrolysis oil as well as the phase separation that occurs in many of the samples.

Cottonwood leaves fractionated oil has a very large 95% error bars due to a large amount of solids that had an affinity to float on the surface in addition to phase separation. Fractionated pyrolysis oils have higher viscosities versus total pyrolysis oil and water condensate. In addition the water condensate also has the lowest in comparison of the fractionated and total oils. Total pyrolysis oil, produced from leaves, and water condensate, produced from leaves and bark, have very low viscosity when compared to the clear wood, whole tree and bark pyrolysis oils.

For bark, clear wood, and whole tree samples, the total pyrolysis oil had measured viscosities in the range of 22.2-245 cP and the water condensate ranged from 1.31-41.4 cP. Fractionated pyrolysis oil showed tremendously different viscosities depending upon the feedstock with bark pyrolysis oil having the largest viscosity followed by whole tree and then clear wood. For the whole tree pyrolysis oil compositions, the significantly larger viscosity for the fractionated sample, similar to the behavior of the bark samples, is in line with the presence of the bark in the feedstock and has significant effect on pyrolysis oil properties as evidenced by the viscosity, pH, and density data.

Pine needle pyrolysis oils and water condensate have very different properties when compared to all the other samples where the fractionated oil viscosity is the largest of the pine pyrolysis oil and the second largest overall. In addition the pine needle water condensate has a 216 % larger viscosity than the total pine needle pyrolysis oil and a viscosity larger than all the water condensate and total pyrolysis oil samples. This larger difference is largely due to a high concentration of solids in all of the samples, some of which appear to be pine needle shape biomass and/or char and water condensate visually

appears more similar to the other total pyrolysis oils with a top and bottom phase and a more opaque top phase rather than translucent.

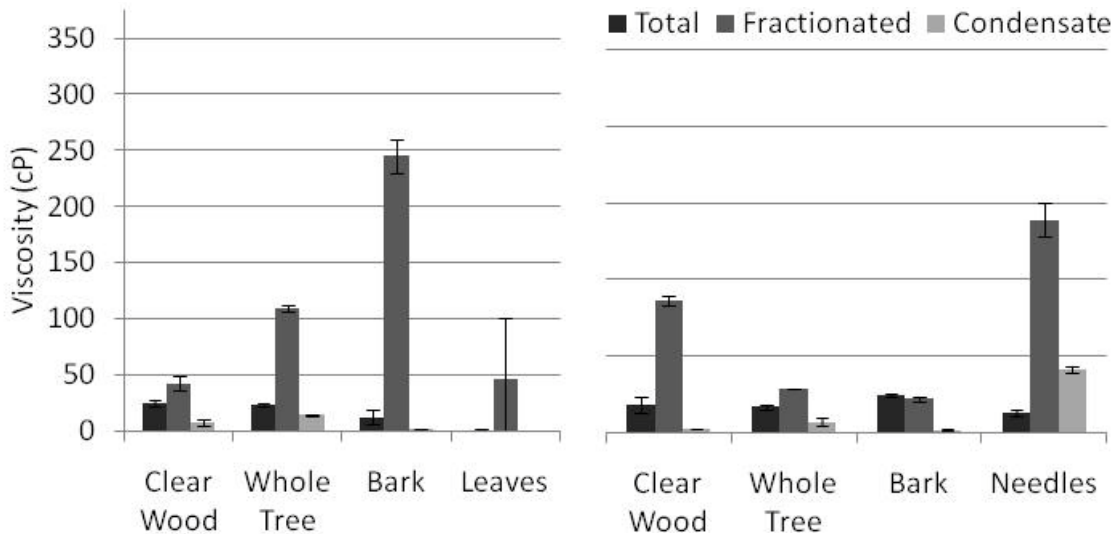


Figure 2.12 Average viscosity measurements (as determined by rheology) for neat (non-aged) cottonwood (left) and pine (right) pyrolysis oil comparing bark, clear wood, leaves/needles and whole tree oil including total, fractionated and condensate produced from cottonwood. Error bars represent 95 % confidence intervals.

2.4.10 ATR-FTIR Spectra- need to insert the spectra for the pyrolysis oil and compare

2.4.10.1 Cottonwood Pyrolysis Oil

Figures 2.13 to 2.16 display the ATR spectra for neat cottonwood total and fractionated pyrolysis oils in addition to the corresponding water condensates. In general all of the spectra are similar with hydroxyl peaks ($3700-3000\text{ cm}^{-1}$; O-H st), C-H st ($3000-2800\text{ cm}^{-1}$), carbonyl peak ($\sim 1700\text{ cm}^{-1}$; C=O st) coupled with aromatic/ skeletal stretching peaks (~ 1600 and $\sim 1515\text{ cm}^{-1}$; C=C st) and peaks at ~ 1268 identified as an aromatic ether (=C-C-O st)[Pretsch, Nakanishi, Silverstein, Kuptsov] or a carboxylic

acid (O-H bend and C-O st) [Nakanishi, Silverstein] and $\sim 1051\text{ cm}^{-1}$ due to primary alcohol (C-O st) [Kuptsov, Silverstein, Nakanishi].

The two peaks were the most variance occurs between pyrolysis oil types and biomasses are the C-H peaks and the carbonyl/ aromatic region ($1800\text{-}1550\text{ cm}^{-1}$). For all of the water condensates and top phases (when there was phase separation) the C-H peaks were small if present at all. This indicates that there is much less C-H bonding which could indicate substituted compounds and/or double bonding.

In the carbonyl region there is a larger variance in both the strength of the two peaks in addition to the shape of the region in general. Fractionated pyrolysis oils have a dominant peak at $\sim 1710\text{ cm}^{-1}$ which could be due to a C=O stretch in an aliphatic/cyclic ketone and/or a carboxylic acid dimer [Silverstein, Pretsch, Nakanishi]. With the presence of the water condensate either separately or in the total pyrolysis oil this peak diminishes to be approximately equal to the aromatic peak at $\sim 1600\text{ cm}^{-1}$ (C=C in aromatic hydrocarbons and/or skeletal stretching) [Silverstein, Pretsch]. Outside these differences the only spectrum that stands apart is the water cottonwood clear wood condensate bottom phase (Figure 2.13 c) that has two stronger peaks at 1114 and 1034 cm^{-1} . A peak at 1140 cm^{-1} can be due to either a secondary alcohol C-O stretch [Pretsch, Nakanishi, Silverstein] and/or aliphatic or ring ether C-O-C stretch [Nakanishi, Silverstein] and the peak at 1034 cm^{-1} is due to primary alcohol. In addition the water condensate and top phases have smaller peaks in the fingerprint region ($1800\text{-}900\text{ cm}^{-1}$) that could be due to dilution by high water content.

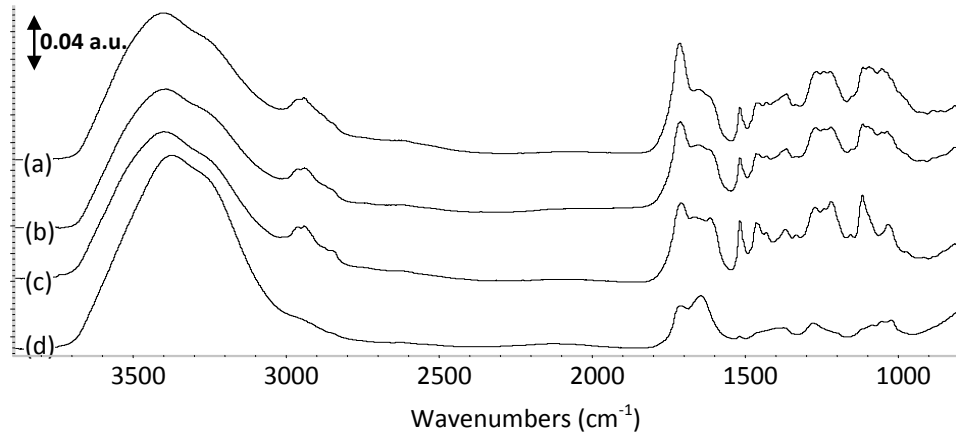


Figure 2.13 Cottonwood clear wood fractionated (a) and total (b) pyrolysis oil and water condensate top bottom (c) and water condensate top phase (d) ATR spectra (common scale, ATR corrected).

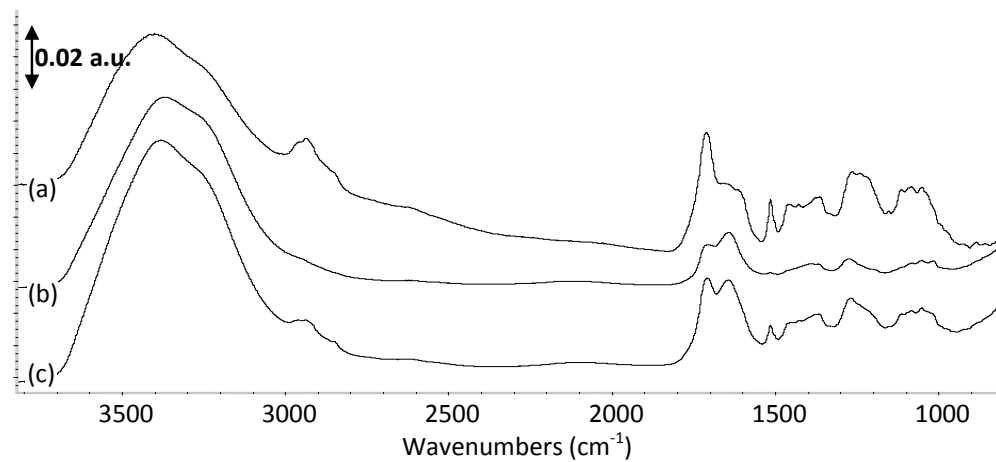


Figure 2.14 Cottonwood whole tree fractionated (a) and total top (c) and bottom (b) phases pyrolysis oil and water condensate (d) ATR spectra.

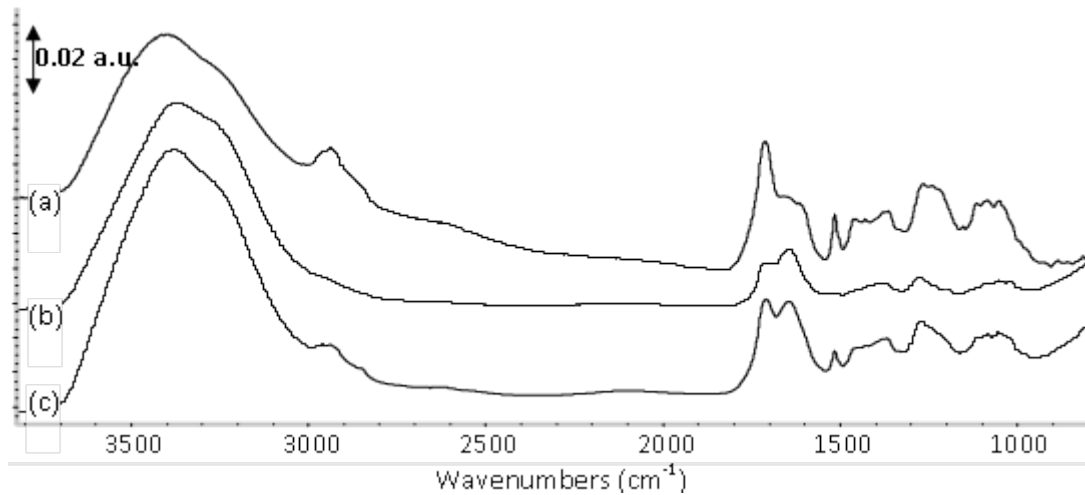


Figure 2.15 Cottonwood bark fractionated (a) and total (c) pyrolysis oil and water condensate (b) ATR spectra.

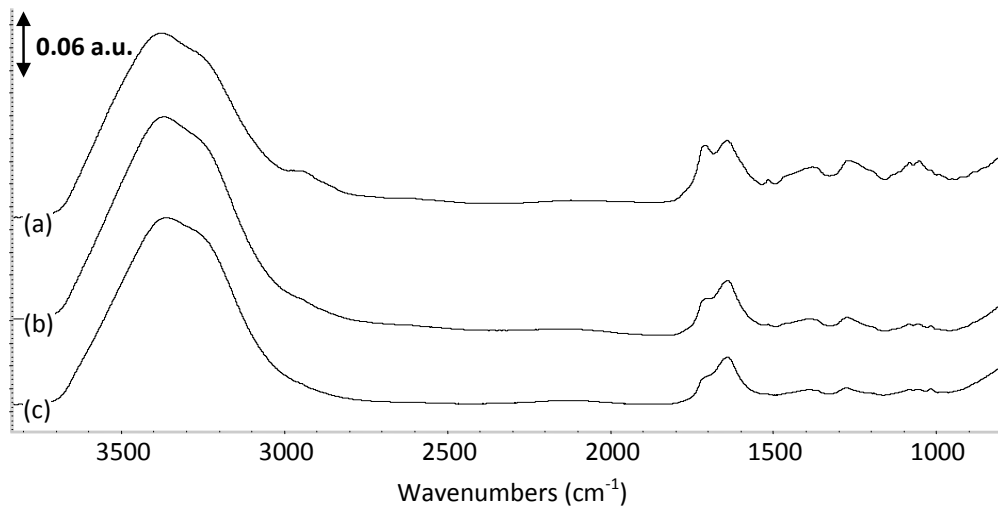


Figure 2.16 Cottonwood leaves fractionated (a) and total (b) pyrolysis oils and water condensate (c) ATR spectra.

2.4.10.2 Pine Pyrolysis Oil

When comparing all of the biomass spectra for pine pyrolysis oil there is also no significant change in the fractionated samples which have the dominant ketone/ carboxylic acid peak. With the water condensate the carbonyl region also changes as in the cottonwood pyrolysis oil with a decrease in the ketone/ carboxylic acid peak. In

addition water content and top phases do not have strong peak present in the fingerprint region. This indicates a lower concentration of these compounds which may be due to the elevated water content in the water condensate and total pyrolysis oil.

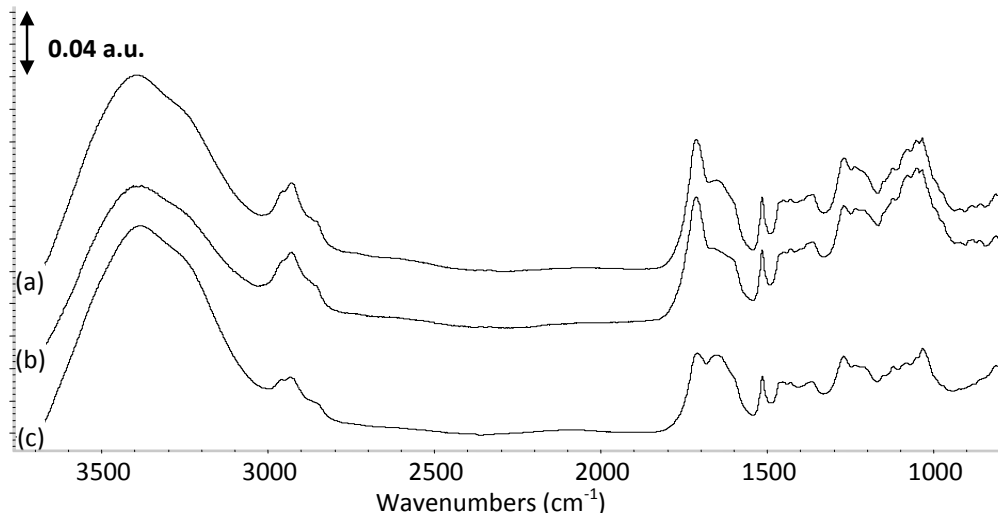


Figure 2.17 Pine clear wood total (a) and fractionated (b) pyrolysis oil and water condensate (c) ATR spectra.

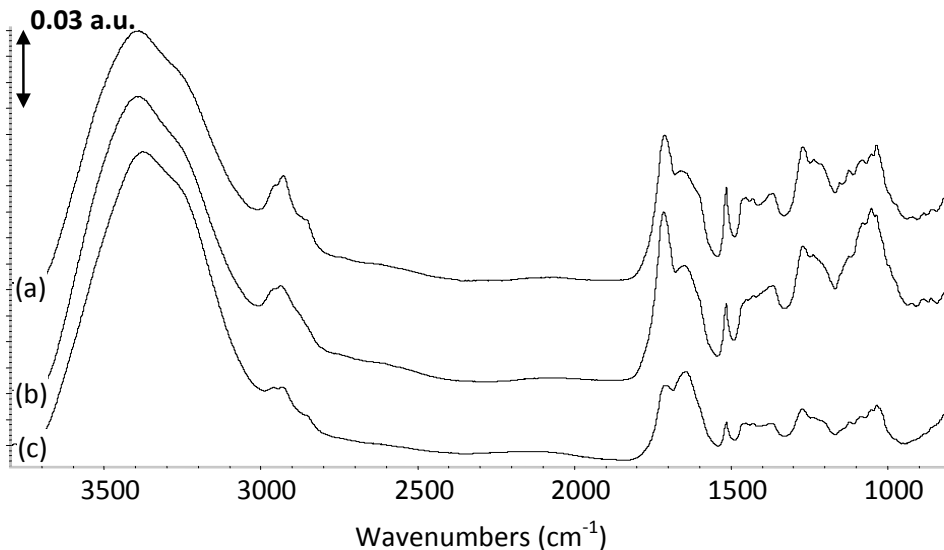


Figure 2.18 Pine whole tree total (a) and fractionated (b) pyrolysis oil and water condensate (c) ATR spectra.

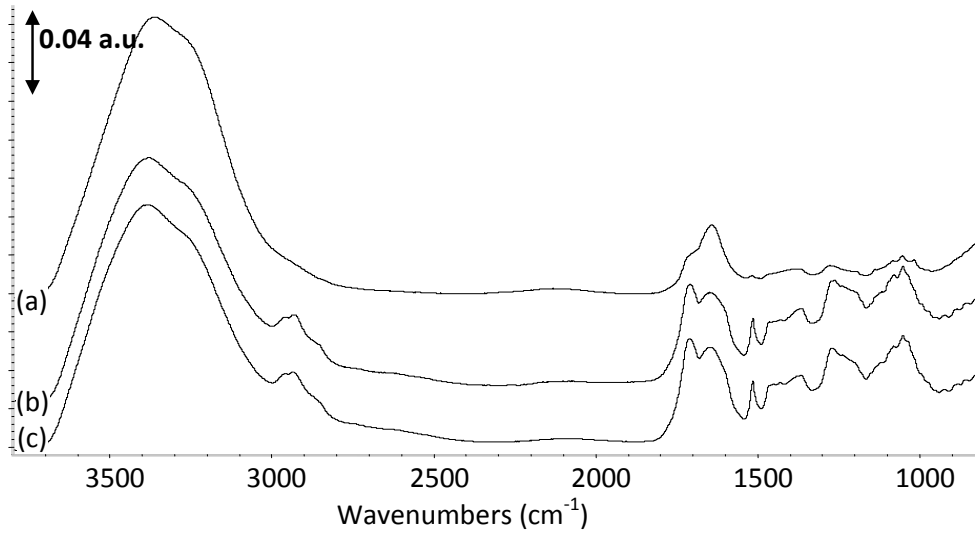


Figure 2.19 Pine bark water condensate (a) and fractionated (b) and total (c) pyrolysis oil ATR spectra.

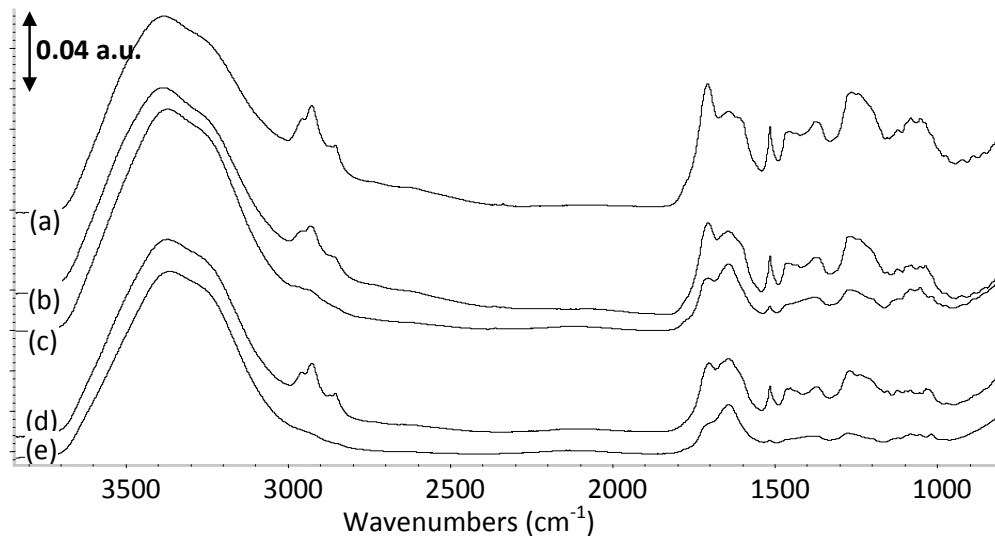


Figure 2.20 Pine needles fractionated (a) and total bottom (b) and top (c) and water condensate bottom (d) and top (e) ATR spectra.

2.4.10.3 Cottonwood vs. Pine Pyrolysis Oil

Pyrolysis oils produced from pine and cottonwood biomass are very similar and Figures 2.21 and 2.22 compare the fractionated pyrolysis oils. Fractionated spectra were selected to compare the composition of the two types of pyrolysis oil so that the water

condensate does not play a role in the spectra. Within the pine spectra there is a significant difference in the shape of the carbonyl region the bark spectrum (Figure 2.21 c) where the as C=O stretch in an aliphatic or cyclic ketone and/or a carboxylic acid dimer ($1714-1711\text{ cm}^{-1}$) [Silverstein, Pretsch, Nakanishi]. In addition the whole tree spectrum appears to have a stronger primary alcohol peak.

Comparing cottonwood and pine there does not appear to be a significant difference other than potentially a stronger C-O st at 1034 cm^{-1} due to primary alcohols and a smaller peak at 1110 cm^{-1} identified as either a secondary alcohol or aromatic ether. In general the ATR spectra for all of the biomass from pine and cottonwood have a lot in common and therefore there should also be similar aging reactions during aging.

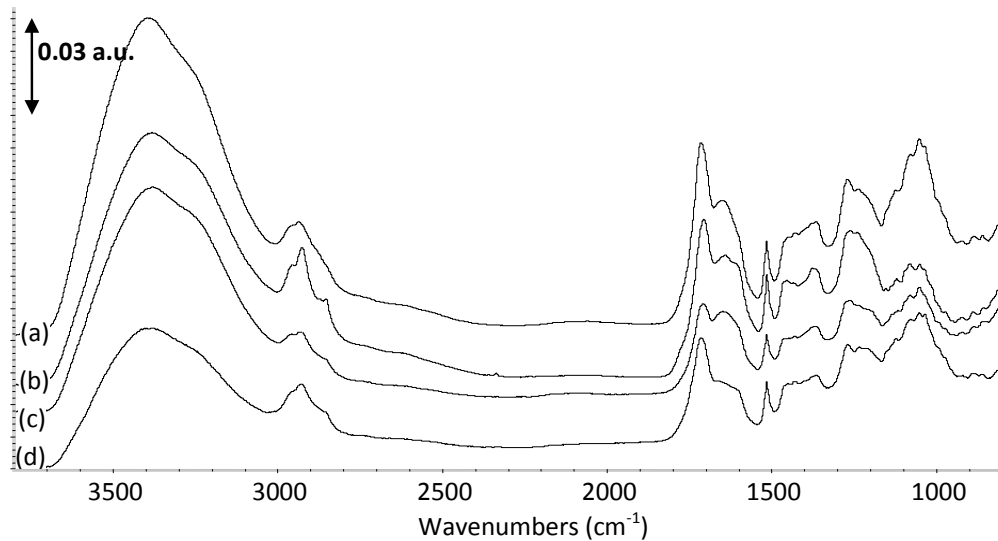


Figure 2.21 Pine fractionated pyrolysis oils derived from whole tree (a), needles (b), bark (c), and clear wood (d)

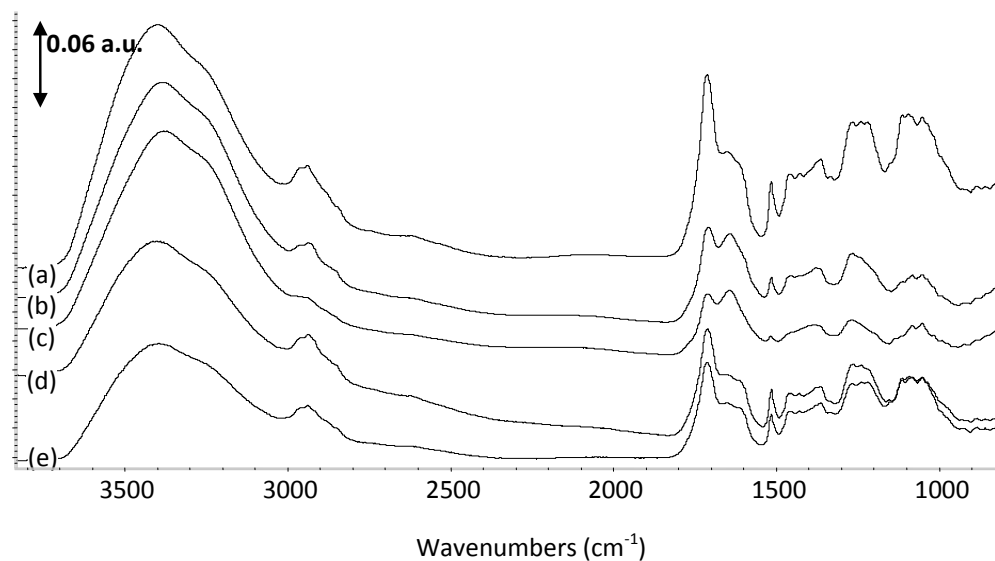


Figure 2.22 Cottonwood fractionated pyrolysis oils derived from clear wood (a), leaves top (c) and bottom (b) phases , bark (d) and whole tree (e).

2.5 Conclusions

Overall, pyrolysis oil water condensate fractions are acidic with nominal pH values of 3 and for pine bark and whole tree (which also contains bark) pyrolysis oils showed lower pH values of 2.51 and 2.87, respectively. Water condensates had 50-75 wt% and 48-75 wt% water in pine and cottonwood respectively and whole tree, bark and needle/leaf derived pyrolysis oils have elevated water content compared to clear wood.

FTIR analyses of the biomass from which the pyrolysis oil was produced as well as the char byproduct also show chemical differences between the feedstocks and also between the bark/leaves and clear wood. Also the leaves and bark biomass have more aromatic compounds and the char has more aromatic, alcohol, ether and/or ester group.

The change in pyrolysis oil properties such as pH, water content and viscosity due to the addition of non heart wood materials could be partly due to the increasing concentration of alkali metals in the biomass and subsequent char in the bark, leaves or needles.

2.6 References

ASTM Standard E 203-01 Standard method for water using volumetric Karl Fischer Titration p. 396-405.

Ba, T.; Chaala, A.; Garcia-Perez, M.; Roy, C. Colloidal Properties of Pyrolysis oils Obtained by Vacuum Pyrolysis of Softwood Bark. Storage Stability. *Energy & Fuels* 2004, 18, 188-201.

Boucher, M.E.; Chaala, A.; Roy, C. Pyrolysis oils obtained by vacuum pyrolysis of softwood bark as a liquid fuel for gas turbines. Part I: Properties of pyrolysis oil and its blends with methanol and a pyrolytic aqueous phase. *Biomass & Bioenergy* 2000, 19, 337-350.

Chaala, A.; Ba, T.; Garcia-Perez, M.; Roy, C. Colloidal Properties of Pyrolysis oils Obtained by Vacuum Pyrolysis of Softwood Bark: Aging and Thermal Stability. *Energy & Fuels* 2004, 18, 1535-1542.

Czernik, S. Bridgwater, A.V. Overview of Applications of Biomass Fast Pyrolysis Oil. *Energy & Fuels* 2004, 18, 590-598.

Diebold, J.P. A Review of the Chemical and Physical Mechanisms of Storage Stability of fast Pyrolysis Pyrolysis oils. Subcontractor Report for the National Renewable Energy Laboratory NREL/SR-570-27613; National Renewable Energy Laboratory: Golden, CO, 2000.

Fratini, E.; Bonini, M.; Oasmaa, A.; Solantausta, Y.; Teixeira, J.; Baglioni, P. SANS Analysis of the Microstructural Evolution during the Aging of Pyrolysis Oils from Biomass. *Langmuir* 2006, 22, 306-312.

Garcia-Perez, M.; Wang, S.; Shen, J.; Rhodes, M.; Lee, W.; Li, C. Effects of Temperature on the Formation of Lignin-Derived Oligomers during the Fast Pyrolysis of Mallee Woody Biomass. *Energy & Fuels* 2008, 22, 2022-2032.

McKendry, P. Energy Production From Biomass (Part 1): Overview of Biomass. *Bioresour. Technology* 2002, 83, 37-46.

Mohan, D.; Pittman, C.U.; Steele, P.H. Pyrolysis of Wood/Biomass for Pyrolysis oil: A Critical Review" *Energy & Fuels* 2006, 20, 848-889.

Mullaney, H. Technical, Environmental and Economic Feasibility of Pyrolysis oil in New Hampshire's North Country. New Hampshire Industrial Research Center (NHIRC) 2002.

Oasmaa, A.; Peacocke, C.; A guide to physical property characterisation of biomass-derived fast pyrolysis liquids. Technical Research Centre of Finland, VTT Publication 450, ESPOO 2001.

Oasmaa, A.; Kuoppala, E.; Gust, S.; Solantausta, Y. Fast Pyrolysis of Forestry Residue. 1. Effect of Extractives on Phase Separation of Pyrolysis Liquids. *Energy & Fuels* 2003, 17, 1-12.

Oasmaa, A.; Sipila, K.; Solantausta, Y.; Kuoppala, E. Quality Improvement of Pyrolysis Liquid: Effect of Light Volatiles on the Stability of Pyrolysis Liquids. *Energy & Fuels* 2005, 19, 2556-2561.

Oasmaa, A.; Kuoppala, E.; Solantausta, Y. Fast Pyrolysis of Forestry Residue. 2. Physicochemical Composition of Product Liquid. *Energy & Fuels* 2003, 17, 433-443.

Oasmaa, A.; Kuoppala, E. Fast Pyrolysis of Forestry Residue. 3. Storage Stability of Liquid Fuel. *Energy & Fuels* 2003, 17, 1075-1084.

Polagye, B. L.; Malte, P.C. Overview of Potential Conversion Technologies for Forest Thinnings. Department of Mechanical Engineering, University of Washington, Laboratory for Energy and Environmental Combustion

CHAPTER III
STATISTICAL ANALYSIS OF THE EFFECT OF FEEDSTOCK ON ACCELERATED
AGING ON PINE AND COTTONWOOD PYROLYSIS
OIL PROPERTIES

3.1 Abstract

Neat pine and cottonwood pyrolysis oils produced from clear wood, whole tree, bark and needles/leaves were examined before and after accelerated aging at 80 °C for 24 h and 504 h. Minitab software was used with a 2^k factorial statistical method to examine the effects of tree type, forestry residue (bark needles and/or leaves), oil type and aging time on pyrolysis oil properties: pH, water content, viscosity and molecular weight. It was determined that forestry residue present in biomass prior to pyrolysis affects the water content of un-aged pyrolysis oil. In addition, the tree type (cottonwood or pine) had no impact on the pyrolysis properties and the pyrolysis oil collection method (total vs. fractionated oil) played a larger role. The total oil, fractionated oil plus water condensate, affects all of the properties examined and had the largest impact on viscosity and initial molecular weight. After 24 h of accelerated aging, a correlation was only found with increased molecular weight while 504 h of aging correlated to changes in pH, water content, viscosity, and molecular weight.

3.2 Introduction

Pyrolysis is defined as the thermal decomposition in the absence of oxygen [Diebold, Bridgewater 1997]; when pyrolyzing biomass there is only a partial

decomposition resulting in highly organic reactive components [Diebold 1997]. Due to the partial composition, the composition of pyrolysis oil is highly dependent on biomass and is comprised of fragmented portions of cellulose, hemicelluloses and lignin [Diebold, Bridgewater 1997]. In addition to feedstock, pyrolysis parameters such as pressure, temperature, heating rate and residence time also have a large effect on the composition of pyrolysis oil [Sensoz 2003, DeSisto 2010].

Storage instability, or aging, is a significant problem resulting in increased viscosity when stored at room temperature [Diebold, 1997] and preventing the direct application of pyrolysis oil as a fuel [Garcia-Perez 2006]. During aging reactive organic components react to produce large molecules changing the physical properties [Diebold 1997]. Therefore, as expected, the rate of aging is dependent on the composition of the biomass [Diebold 2000].

In this study, four categories wood feedstocks (clear wood, whole tree, bark and leaves/needles) were investigated for cottonwood and pine to determine the statistical effects of feedstock and liquid fraction collected on pyrolysis oil properties, both before and after accelerated aging. Since these pyrolysis oils were then used in further studies (e.g., particulate addition, filtration, solvent addition), a preliminary analysis of unaltered pyrolysis oil properties is important to determine potential anomalies or unique properties based on tree species, feedstock and liquid fraction.

3.3 Statistical Method

Minitab 15[®] software (Minitab, Inc.) was used to statistically analyze pyrolysis oil properties characterized, including pH, water content, viscosity and molecular weight, and if and how these properties are related to tree species, feedstock composition, oil

type, and aging time. Pine and cottonwood properties were compiled for each specific type (i.e., total, fractionated, condensate) of pyrolysis oil. Three data points were included for each property when available resulting in 24 pyrolysis oil types and 72 data points per property.

For data analysis, a custom factorial design of experiment (DOE) function was defined and used. Four two-level factors were defined for (i) tree type (pine/cottonwood), (ii) forestry residue (yes/no), (iii) total and fractionated oils (yes/no), and (iv) aging for 24 and 504 hours (yes/no).

3.4 Results and Discussion

3.4.1 Phase Separation

Phase separation details after 24 and 504 hours of aging at 80 °C are presented in Table 3.1 and Table 3.2. Total pyrolysis oils and water condensates were more likely to phase separate prior to aging due to the high water concentrations. The only fractionated pyrolysis oils that phase separated after aging were derived from pine needles, pine bark, or cottonwood leaves. Also, several of the total pyrolysis oils formed tar-like pseudo solid disks at the bottom of the sample bottles after 504 hours of aging.

Table 3.1 Identification of phase separation in neat and aged (80 °C for 24 or 504 hours) cottonwood pyrolysis oil samples.

Cottonwood Feedstock Composition	Pyrolysis Oil Type	Aging Time at 80 °C		
		0 h	24 h	504 h
Heart Wood	Fractionated	N	-	N
	Total	Y	Y	Y
	Condensate	Y	-	Y
Whole Tree	Fractionated	N	N	N
	Total	Y	Y	Y
	Condensate	N	-	Y
Bark	Fractionated	N	N	N
	Total	Y	Y	Y
	Condensate	Y	-	Y
Leaves	Fractionated	Y	Y	Y
	Total	N	Y, sm	Y
	Condensate	N	-	Y, sm
	<i>Thick and Tacky</i>		<i>Solid bottom</i>	

Table 3.2 Identification of phase separation in neat and aged (80 °C for 24 or 504 hours) pine pyrolysis oil samples.

Pine Feedstock Composition	Pyrolysis Oil Type	Aging Time at 80 °C		
		0 h	24 h	504 h
Heart Wood	Fractionated	N	N	N
	Total	Y	Y	Y
	Condensate	Y	-	Y
Whole Tree	Fractionated	N	N	Y
	Total	Y	Y	Y
	Condensate	Y	-	Y
Bark	Fractionated	N	N?	Y
	Total	Y		
	Condensate	N	-	Y
Needles	Fractionated	N	Y, 3	Y, 3
	Total	Y	Y, 3	Y, 3
	Condensate	Y	-	Y, 3
	<i>Thick and Tacky</i>		<i>Solid bottom</i>	

3.4.2 Statistical Analysis: 2^k Factorial Method

Statistical analysis by factorial method is typically used when there are several factors of interest. A 2^k factorial method allows for the smallest number of samples for several factors that each have two levels [Montgomery]. This method is especially useful for pyrolysis oil given the many parameters that are expected to affect its composition and properties such as feedstock, oil type and age. The P-value can be used to evaluate each factor for correlation. A correlation or statistically significant effect between the response and the two-level factors can be determined [Montgomery].

For neat (unaged) pyrolysis oil, sample factors were defined as (i) tree type (pine or cottonwood), (ii) the presence of forestry residue (contains bark, needles, and/or

leaves), (iii) total and fractionated oil and (iv) aging for 24 and 504 hours with responses in some measured quantities (pH, water content, molecular weight and viscosity). To determine if the effect of the factors are significant for each response, the P-values were examined using $\alpha = 0.05$ (95 % confidence).

When compiling data for analysis and phase separation occurred in the sample (e.g., 504 h data points), the extreme values were used; water content for the top phase and molecular weight for the bottom phase.

In terms of feedstock, tree type and the presence of forestry residue factors were examined with respect to the properties (responses) of cottonwood and pine neat pyrolysis oil (pH, water content, viscosity and molecular weight) for significant effects; these statistical results are presented in Table 3.2. Tree type (cottonwood vs. pine) has a significant impact on pH but does not affect water content, viscosity or MW. Forestry residue present in the biomass does influence the water content with a significant effect of 14. Tree type and the interaction between tree type and forestry residue are not important factors in the properties due to the P-values $> \alpha=0.05$.

Table 3.3 Statistical P-test comparison for neat (unaged) pyrolysis oil based on tree species and forestry residue content.

	Factor					
	Tree Species		Forestry Residue		Tree Type * Forestry Residue	
Responses	Effect	P-value	Effect	P-value	Effect	P-value
pH	0.1475	0.034	-0.1283	0.064	0.032	0.634
Water Content	-1.256	0.813	14.099	0.010	-0.664	0.900
Viscosity	3.237	0.848	9.511	0.573	16.345	0.334
MW	37.300	0.206	-40.54	0.170	-2.590	0.929

Oil type, total or fractionated, does impact the water content and molecular weight significantly (Table 3.3). Also, the total oil that contains the water condensate has an effect on all four properties with the largest impact on the viscosity and initial molecular weight where the fractionated oil only has an effect on water content and molecular weight.

Table 3.4 Statistical P-test comparison for neat (unaged) pyrolysis oil based on oil type/fraction, total and fractionated.

	Factor			
	Total Oil		Fractionated Oil	
Response	Effect	P-value	Effect	P-value
pH	0.17474	0.023	0.10083	0.183
Water Content	-37.84	0.0	-19.88	0.0
Viscosity	83.558	0.0	6.991	0.606
MW	156.83	0.0	95.81	0.0

These analyses indicate that the presence of forestry residue (bark needles and/or leaves) in the starting biomass affects only the water content of the un-aged pyrolysis oil properties and the tree type (cottonwood or pine) has no impact. In contrast, the fractions of the pyrolysis oil collected during condensation plays a much larger role. The total oil, which contains the water condensate, affects all of the properties measured in this study (pH, water content, viscosity, and MW); viscosity and initial molecular weight showed the strongest correlations with total oil.

3.4.3 Comparison of Pyrolysis Oil Properties During Aging

Pine and cottonwood pyrolysis oils and water condensates were aged at 80 °C for 24 and 504 hours. After aging pine and cottonwood pyrolysis oil for 24 h the tree type and forestry residue factors were tested again (Table 3.4). After aging the tree type now

has significant effects with pH, water content and molecular weight. In addition the forestry residue no longer has a significant impact on the water content but instead the pH value after aging. A change in the effects of tree type and forest residue indicate that although the initial properties were not influenced by the tree type it does have a large impact during aging and has the highest effect on molecular weight increase. This may be due to variances in the chemical composition of the pyrolysis oil that could lead to an increase in the aging or conversely retard the aging reactions.

In contrast the factors were tests again after 504 hours of aging (Table 3.5) resulting in no significant effects with tree type having. This indicates that after 504 h of aging the three time no longer has any role in the pyrolysis oil properties. Forestry residue continued to have to affect the pH values where forestry residue actually increases the average pH.

Table 3.5 Statistical P-test comparison for pyrolysis oil aged for 24 h based on tree species and forestry residue content.

Responses	Factor					
	Tree Species		Forestry Residue		Tree Type * Forestry Residue	
	Effect	P-value	Effect	P-value	Effect	P-value
pH	0.29345	0.014	0.6425	0.0	-0.05988	0.599
Water Content	15.53	0.016	5.098	0.406	-12.371	0.05
Viscosity	-30.7	0.202	3.23	0.892	42.53	0.08
MW	120.45	0.049	-14.75	0.8	-95.55	0.113

Table 3.6 Statistical P-test comparison for pyrolysis oil aged for 504 hours based on tree species and forestry residue content.

	Factor					
	Tree Species		Forestry Residue		Tree Type * Forestry Residue	
Responses	Effect	P-value	Effect	P-value	Effect	P-value
pH	0.19125	0.108	0.51375	0.0	-	-
Water Content	45.93	0.118	52.6	0.074	39.77	0.174
Viscosity	-208.5	0.101	-8.8	0.944	51	0.685
MW	56.502	0.505	2.231	0.979	47.902	0.571

Pine pyrolysis oil properties were compared to the factors of 24 and 504 h of aging (Table 3.6) that determined that there is a significant correlation between 24 h of aging and pH, water content, molecular weight and phase separation, but not viscosity. This is interesting in that typically aging is defined by a viscosity increase which 24 hours of aging at 80 °C does not have a significant effect. Molecular weight has the largest effect magnitude indicating that it has the largest effect over 24 h. In addition after 504 hours of aging viscosity becomes a significant effect but water content is no longer. When comparing the 24 and 504 h aging factors it may be possible that multiple reactions have different reactions times. If condensation reactions, producing water, occur within 24 h then the viscosity may not increase due to the increase in water. Also, a polycondensation reaction could produce water while reacting small molecular weight molecules and as the reaction proceeds the molecules involved become larger and do not affect the viscosity until the polymer chains become larger after longer aging times.

Table 3.7 Aging of Pine Pyrolysis oil for 24 and 504 hours

	Factor			
	24 hours		504 hours	
Response	Effect	P-value	Effect	P-value
pH	-0.3444	0.003	-0.5057	0.0
Water Content	-12.137	0.018	7.061	0.104
Viscosity	25.12	0.791	285.66	0.002
MW	163.08	0.002	408.88	0.0
Phase Separation	-0.525	0.036	0.675	0.003

Cottonwood pyrolysis oil aging when analyzed had a much different result when compared to pine pyrolysis oil. The only factor with a significant effect after 24 h was molecular weight. After 504 hours of aging all of the properties are correlated to the aging time with molecular weight with the highest effect. This indicates that the properties of the pyrolysis oil are not significant effected by aging at 80 °C for 24 h, but aging for 504 h will affect all properties. Considering that both pine and cottonwood pyrolysis oils have significant effects in molecular weight after 24 and 504 h of aging, viscosity and molecular weight should be considered during aging rather than viscosity alone.

Table 3.8 Aging of Cottonwood Pyrolysis oil for 24 and 504 hours

	Factor			
	24 hours		504 hours	
Response	Effect	P-value	Effect	P-value
pH	-0.1653	0.101	-0.4814	0.0
Water Content	0.8705	0.975	66.9038	0.003
Viscosity	6.506	0.856	67.022	0.036
MW	179.21	0.001	449.07	0.0
Phase Separation	0.4286	0.108	0.4706	0.044

3.5 Conclusions

Forestry residue (bark needles and/or leaves) present biomass prior to pyrolysis affects the water content of neat pyrolysis oil where the tree type (cottonwood or pine) had no impact. On the contrary pyrolysis oil collection plays a much larger role where the total oil containing the water condensate affects all of the properties with the largest impact on viscosity and initial molecular weight. Post aging there is a significant effect relating pH and forestry residue suggesting the contents of forestry residue potentially aid in the alteration of the pH during aging.

After aging for 24 hours pine and cottonwood pyrolysis oil viscosities did not show significant correlation with the aging. It is suggested that molecular weight, which was significantly affected, would be a better aging indicator for short times rather than viscosity. For long term aging, such as 504 hours, all of the properties are significantly affected by aging time. Therefore, the increase in water, viscosity or molecular weight can be used to monitor aging in the pyrolysis oils.

3.6 References

Montgomery, D.C., Runger, G.C., Applied Statistics and Probability for Engineers. John Wiley & Sons, Inc.: MA, 2007.

CHAPTER IV
EVOLUTION OF PHASE SEPARATION DURING ACCELERATED AGING IN
PINE PYROLYSIS OIL

4.1 Abstract

Pine whole tree fractionated [PWTF] pyrolysis oil was examined during accelerated aging to observe the evolution of phase separation. Neat PWTF samples were aged at 80 °C for 6, 12, 24, 168, 336 and 504 h and after 336 h of aging phase separation was visible. Characterization for phase separated samples was conducted for top and bottom phases in addition to mixing them together. Characterizations included pH, water content and viscosity measurements, gel permeation chromatography (GPC), attenuated total reflectance Fourier transform infrared (ATR-FTIR) spectroscopy and coupled gas chromatography-mass spectroscopy (GC/MS) were utilized to identify and monitor chemical composition. Top and bottom phases had very different properties were the top phase had high water content (34.5-37.5 wt%) and low molecular weight (545-599 Da) and the bottom phase had low water content (26.3-18.0 wt%) and high molecular weight (997-1104 Da). In addition aging continued after phase separation with reaction products concentrated in the bottom phase indicating the reaction occurs in the bottom phase or the products precipitate out of the top phase. ATR peak height ratios showed increased amounts of ketone and/or carboxylic acid functional groups along with decreases in alcohol, ether and/or ester groups. Oxidation of alcohols to form carboxylic acids and ketones explains the increase in water content and decrease in ketones with aging. In

addition, polycondensation may account for the increase in molecular weight in addition to the water formation.

4.2 Introduction

Multiple alternatives to petroleum and coal have been tested and even more suggested to supplement the growing need for energy have been suggested; none of these have demonstrated the potential to completely replace traditional petroleum fuels. One alternative to conventional petroleum fuels is liquid pyrolysis oil that can be used for transportation, heating or electricity generation and are currently the only liquid renewable fuel [Bridgewater 2003]. Fast pyrolysis produces high volumes of energy dense, transportable liquid oil from a heterogeneous, bulky biomass source [Westerhof 2007].

Pyrolysis oil is a complex, multiphase oil with upwards of 400 components [Diebold, 1997] and a large amount of water emulsified with the oil [Boucher 2000], ranging from 15 wt % up to 30-50 wt% [Bridgewater 2003]. In addition, it has also been described as a multiphase fluid with a network structure of oligomers and nonpolar oligomeric micelles [Garcia-Perez, 2006]. Major chemical compounds include water, ketones, aldehydes, organic acids, phenolics, esters and furans [Diebold, 1997]. Pyrolysis oils are miscible with polar solvents (e.g., acetone, methanol, ethanol), but totally immiscible with petroleum-derived fuels [Bridgewater 2003] without an additive. The heating value of pyrolysis oil is about half that of petroleum fuels [Oasmaa 2001].

As produced, multiple properties of pyrolysis oils present a barrier to the direct application, including instability during storage [Garcia-Perez 2006, Ba 2004], high acidity [Garcia-Perez, 2006] and water content leading to corrosion, phase separation

[Mohan, 2006], char containing alkali metals and low burning times [Garcia-Perez, 2006]. Also processing difficulties include clogging nozzles, injectors or filters and/or agglomeration of components in recirculation systems [Ba, 2004]. Storage instability and combustion difficulties is the result of a combination of properties including the breakdown of the microemulsion, chemical reactions [Mohan, 2006], and colloidal nature due the water-insoluble materials [Ba, 2004].

One of the major barriers is instability during storage, otherwise referred to as aging, and is primarily characterized as an increase in viscosity, but is also connected to an increase in water content and molecular weight [Mohan]. Over time reactive organic components within the pyrolysis oil react to produce large molecules resulting in changes to physical properties such as viscosity [Diebold 1997]. Etherification and esterification mechanisms proposed based on FTIR analyses where hydroxyl and carbonyl components react resulting in molecular weight increase during storage [Diebold 1997]; as a byproduct of condensation reactions, water is typically formed [Mullaney 2008]. During aging, phase separation is often observed and is thought to be partly the result of the water formation from the condensation reactions. It has also been suggested that polycondensation reactions produce three dimensional polymer structures forming layer networks and resulting in phase separation [Chaala, 2004]. Preventing these reactions would be advantageous, resulting in a liquid fuel that can be stored for long periods of time without the formation of thick tar and phase separation [Diebold 1997].

The optimum water content for pyrolysis seems to be between 15-30 wt%. Water contents above 30 wt% lead to phase separation, ignition delay, and emissions of particles. And in general less water in pyrolysis oil is favorable for transportation costs, stability, acidity and energy density [Westerhof 2007]. However, below 15 wt% water

the viscosity of pyrolysis oil increases exponentially leading to processing and pumping obstacles [Westerhof 2007].

Two distinct types of phase separation occur in pyrolysis oils due to either large percentage of water content or high concentrations of lignin derived material [Oasmaa 450 2001]. Approximately 30 wt% water or more will result in phase separation and feedstocks including forest residue, barks, pine, straw, tropical hardwood and eucalyptus produce multiple phases due to high levels of hydrocarbon-soluble extractives and/or alkali metals [Oasmaa 2001].

Lignin-rich phase separation is observed in the pyrolysis of forestry residue and results in lower yields, compared to bark-free wood pyrolysis oil, and phase separation with 10-15 wt% extractive-rich top phase and a bottom phase resembling bark-free pyrolysis oil [Oasmaa 2003]. A significant amount of hydrocarbon-soluble extractives and low amount of water-soluble polar compounds are present in the bottom phase and the top phase has significantly higher heating value, viscosity, and solid content and lower water content and density [Oasmaa 2003]. Phase separation takes place due to significant solubility, polarity and density difference of extractives and polar pyrolysis liquid compounds [Oasmaa 2003]. In a second study, phase separation in pyrolysis oil derived from softwood bark (white spruce, balsam fir and larch) occurred due to the presence of waxy materials which crystallize on cold surfaces or at cold temperatures and melt at 45 °C [Garcia-Perez 2006]. Softwood bark-derived pyrolysis oil is characterized as a colloidal system with a bottom phase similar to whole pyrolysis oils, but with higher ash and water content, and a top phase (16 wt%) rich with extractives [Ba 2004]. Whole pyrolysis oil viscosity was measured as 62 cSt at 50 °C while the upper phase had a higher viscosity of 88 cSt and the bottom phase viscosity was reported as 66 cSt [Ba

2004]. In a separate study, it was determined that aging was more pronounced in the bottom layer of softwood bark-derived pyrolysis oil and when the top and bottom phases were aged together the aging rate was reduced [Chaala 2004]. In addition to the top phase container higher calorific value than the bottom phase and the reduced aging rate when phases were aged together, it was suggested to leave top phase in the pyrolysis oil and would be mixed using stirring or recirculating at 45-50 °C [Chaala 2004].

Phase separation due to water results in the precipitation of a heavy oil and tar bottom phase and is exhibited both in fresh pyrolysis oil when the moisture content of the feedstock was >15 wt% prior to pyrolysis [Oasmaa 2001] and also with the addition of water post-production [Elliot 1994]. In pine- and oak-derived pyrolysis oils, phase separation occurred at 25-30 and 35 wt % water, respectively [Elliot 1994]. In another study, water was added incrementally to pine pyrolysis oil, mixed and allowed to sit for 7 days to determine that a minimum of 32 wt % water is required to induce phase separation leaving the water content of the heavy organic phase approximately constant [Westerhof 2010].

In addition to phase separation occurring due to lignin-rich feedstocks and high water content, phase separation also occurs during storage and accelerated aging. During heating of pyrolysis oils phase separation can occur due to water formation when the total water content exceeds 30 wt%; described as a by-product of aging reactions and results in an aqueous phase and a heavy lignin-rich phase [Oasmaa 2001]. Phase separation during aging has also been described as the result of elevated water content and the formation of large molecules by reactions such as polymerization (large molecules) and etherification and esterification (water by-product) leading to a tar-like bottom phase and an acidic top phase with high water content [Mullaney 2008]. Pine-derived pyrolysis oil containing 21

wt % water (viscosity of 35 mPas at 40 °C) aged at 80 °C for 24 hours had a 95 % increase in viscosity correlating to 1 year of storage at room temperature [Oasmaa 2001]. Forestry residue pyrolysis oil phase separates at 80 °C after 24 h thus 1 week at 40 °C was used for test conditions correlating to three months at room temperature [Oasmaa 2001].

It has also been proposed that lignin oligomers polymerize during storage within the first 6-7 months and that this process continues until the heaviest lignin-rich fraction separates out of the matrix after approximately one year of storage (with the exact time dependent on water content) [Fratini 2006].

Pyrolysis oils derived from hardwood bark and softwood bark were compared during accelerated aging [Garcia-Perez 2006]. Softwood bark pyrolysis oil phase separated after 96 h at 80 °C. After 168 h at 80 °C, the aqueous phase that was formed comprised approximately 20 wt% of the total sample [Garcia-Perez 2006]. Softwood bark-derived pyrolysis oil contained polyaromatic compounds thought to participate in aging reactions whereas hardwood bark-derived pyrolysis oil did not show phase separation and contained dimethoxy phenols thought to react and form lower molar mass material [Garcia-Perez 2006]. In addition, it was determined that the formation of the aqueous phase resulted in further degradation of the pyrolysis oil leading to heavy methanol insoluble materials [Garcia-Perez 2006].

Given the components of pyrolysis oil and proposed aging reactions, it has been suggested to add solvents for the reduction of esterification, acetalization and phenol/formaldehyde reactions, to add antioxidants to reduce olefin polymerization reactions, and to include emulsifiers to prevent/minimize phase separation [Qi 2007].

Water-and lignin-rich phase separation have been investigation previously and are well understood. Pine whole tree pyrolysis fractionated oil was investigated to observe phase separation evolution during accelerated aging in order to determine the type of phase separation, when it occurs and the effect of bark and leaves in the biomass.

4.3 Methods and Materials

Feedstock: Plantation grown Loblollypine trees (*Pinus taeda*) were harvested and needle biomass was separated from the bole wood (bark, limbs and wood). All biomass was dried to 10-15% moisture content (MC) in an oven (Despatch V series VREZ-19-ZE) at 103 °C. Bole wood was chipped to 1-2 inch chips (Carthage Machine Inc., Model 39 chipper, 1470 rpm) prior to the needles being added back in and the total ground (Bauer Bro. Co., 25 Hp, 1465 rpm), and screened to particles sizes between ~4 to 6 mm (Universal Vibrating Screener, Type S #1354). Prior to pyrolysis the whole tree mixture was dried to 1-2 % MC.

Pyrolysis: MSU Forest Products Laboratory produced the pine whole tree pyrolysis oil using an auger pyrolysis reactor operated under vacuum at 400 °C, 25 °C (± 1 °C) water condensers and an average flow rate of 15-20 L/min. Fractionated oil was collected referring to the exception of one condenser during oil collection where high concentrations of water are produced in addition to organic acids and during oil production the first condenser was not cooled. Pyrolysis oil samples were at ~5 °C within 1 h of production minimizing aging prior to aging. Produced pyrolysis oil was dark in color with a pungent smell, one phase and pyrolysis oil samples were aliquots from the same 1 L production batch.

The pine whole tree fractionated [PWTF] pyrolysis oil was compared to PWTF pyrolysis oil produced 3 weeks earlier using a different harvest of pine trees, but with the same method and same auger reactor operated at 450 °C. An in-depth description of the properties for PWTF pyrolysis oil produced used in this study is presented in earlier work [ref filtration #1 draft/ chapter 1].

Aging Conditions: Triplicate 27 mL samples of pine whole tree fractionated [PWTF] pyrolysis oil were prepared in 30 mL amber bottles with PTFE lined caps (in accordance to recommendations in Oasmaa, 2001). These samples were then aged in a convection oven at 80 °C for 6, 12, 24, 168, 336 and 504 h; control samples were stored in a refrigerator at 5 °C to prevent aging. Throughout aging the caps were retightened periodically to minimize material/weight loss. In addition to characterization methods described below, the initial and final weights were recorded and the average weight loss range was 0.02 to 0.38 wt %.

pH and Water Content: pH measurements were collected on the pyrolysis oil using an Accumet Basic pH meter (calibrated using five phosphate buffer solutions: 2, 4, 7, 10 and 12). Karl Fischer titrations (Barnstead International Aquametry II Apparatus) were conducted following ASTM E 203-01 for water content determinations using Hydranal Solvent CM (chloroform-methanol) and Hydranal Titrant 2E [Oasmaa, 2001]. For pH and water content, a minimum of three measurements were collected in order to calculate average values and 95 % confidence intervals.

Viscosity: Step-flow shear tests were used to determine the pyrolysis oil viscosity using a TA Instruments AR 1500x rheometer with a Peltier heater (40 °C) and 60 mm aluminum parallel plate geometry. Sample volumes varied from 500 to 1200 μm , maximizing the volume for each experiment, but dependant on the sample viscosity and

gap distance. Viscosity was measured over the shear rate range 0.1 to 1000 Hz (1/s) and a minimum of 10 data points were averaged over a plateau region observed at higher shear rates (10-1000 1/s). A minimum of three measurements were collected to calculate average viscosity values and 95 % confidence intervals.

Pendant Drop: A Krüss Easydrop contact angle measuring instrument with a Teli CCD camera was used to collect interfacial tension data using disposable PP 1 mL syringes with 2 mm inner diameter stainless steel needles. Pendant drops with a volume of 10 μ L were formed at ambient temperature. A minimum of 9 pendant drops were formed with each pyrolysis oil sample and evaluated using Drop Shape Analysis software (version 1.90.0.14) to obtain interfacial tension values (mN/m).

Calorimetry: An adiabatic PARR 1535EA oxygen bomb calorimeter, operated at 115V and 60 Hz in accordance with ASTM D 240-92.

Molecular Weight Determination: Molecular weight was determined by gel permeation chromatography (GPC). Pyrolysis oil samples were prepared in Optima tetrahydrofuran (THF, >95 wt%) at 1-2 mg/mL, sonicated, and then filtered with 0.45 μ m syringe filters. A custom-built GPC instrument was constructed using a Varian Star 9040 refractive index detector, Waters 610 Fluid pump, Waters 600 Controller, Varian Mesopore guard column (50 x 4.6 mm ID) and Varian Mesopore column (250 x 4.6 mm ID) operated at 0.3 mL/min and 50 μ L of sample was injected at room temperature. A nine point polystyrene calibration (162, 266, 486, 582, 891, 2780, 6480, 10261, 18200 MW standards, PSS Polymer Standards) was used in addition to an internal polystyrene standard (Mw = 177,000) to account for pressure changes and shifting retention time. Calibration points were shifted to a common internal standard position and then shifted collectively to each sample internal standard position. Star WS and Waters Breeze

software packages were used collectively for data analysis performing a minimum of 4 replicates data point to obtain average values and 95 % confidence intervals.

FTIR Spectroscopy: Attenuated total reflectance Fourier transform infrared (ATR-FTIR) spectra were collected using a Nicolet 6700 spectrometer on a ZnSe 60-degree ATR crystal (liquid nitrogen cooled MCT-A* detector, 4 cm^{-1} resolution, 256 scans). All ATR spectra were ATR corrected using Thermo Electron OMNIC software and peak height ratios (PHR) were calculated by measuring peak heights of interest and normalizing with a reference peak (asymmetric methyl C-H stretch peak, 2929 cm^{-1}) [Silverstein]. A minimum of 3-5 spectra were collected for each sample to check for sample homogeneity and so that average PHRs could be calculated along with 95 % confidence intervals. Peak resolution was performed for neat and samples aged for 24, 168, 336 and 504 hours using Omnic software over the range of 1800-1560 cm^{-1} .

GC/MS Analysis: Samples were analyzed using a Varian 3600 gas chromatogram coupled with a Varian Saturn 2000 mass spectrometer (GC-MS; Varian Inc., Walnut Creek, CA) using a fused silica column Rtx-1MS (30 m \times 0.25mm, film thickness 0.25 μm). The system was operated over an oven temperature range of 50-300 $^{\circ}\text{C}$ with a heating rate of 10 $^{\circ}\text{C}/\text{min}$, helium carrier gas, 1.2 mL/min volumetric flow rate, and 250 $^{\circ}\text{C}$ detector temperature. Unknown compounds were identified by comparing spectra obtained to the NIST 2005 organic compound database with MASPEC II 32 data system software. A GC/MS data analysis method was developed for peak height comparisons where all peak height data were normalized using the sample concentration. One sample was analyzed by GC/MS for each aging time in both the unfiltered and filtered pyrolysis oil sample sets.

4.4 Results and Discussion

During accelerated aging the sample jars lost small percentages of volatile materials which increased with aging time but did not exceed 0.4 wt%. After the samples were aged for a specified period of time, the jars were quenched in ice water and when opened the jars were under vacuum and ‘popped’ when opened. It was noted that a white vapor was present in the headspace of the jars when first opened. There was a noticeable decrease in the weight of the jars when the vapor leaves. When measured, the white vapor accounted for approximately 0.35 wt% of the sample (oil +jar/lid).

Two batches of pine whole tree fractionated pyrolysis oil produced 3 weeks apart with identical reactor conditions are compared in Table 4.1 including pH, water content, viscosity and weight average molecular weight (Mw). The PWTF-319 oil had 11-25 % lower pH when compared to PWTF-94 and 35-62 % larger water content. The Mw for the PWTF-319 oil was 32 % higher for the neat sample and only 8 % higher after aging for 3 weeks. The largest difference between the two batches/lots is the viscosities where the PWTF-319 control is 58 % lower, after 2 weeks aging is 70 % lower, but after 3 weeks is 141 % larger than the PWTF-94 viscosity. Comparison of the PWTF-319 and PWTF-94 pyrolysis oils show the reactor temperature and possibly the origin and/or lot of the feedstock can affect the pH, water content, viscosity and Mw and also how these properties change during aging.

Table 4.1 Comparison of pH, water content, viscosity, and weight average molecular weight (Mw) for two batches of PWTF pyrolysis oil over the duration of an aging study at 80 °C

Aging Time at 80 °C (h)	pH		Water Content (wt%)		Viscosity (cP)		Mw (Da)	
	PWTF-319	PWTF-94	PWTF-319	PWTF-94	PWTF-319	PWTF-94	PWTF-319	PWTF-94
0	2.74	3.08	35.16	21.87	11.4	27.2	1220	921
168	2.54	3.02	30.27	22.28	8.94	73.3	1443	1198
336	2.34	3.12	34.39	21.21	19	63.9	1583	1461
504	2.47	3.16	46.66	26.29	47.18	19.5	1512	1403

4.4.2 Phase Separation

Pine whole tree fractionated (PWTF) pyrolysis oil aged at 80 °C for 336 and 504 h has a distinct phase separation when cold (~5 °C). As is shown in Figure 4.1, when a vial containing this material is removed from the refrigerator and inverted, the viscous bottom phase remains at the bottom of the vial and the liquid top phase moves freely. As the pyrolysis oil sample is warmed to room temperature, the bottom phase becomes mobile and moves slowly downward and the phase separation becomes hard to distinguish due to the phases being identical in color.

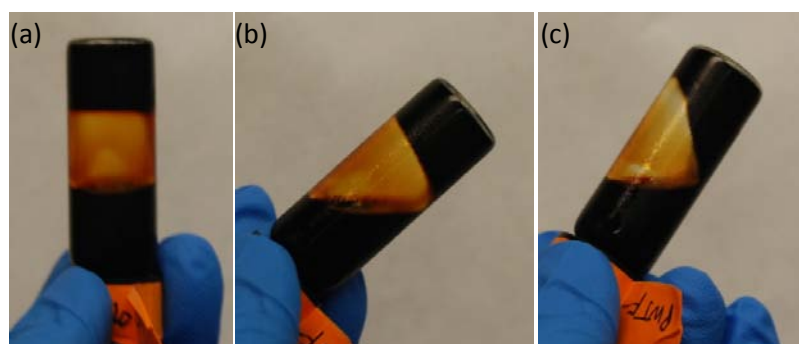


Figure 4.1 Photographs displaying phase separation in PWTF pyrolysis oil aged at 80 °C for 504 hours at 5 °C (a) and as it begins to warm to room temperature (b and c).

4.4.3 pH measurement

Measured pH of the pine whole tree fractionated [PWTF] aged at 80 °C for up to 504 h is presented in Figure 4.2. There is no definitive trend in the pH measurements and overall the pH remained constant with an average pH value of 3.1 ± 0.08 .

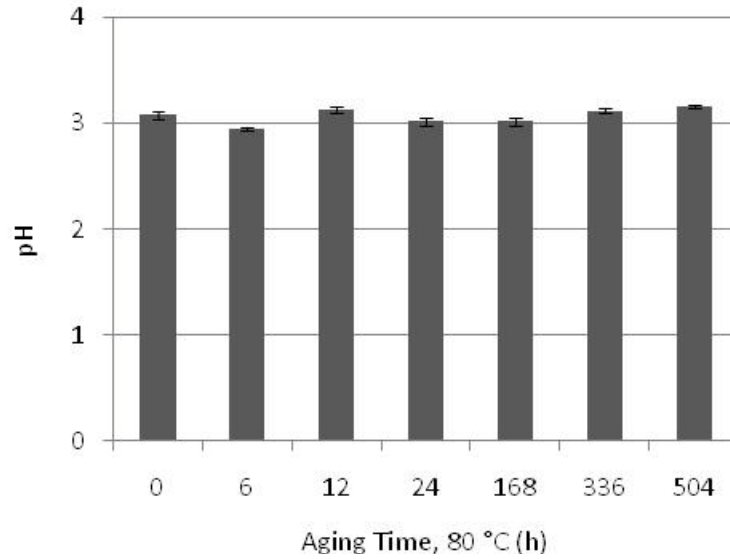


Figure 4.2 pH measurements for the PWTF pyrolysis oil samples aged at 80 °C for up to 504 h.

4.4.4 Water Content

Average water contents were measured and are presented in Figure 4.3 along with 95 % confidence intervals error bars—for both combined and separate phases—during the aging study at 80 °C for up to 504 h. When examining the combined phase, water content remained approximately constant within the first 168 h (1 week) of aging and started to increase after 336 h (2 weeks) with measured 9 and 19.5 % increases after 336 and 504 h of aging, respectively. After 336 h of aging, the top phase water content had increased by 57 % and the bottom phase had decreased by 19 %. After 504 h, the top phase had increased by 70 % and the bottom phase decreased by 18 % compared to the

control. It is easy to conclude that the phase separation occurring is the water induced phase separation rather than the lignin-rich phase separation especially because as the top phase water content surpasses the 30-35 wt% of water described as the maximum amount prior to phase separation [Bridgewater 2003].

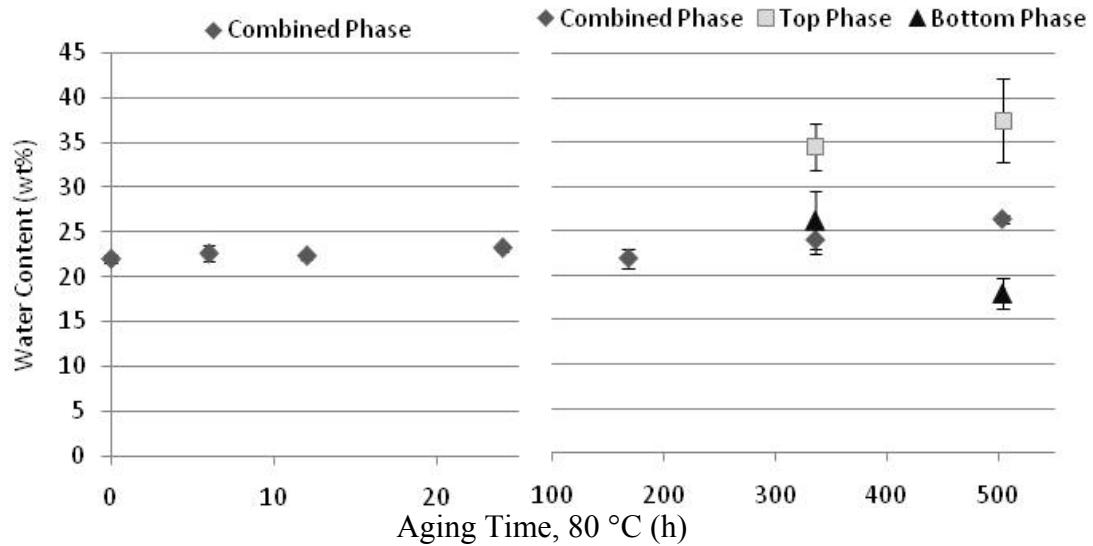


Figure 4.3 Water content for PWTF-94 pyrolysis oil aged at 80 °C for up to 24 h (left) and 168 to 504 h (right) for combined, top and bottom phases (with 95% CI error bars).

4.4.5 Calorimetric Analysis

Caloric data was obtained for combined phase PWTF-94 pyrolysis oil at each aging time in the study and for the 3 week top and bottom phases (Figure 4.4). An error bar is included for the 6 h aging time. This large variability in the energy density may be due to the heterogeneous nature of pyrolysis oil. There was no substantial change in the heating values of the combined phase pyrolysis oil samples during aging, but there was a large difference between the top and bottom phases. The top phase had a lower caloric value and may be the result of the high water content in that phase. This suggests that the presence of the top phase may reduce the combined caloric value of the pyrolysis oil as a

fuel and with the removal of the top phase after aging may actually increase the caloric value of the pyrolysis oil.

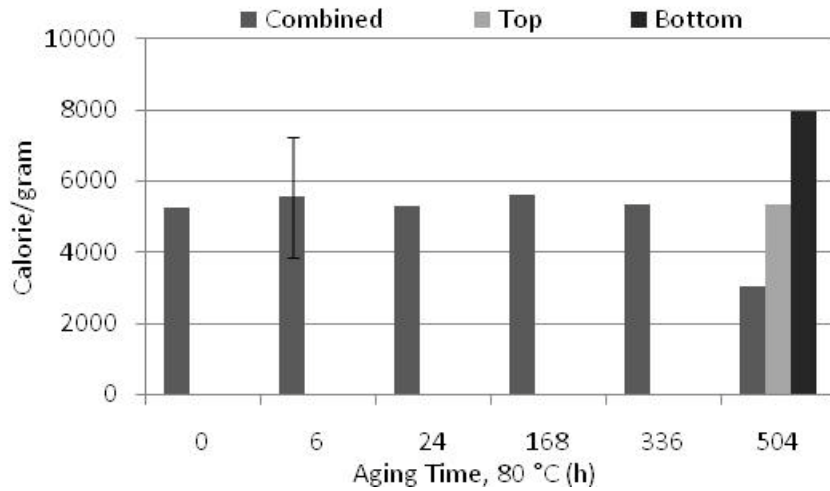


Figure 4.4 Calorimetry data (Calorie/gram) for combined and separate phases of PWTF-94 pyrolysis oil aged at 80 °C for up to 504 h. A 95% CI error bar is presented for the 6 h sample.

4.4.6 Viscosity

Viscosity data collected for the PWTF-94 pyrolysis oil aged at 80 °C for up to 504 hours is presented in Figure 4.5. Viscosity increased with aging time through the 168 h samples (1 week). The viscosities increased 24.7, 35.7, 66 and 170 % for 6, 12, 24 and 168 hours of aging, respectively, as compared to the neat viscosity of 27.2 cP ± 0.52. The viscosity then decreased by 13 % between 168 (1 week) and 336 h (2 weeks) and further decreased another 70 % between 336 (2 weeks) and 504 h (3 weeks). The 504 h sample viscosity, 19.5 cP ± 2.3, was 28 % lower than the neat value of 27.7 cP ± 0.52.

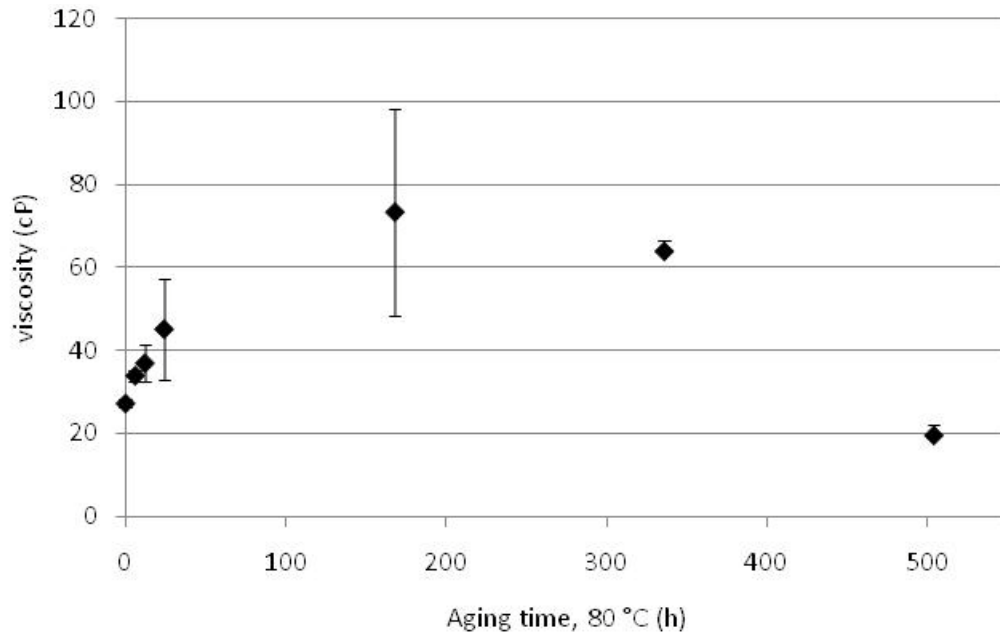


Figure 4.5 Average viscosities for PWTF pyrolysis oil aged at 80 °C for up to 504 h. Error bars represent 95% CI.

Samples aged up to 168 h displayed Newtonian properties while the samples aged for 336 h and 504 h displayed non-Newtonian properties. In addition, the samples aged for 504 h were also phase separated. Stepped shear data is presented in Figure 4.6 comparing for the unaged and aged PWTF oil samples. The phase separation can explain the non-Newtonian behavior observed in the 336 h and 504 h samples due to the creation of an emulsion between the polar and non-polar phases.

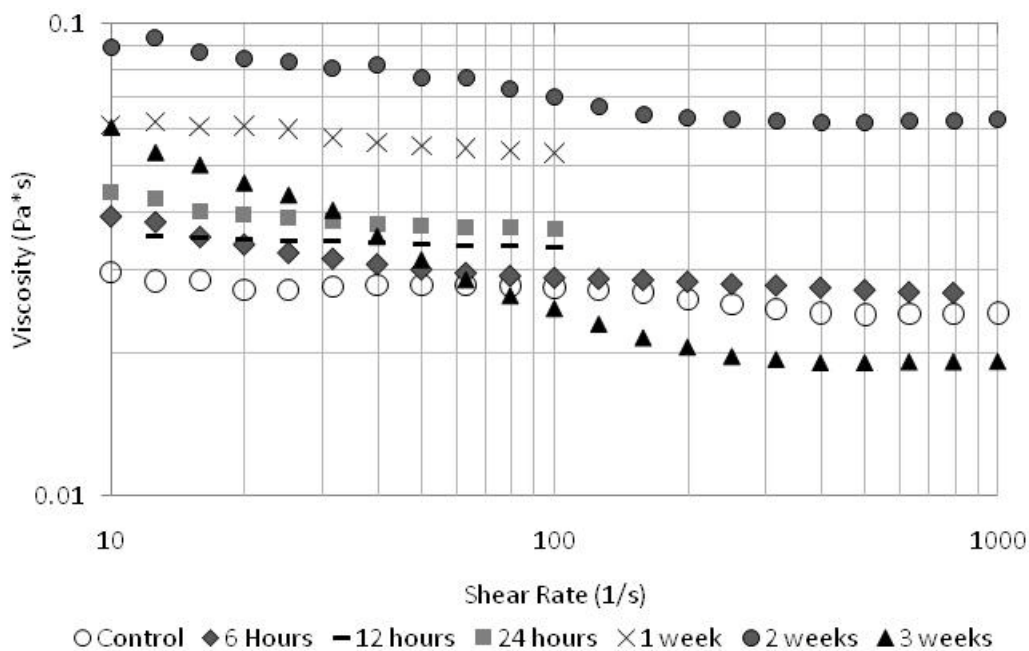


Figure 4.6 Rheology data (collected at 40 °C; 10-1000 1/s) for PWTF-94 pyrolysis oil aged at 80 °C for up to 504 h.

4.4.7 Pendant Drop

Pyrolysis oil pendant drop was conducted in air for the neat and aged samples to better understand the age-dependent changes. The evolution of a second liquid phase, potential containing particulates, during aging was evidenced by the increasing volume of the second phase over time as displayed in Figure 4.7. Photographs of pendant drop of the neat PWTF and 6 and 12 h aged samples have some small droplets within the total oil sample and can be seen in the pendant drop. The sample aged at 80 °C for 24 h has a much larger concentration of the second phase droplets. For the 1 week and 3 week samples the top phase was examined due to the opacity of the bottom phase. Even post phase separation the 1 and 3 week samples have large amount of phase droplets with the apparent largest concentration in the 3 week sample displaying the evolution of the phase formation during aging.

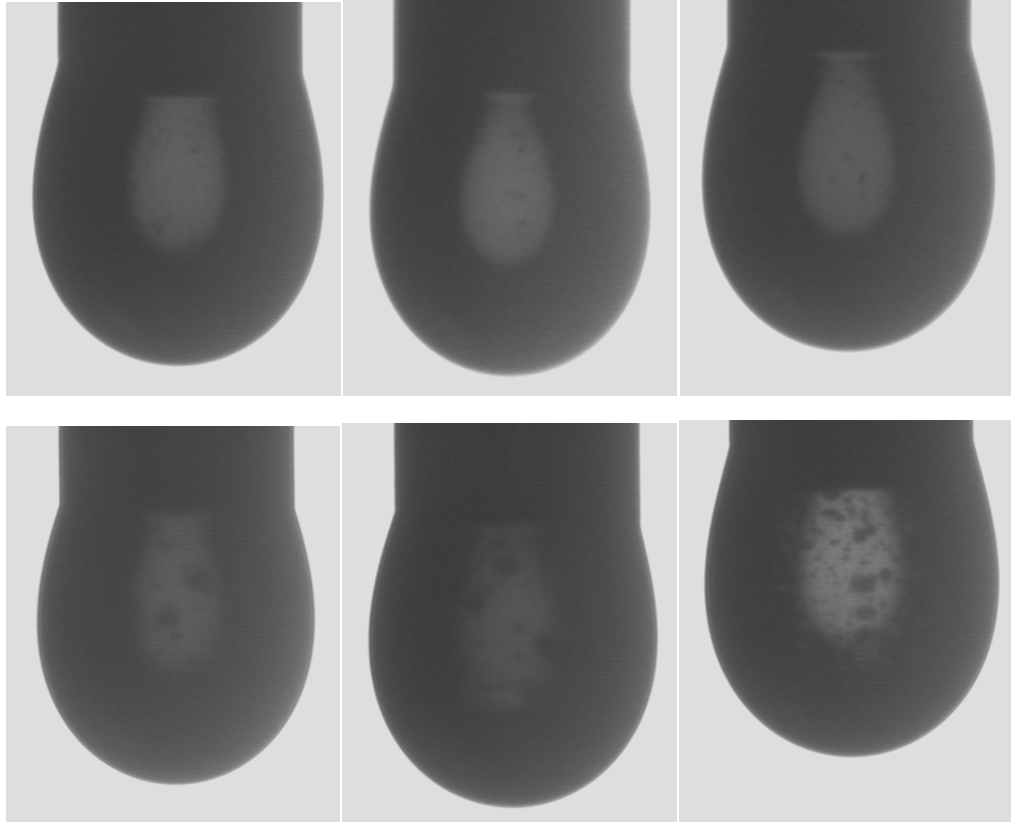


Figure 4.7 Pendant drop images for PWTF pyrolysis oil aged at 80 °C for 6 h and 12 h [top L-R] and 24 h, 336 h (1 week)* and 504 h (3 weeks)* [bottom L-R]. (* Droplets of the top phase only.)

Interfacial tension (IFT) can be a tool to gain more insight into the cause of phase separation during aging and can be measured using pendant drop analysis. Figure 4.8 presents the IFT for the complete pyrolysis oil prior to phase separation and the IFT of the top and bottom phases individually afterwards.

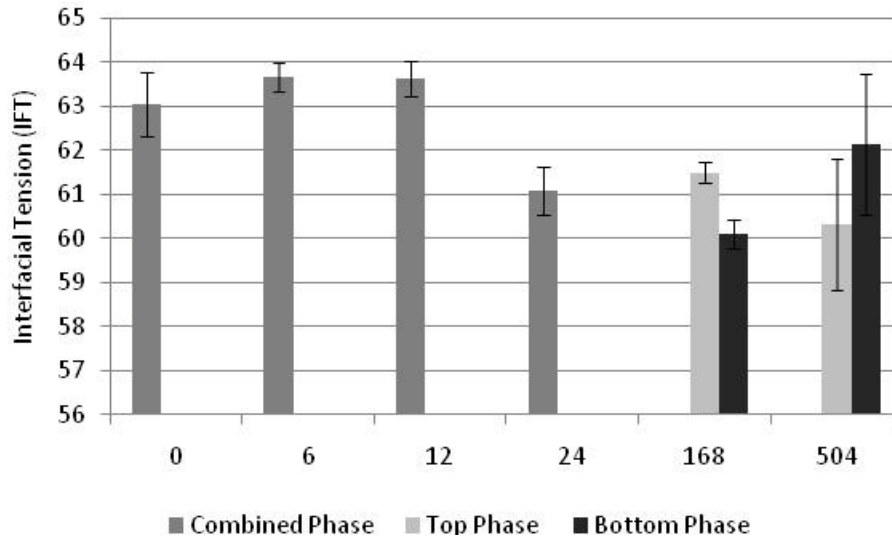


Figure 4.8 Interfacial tensions (IFT) measured using the pendant drop method for PWTF oil samples as a function of aging time at 80 °C.

4.4.8 GPC

Trends in the weight average molecular weight (Mw) over the course of aging at 80 °C are shown for the combined and separate phases of PWTF pyrolysis oil in Figure 4.9. For the combined phase samples, the Mw increased as a function of aging time demonstrating increases of 24, 44 and 83 % after 24, 168 and 336 hours of aging, respectively. After 336 hours, the average Mw decreased only slightly (3 %) between 336 and 504 h indicating a possible plateau after 336 hours of aging. In contrast, after 336 h the top layer decreased in Mw returning to the original Mw and the bottom phase increased by 83 and 103 % after 336 h and 504 h of aging, respectively. This trend is similar to that in the water content but in reverse. A condensation reaction resulting in water formation could produce larger molecular weight compounds such that after phase separation the water remains in the top phase and the higher molecular weight (“heavy”) molecules precipitate out forming the bottom phase. A further increase in molecular weight in the bottom phase and increase in the water content in the top phase after phase

separation indicates the aging reaction(s) continue after phase separation but it is difficult to determine if these reactions are occurring solely in one phase by examining only the water content and molecular weight.

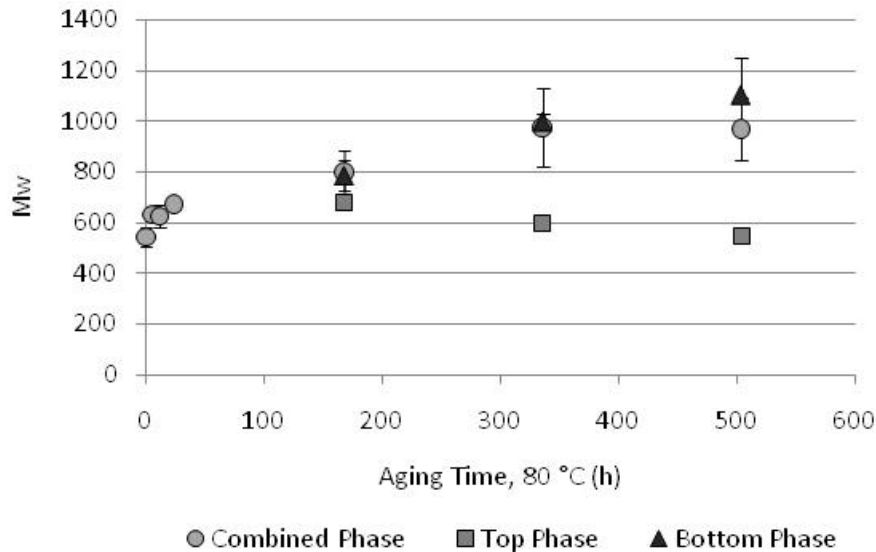


Figure 4.9 Measured weight average molecular weight (Mw) as a function of aging time (at 80 °C) up to 504 h for combined, top and bottom phases. All data points include 95 % confidence interval error bars.

An overview of the GPC data results are presented in Table 4.2 including the number average (Mn), weight average (Mw), and size average (Mz) molecular weights as well as the polydispersity (PDI) as a function of aging time at 80 °C for PWTF pyrolysis oil. Mn and Mz follow the same trend as the Mw and increase during aging. The polydispersity index (PDI) indicates the relative distribution of the molecular weight of the samples and is calculated by dividing Mw by Mn. PDI increased during aging indicating a broader distribution of molecular weights in the aging samples.

Table 4.2 GPC data overview including number average (Mn), weight average (Mw), and size average (Mz) molecular weights and polydispersity index (PDI) for PWTF pyrolysis oil combined phase after aging at 80 °C up to 504 hours.

Aging Time (hours)	Mn	Mw	Mz	PDI
0	363	551	956	1.52
6	385	632	1178	1.64
12	382	627	1123	1.64
24	394	674	1212	1.71
168	442	798	1462	1.80
336	472	975	2093	2.06
504	474	971	2039	2.04

Table 4.3 GPC data overview including number average (Mn), weight average (Mw), and size average (Mz) molecular weights and polydispersity index (PDI) for PWTF pyrolysis oil top and bottom phases after aging at 80 °C up to 504 hours.

Hours	Mn	Mw	Mz	PDI
168 Top	387	683	1349	1.77
168 Bottom	423	785	1570	1.86
336 Top	360	599	1148	1.66
336 Bottom	469	998	2176	2.13
504 Top	345	546	995	1.58
504 Bottom	481	1104	2613	2.29

4.4.9 GC/MS

Chromatograms for the PWTF samples are presented in Figure 4.10 for the single-phase neat sample and top and bottom phases after 336 and 504 h of aging at 80 °C. After 336 h there is little to no difference in the bottom phase chromatogram but some increases were observed in the top phase. In contrast, after 504 h of aging the bottom phase showed the larger changes in peak heights than in the top phase. This may be due to difficulty in consistently sampling the two separate phases, single samples, or it is possible that at shorter times reactions occur in the top phase and then at longer times the product precipitates into the bottom phase.

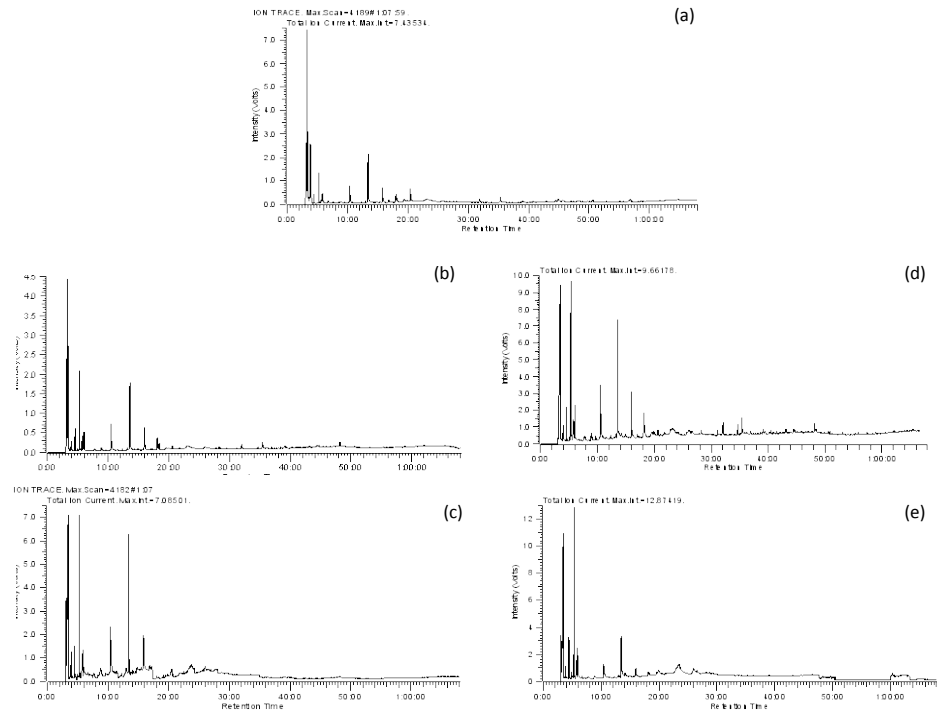


Figure 4.10 GC-MS Ion Chromatogram for PWTF-94 neat (a), 336 h bottom (b) and top (c) phases and 504 h bottom (d) and top (e) phases.

After two weeks of aging, there were overall increases in the percent change in height compared to the control in the top phase including 2-heptyn-1-ol, 2-methyl-trans-1,1-bicyclohexyl and 2-methoxy-2-methyl-phenol and there were small decreases or no change in the bottom phase when compared to the neat pyrolysis oil. In the three week samples, the larger increases were in the top phase including 2-heptyn-1-ol, tetrahydro-2-furanmethanol and 2-methoxy-2-methyl-phenol and the bottom phase had large increases over all especially in the phenolic compounds such as 2-methoxy-phenol, 3, 4-dimethyl-phenol, 2-methoxy-4-methyl-phenol, 4-ethyl-2-methoxy-phenol, and 1-(cyclohexylmethyl)-2-methylcyclohexane.

Considering there was little to no change observed in the bottom phase after two weeks of aging and then the large increase in phenolic compounds after three weeks suggests that the aging reaction(s) may occur in the top phase after phase separation and

the product precipitates to the bottom phase after a significant amount or high enough molecular weight has formed. Also, phenolic compounds abundant in the PWTF pyrolysis oil are the result of lignin [Diebold 2000] and thus lignin rich phase separation could also play a role in phase separation. In addition, the phenolic structures observed are very similar to those identified in to increase in pine whole tree fractionated pyrolysis oil [Chapter 5] showing a similarity in these aging reactions.

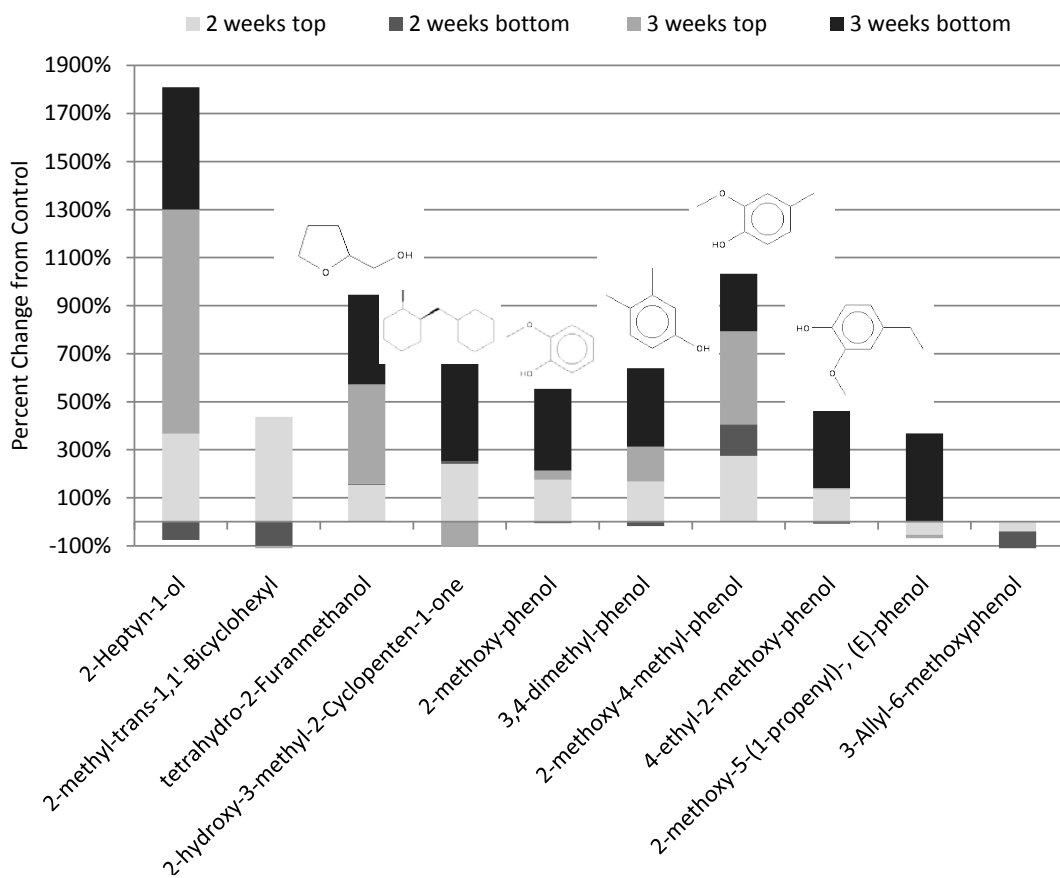


Figure 4.11 GC-MS determined percent change in concentrations, based on the control, for the top and bottom phases of PWTF-94 pyrolysis oil after aging at 80 °C for 336 and 504 h along with chemical structures.

4.4.10 ATR-FTIR Spectroscopy

ATR spectra collected for the PWTF pyrolysis oil combined phase aged at 80 °C for up to 504 hours are displayed in Figure 4.12 and the separate phases for the 336 h and 504 h samples in Figure 4.13. When comparing the ATR spectra, there are no significant changes in the peaks during aging. There appears to be a minor change in the shape of the carbonyl peak (C=O st; 1710 cm⁻¹) and aromatic peak (C=C st.; 1639 cm⁻¹) [Pretsch]. Surprisingly there is no significant difference when comparing the top and bottom phases even though the water content and molecule weight have very different values. This suggests that there is no chemical difference between the functional groups in each phase and perhaps a polymerization reaction is simply adding monomers/oligomers and increasing the molecular weight.

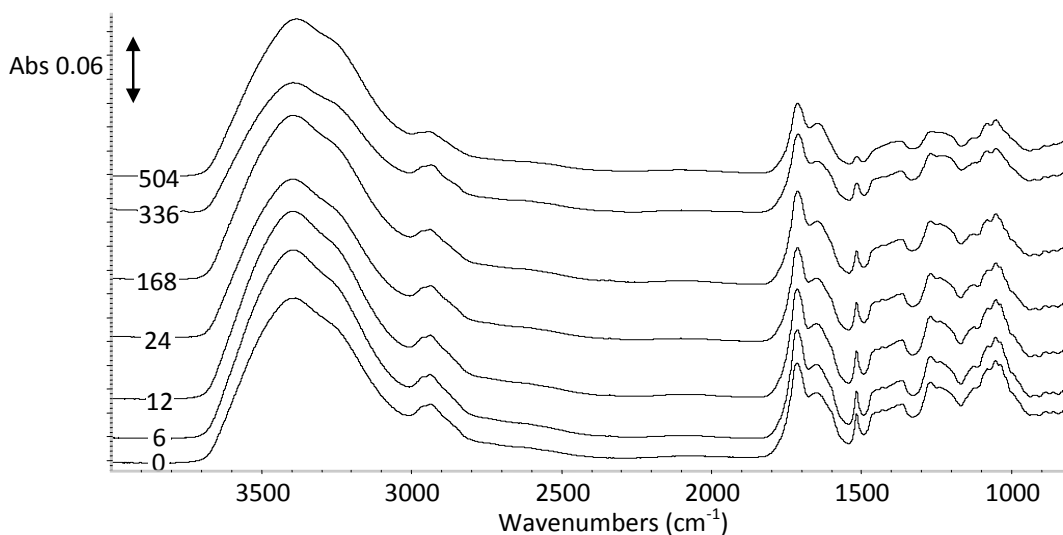


Figure 4.12 ATR FTIR spectra of the PWTF pyrolysis oil neat (0 hours) and aged at 80 °C for up to 504 h.

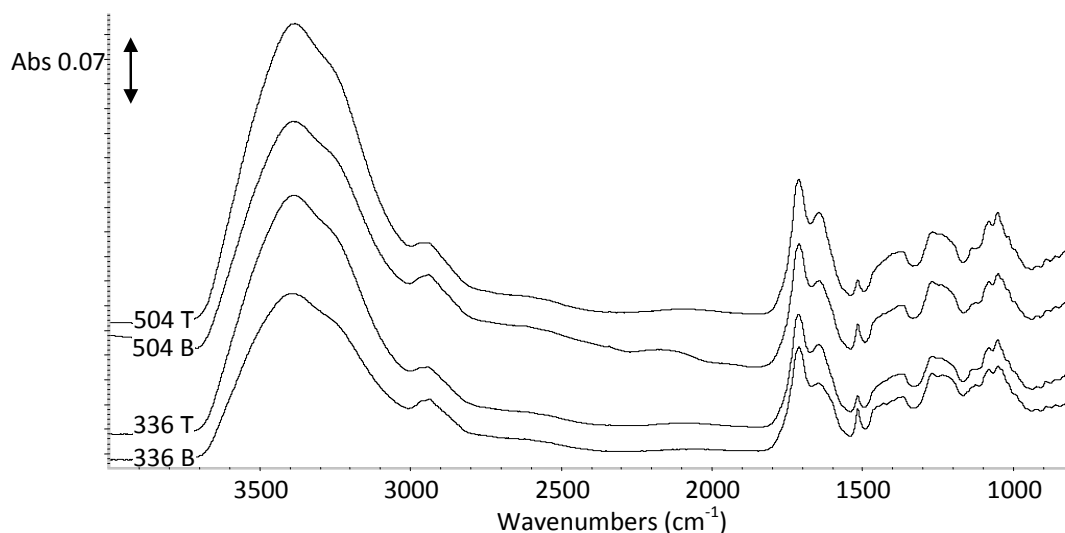


Figure 4.13 ATR-FTIR spectra of the top and bottom phases of PWTF pyrolysis oil aged at 80 °C for 336 and 504 h.

Quantitative FTIR analysis by peak height ratio (PHR) was conducted with the result of significant changes in five major peaks. First, an increase was observed in the hydroxyl peak ($\sim 3350\text{ cm}^{-1}$) representing the hydrogen bonded OH stretch [Pretsch, Silverstein]. PHR decreased for the peaks at 1133 cm^{-1} and 1079 cm^{-1} that can be assigned to the C-O stretch in alcohol, ester and/or ether [Silverstein, Pretsch]. The peaks at 1051 cm^{-1} (C-O stretch, primary alcohol; Kuptsov, Silverstein, Nakanishi) and 1035 cm^{-1} (C-O stretch of an alcohol or ester; Silverstein, Nakanishi or the =C-O-C stretch of an aromatic or vinyl ether; Pretsch, Nakanishi) also has PHRs that decreased during aging.

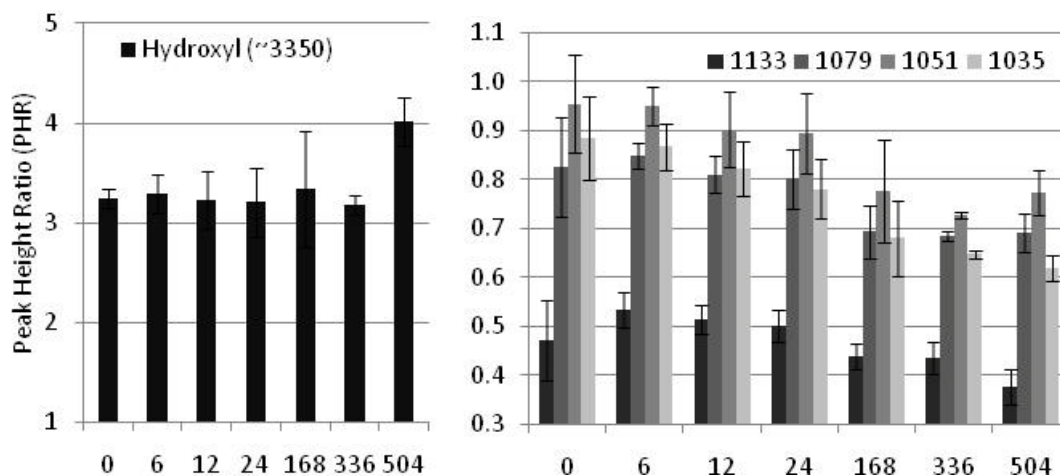


Figure 4.14 Peak height ratios calculated for five key peaks over aged up to 504 h at 80 °C.

Peak fitting was conducted over the region between 1800-1560 cm^{-1} and resulted in three peaks (Figure 4.15). Peaks were identified as C=O stretch in an aliphatic or cyclic ketone and/or a carboxylic acid dimer (1714-1711 cm^{-1}) [Silverstein, Pretsch, Nakanishi], C=C stretch in alkenes and/or C=O stretch in a conjugated ketone (1653-1644 cm^{-1}) [Silverstein, Pretsch, Nakanishi] and C=C in aromatic hydrocarbons and/or skeletal stretching in heteraromatics (1613-1602 cm^{-1}) [Silverstein, Pretsch]. Peak height ratios were conducted using the heights for the fitted peaks and are presented in Figure 4.16. There was little to no change in the aromatic C=C peaks (1653-1644, 1613-1602 cm^{-1}) but the ketone/acid peak did increase during aging.

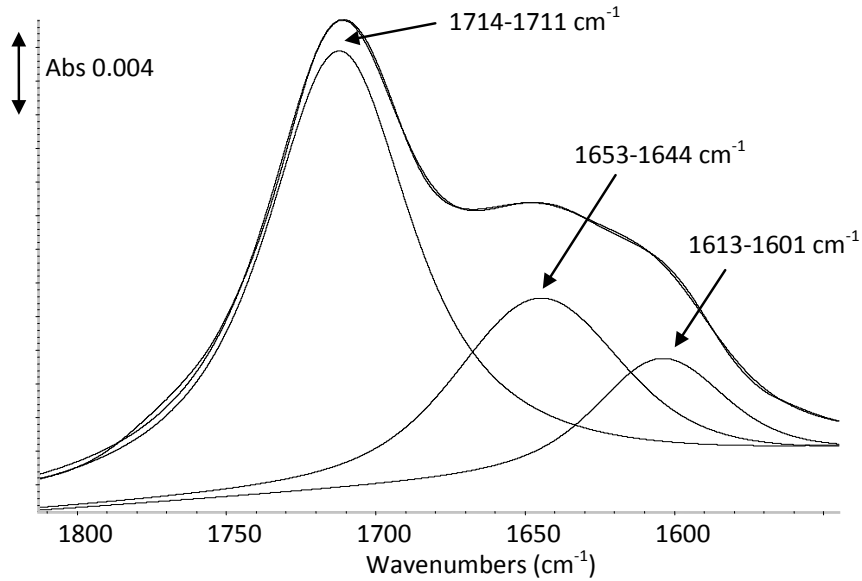


Figure 4.15 Peak resolution representation for neat PWTF-94 pyrolysis oil.

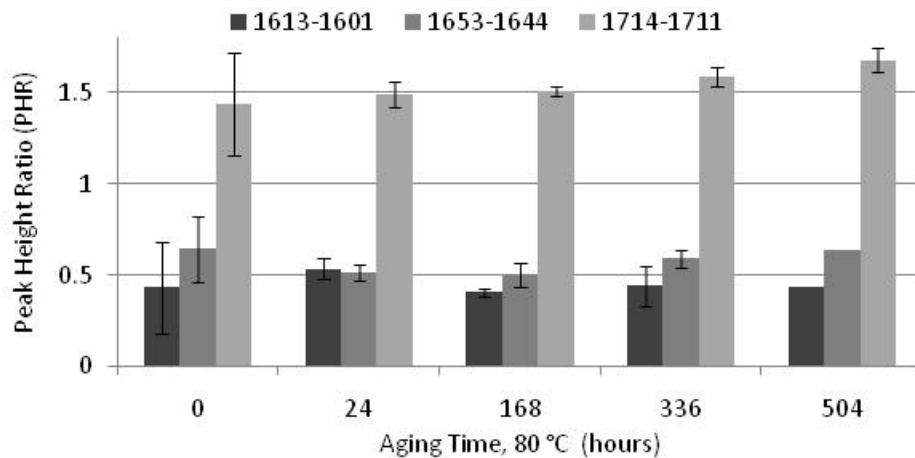


Figure 4.16 Peak height ratios for peaks found in peak resolution.

4.4.11 Proposed Reactions/ Phase Separation Mechanisms

Phase separation is most likely due to the increase water content due to condensation reactions occurring throughout aging as described in previous research where water content is above 30-35 wt% [Bridgewater 2003]. In addition, it has been previously postulated that etherification and esterification between hydroxyl, carbonyl

and carboxyl groups occurs to form water [Diebold 1997]. When considering the phenolic compounds containing hydroxyl and ether functional groups observed in GC/MS combined with the decrease in alcohol, ether and/or ester functional groups observed with ATR, there are a wide variety of possible reactions that could be occurring. However, there was not any evidence of an increase in ester or ether functionality in the ATR analysis to support etherification or esterification. When looking at the overall changes occurring during aging in the ATR data there are increases C=C and/or C=O bonds and decreases C-O bonds which indicates a C-O bond reacts to form C=C and/or C=O bonds.

Common condensation reactions that may produce water include alcohols reacting to produce either ethers or alkenes [Carey], but ethers are not being produced but rather consumed. Oxidation of primary alcohols can produce carboxylic acids and secondary alcohols can easily produce ketones in the presence of a strong oxidizing agent at room temperature or slightly elevated [Smith 2007]. This reaction proceeds rapidly when secondary alcohols are in acetone and Jones reagent (solution of chromic acid and sulfuric acid in water) is titrated [Smith 2007]. It would be possible to have oxidation occur in pyrolysis oil if an oxidizing agent was present, and with the 400 compounds reported this could be possible. Oxidation can also occur in benzylic positions which could lead to substituted phenolic compounds.

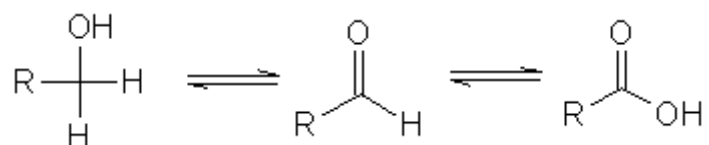


Figure 4.17 Oxidation of primary alcohol to produce a carboxylic acid with an aldehyde intermediate [Carey ochem]

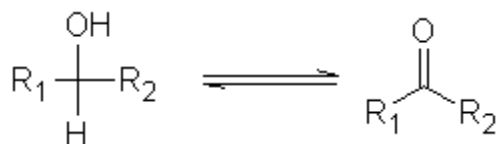


Figure 4.18 Oxidation of secondary alcohol to produce a ketone [Carey ochem]

Examining all of the data collected oxidation of alcohols accounts for the decrease in alcohols and increase in ketones and/or carboxylic acids in addition to the formation of water. On the other hand, it does not account for the increase in molecular weight.

Previous pyrolysis oil research has suggested condensation and polymerization reactions to play a larger role in aging [Chaala 2004]. Polycondensation is described as a reaction involving OH, COOH, etc. that forms new compounds with the release of low molecular weight materials such as water, alcohol, etc. [Chaala 2004]. When molecules involved in polycondensation contain more than two functional groups, high molecular weight, three dimensional polymers can be produced which were shown to be present in bottom phases of softwood bark pyrolysis oil in previous work [Chaala 2004]. Additional research has also proposed polycondensation as a mechanism for the increasing molecular weights [Boucher 2000, Garcia-Perez 2006]. In chain growth polymerization reactions, C=C in alkenes and C=O bonding in ketones and aldehydes are the most important participating functional groups where an active molecule added to one atom of the double bond producing a new active species on the other atom [Rudin 1982]. In addition ketones and aldehydes are polymerized by ionic or heterogenous catalytic processes rather than a radical polymerization [Rudin 1982]. It is possible that ketones are produced that then participate in a polymerization reaction. If this is the case, the production of ketones would have to be larger than the polymerization consumption for there to be an increase

indicated in ATR or it could be possible that there are one or more intermediates that are not detected during characterization.

4.5 Conclusions

Phase separation occurred between 168 and 336 h of aging at 80 °C and was due to the increase in water content above 30-35 wt%. Evolution of phase separation was visually observed in pendant drop samples throughout aging process (0-504 h). Top and bottom phases were characterized separately and found to have very different properties. The top phase had high water content (34.5-37.5 wt%) and low molecular weight (545-599 Da) and the bottom phase had low water content (26.3-18.0 wt%) and high molecular weight (997-1104 Da). The caloric value of the bottom phase (7965.7 Cal/g) was significantly larger than the top phase (3064.4 Cal/g). Molecular weight and water content continued to increase after phase separation and reaction products concentrated in the bottom phase indicating the reaction occurs in the bottom phase or the products precipitate out of the top phase.

Increased amounts of ketone and/or carboxylic acid functional groups were observed in IR analysis along with decreases in alcohol, ether and/or ester groups. Oxidation of alcohols to form carboxylic acids and ketones explains the increase in water content and decrease in ketones with aging. In addition, polycondensation may account for the increase in molecular weight in addition to the water formation.

4.6 References

ASTM Standard E 203-01 Standard method for water using volumetric Karl Fischer Titration p. 396-405.

ASTM Standard D 240-92 Standard method for Heat of Combustion of Liquid Hydrocarbon Fuels by Bomb Calorimetry p. 133-140.

Ba, T.; Chaala, A.; Garcia-Perez, M.; Roy, C. Colloidal Properties of Pyrolysis oils Obtained by Vacuum Pyrolysis of Softwood Bark. Storage Stability. *Energy & Fuels* 2004, 18, 188-201.

Boucher, M.E.; Chaalab, A.; Roy, C. Pyrolysis oils obtained by vacuum pyrolysis of softwood bark as a liquid fuel for gas turbines. Part I: Properties of pyrolysis oil and its blends with methanol and a pyrolytic aqueous phase. *Biomass & Bioenergy* 2000, 19, 351-361.

Bridgewater, A.V. Renewable fuels and chemicals by thermal processing of biomass. *Chemical Engineering Journal* 2003, 91, 87-102.

Bruice, P.Y., Organic Chemistry, Fourth Edition. Prentice Hall, 2004.

Carey, F.A., Sundberg, R.J. Advanced Organic Chemistry, Fourth Edition. Part B: Reactions and Synthesis. Kluwer Academic/Plenum Publishers: New York, 2000; p. 332-339, 693-695.

Chaala, A.; Ba, T.; Garcia-Perez, M.; Roy, C. Colloidal Properties of Pyrolysis oils Obtained by Vacuum Pyrolysis of Softwood Bark: Aging and Thermal Stability. *Energy & Fuels* 2004, 18, 1535-1542.

Diebold, J.P.; Czernik, S. Additives To Lower and Stabilize the Viscosity of Pyrolysis Oils during Storage. *Energy & Fuels* 1997, 11, 1081-1091.

Elliot, D.C. Water, Alkali and Char in Flash Pyrolysis Oil. *Biomass & Bioenergy* 1994, 7, 79-185.

Garcia-Perez, M.; Chaala, A.; Pakdel, H.; Kretschmer, D.; Rodrigue, D.; Roy, C. Multiphase Structure of Pyrolysis oils. *Energy & Fuels* 2006, 20, 364-375.

Garcia-Perez, M.; Chaala, A.; Pakdel, H.; Kretschmer D.; Rodrigue, D.; Roy, C. Evaluation of the Influence of Stainless Steel and Copper on the Aging Process of Pyrolysis oil. *Energy & Fuels* 2006, 20, 786-795.

Mohan, D.; Pittman, C.U; Steele, P.H. Pyrolysis of Wood/Biomass for Pyrolysis oil: A Critical Review” *Energy & Fuels* 2006, 20, 848-889.

Mullaney, H. Technical, Environmental and Economic Feasibility of Pyrolysis oil in New Hampshire's North Country. New Hampshire Industrial Research Center (NHIRC) 2002.

Nakanishi, K.; Solomon, P.H. Infrared Absorption Spectroscopy. Holden Day: Oakland, 1977; p. 14, 19, 25,26, 31, 38-40.

Oasmaa, A.; Peacocke, C.; A guide to physical property characterisation of biomass-derived fast pyrolysis liquids. Technical Research Centre of Finland, VTT Publication 450, ESPOO 2001.

Oasmaa, A.; Kuoppala, E. Fast Pyrolysis of Forestry Residue. 3. Storage Stability of Liquid Fuel. *Energy & Fuels* 2003, 17, 1075-1084.

Oasmaa, A.; Kuoppala, E.; Gust, S.; Solantausta, Y. Fast Pyrolysis of Forestry Residue. 1. Effect of Extractives on Phase Separation of Pyrolysis Liquids. *Energy & Fuels* 2003, 17, 1-12.

Oasmaa, A.; Kuoppala, E.; Selin, J.; Gust, S.; Solantausta, Y. Fast Pyrolysis of Forestry Residue and Pine. 4. Improvement of the Product Quality by Solvent Addition. *Energy & Fuels* 2004, 18, 1578-1583.

Pretsch, E.; Buhlmann, P.; Affolter, C. Structure of Determination of Organic Compounds, Tables of Spectral Data; Springer: New York, 2000; p. 245, 255, 263, 264, 286, 287, 291, 293.

Qi, Z.; Jie, C.; Tiejun, W.; Ying, X. Review of biomass pyrolysis oil properties and upgrading research. *Energy Conversion and Management* 2007, 48, 87-92.

Rudin, A., The Elements of Polymer Science and Engineering; Academic Press, Inc.: New York, 1982; p. 192.

Silverstien, R.M.; Webster, F.X. Spectrometric Identification of Organic Compounds; John Wiley & Sons Inc.: New Jersey, 1998; p. 82, 86, 87, 90-92, 94 95, 97.

Smith, M.B.; March, J. March's Advances Organic Chemistry; Wiley-Interscience; 2007.

Wang, J.; Chang, J.; and Fan, J. Upgrading of Pyrolysis oil by Catalytic Esterification and Determination of Acid Number for Evaluating Esterification Degree. *Energy Fuels* 2010, 24, 3251-3255

Westerhof, R.J.M.; Kuipers, N.J.M.; Kersten, S.R.A.; Swaij, W.P.M. Controlling the Water Content of Biomass Fast Pyrolysis Oil. *Industrial and Engineering Chemistry Research* 2007, 46, 9238-9247.

Westerhof, R.J.M.; Brilman, D.W.F.; van Swaaij, W.P.M.; Kersten, S.R.A. Effect of Temperature in Fluidized Bed Fast Pyrolysis of Biomass: Oil Quality Assessment in Test Units. *Industrial and Engineering Chemistry Research* 2010, 49, 1160–1168.

CHAPTER V

POST CONDENSATION FILTRATION OF PINE AND COTTONWOOD PYROLYSIS OIL AND THE IMPACT ON ACCELERATED AGING REACTIONS

5.1 Abstract

Effects of filtration on pine pyrolysis oil were investigated under accelerated aging conditions, 80 °C for up to 3 weeks. Neat (as produced) pyrolysis oil underwent a serial filtration by vacuum filtration [20-25 µm] followed by centrifugal filtration [0.2 µm]. Neat and filtered pyrolysis oil samples were then aged at 80 °C for 1, 2 and 3 weeks. Physical characterization included pH, water content and viscosity measurements and attenuated total reflectance Fourier transform infrared (ATR-FTIR) spectroscopy, gel permeation chromatography (GPC), and coupled gas chromatography-mass spectroscopy (GC/MS) were utilized to identify and monitor chemical composition. The filtered solids were characterized by particle size distribution and diffuse reflectance FTIR (DRIFT) spectroscopy. Serial filtration removed over 80 % of the particles in the pyrolysis oil and DRIFT analysis showed the particles were likely entrained char. A 288 % increase in viscosity was observed in the unfiltered pine pyrolysis oil upon aging at 80 °C for 3 weeks. Filtration prevented this viscosity increase. However, filtered samples were shown to have lower pH, higher water content, and higher average molecular weight. Considering the possibility of chemical reactions during aging, GC/MS analyses indicated higher concentrations of substituted phenolic and ether compounds in both unfiltered and filtered samples and these chemical changes were confirmed by ATR-

FTIR. It is concluded that filtration can prevent the viscosity increase that is commonly encountered in pyrolysis oil during storage/aging, but filtration did not impact chemical changes that are observed during aging.

A second, more extensive serial filtration study was conducted with pine and cottonwood pyrolysis oils with 2- and 3-step filtrations to further investigate the effect of filtration on pyrolysis oil properties during accelerated aging. Neat pine bark fractionated [PBF] and cottonwood clear wood fractionated [CCWF] pyrolysis oil underwent a serial filtration by vacuum filtration [20-25 μm] followed by centrifugal filtration [0.2 μm]. Neat pine clear wood total [PCWT] and fractionated [PCWF] pyrolysis oils also underwent a serial filtration by vacuum filtration [20-25 μm] followed by a second vacuum filtration [2.5 μm] and concluding with a centrifugal filtration [0.2 μm]. Unfiltered and filtered pyrolysis oils were then aged at 80 °C for 6, 12, 24, 168, 336 and 504 hours. Unfiltered and filtered sample characterizations included pH, water content and viscosity measurements and attenuated total reflectance Fourier transform infrared (ATR-FTIR) spectroscopy, gel permeation chromatography (GPC), and coupled gas chromatography-mass spectroscopy (GC/MS) were utilized to identify and monitor chemical composition. After filtration but prior to aging, the water content of the samples decreased and the viscosity increased. After aging, pyrolysis oil samples increased in viscosity, water content and molecular weight regardless of filtration suggesting that the filtration did not prevent or retard the aging reactions. All pyrolysis oil samples exhibited decreases in primary or secondary alcohols and/or ethers in addition to an increase in aromatics and ketones or carboxylic acids showing a similarity in the aging reactions between the samples. GC/MS analysis demonstrated that filtration did alter the aging reactions in PBF, PCWF and PCWT, but not CCWF.

5.2 Introduction

In 2008, 7% of the United States total energy consumption was from alternative energy sources, of which bio-fuels contributed only 0.1% [EIA]. As world energy consumption continues to rise [EIA], interest and research in alternative energy has been renewed in the United States and other countries. Biomass-derived pyrolysis liquids (pyrolysis oils) have the demonstrated potential to contribute to the wide variety of emerging fossil fuel alternatives, as a replacement fuel or a supplement to petroleum-based fuel oil in boilers, furnaces, engines, and turbines [Bridgewater 2003; Fratini, 2006]. With transportation comprising 28% of the total energy consumption in the United States [EIA], significant alternative energy gains could be made through the use of upgraded pyrolysis oil (e.g., emulsification with diesel fuel, hydrotreatment, catalytic vapor cracking) as an extender in transportation fuels [Bridgewater 2004 therm sci]. Use of forestry residue as the biomass feedstock for pyrolysis oil production could provide a low-cost fuel for the southeastern United States where forestry industry is prevalent. There is also potential for fast-growth tree farms where young whole trees are harvested and chipped to provide another renewable timber biomass source for biofuel production. This type of fast growing feedstock could provide a sustainable source for energy and spur economic growth in the forestry industry. Fast pyrolysis can be implemented with various reactor designs to produce pyrolysis oil, but the physical and chemical properties of the oil product can vary greatly depending on the biomass feedstock [Bridgewater 2004] and reactor operating conditions [Ba 2004]. Bubbling fluid bed, circulating fluid bed, ablative pyrolysis, rotating cone, and vacuum pyrolysis reactors have been used for pyrolysis oil production [Bridgewater 2003]. While multiple reactor configurations have been designed to provide high heating rates, it has been shown that fluidized and

transport bed reactors produce the highest yields [Ringer]. Although high yields can be achieved, there are still several barriers preventing the direct utilization of pyrolysis oil as a fuel including thermal instability, low pH [Garcia-Perez 2006, 2007], low colorific value [Garcia-Perez 2007], high viscosity, water content and inorganic content [Agblevor, 1996], and poor lubrication [Garcia-Perez 2007] compared to petroleum-derived fuels.

Throughout the years, pyrolysis oil has had many names including pyrolysis oil, bio-crude, wood liquids, liquid smoke and wood distillates [Bridgewater 2003]. Pyrolysis oil has been described as a microemulsion where hydrogen bonding stabilizes an aqueous phase of holocellulose-derived compounds and a discontinuous phase of pyrolytic lignin macromolecules [Bridgewater 2003]. Crude pyrolysis oil is relatively polar and contains 33-45 mass % oxygen [Garcia-Perez 2007]. Physical and chemical characterization of pyrolysis oil is complicated by the large number, generally 300+, of chemical compounds [Ringer], 5-30 wt % water [Garcia-Perez 2007], and a wide variety of highly reactive compounds including carboxylic acids, alcohols, aldehydes, ketones, carbohydrates, and degraded lignin [Oasmaa 2003]. Pyrolysis oil is therefore a complex mixture and contains compounds with a wide range of boiling points, from volatile compounds with boiling points under 150 °C, to those similar to gasoline and diesel fuels, to oligomers with high molecular weights and high boiling points [Garcia-Perez 2007].

Storage of pyrolysis oil has been shown to result in increased viscosity at room temperature [Diebold, 1997, Oasmaa 2004] and the rate of this viscosity instability can be accelerated by heat or reduced by cooling [Diebold, 1997]. In addition to increased viscosity, increased water content [Oasmaa, 2004], increased molecular weight,

decreased volatile material concentrations, and phase separation have also been observed when stored especially at elevated temperatures [Bridgewater 2004]. Research by Czernik and coworkers has demonstrated that equivalent viscosities are obtained in oak pyrolysis oil after 3 months of aging at 37 °C, 4 days of aging at 60 °C, or 6 hours of aging at 90 °C [Czernik, 1994]. First order kinetics were successfully used to correlate the observed viscosity increase during aging by modeling the molecular weight increase, but the model may not be applicable to pyrolysis oil from other feedstocks or reactor configurations due to the dependence of viscosity on water content and high molecular weight compounds [Czernik 1994].

It has been proposed that the viscosity increase during storage/aging is the result of molecular weight increases caused by polymerization reaction(s) [Boucher 2000, Czernik 1994]. Using FTIR analysis, it was concluded polymerizations were occurring during storage due to etherification and esterification reactions between hydroxyl, carbonyl, and carboxyl groups [Diebold 1997] resulting in an increase in water due to the condensation reactions [Fratini, 2006].

Inorganic compounds, including alkali metals, are concentrated in char particles [Elliot 1994] and it has been suggested these alkali metals in the char act as catalysts for polymerization reactions [Ringer 2006, Diebold 2000] leading to an increase in viscosity and visible growth in particle diameter [Diebold 2000]. Alkali metals have been found to not leach from char particles into pyrolysis oil [Agblevor 1996], therefore the removal of the char particles reduces the alkali content and has been examined to prevent and/or reduce the (polymerization) reactions that result in increased viscosity during aging.

In addition to catalyzing reactions, alkali metals have been attributed to pyrolysis oil corrosion [Agblevor 1996, Darmstadt 2004] where ash containing alkali metals results

in hot corrosion, fouling steam boiler tubes and erosion of turbine blades [Agblevor 1996]. Thus it is ideal to remove the alkali metals to prevent corrosion and catalyzing aging reactions. Cyclone filtration is included in most pyrolysis reactor systems to remove large char particles such that the char that remaining in the pyrolysis oil is ≤ 10 μm in diameter [Diebold, 2000]. Hot gas filtration in conjunction with a cyclone produces relatively char-free oil [Diebold 1997]. Hot gas filtration can also reduce alkali metals—thought to cause fouling corrosion and erosion in steam boilers and turbines—to 10 ppm [Agblevor, 1996]. The drawback to hot gas filtration is the reduction in yield by 10-20 % [Bridgewater 2003]. Recent research has shown that *in situ* hot gas filtration alone results in higher quality oil without a reduction in yield when compared to oil produced from the same reactor using only a cyclone for filtration [Hoekstra 2009].

Removal of char particles using hot gas filtration and a cyclone prior to condensation significantly slowed pyrolysis oil aging (as monitored by changes in viscosity) when compared to pyrolysis oil filtered only by cyclone [Diebold 1997]. Conversely, the addition of char to pyrolysis oil has been found to accelerate the rate of the viscosity increase during storage at 45 °C over 16 days [Agblevor 1998]. In another study, char/sand particles were collected by successive wire mesh filters integrated into a fluidized bed reactor and external glass filters directly after the reactor that collected char indicating that char formation may occur in particle free vapor outside of the reactor [Hoekstra 2009]. Resulting pyrolysis oil, filtered by both hot gas filtration and a cyclone, was then aged at 80 °C for 24 h and showed increased molecular weights potentially as the result of reactions involving some of the highly reactive compounds found in pyrolysis oil [Hoekstra 2009]. Diebold et al. found that particles had agglomerated during aging in pre-filtered pyrolysis oil and hypothesized that the entrained char

particles that were not filtered just after pyrolysis may have acted as catalytic condensation sites [Diebold 2000].

So, char removal (prior to condensation) was shown to reduce viscosity increases generally observed with aging and the addition of char has been found to accelerate the rate of this aging process [Diebold 1997]. However, even with char filtration, residual char has been found to aggregate during again and possibly serve as catalytic sites for condensation reactions [Diebold 2000]. It has also been theorized that reactions involving reactive species are responsible for forming higher molecular weights compounds and do not require the presence of char or ash [Hoekstra 2009]. So filtration—*in situ*, hot gas, and/or post-condensation—may not be sufficient to prevent pyrolysis oil property changes during aging. It is not clear then the number or type of mechanism that may be causing the viscosity and molecular weight increases during aging. is causing the change in aging reactions.

To determine the role of char in aging reactions, pine whole tree fractionated pyrolysis oil, produced without a cyclone or hot gas filtration, was filtered after condensation, but prior to aging and compared to unfiltered pyrolysis oil. Removed solids were also characterized to determine their composition and microscopy was conducted for unaged and aged pyrolysis oil sampled to observe any changes in solids due to aging.

5.3 Methods and Materials

Feedstock: Plantation grown Loblollypine (*Pinus taeda*) was harvested and the whole tree was divided into needles and bole wood (bark, limbs and wood) and dried to 10-15% moisture content (MC) in an oven (Despatch V series VREZ-19-ZE). Bole wood

biomass was chipped to 1-2 inch chips (Carthage Machine Inc., Model 39 chipper, 1470 rpm), the leaves were added and the resulting total was ground (Bauer Bro. Co., 25 Hp, 1465 rpm), and screened using 30 mesh resulting in particles nominally ≤ 4 mm in diameter (Universal Vibrating Screener, Type S #1354).

Feedstock Part II: Seven trees each of cottonwood and plantation grown Loblollypine (*Pinus taeda*) were harvested; four of which were separated into heart wood, bark and leaf/needle biomass and three were separated into bole wood (bark, limbs and wood) and leaves/needles. This biomass was then dried to 10-15% moisture content (MC) using a Despatch V series oven (VREZ-19-ZE). Both bole wood and heart wood was chipped (separately) to 1-2 inch chips (Carthage Machine Inc., Model 39 chipper, 1470 rpm). Bole wood and leaves/needles were mixed, ground (Bauer Bro. Co., 25 Hp, 1465 rpm), and screened to particles sizes of 4 mm to 6 mm (Universal Vibrating Screener, Type S #1354). Heart wood, bark and leaf/needle biomass was also ground and screened separately prior to pyrolysis and all biomass was dried to 1-2 % MC before pyrolysis.

Pyrolysis Part I: Pyrolysis oil samples were produced by the MSU Forest Products Laboratory using an auger pyrolysis reactor operated under vacuum at 450 °C, an average flow rate of 15-20 L/min, and 25 °C (± 1 °C) water condensers. Fractionated oil refers to a product collected without including the material collected from one of the condensers that contained high concentrations of water and organic acids. Within 1 h of production, samples were stored at ~ 5 °C to minimize aging prior to experiments. Produced pyrolysis oil was dark in color with a pungent smell and consisted of two phases. The top phase exhibited lower viscosity, higher water content, and a translucent yellow/brown color that could be seen easily when separated into small volumes. The bottom phase was more

viscous than the top with lower water content and an opaque dark brown color. Phases were mixed by warming to room temperature and shaking by hand until phases were visibly mixed. All pyrolysis oil samples used in this study were taken from a single 1 L production batch.

Pyrolysis Part II: Auger reactor configuration was altered after Part I study and operated under vacuum at 400 °C.

Filtration Part I: Pine whole tree fractionated [PWTF] pyrolysis oil was filtered prior to aging by vacuum filtration (Whatman Grade 41 filter paper, 20-25 µm pores) followed by centrifugal filtration (Grace 50 mL filter centrifuge tubes, PVDF hydrophobic membrane, 0.2 µm pores) using an Eppendorf 5810R centrifuge at 2500 rpm for up to 30 min. Samples were then removed from the centrifuge tubes and solids were washed from the filters with methanol (99%) and sonicated until methanol remained clear. It is noted that 3-5 wt % of the total sample was lost due to residual oil coating glassware and centrifuge tubes. Vacuum filtration (20-25 µm pore size) resulted in the removal of 4 wt % (based upon initial pyrolysis oil sample mass) of oil-coated solids, and an additional 2.2 ± 0.5 wt % was then removed by centrifugal filtration (10, 0.2 µm pore size filters) resulting in a total weight loss of 6 %.

Filtration Part II: All four sets of pyrolysis oil underwent a crude filtration (SS wire mesh; 1183 µm pores) and then filtered by vacuum filtration (Whatman Grade 41 filter paper, 20-25 µm pores) followed by centrifugal filtration (Grace 50 mL filter centrifuge tubes, PVDF hydrophobic membrane, 0.2 µm pores) using an Eppendorf 5810R centrifuge at 2500 rpm for up to 30 min prior to aging. Pine clear wood total (PCWT) and pine clear wood fractionated (PCWF) pyrolysis oils had an additional, intermediate vacuum filtration step (Whatman Grade 5 filter paper, 2.5 µm pores). Some

of the samples in Part II did phase separate as produced, after filtration or after aging. When phase separation occurred the two phases were analyzed separately.

Aging Conditions Part I: In preparation for the aging studies, 27 mL aliquots of PWTF pyrolysis oil was placed into 30 mL amber bottles with PTFE lined caps (in accordance to recommendations in Oasmaa, 2001). Aged samples were heated in a convection oven at 80 °C for 1, 2, and 3 weeks while control samples were stored in a refrigerator at 5 °C to prevent aging. Caps on the heated jars were retightened daily to minimize weight loss. In addition to the characterizations described below, initial and final weights were recorded at room temperature; the average weight loss during aging was 0.23 +/- .07 wt % and there was only one sample per aging time. Unfiltered and filtered control samples (unaged) had two replicate samples and aged samples had one sample each.

Aging Conditions Part II: Samples were heated in a convection oven at 80 °C for 6, 12, 24, 168, 336 and 504 hours while control samples were stored in a refrigerator at 5 °C to prevent aging. Note: There were one to three samples per aging time depending on the production batch size.

pH and Water Content: The pH of the pyrolysis oil was measured (Mettler Toledo SevenEasy S20 pH meter) with a three point phosphate buffer solution (pH 4, 7 and 10) calibration. Water content was determined by Karl Fischer titration (Barnstead International Aquametry II Apparatus) following ASTM E 203-01 with Hydranal 2E titrant and chloroform-methanol (CM) solvent. Three measurements were collected and averaged to calculate the pH and 95 % confidence intervals.

Viscosity: Step-flow shear tests were conducted using a TA Instruments AR 1500x rheometer and 60 mm aluminum parallel plate geometry. Sample volumes ranged

from 500 to 1200 μm as the volume was maximized in all runs but was dependant on the gap distance and sample viscosity. Temperature was fixed at 40 °C using a Peltier plate and then the sample viscosity was measured over the shear rate range 0.1 to 1000 Hz (1/s). To obtain an average sample viscosity, a minimum of 10 data points were averaged over a plateau region that was observed for these sample at higher shear rates (10-1000 1/s).

Particle Size: Optical micrographs were collected for the neat and filtered pyrolysis oil and the filtered solids were collected at 10, 25 and 63 X magnifications on a Zeiss Axiovert inverted light microscope. Particle size distribution analyses were conducted with Olympus BX51 and Image-Pro Plus software for neat and filtered pyrolysis oil before and after aging.

Molecular Weight Part I: Gel permeation chromatography (GPC) was used for molecular weight (MW) determination based on a seven point polystyrene calibration (486, 582, 891, 2780, 6480, 10261, 18200 MW standards, PSS Polymer Standards). Pyrolysis oil samples were diluted to 1-2 mg/mL using Optima tetrahydrofuran (THF, >95 wt%), sonicated, and then filtered with 0.45 μm syringe filters. A custom-built GPC instrument with a Varian Star 9040 refractive index detector, Waters 610 Fluid Unit, Waters 600 Controller, Varian Mesopore guard column (50 x 4.6 mm ID), and Varian Mesopore column (250 x 4.6 mm ID) was operated at 0.3 mL/min and 50 μL of sample was injected. To account for pressure changes and shifting retention time, a polystyrene standard (Mw = 177,000) was used as an internal standard. Based upon this internal standard, calibration points were shifted to a common position and then shifted collectively to the sample internal standard position. Data analyses were performed using

Star WS and Waters Breeze software packages with a minimum of 4 replicates were examined in order to obtain average values and 95 % confidence intervals.

Molecular Weight Part II: For this second filtration study, two additional polystyrene standards were used with molecular weights of 266 and 126 Da.

FTIR Spectroscopy: Transmission Fourier transform infrared (T-FTIR) spectra were collected of pyrolysis oil smears on KBr crystals using a Nicolet 6700 spectrometer (DTGS detector, 4 cm^{-1} resolution, 128 scans). Attenuated total reflectance Fourier transform infrared (ATR-FTIR) spectra were collected with a ZnSe 60-degree ATR crystal (liquid nitrogen cooled MCT-A* detector, 4 cm^{-1} resolution, 256 scans). All ATR spectra were ATR corrected using Thermo Electron OMNIC software. Diffuse reflectance infrared Fourier transform (DRIFT) spectra of the filtered solids were collected after preparation with 95% KBr powder (liquid nitrogen cooled MCT-A* detector, 4 cm^{-1} resolution, 256 scans). Peak height ratios were calculated by measuring the height of a peak of interest and dividing it by the peak height for the asymmetric methyl C-H stretch peak (2929 cm^{-1}) [Silverstein]. A minimum of 3-5 spectra were collected for each sample to check for sample homogeneity and so that average PHRs could be calculated along with 95 % confidence intervals.

Two methods of Fourier transform infrared spectroscopy were used to analyze the pyrolysis oil, transmission (T) and attenuated total reflectance (ATR). Transmission spectra tended to have larger variations in replicate spectra and subsequently the calculated peak height ratios (PHR). The non-homogeneous nature of pyrolysis oil and the removal of volatiles in the vacuum oven prior to T-FTIR likely caused this variation. ATR-FTIR spectra were found to be much more reproducible than T-FTIR. In addition, since volatiles did not need to be removed prior to ATR-FTIR, the sample preparation

time was significantly reduced and peaks for the volatile materials could be observed in the spectra.

GC/MS Analysis Part I: Coupled gas chromatography-mass spectroscopy (GC/MS) analyses were conducted using a Thermo Finnigan MAT95XL high resolution magnetic sector MS coupled to a HP 6890 GC with a using a Restek Rtx-5MS[®] fused silica column (30 m x 0.25 mm, 0.25 μ m film thickness). GC operating conditions follow. The oven temperature was maintained at 30 °C for 4 min, increased to 290 °C at a rate of 5 °C/min, and then held at 290 °C for 10 minutes. The injector was maintained at 300 °C with a column flow rate of 1.5 mL/min, operated in splitless mode with purge closed for 0.75 min, and then opened with a 75 mL/min flow rate to sweep out residual solvent from the injection port. A GC/MS data analysis method was developed for peak height comparisons where all peak height data were normalized using the sample concentration. Chemical identification was based on the National Institute of Standards and Technology (NIST) database used with MASPEC II 32 data system software. One sample was analyzed by GC/MS for each aging time in both the unfiltered and filtered pyrolysis oil sample sets.

GC/MS Analysis Part I: Unknown chemical compositions were determined using a Varian 3600 gas chromatogram with a Varian Saturn 2000 mass spectrometer (Varian Inc., Walnut Creek, CA) using a fused silica column Rtx-1MS (30 m \times 0.25mm, film thickness 0.25 μ m). The operating conditions were as follows: oven temperature 50-300 °C with a heating rate of 10 °C/min; helium carrier gas; 1.2 mL/min volumetric flow rate; 250 °C detector temperature. Unknowns were identified by comparing sample spectra to the NIST 2005 organic compound database.

5.4 Results and Discussion Part I

Neat (unaltered) pine whole tree fractionated [PWTF] pyrolysis oil flowed freely with a visually low viscosity and little to no bottom phase present. During aging at 80 °C, unfiltered PWTF pyrolysis oil separated into two phases with ~50% (v/v) bottom phase after one week and ~90% (v/v) bottom phase after two weeks. After three weeks of aging at 80 °C, there was little to no top phase present. In stark contrast, the filtered PWTF pyrolysis oil remained one phase even after three weeks of aging at 80 °C. The lack of a bottom phase in the filtered pyrolysis oil prior to and during aging may indicate the bottom phase was filtered from the oil and that any reactions resulting in increased viscosity occur in the bottom phase.

5.4.1 Water Content

It has been suggested that phase separation of pyrolysis oil is due to increased water content [Oasama, 2003, 1-12] and so water content was monitored for both the unfiltered and filtered samples. Average water content data is plotted in Figure 5.1 as a function of aging for both the filtered and unfiltered samples. For the unfiltered pyrolysis oil, water content initially decreased and then steadily increased after 1 week of aging with a 33 % increase in measured water content after 3 weeks at 80 °C. Pyrolysis oil filtered prior to aging showed larger water contents at 1 and 2 weeks versus the unfiltered samples. Water content of the filtered pyrolysis oil increased by 37 % after 2 weeks of aging. (Note: Reliable data could not be obtained for the 3-week, filtered samples due to insolubility of the sample in the titration solvent.) Filtration prior to aging resulted in elevated water contents during aging that may be due to the removal of material during filtration resulting in an increase in water weight percent.

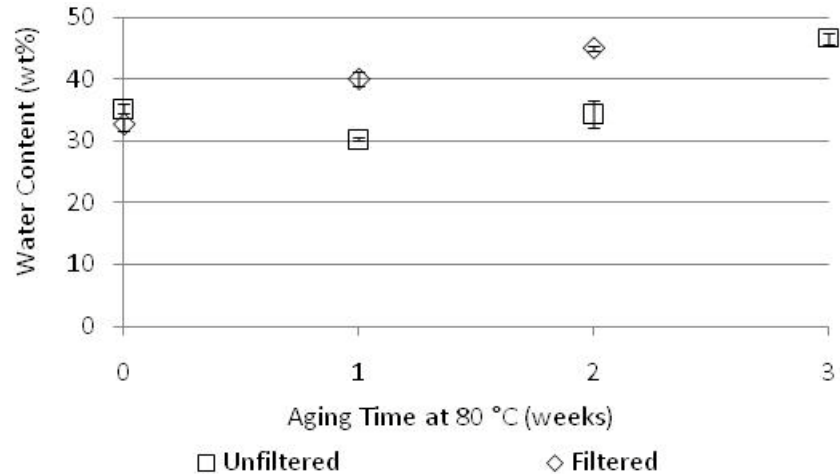


Figure 5.1 Water content data (with 95% CI error bars) as determined by Karl Fischer titration for PWTF pyrolysis oil aged at 80 °C for up to 3 weeks.

5.4.2 pH Measurements

Figure 5.2 displays the measured pH values for the unfiltered and filtered PWTF pyrolysis oil as a function of aging time. There is no significant difference in the pH between the unfiltered and filtered pyrolysis oil for the unaged (0 weeks) samples and so the removal of some solids has not significantly affected the pH. There is also no difference between the pH of the unfiltered and filtered samples at 1 and 2 weeks of aging. At 3 weeks, the unfiltered samples show a slightly higher pH (2.47) than the filtered samples (2.3). The average pH of the PWTF pyrolysis oil decreased slightly from ~ 2.75 to ~ 2.30 over 3 weeks when aged at 80 °C.

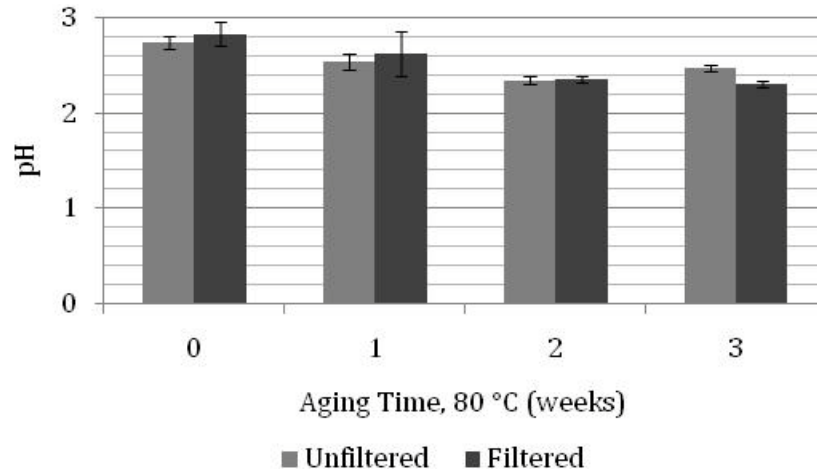


Figure 5.2 Average measured pH values for unfiltered and filtered PWTF pyrolysis oil aged at 80 °C for up to 3 weeks (with 95% CI error bars).

5.4.3 Particle Size Analysis

Optical micrographs are presented in Figure 5.3 comparing neat and filtered pyrolysis oil, with top and bottom phases mixed, prior to and after aging. A reduction in the number of particles due to filtration is evident. Also, there appears to be a change in particle size and shape upon aging that can be most easily observed in the unfiltered aged sample (Figure 3c). A previous study also observed an increase in particle size in a recirculation loop post heating [Chaalal 2004]. Particle size analyses of 50 images per sample were conducted on the unfiltered and filtered controls in addition to the pyrolysis oils aged for 3 weeks and resulted in particle size distributions (Figure 5.4). Due to a reduced number of particles in the filtered aged sample in addition to the increased opacity of the same after aging it was difficult to collect enough data for a particle size distribution and therefore was not included. For the control samples, filtration resulted in a ~81% decrease in particle concentration. The particle size distributions for unfiltered and filtered samples have the same general shape and maxima position; however, the filtered sample shows a lower number of total particles. It would be expected that after

filtration the particle size distribution would shift with a smaller average particle size. This was not found to be the case and may be due to particle agglomeration, limitations of the microscope, or undetected tears in the filters (most likely during centrifuge filtration). In addition when comparing the neat pyrolysis oil to the unfiltered aged pyrolysis oil there is little to no difference in the particle size distribution indicating there is no significant change in the area of the particles during aging.

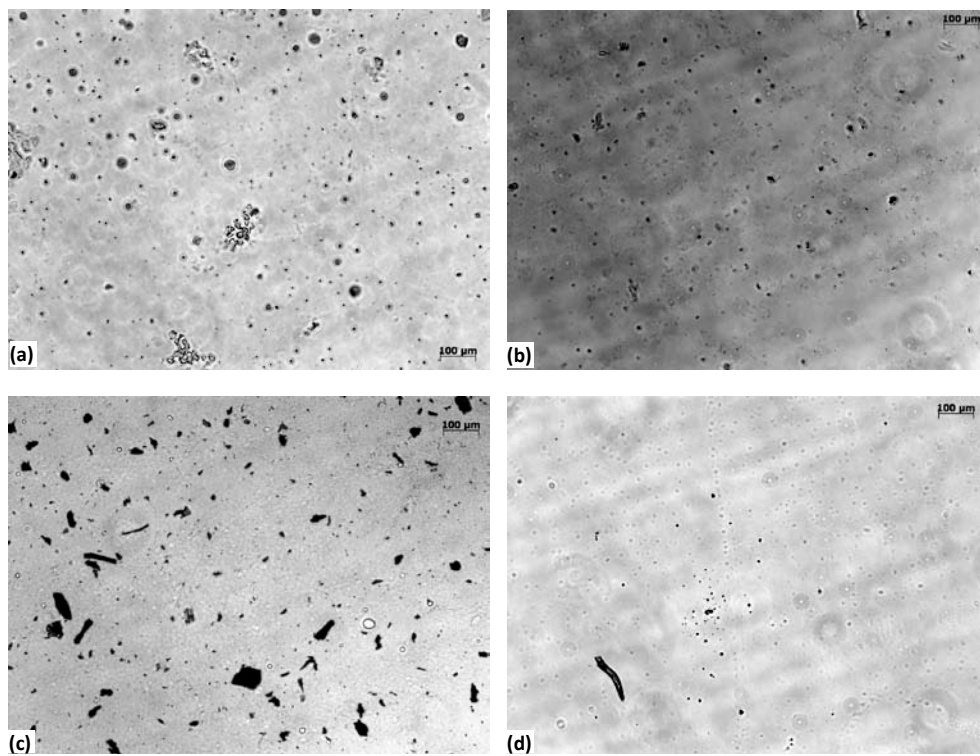


Figure 5.3 Representative optical micrographs showing particle shape, size, and distribution in unaged samples: (a) unfiltered and (b) filtered PWTf pyrolysis oil. Corresponding micrographs showing particles in aged samples (80 °C, 3 weeks) for (c) unfiltered and (d) filtered PWTf pyrolysis oil. All images are at 10X magnification. Note: light rings in the micrographs are artifacts from the microscope lens.

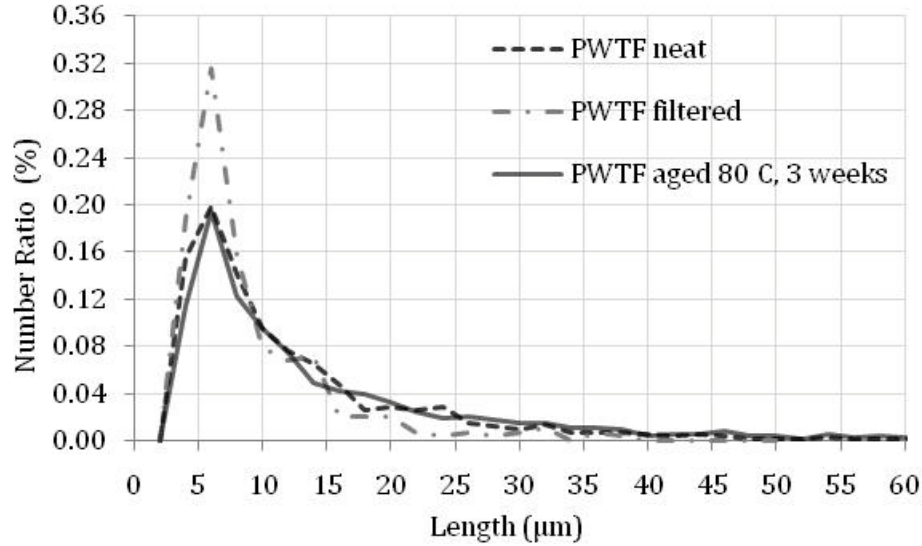


Figure 5.4 Major axis particle size distributions for the PWTF pyrolysis oil: neat (unfiltered, unaged), filtered, and unfiltered aged at 80 °C for 3 weeks.

5.4.4 FTIR Characterization of Filtered Particles

To identify the chemical composition of the filtered particles, transmission-FTIR and DRIFTS analyses were conducted (Figure 5.5). Initially, the particles were observed by transmission-FTIR 'as filtered' (Fig. 5.5a), and as expected showed spectra almost identical to the pyrolysis oil (Fig. 5.5b) from which they were removed. The filtered particles were then washed sequentially with acetone and methanol to remove the pyrolysis oil coating the particles. DRIFTS spectra were then collected on the washed solids (Fig. 5.5c) and indeed the FTIR signature was different from the pyrolysis oil. The washed, filtered particles show similar peaks positions and relative peak heights as the DRIFTS spectra for pine char (Fig. 5.5d). So, the filtered solids are most likely char entrained in the oil from the pyrolysis process. Functional groups corresponding to the peaks in Figure 5.5 are identified in Table 5.1.

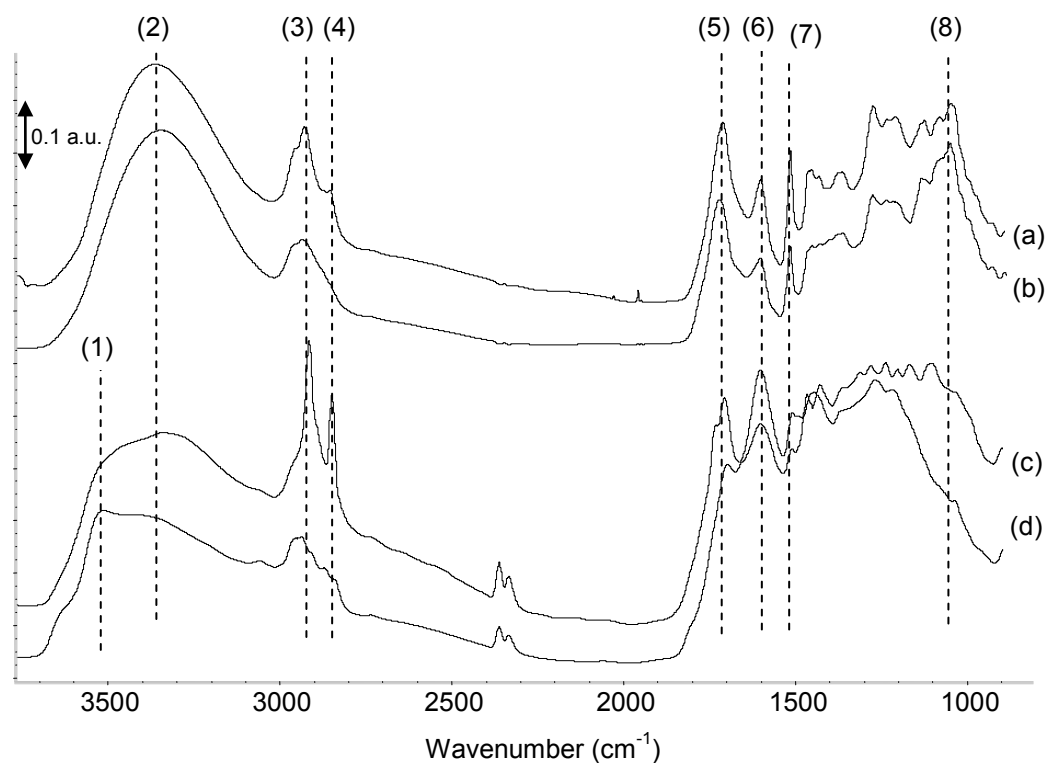


Figure 5.5 Transmission-FTIR and DRIFTS spectra of the filtered solids before (a) and after (c) solvent washing along with spectra for PWTF pyrolysis oil (b) and pine whole tree [PWT] char (d).

Table 5.1 Functional group identifications for the major FTIR peaks in Figure 5.

#	Peak Position (cm ⁻¹)	Identification	Reference
1	3513	O-H stretch; H-bonded	Nakanishi, Silverstein
2	3355	O-H stretch	Pretsch, Nakanishi
3	2937-2913	C-H stretch; CH ₂	Nakanishi, Silverstein
4	2850-2844	C-H stretch; CH ₂ , aromatic ether (-OCH ₃ or -OCH ₂ -)	Pretsch, Nakanishi, Silverstein
5	1731-1697	C=O stretch; ester, ketone, aldehyde, carboxylic acid	Pretsch, Nakanishi, Silverstein
6	1600	ar. C-C/ C=C; ring stretching and skeletal vibrations	Pretsch, Nakanishi, Silverstein
7	1515-1510	ar. C-C/ C=C; ring stretching and skeletal vibrations	Pretsch, Nakanishi, Silverstein
8	1051	C-O stretch; primary alcohol (CH ₂ -OH)	Pretsch, Nakanishi, Silverstein

5.4.5 Rheology

Rheological studies revealed shear thinning behavior in the unfiltered pyrolysis oil. In contrast, the filtered pyrolysis oil samples displayed Newtonian behavior with constant viscosity as the shear rate was increased. After 3 weeks of aging, the shear thinning behavior changed to shear thickening in the unfiltered samples whereas the filtered samples remained Newtonian. Average viscosities of unfiltered and filtered PWTF pyrolysis oil are plotted as a function of aging time and presented in Figure 5.6. The unfiltered pyrolysis oil viscosity increased 11 cP to 42 cP after 3 weeks of aging, a 288 % increase. For the filtered pyrolysis oil, the viscosity decreased substantially during the first and second weeks of aging and decreased only slightly during the third week of aging. Filtration not only prevented a viscosity increase during aging, but appears to have contributed to a 66% decrease in viscosity during the 3 weeks of aging at 80 °C. At the end of the study, there was an order of magnitude difference in the viscosities measured for the unfiltered and filtered PTWF pyrolysis oil.

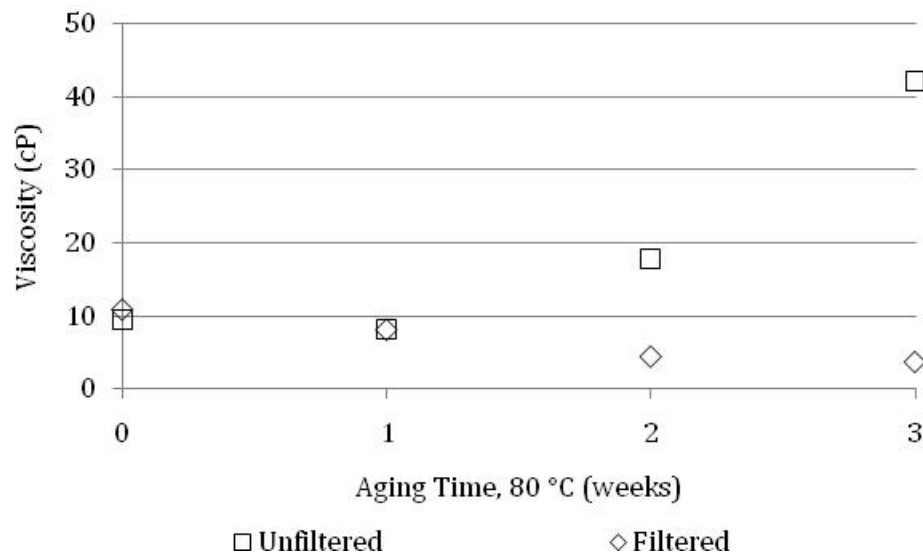


Figure 5.6 Rheologically determined average viscosities (averaged over 100-1000 1/s) for unfiltered and filtered PWTF pyrolysis oil aged at 80 °C.

5.4.6 Molecular Weight Determination

GPC-determined weight averaged (M_w) molecular weights for the filtered and unfiltered pyrolysis oil samples are presented in Figure 5.7 as a function of aging time at 80 °C. There was a slight M_w difference between the unfiltered (1200 ± 56 Da) and filtered (1120 ± 48 Da) pyrolysis oil before aging, but this difference was not statistically significant. After one week of aging, the unfiltered and filtered pyrolysis oils had nearly identical M_w of ~ 1430 Da—a 20 % increase for unfiltered pyrolysis oil and a 29 % increase for filtered oil versus the unaged samples. Two weeks of aging resulted in 1580 Da (32 % increase) in the unfiltered pyrolysis oil and 1960 Da (75 % increase) in the filtered sample. After the third week of aging the weight average molecular weight decreased in both the unfiltered and filtered pyrolysis oil.

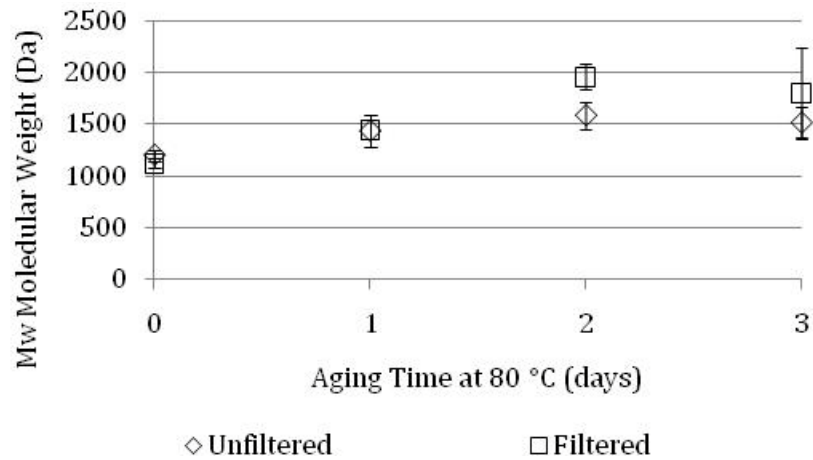


Figure 5.7 Weight averaged (M_w) molecular weight for unfiltered and filtered PWTF pyrolysis oil aged at 80 °C.

5.4.7 Gas Chromatography/Mass Spectroscopy (GC/MS)

Chromatograms collected via gas chromatography/mass spectroscopy (GC/MS) are presented in Figures 5.8 and 5.9 for the unfiltered and filtered PWTF pyrolysis oil samples respectively. After aging, large increases were observed in the peaks at $\sim 22:03$,

25:47 and 29:01 min retention times for both the unfiltered and filtered samples. Peaks for each retention time from the aged samples were compared to the control (unaged) peak height and the peak height difference calculated and plotted for trends during aging. In Figure 5.10 peak heights differences between the aged and unaged samples are displayed for the unfiltered (a) and filtered (b) samples along with the corresponding resonance times for the unfiltered PWTF pyrolysis oil aged at 80 °C for 1, 2 and 3 weeks. Significant increases in the normalized peak heights (22:03, 25:05, 25:47, 29:01 and 31:33 min) were observed during aging for both unfiltered and filtered samples and correspond to the substituted aromatic structures presented in Figure 5.10 demonstrating a ring forming or substitution reaction may be occurring during aging. In addition, the peak height difference continuously increases as a function of aging time and demonstrates that these GC/MS peak height increases are related to the aging process(es) occurring in the pyrolysis oil.

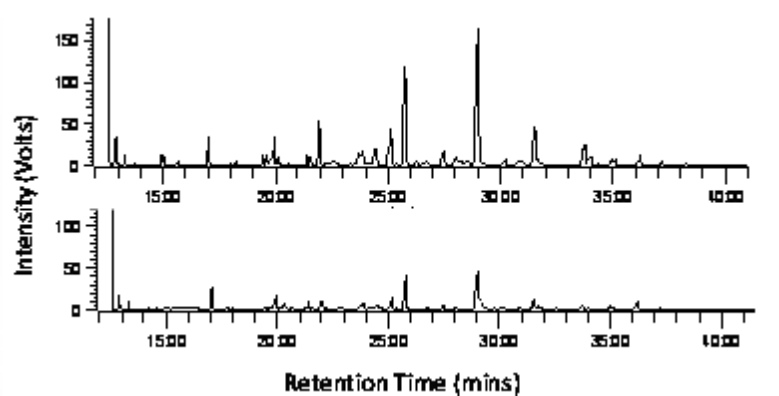


Figure 5.8 GC-MS ion chromatogram for the neat PWTF pyrolysis oil (bottom) and the aged unaltered PWTF pyrolysis oil at 80 °C for 3 weeks (top).

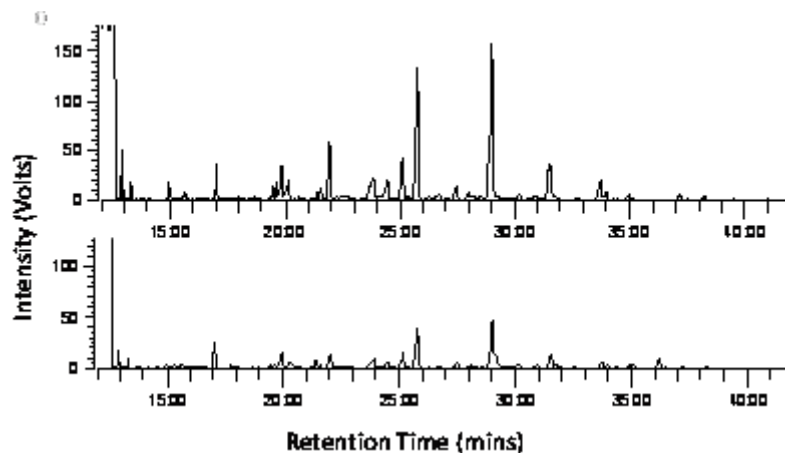


Figure 5.9 GC-MS ion chromatogram for the un-aged filtered PWTF pyrolysis oil (bottom) and aged filtered PWTF pyrolysis oil at 80 °C for 3 weeks (top).

For unfiltered PWTF pyrolysis oil, retention times of 21:56, 25:05, 25:44, 29:01 and 31:33 were identified as phenol, 4-methyl-phenol, 2-methoxy-phenol, 2-methoxy-4-methyl-phenol, and 4-ethyl-2-methoxy-phenol, respectively (Figure 5.10). All of the identified compounds are phenolic and increase in concentration with aging. It is likely that phenol is being formed and concurrently being (successively) substituted by ether [R-O-R'] and (m)ethyl functional groups. In addition, there is a higher concentration of phenolic compounds in the filtered samples suggesting filtration may have encouraged the phenol producing reaction(s).

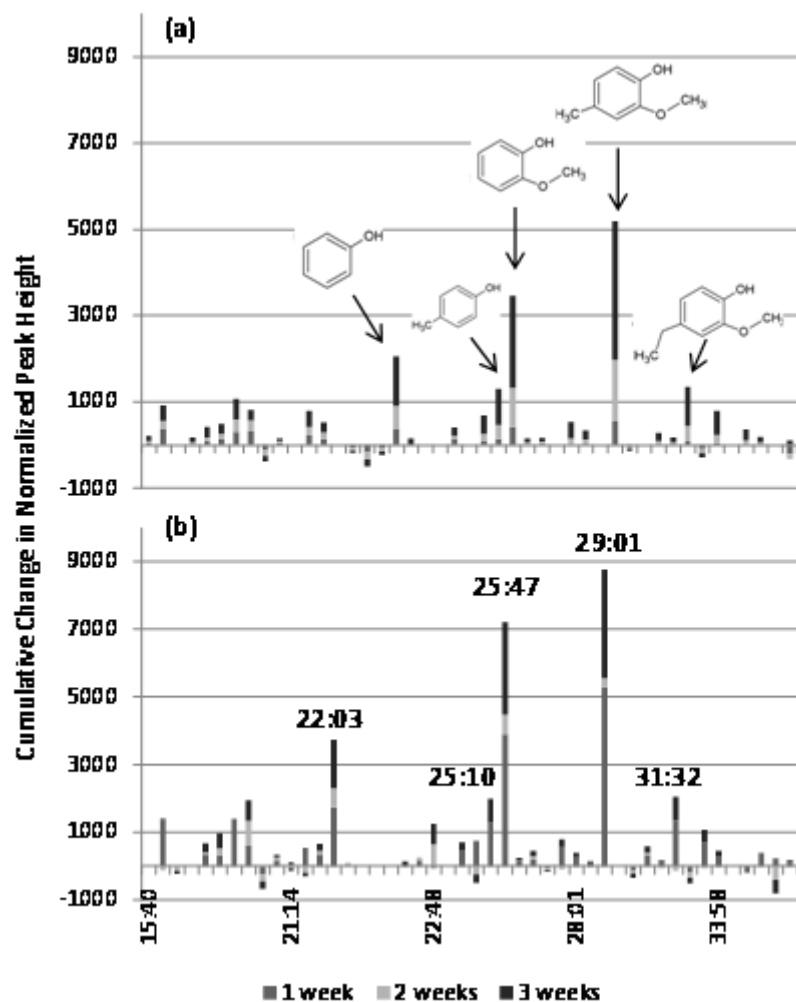


Figure 5.10 Major changes in GC-MS normalized peak heights (versus the controls) displayed as a function of the resonance time for unfiltered (a) and filtered (b) pyrolysis oil. Peak height differentials increase over the course of the 3 week aging study for the unfiltered PWTF pyrolysis oil aged at 80 °C.

5.4.8 FTIR Spectroscopy

ATR-FTIR spectra for unfiltered and filtered PWTF pyrolysis oil are shown for the unaged control and 80 °C/3 week aged samples in Figure 5.11. After 3 weeks of aging, the peak at 1050 cm^{-1} (C-O st, primary alcohol) appears to have decreased in the unfiltered sample and the peaks at $\sim 1270\text{ cm}^{-1}$ (=C-C-O st, aromatic ether) and $\sim 1710\text{ cm}^{-1}$ (C=O of ketone, aldehyde, ester or carboxylic acid) appear to have increased in the filtered sample. To quantify these and more subtle spectral differences, peak height

ratios (PHR) were calculated for eight peaks of interest in both the unfiltered and filtered samples (Figure 5.12). In the unfiltered samples, PHRs for the peaks at 1710 (C=O of ketone, aldehyde, ester or carboxylic acid) and 1643 cm^{-1} (ar. C=C st, skeletal st) vary from sample to sample and do not show obvious trends. Definitive PHR increases during aging were measured for the peaks at 1602, 1513, 1268, and 1193 cm^{-1} . The peaks at 1602 and 1513 cm^{-1} are signatures for C=C aromatic skeletal stretching [Kuptsov, Silverstein]. The peak located at 1268 cm^{-1} represents the =C-C-O stretch in an aromatic ether [Pretsch, Nakanishi, Silverstein, Kuptsov] or an O-H bend and C-O stretch of carboxylic acid [Nakanishi, Silverstein]. The 1193 cm^{-1} peak corresponds to the C-O stretch of phenol [Kuptsov, Silverstein, Nakanishi]. The increase in phenol in addition to aromatic compounds verifies the increase in phenolic compounds determined by GC-MS.

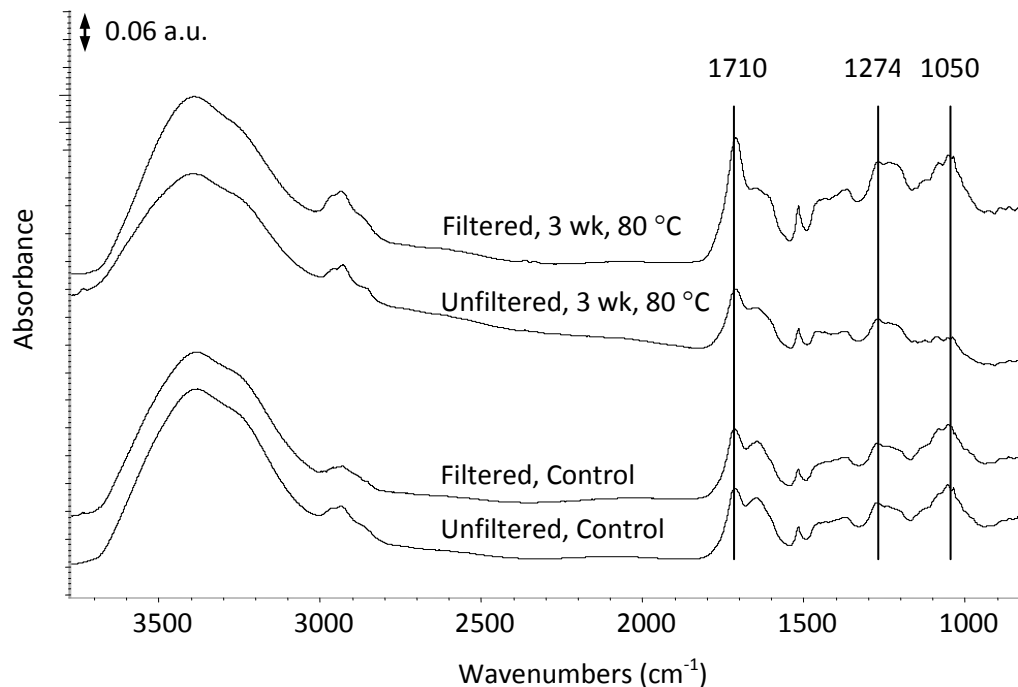


Figure 5.11 ATR spectra of unfiltered and filtered PWTF pyrolysis oil sample before (control) and after storage for 3 weeks at 80 °C.

Peaks located at 1051 and 1033 cm^{-1} decreased as a function of aging time. The 1050 cm^{-1} peak corresponds to the C-O stretch of a primary alcohol [Kuptsov, Silverstein, Nakanishi] and 1033 cm^{-1} peak is the C-O stretch of an alcohol or ester [Silverstein, Nakanishi] or the =C-O-C stretch of an aromatic or vinyl ether [Pretsch, Nakanishi]. The decrease in the primary alcohol and either an ether or alcohol suggests that an alcohol, ether and/or ester group is reacting to produce a phenolic compounds and ether substituted phenolic compounds.

As shown in Figure 5.12, the filtered samples show no definitive trend for the PFR of the peak at 1643 cm^{-1} , but PHR increased for the peaks at 1710, 1602, 1513, 1268 and 1193 cm^{-1} . The 1710 cm^{-1} peak is the result of a C-O stretch of a carboxylic acid, aromatic ketone [Kuptsov, Nakanishi, Pretsch] or aromatic aldehyde [Nakanishi]. Increased PHRs for the remaining peaks indicate an increase in phenol C-O stretching [Kuptsov, Silverstein, Nakanishi] and C=C aromatic skeletal stretching [Kuptsov, Silverstein] in the unfiltered oil.

The peaks at 1051 and 1033 cm^{-1} decrease during aging for both the filtered and unfiltered pyrolysis oil samples. This indicates a decrease in primary alcohol and/or ether also occurred in the filtered samples. The one difference between unfiltered and filtered PHRs during aging is the increase in the carbonyl peak where there is a definitive increase due to a ketone, aldehyde, carboxylic acid and/or ester functional group [Nakanishi, Pretsch, Silverstein].

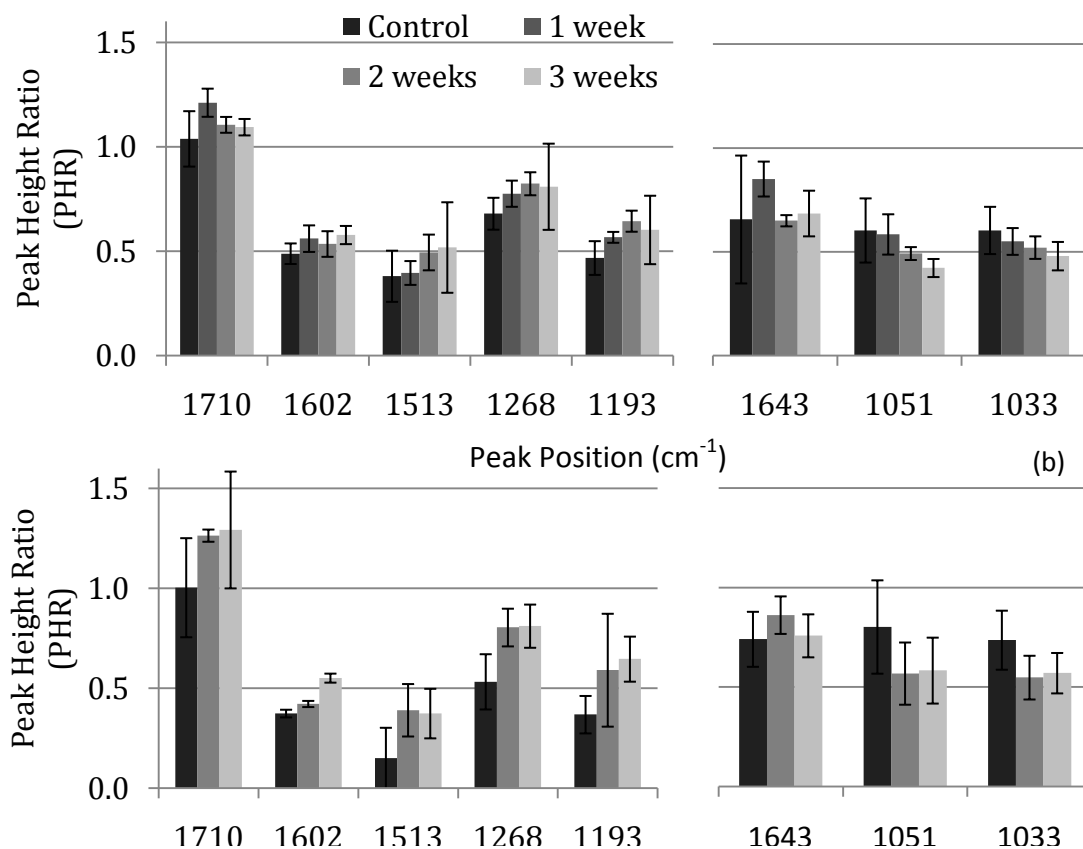


Figure 5.12 Average peak height ratios (PHR) and 95% confidence intervals error bars for key peaks identified in unfiltered neat and aged PWTF pyrolysis oil samples (a) and filtered neat and aged PWTF pyrolysis oil samples (b).

5.4.9 Postulated Aging Reactions

There are several possible reactions that may produce both phenolic compounds and water, including Diels-Alder reaction, electrophilic aromatic substitution, and etherification [Carey, Adv Chem 2000]. Diels-Alder reaction is a ring-forming reaction that combines an alkene with a diene and proceeds forward with the addition of heat. Alkenes are most reactive with simple dienes with strong electron-attracting groups which include esters, ketones and α,β -unsaturated aldehydes [Carey, Adv Chem 2000]. Figure 5.13 shows a generic Diels-Alder reaction and shows how substituted aromatic compounds can be formed where the substituents would be any of the R groups.

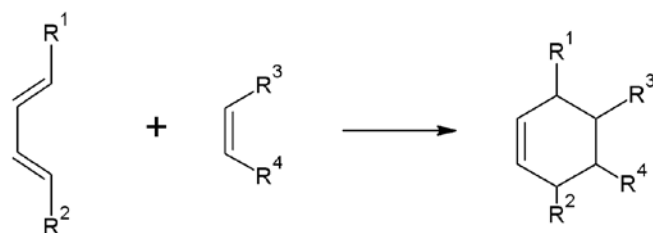


Figure 5.13 Diels-Alder reaction resulting in substituted aromatic compounds [Carey, Adv Chem 2000].

Electrophilic aromatic substitution begins with an aromatic ring such as benzene and a substituent is catalytically added to the ring; the substituent can include -OH, -OR, -R or -H groups. The electrophilic substitution of phenol of ethyl, methyl, or methoxy groups would match the observed GC/MS trends. C-acylation and O-acylation are the two types of electrophilic aromatic substitution [Carey, Ochem]. C-acylation requires an acylating agent such as anhydride or acyl chloride or AlCl_3 , is thermodynamically controlled, and generally predominates versus O-acylation. O-acylation requires an acylating agent such as acyl chloride or anhydride and is kinetically controlled [Carey, Ochem].

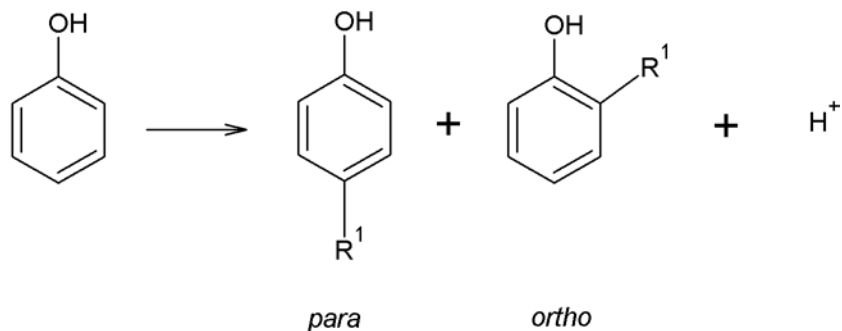


Figure 5.14 Electrophilic aromatic substitution [Carey, Ochem]

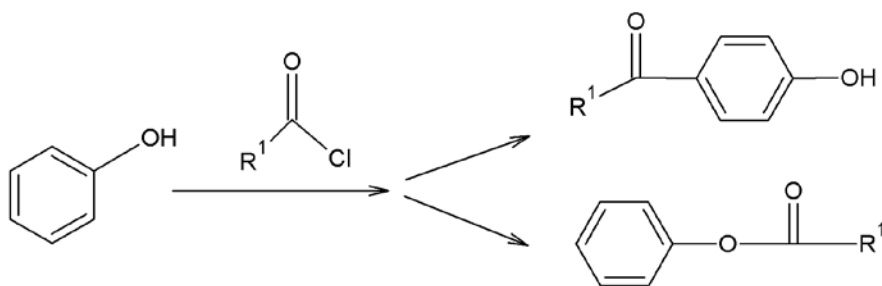


Figure 5.15 Electrophilic aromatic substitution; C-acylation (top) and O-acylation (bottom) [Carey, Ochem]

In addition to Diels-Alder reaction and electrophilic aromatic substitution, etherification can also produce aromatic ethers such as the phenol and substituted phenolic compounds formed during pyrolysis oil aging which can explain the observed increase in water. Acid-catalyzed condensation of alcohols can produce ethers via a nucleophilic substitution (S_N2) reaction that usually requires heat and H_2SO_4 and is typically limited to symmetrical ethers of primary alcohols [Carey]. Figure 5.16 represents an example of acid-catalyzed alcohol condensation which produces water as a byproduct and could account for the formation of water during pyrolysis oil aging.

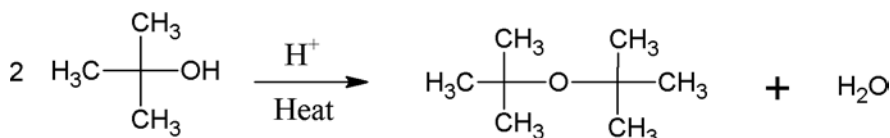


Figure 5.16 Acid-catalyzed condensation of alcohols to form ether and water [Carey, Ochem].

There is no evidence to show that the ethers are forming prior to the phenol/ aromatic ring formation. It may be possible that the acid catalyzed condensation is occurring to phenol rather than a primary alcohol or the reaction between the ether and the phenolic groups is fast enough the ether is not observed.

5.4.10 Conclusions

Accelerated aging of pyrolysis oil results in increased viscosity accompanied by increased water content and average molecular weight. Removal of char particles by serial filtration prior to aging prevented the viscosity increase but an increase in water content and average molecular weight was still observed. This suggests that the viscosity increase and increase in water and molecular weight are not interconnected as previously thought. The concentration of phenolic and aromatic ether compounds increased in both unfiltered and filtered samples during aging. Considering the large number of compounds in pyrolysis oil, multiple reactions are likely to occur during aging. During aging, one or more reactions may be occurring that are related to char solids and viscosity increase and different co-current reaction(s) resulting in the increases observed in Mw, water, phenolic and ether compounds. Etherification during aging was determined by GC-MS and FTIR analyses by the formation of aromatic ethers and phenolic compounds in both the filtered and unfiltered pyrolysis oil samples. Specific reactions that may form these compounds include electrophilic aromatic substitution, Diels-Alder reaction and acid-catalyzed condensation of alcohols.

5.5 Results and Discussion Part II

5.5.1 Filtering Pyrolysis oil

Percent solids removed from the pyrolysis oil samples was estimated by initial and final weights of the vacuum and centrifuge filters in addition to the pre- and post-filtration weights of the oil samples. The percent removed solids are shown in Table 5.2 in terms of each sequential filtration step and overall. The first vacuum filtration (VF) averaged ~15 wt % solids removal, the second VF 18 wt %, and centrifugal filtration

(CF) then removed an additional ~3 % material. Note: The CCWF pyrolysis oil was vacuum filtered but the measurements had larger error and did not allow for the calculation of solids removed.

Table 5.2 Percent solids removed by each filtration step: two vacuum filtrations (VF) followed by centrifugal filtration (CF). Note the PBF and CCWF oils were not subjected to the second vacuum filtrations.

Pyrolysis oil	Solids removed (wt %)		
	1: VF (20-25 μm)	2: VF (2.5 μm)	3: CF (0.2 μm)
PBF	19.4	-	2.8
PCWT	10.75	19.1	3.12
PCWF	13.5	17.3	2.94
CCWF	-	-	2.92

5.5.2 Filtration

Photos collected during filtration are presented in Figure 5.17 and show the consistency of the pyrolysis oil and some of the filtration methods including crude filtration ('screening'), vacuum filtration, and a vacuum filter post-filtration.

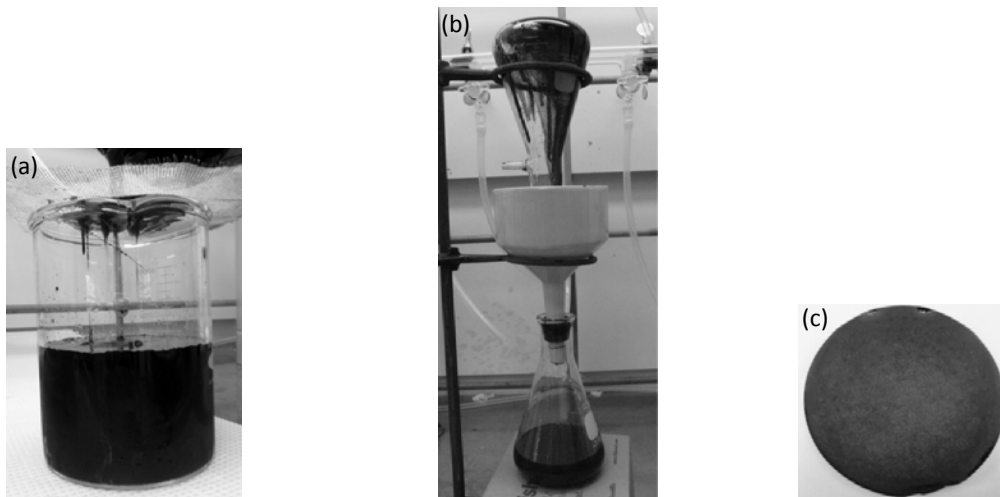


Figure 5.17 Photos of crude filtration ('screening') (a), vacuum filtration (b) and a vacuum filter post-filtration (c).

5.5.3 Visual Observation of Phase Separation

All samples were monitored for phase separation throughout aging and the approximate volume % was recorded when phase separation occurred. Tables 5.3 and 5.4 display the phase separation and observations recorded after aging. Pine bark fractionated [PBF] and pine clear wood total [PCWT] were the two pyrolysis oils that exhibited phase separation during aging for both unaltered and filtered samples. In PBF phase separation occurred between 24 and 504 h where after 504 h of aging the filtered sample had a larger bottom phase volume of 50-70 vol % compared to the unaltered that had 30 vol% bottom phase. In PCWT phase separation occurred between 24 and 168 h of aging and both unaltered and filtered samples resulted in 50 vol % bottom phase. PCWF and CCWF did not exhibit phase separation and resulted in very thick pyrolysis oil after 504 h of aging.

Table 5.3 Phase separation observations for pine-derived pyrolysis oils

Sample Name	Phase Separation	Observations
PBF Unfiltered		
Neat	No	-----
24 hours	No	-----
504 hours	Yes	~30 vol% bottom phase
PBF Filtered		
Unaged	No	-----
24 hours	No	-----
2 weeks	Yes	50 vol% split into 2 phases; bottom flows
504 hours	Yes	50-70 vol% bottom phase
PCWT Unfiltered		
Neat	No	-----
1 week	Yes	40-50 vol% bottom phase; bottom flows
2 weeks	Yes	~60 vol% bottom phase; bottom little flow
504 hours	Yes	~50 vol% bottom phase
PCWT filtered		
Unaged	No	-----
24 hours	No	-----
2 weeks	Yes	50 vol% split in phases; bottom flows
504 hours	Yes	~50 vol% bottom phase
PCWF Unfiltered		
Neat	No	-----
24 hours	No	-----
504 hours	No	Very thick
PCWF Filtered		
Neat	No	-----
24 hours	No	-----
504 hours	No	Very thick

Table 5.4 Phase separation observations for cottonwood-derived pyrolysis oils

Sample Name	Phase Separation	Observations
CCWF Unfiltered		
504 hours	No	Very thick
CCWF Filtered		
504 hours	No	Very thick

5.5.4 pH

pH measurements for cottonwood clear wood fractionated (CCWF) pyrolysis oil are presented in Figure 5.18. Note: The non-filtered samples were not aged for 24 h due to lack of material. There was no significant change in pH after the filtration. During aging, the pH of the unfiltered and filtered pyrolysis oil remains constant at 2.34 ± 0.01 and 2.4 ± 0.03 respectively. Therefore, filtration of CCWF resulted in a pH stabilization during aging/storage.

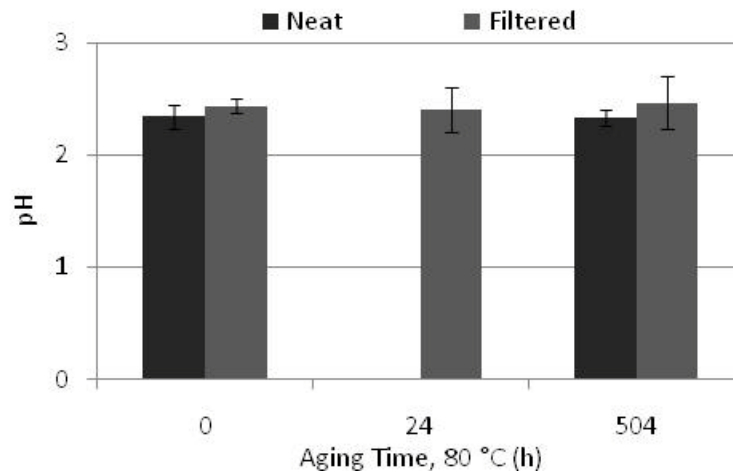


Figure 5.18 pH measurements of cottonwood clear wood fractionated [CCWF] pyrolysis oil, neat and filtered, as a function of aging at 80 °C for up to 504 h (3 weeks).

Pine clear wood total (PCWT) and fractionated (PCWF) pyrolysis oils, both non-filtered and filtered, are compared in Figure 5.19. This PCWF sample set includes three samples where the centrifuge filters tore and the pyrolysis oil was aged as a separate sample set. In PCWT and PCWF, the pH increases after filtration only by 4 and 8 %, respectively, and the PCWF torn filter samples showed a 18 % increase in pH. During aging, the pH decreases in both the non-filtered and filtered PCWT samples and by 17 and 15 %, respectively, showing little difference after filtration. PCWF samples have a

less defined trend in pH; the non-filtered samples increase or decrease by $\pm 7\%$ and the filtered and torn filter samples change by 8 and 28%, respectively. The pH of non-filtered and filtered PCWT and PCWF samples have similar changes in pH during aging indicating that the filtration has no effect on the pH change during aging, only on the initial pH. It should also be noted that the total and fractionated pyrolysis oils have similar pH ranges.

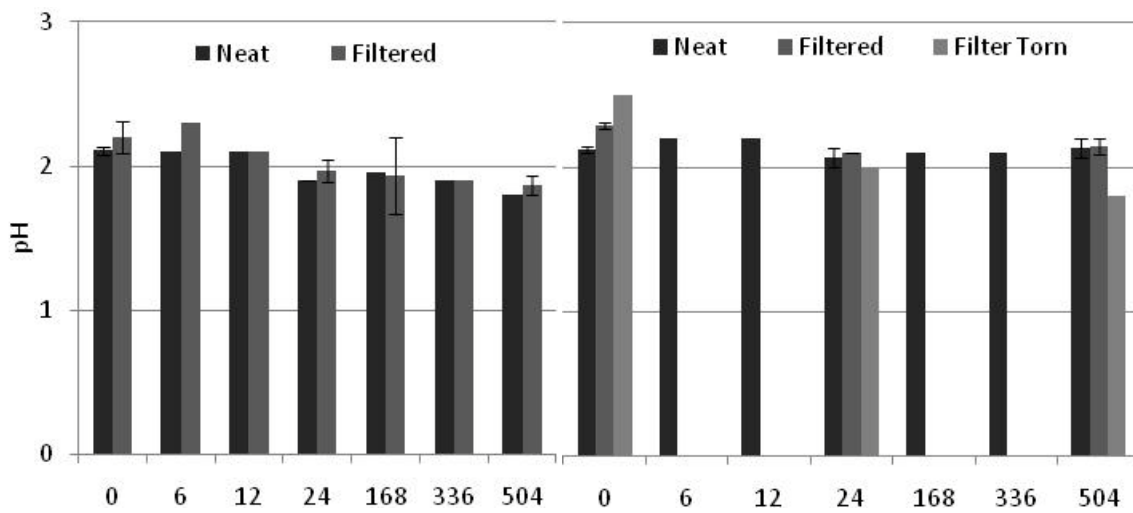


Figure 5.19 pH measurements of pine clear wood total [PCWT, left] and pine clear wood fractionated [PCWF, right] pyrolysis oil, both neat and filtered, as a function of aging at 80 °C for up to 504 h.

Pine bark fractionated (PBF) pyrolysis oil was also examined and the pH for non-filtered and filtered samples is presented in Figure 5.20. There was so significant change in pH after filtration and during aging the unaltered pH varied by 7% and the filtered varied by 12%. When considering the 95% confidence intervals, there is no significant difference between the non-filtered and filtered samples during the aging study and overall the pH values remain relatively stable.

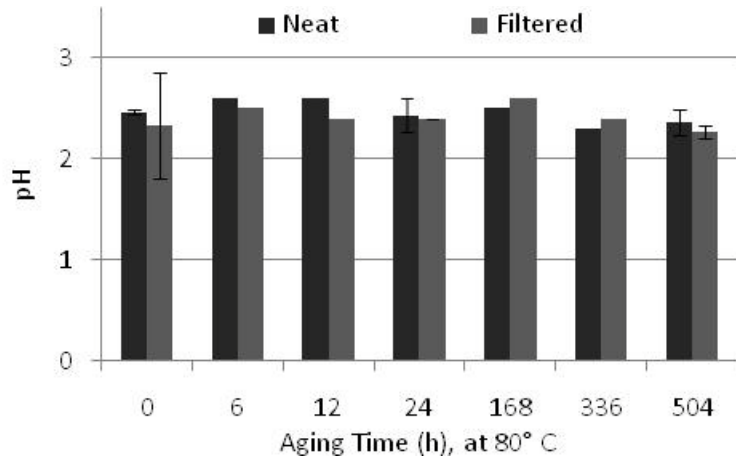


Figure 5.20 pH measurements of pine bark fractionated [PBF] pyrolysis oil neat and filtered as a function of aging at 80 °C for up to 504 h.

When considering all four sets of pyrolysis oils the lowest pH was found in the PCWT samples and during aging the nominal values dropped below pH of 2 thus classifying it as a hazardous waste resulting in high disposable costs but also additional corrosion impacts.

5.5.5 Water Content

CCWF water content is displayed in Figure 5.21 where the pyrolysis oil samples remained on phase throughout aging. Unfiltered samples increased in water content from 19.8 to 22 wt% water (11 % change). After filtration, the water content decreased by 28 % and varied only slightly during aging with no statistically significant change in water content. Water may have been lost in the filtration process which may have aided in the stabilization of the pyrolysis oil during aging.

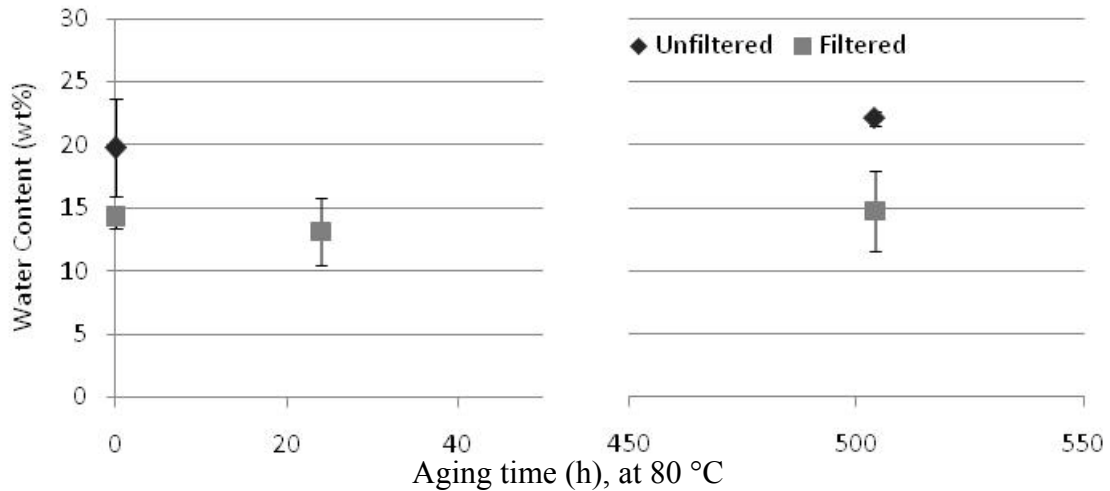


Figure 5.21 Water content for CCWF unaltered and filtered aged up to 504 h at 80 °C.

Water content measurements for PCWT and PCWF are presented in Figures 5.22 and 5.23. It should be noted that PCWT exhibited phase separation at 336 h of aging and PCWF remained one phase. Within the first 24 h of aging the unfiltered PCWT water content decreased by 22 % and then increased to 32 wt % after 168 h. PCWT top phase water content continued to increase up to 40 wt% after 504 h were the bottom phase decreased in water content by 31 % after 504 h. After filtration the water content dropped to 23 wt% (a 22 % reduction) and the water content remained approximately constant within the first 24 h. After 168 h the filtered pyrolysis oil increased in water content by 23 % prior to phase separation. After phase separation at 336 h, the top phase continued increased to 40 wt% water and the bottom phase decreased to 22 wt% water. There is little to no difference in the unfiltered and filtered pyrolysis oil after 504 h of aging and filtration did not prevent phase separation of the water content increase.

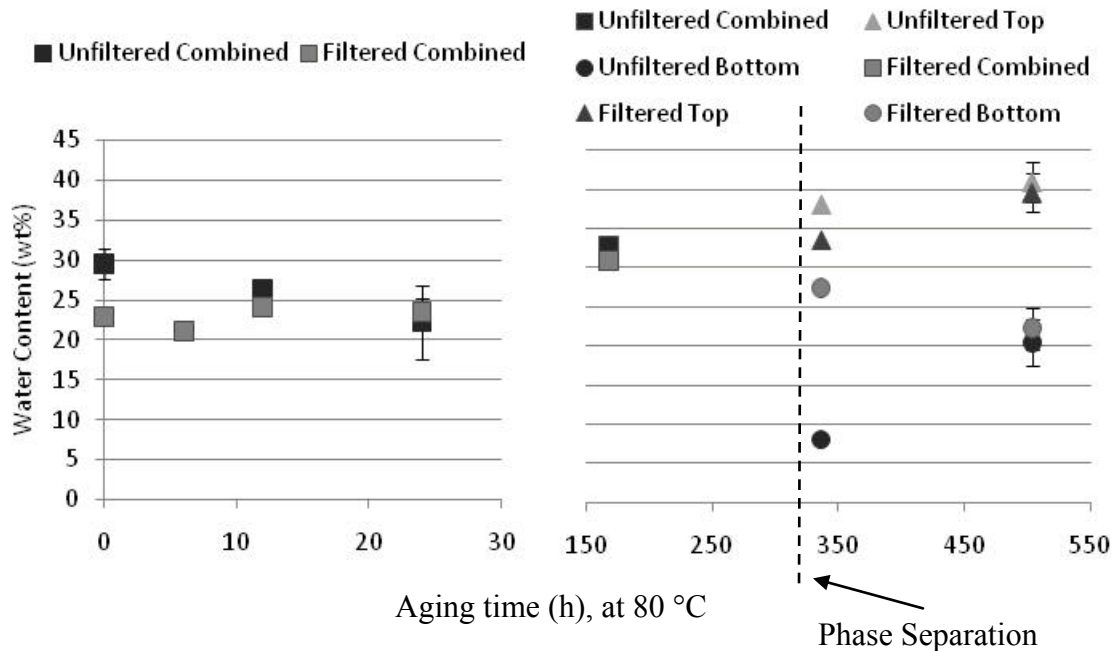


Figure 5.22 Water content for PCWT unaltered and filtered aged up to 504 h at 80 °C.

PCWF samples did not exhibit phase separation at any point during aging, but the water content measurements did vary. Unfiltered water content decreased within the first 24 hours by 22 % and then increased again resulting in 18 wt% water content after 504 h, a value 4 % larger than the neat water content. After filtration the water content was 9 wt% (48 % lower) and remained lower during aging, increasing overall by 47 % after 504 h of aging. There was a very small increase in water content in the non-filtered sample, so filtration may actually have encouraged water increase with almost double the percentage increase. In addition, the torn filtered samples started with slightly higher water content and increased by 21 and 70 % after 24 and 504 h of aging, displaying a drastic different when compared to the non-filtered samples. This suggests that material removed during the filtration of PCWF may help to stabilize the reactions that produce water during aging.

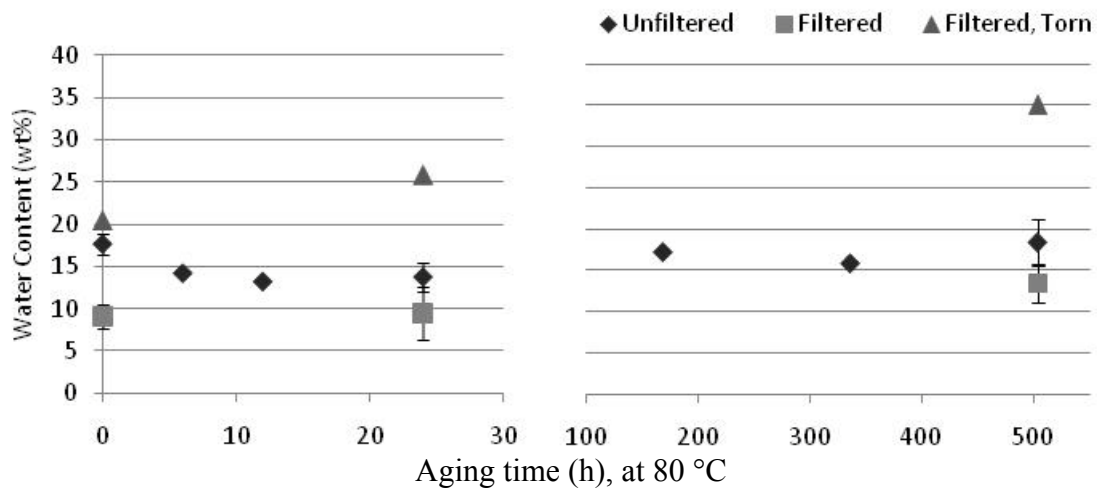


Figure 5.23 Water content for PCWF non-filtered and filtered aged up to 504 h at 80 °C.

PBF pyrolysis oil exhibited relatively high initial water content before and after aging and phase separated after 168 h of aging; both of which are not typical of fractionated pyrolysis oil. After filtration, neat PBF exhibited a decrease in water content by 12 % and in general remained lower during aging. After 168 h the top phases contained most of the water with 50 and 38 wt% for unfiltered and filtered pyrolysis oil; the bottom phases contained only 22 and 18 wt%, respectively. The unfiltered top phase decreased slightly after 336 h and then increased back to 44 wt % after 504 h of aging, a 43 % increase. Filtered top phase increased steadily reaching 45 wt% after 504 h, a 45 % increase from the initial filtered pyrolysis oil a higher increase in water content compared to the unaltered sample (35 % increase). This indicates that filtration of the pyrolysis oil did not prevent any reactions that might result in water formation and may have even encouraged water formation, as was observed in PCWF. Also when compared to the PCWF pyrolysis oil, PBF has a much higher initial water content (100 % larger) which may be due to the use of bark compared to clear wood.

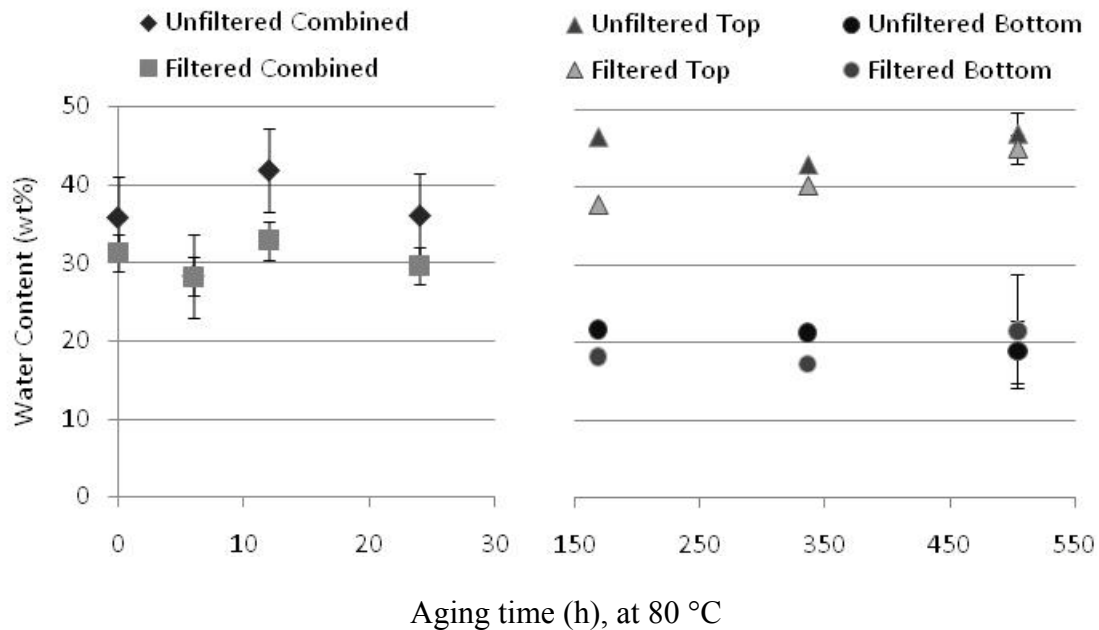


Figure 5.24 Water content of PBF pyrolysis oil, non-filtered and filtered, aged up to 504 h at 80 °C.

5.5.6 Viscosity

Viscosity data are presented for unfiltered, double-filtered pyrolysis oils (PBF and CCWF) and triple-filtered pyrolysis oil samples (PCWT and PCWF) at up to 504 h of aging at 80 °C (Figures 6.9 to 6.12). After filtration CCWF (Figure 5.25) exhibits a larger, unexpected increase of 116 % that may be due to the loss of water during filtration (5.5 %) or may be due to an alteration in the emulsion creating higher viscosity. CCWF did not experience phase separation during aging and the viscosity for both unfiltered and filtered oil increased by 153 and 423 %, respectively, after 504 h. Rather than reducing or preventing a viscosity increase, filtered samples displayed a viscosity more than double that of the unfiltered samples.

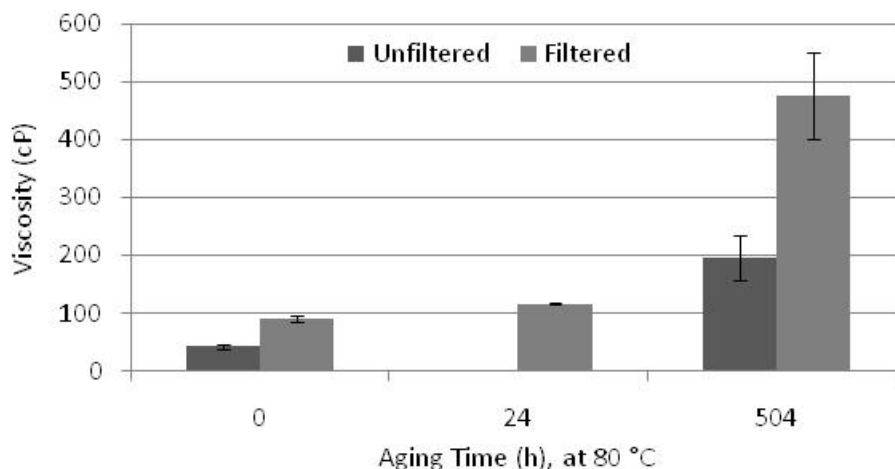


Figure 5.25 Viscosity (cP) for cottonwood clear wood fractionated [CCWF] pyrolysis oil as a function of aging time at 80 °C for up to 504 h (3 weeks).

PCWT viscosity data is presented in Figure 5.26 and for both sets of samples a single data point was collected for 6, 12, 158 and 336 h due to lack of sample and therefore no error bars are included. PCWT samples exhibited a 50 % increase in viscosity post filtration which may also be due to the 22 % decrease in water content in the filtration process. Filtered and unfiltered PCWT viscosity remained approximately constant within the first 24 h of aging. Viscosity increased by 222 and 127 % after 336 h for the unfiltered and filtered samples. Data for 168 and 336 h are single data points so it is possible that the filtered viscosity at 168 h may be an outlier or elevated. After 504 h of aging both unfiltered and filtered PCWT decrease in viscosity significantly, a result of phase separation where the top and bottom phases were approximately 50/50. Using the 168 and 336 h times as a reference it appears that the filtration was able to retard the viscosity increase but did not help with phase separation.

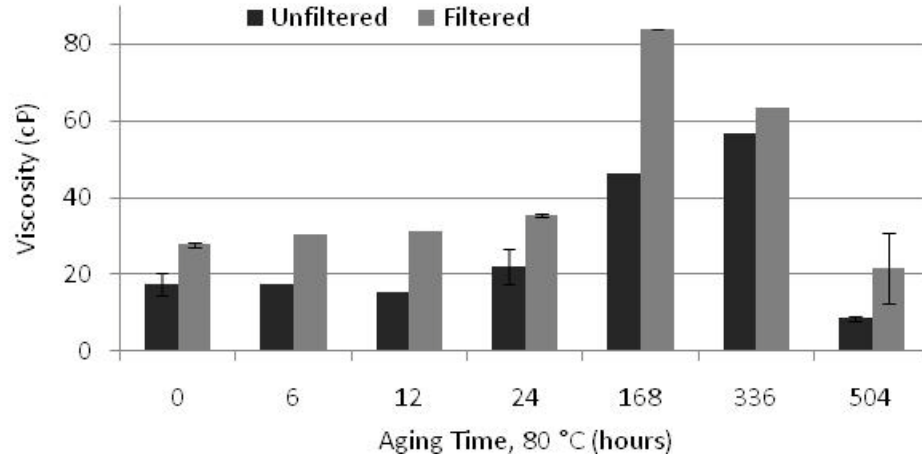


Figure 5.26 Viscosity measurements for pine clear wood total [PCWT] oil as a function of aging time at 80 °C for up to 504 h.

Filtered and unfiltered PCWF viscosity measurements are displayed in Figure 5.27. When comparing PCWF to PCWT, the fractionated oil has a 370 % larger viscosity and 67 % lower water content. In addition, the PCWF pyrolysis oil increases in viscosity after filtration as was also observed in CCWF and PCWT and may be the result of 48 % decrease in water content during filtration. PCWF did not phase separate during aging. Both unfiltered and filtered PCWF viscosities increased during aging resulting in increases of 800 and 481 %, respectively, after 504 h. Viscosity for the torn filtered sample was significantly lower than the unfiltered and filtered samples, did not change significant during aging, and appears either to be an outlier with significantly different properties.

From the data presented above, it is obvious that the filtration did not prevent or reduce the viscosity increase that is generally observed with pyrolysis oil aging, and in fact greatly increased the viscosity. PCWF has the lowest water content initially, which was reduced upon filtration to 9 wt%, and this low water content may have promoted a reaction that resulted in the viscosity increase. It is possible that the reduction of water

content allowed for one reaction to proceed (or dominate) causing a drastic increase in viscosity. Conversely, samples with larger water concentrations, as observed in PNT (Chapter 6), also contain age- and/or temperature-related reactions but result in increased water and molecular weight instead of viscosity.

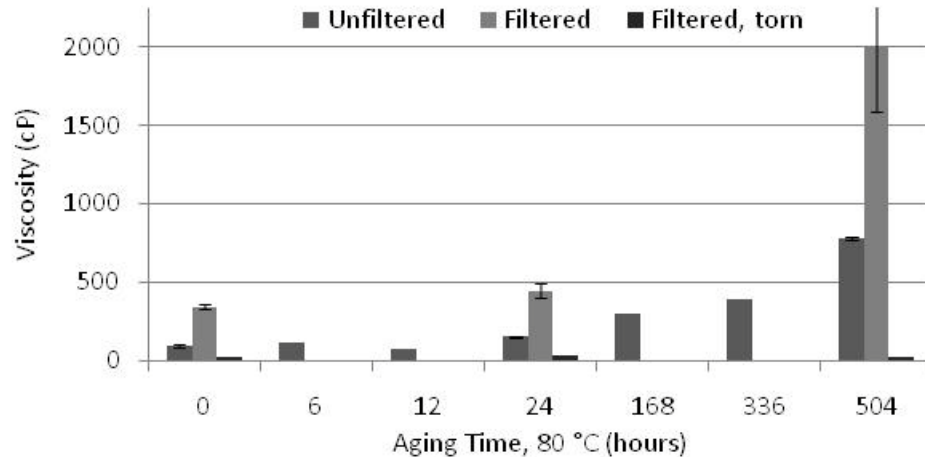


Figure 5.27 Viscosity measurements for pine clear wood fractionated [PCWF] oil as a function of aging time at 80 °C for up to 504 h.

PBF viscosity is presented in Figure 5.28 where, as observed in CCWF, PCWT and PCWF, the viscosity decreased after filtration by 23 % and may be related to the 12 % decrease in water content due to filtration. Unfiltered and filtered viscosities remained approximately constant throughout the first 24 hours of aging. After 336 hours, the filtered oil the viscosity increased by 19 % and unfiltered increased by ~30 %. In both unfiltered and filtered samples, phase separation occurred after 504 hours of aging resulting in 30-50 vol % bottom phase and significantly decreased viscosities for the filtered and unfiltered oils, 75 and 64 % respectively. In PBF pyrolysis oil, filtration failed to prevent age-related viscosity increases (prior to phase separation) or the phase

separation. Either due to the removal of water or other material, the PBF viscosity was increased by filtration.

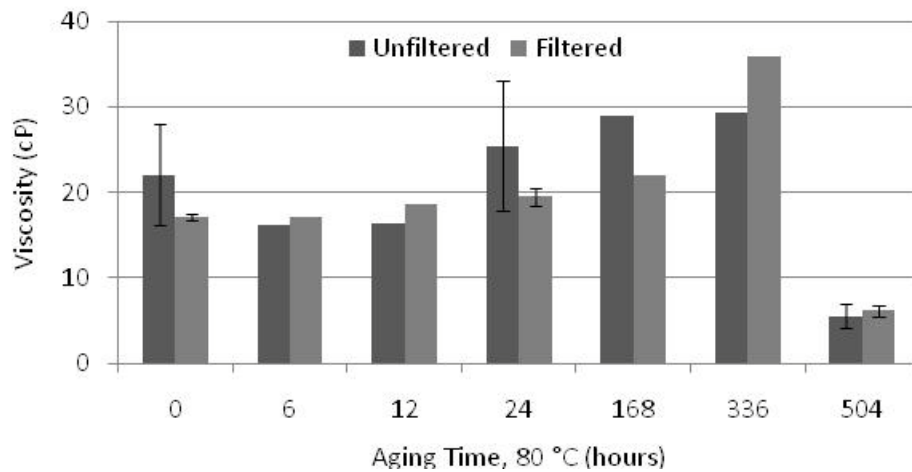


Figure 5.28 Viscosity measurements for pine bark fractionated [PBF] oil as a function of aging time at 80 °C for up to 504 h.

5.5.7 GPC

Weight average molecular weights are displayed for the combined and top and bottom phases (where applicable) for CCWF, PCWT, PCWF and PBF in Figures 5.29-5.32. CCWF unfiltered and filtered pyrolysis oils increased by 70 and 72 % after 504 h respectively to a MW of 1037 Da which indicates there is no significant difference in molecular weight before or after aging due to filtration.

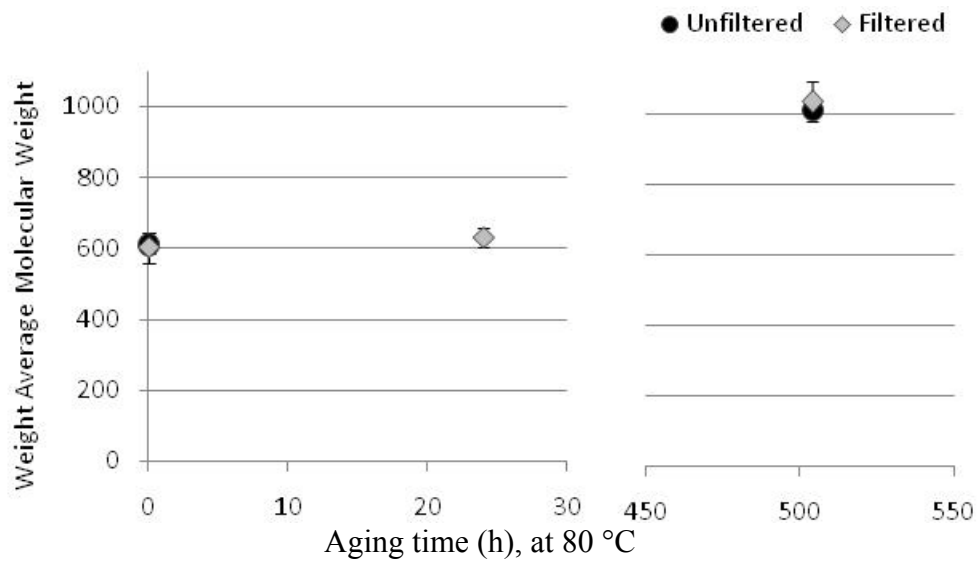


Figure 5.29 Weight average molecular weight for CCWF oil as a function of aging time at 80 °C for up to 504 h.

PCWT exhibited little to no MW change within the first 24 h of aging in both unfiltered and filtered samples (Figure 5.30). After 168 h of aging, both the unfiltered and filtered samples phase separated. After 504 h, the bottom phase MW had increased to 1214 Da, a 120 % increase for the unfiltered sample. Top phase MWs decreased slightly resulting in 537 Da approximately equal to the initial MW. There is no significant difference between the unfiltered and filtered samples showing that that filtration did not impact the reactions in any way.

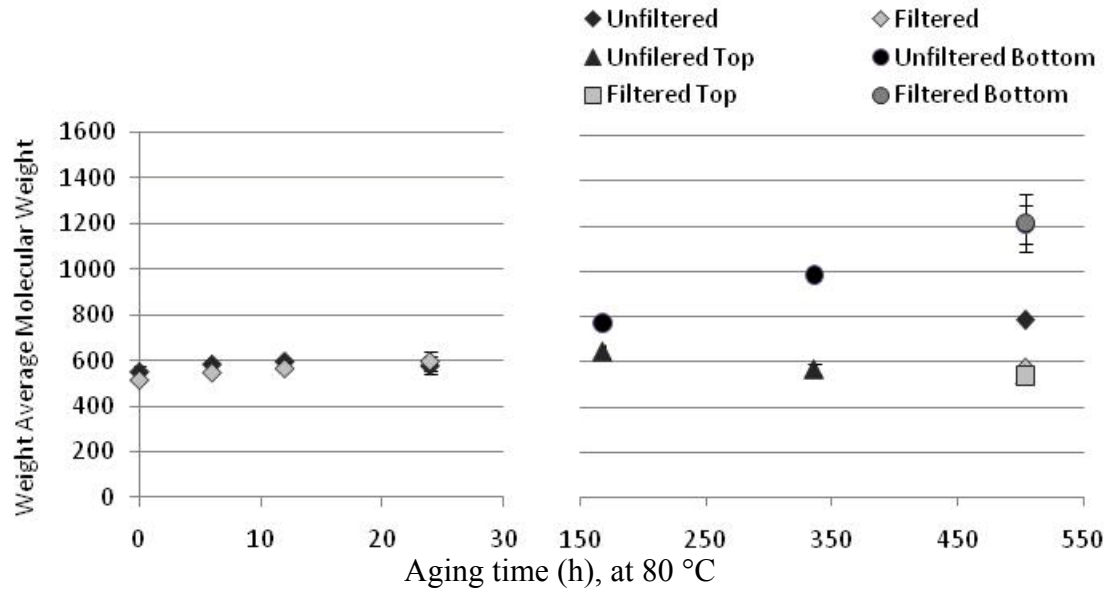


Figure 5.30 GPC results for PCWT oil as a function of aging time at 80 °C for up to 504 h.

PCWF pyrolysis oil remained one phase and increased by 14 % \pm 2 after 24 h of aging for unfiltered, filtered and torn filter samples. After 504 h, the filtered sample had the largest MW of 1082 Da followed by the unfiltered sample (1021 Da) and torn filter (887 Da). Overall the MW increased by 93, 110 and 67 % after 504 h of aging for the unfiltered, filtered and torn filter samples respectively showing that the filtration did not prevent the MW increase.

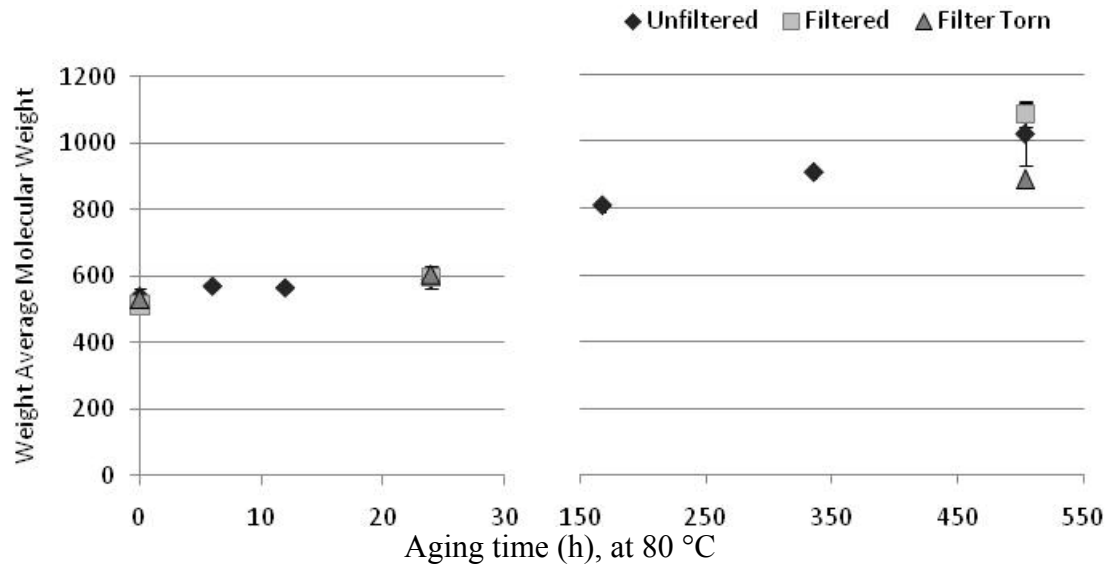


Figure 5.31 Weight average molecular weight for PCWF oil as a function of aging time at 80 °C for up to 504 h.

Weight average molecular weight (MW) was determined using GPC and for phase separated samples the MW was determined for each phase separately. In PBF unfiltered and filtered samples the MW remained relatively stable during the first 24 h and after 168 h of aging phase separated. After 168 h the top phase had a MW approximately the same as the neat pyrolysis oil and a bottom phase with increased MW. After 504 h the unfiltered bottom phase increased by 160 % and the top phase decreased (20 %) and the filtration did not have a significant difference on the MW increase. When comparing the four pyrolysis oils, PBF resulted in the largest molecular weight of 1490 Da and also the largest increase (160 %) after 504 h of aging, which may be due to the addition components in bark when compared to heart wood

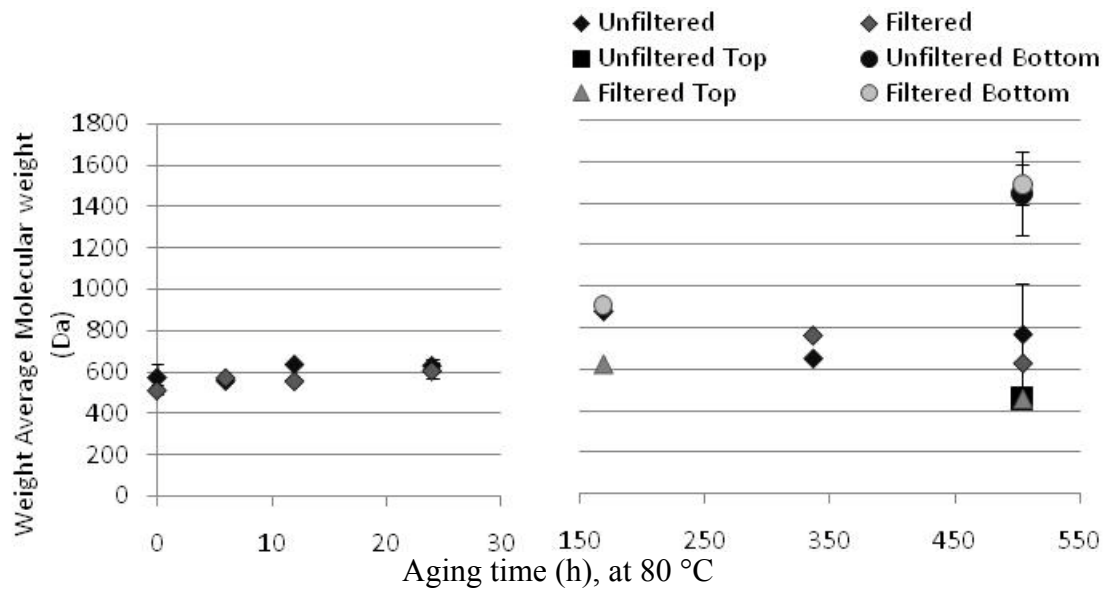


Figure 5.32 Weight averaged molecular weight for PBF oil as a function of aging time at 80 °C for up to 504 h.

5.5.8 ATR Analysis

ATR spectra collected for PBF, PCWF, PCWT and CCWF samples are displayed in Figures 5.33 through 5.40. PCWT and PBF both exhibited phase separation during aging after 504 and 336 hours respectively and top and bottom phase spectra are displayed. Figures 5.33 and 5.34 show the progression during aging for the unfiltered and filtered PBF pyrolysis oil samples where there is no significant change occurring. One main difference is after phase separation there is a change in dominant peaks within the carbonyl region as previously observed in PWTF, PNT and PNF pyrolysis oils (Chapters 4 and 6). No additional peaks were observed to be forming, shifting, increasing or decreasing.

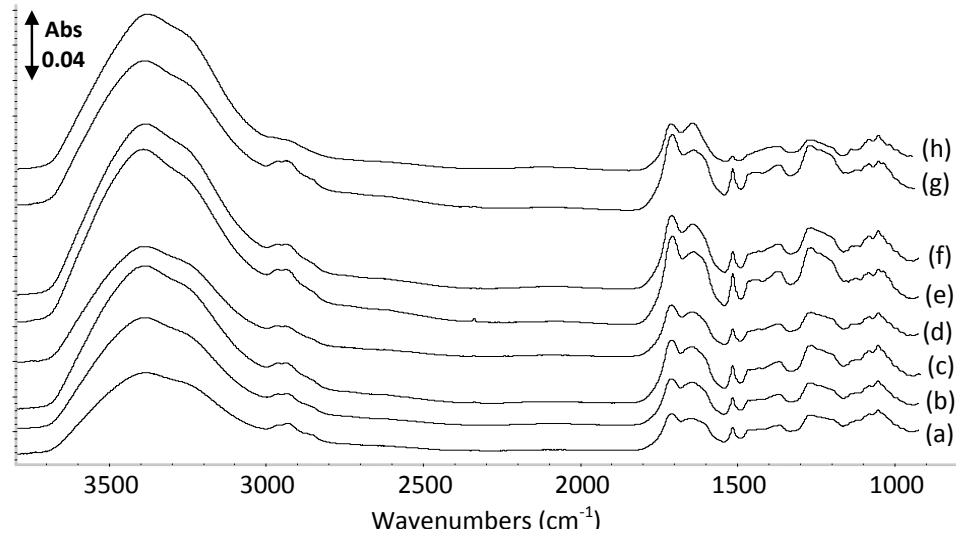


Figure 5.33 PBF unfiltered pyrolysis oil: neat (a) and aged at 80 °C for 12 h (b), 24 h (c), 168 h (d) and phase separated after 336 h [(e) bottom, (f) top], 504 h [(g) bottom, (h) top].

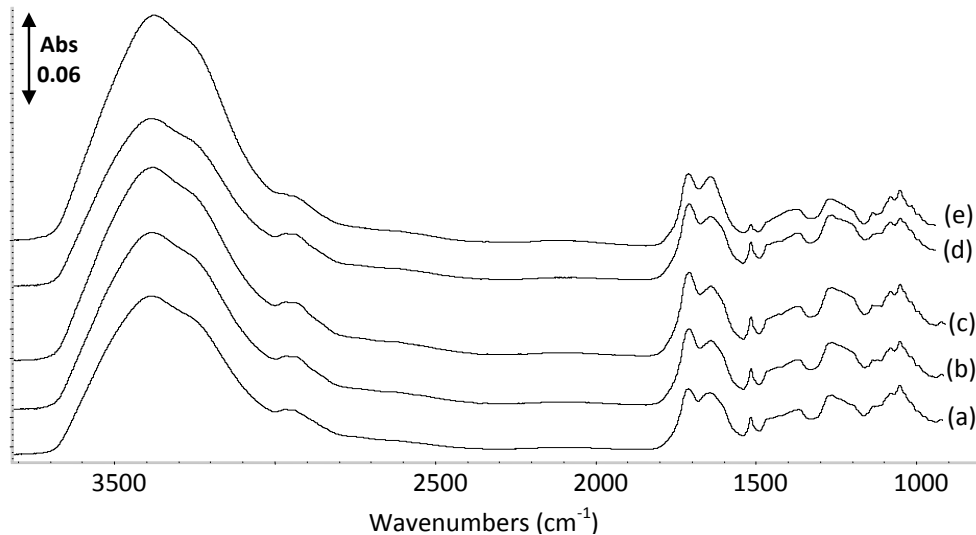


Figure 5.34 PBF filtered samples: unaged (a) and aged at 80 °C for 336 h [top (b), bottom (c)] and 504 h [top (d), bottom (e)] phases.

Figures 5.35 and 5.36 are displayed for the PCWF pyrolysis oil spectra or the unfiltered, filtered and filter torn samples where the unfiltered and filtered samples did not phase separate but the torn filter sample did phase separate. When comparing the

general appearance of the unfiltered and filtered before and after aging there is no difference and the torn filter spectra do not appear different until after phase separation where the carbonyl region also changes shape.

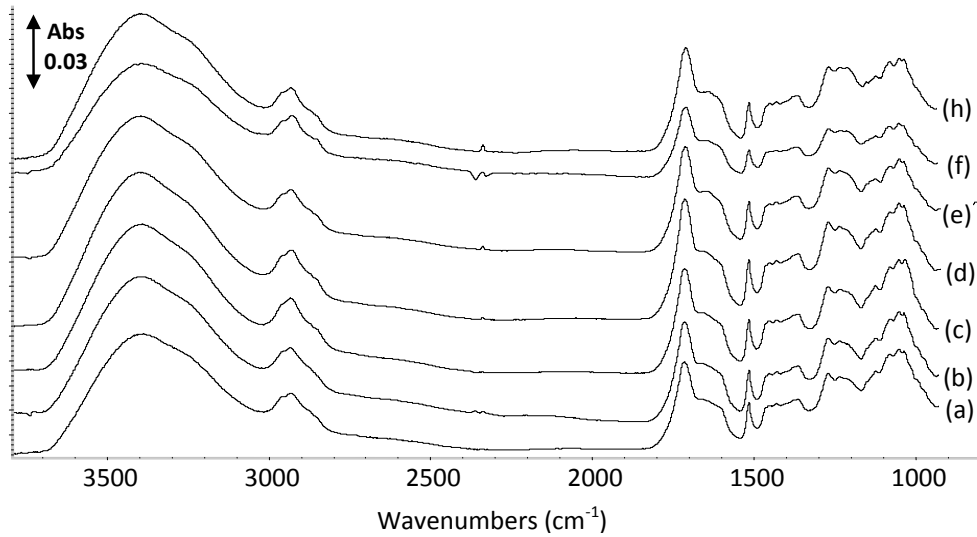


Figure 5.35 PCWF unfiltered pyrolysis oil samples: control (a) and aged at 80 °C for 6 h (b), 12 h (c), 24 h (d), 168 h (e), 336 h (f) and 504 h (g).

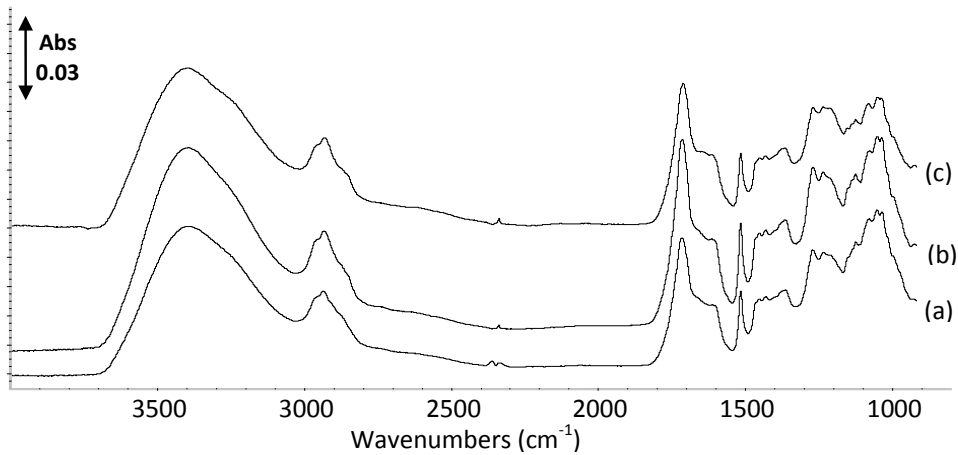


Figure 5.36 PCWF filtered pyrolysis oil samples: control (a) and aged at 80 °C for 24 h (b), and 504 h (c).

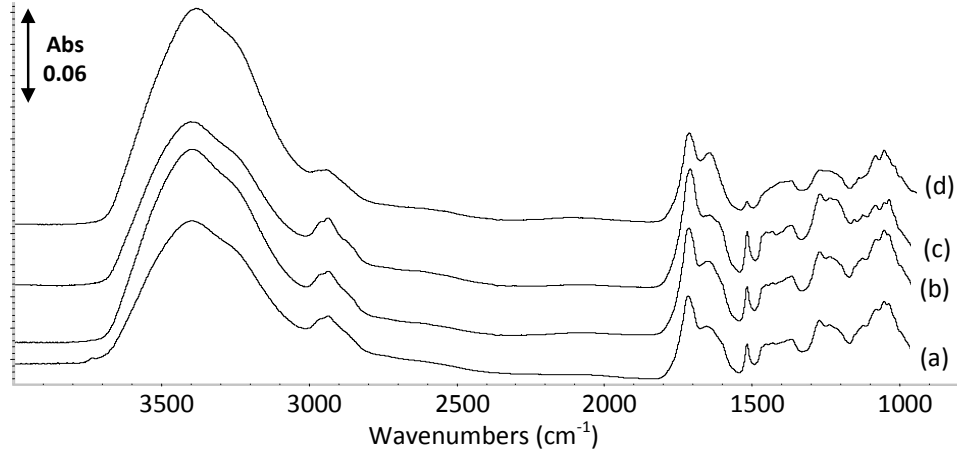


Figure 5.37 PCWF filter torn pyrolysis oil samples: control (a) and aged at 80 °C for 24 h (b) and 504 h [bottom (c), top (d)].

Another comparison of PCWT pyrolysis oil unfiltered (Figure 5.38) and filtered (Figure 5.39) is presented where both the unfiltered and filtered samples phase separated after 504 h of aging. As with the other pyrolysis oil samples there is no visible or significant changes due to filtration or aging in the spectra other than the change due to phase separation.

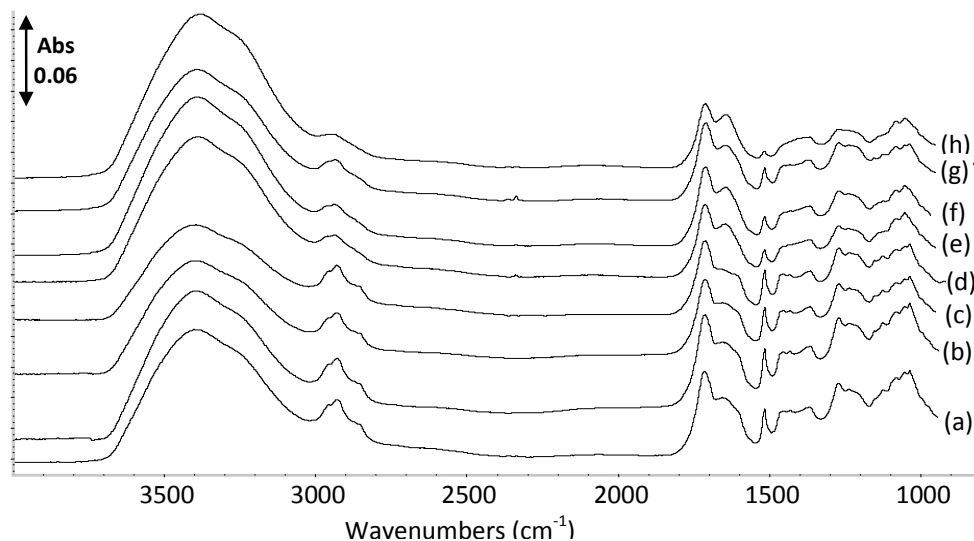


Figure 5.38 PCWT unfiltered pyrolysis oil samples: control (a) and aged at 80 °C for 6 h (b), 12 h (c), 24 h (d), 168 h (e), 336 h (f) and 504 h [bottom (g), top (h)].

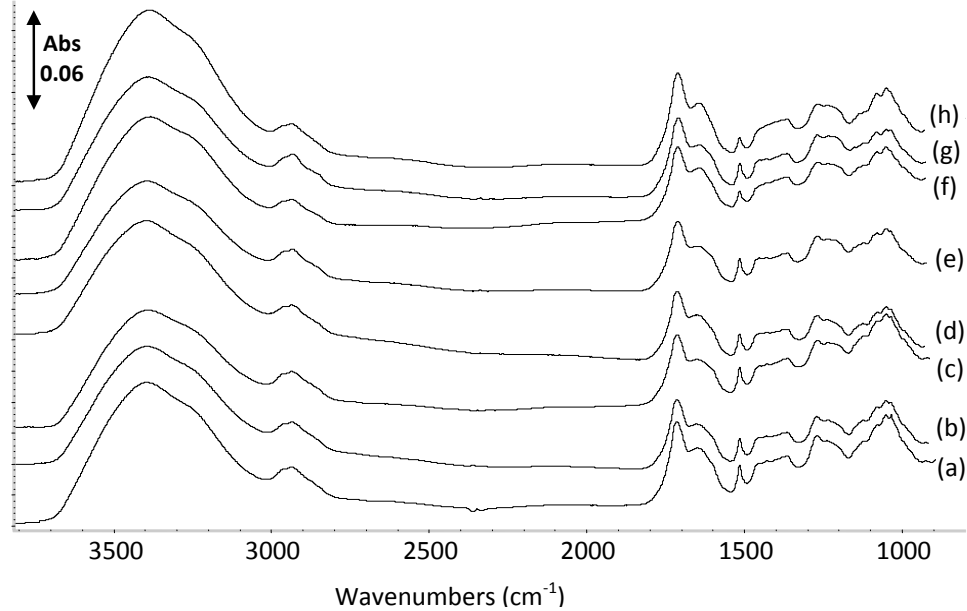


Figure 5.39 PCWT filtered pyrolysis oil samples: control (a) and aged at 80 C for 6 h (b), 12 h (c), 24 h (d), 168 h (e), 336 h (f) and 504 h [top (g), bottom (h)] phases.

During aging, CCWF remained one phase and the spectra collected for both unfiltered and filtered pyrolysis oil are presented in Figure 5.40. As in the other samples, CCWF does not show any significant changes in the samples due to filtration or during aging. For filtration, it is reasonable to suggest that the solids removed were coated in pyrolysis oil and therefore were not detected with the surface sensitive ATR technique. In addition, if the filtered materials were in low concentrations they may not be detected when analyzed in combination with more abundant materials. Regarding aging, a chemical change does not occur during aging, the changes are too subtle when compared to the overall spectral strength, or the reactions include functional group/bonds already present in the pyrolysis oil such that the IR spectra do not change significantly.

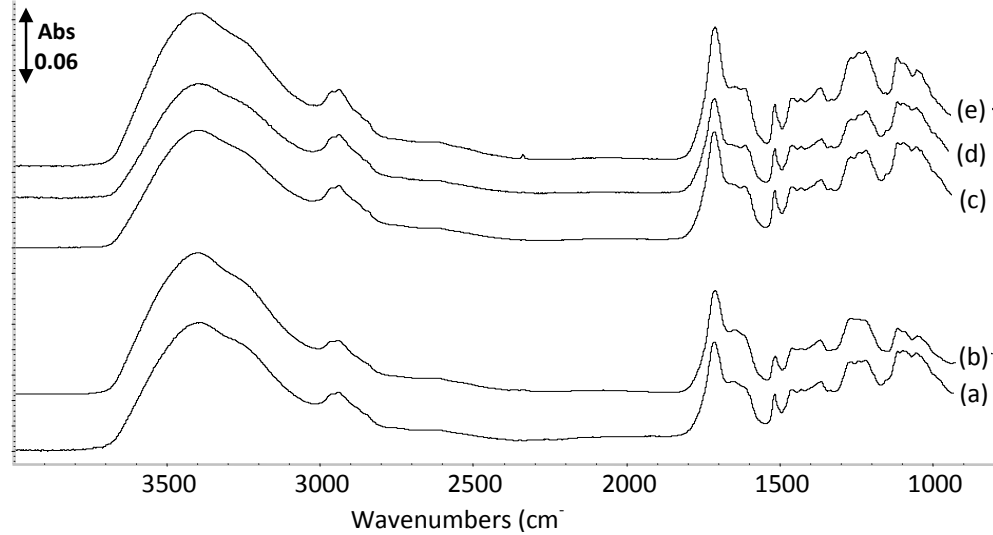


Figure 5.40 CCWF unfiltered neat (a), unfiltered aged for 504 h (b), filtered neat (c), filtered aged for 24 h (d) and 504 h (e).

5.5.9 Quantitative IR Analysis: Peak Height Ratio

For all four pyrolysis oil types, peak heights were measured and peak height ratios (PHRs) calculated for eight peaks of interest located at 3390, 1714, 1645, 1600, 1515, 1268, 1112 and 1051 cm^{-1} . These peaks correspond to Below the PHRs for each pyrolysis oil are discussed separately.

CCWF PHRs are presented in Figure 5.41 showing a decrease in the 3390 cm^{-1} peak after filtration that then increased in the unfiltered samples during aging. This peak is due to the O-H stretch [Silverstein] and is most likely related to the water decrease due filtration and then the water increase during aging. Unfiltered samples observed an increase in the peaks at 1714, 1645, 1600 and 1268 cm^{-1} and a decrease in 1112 and 1051 cm^{-1} during aging. Carbonyl C=O stretches typically occur 1765-1645 cm^{-1} [Pretsch] and given the position (1711-1708 cm^{-1}) it is either an aliphatic/cyclic ketone and/or a carboxylic acid dimer [Silverstein, Pretsch, Nakanishi]. Alkenes or conjugated ketones result in the C=C stretch at 1645 cm^{-1} [Silverstein, Pretsch, Nakanishi] and aromatic or

heteraromatic compounds result in the C=C stretch or skeletal stretching (1600 cm^{-1}) [Silverstein, Pretsch]. A =C-C-O stretch at 1268 cm^{-1} is either an aromatic ether [Pretsch, Nakanishi, Silverstein, Kuptsov] and/or a carboxylic acid [Nakanishi, Silverstein]. Primary alcohol C-O stretching is present at 1051 cm^{-1} [Kuptsov, Silverstein, Nakanishi] and 1112 is due to either a secondary alcohol C-O stretch [Pretsch, Nakanishi, Silverstein] and/or aliphatic or ring ether C-O-C stretch [Nakanishi, Silverstein].

Looking at the similar bonds that are increasing (C=O or C=C) and those decreasing (C-O or C-O-C) there appears to be the formation of double bonds during aging and potentially the formation of aromatic rings. On the other hand there was no significant change in the peak at 1515 cm^{-1} representing a C=C aromatic skeletal stretching [Kuptsov, Silverstein]. When considering the increasing and decreasing peaks there appears to be aromatic formation either with a carbonyl functional group or separately carbonyl C=O is also being formed. This would also suggest that primary and secondary alcohols and/or ethers are reacting to produce these aromatics, ketones and/or carboxylic acids. Several of the error bars (95 % confidence) are large for the filtered pyrolysis oil aged for 504 hours and therefore it is difficult to determine if the filtration altered the aging in any way.

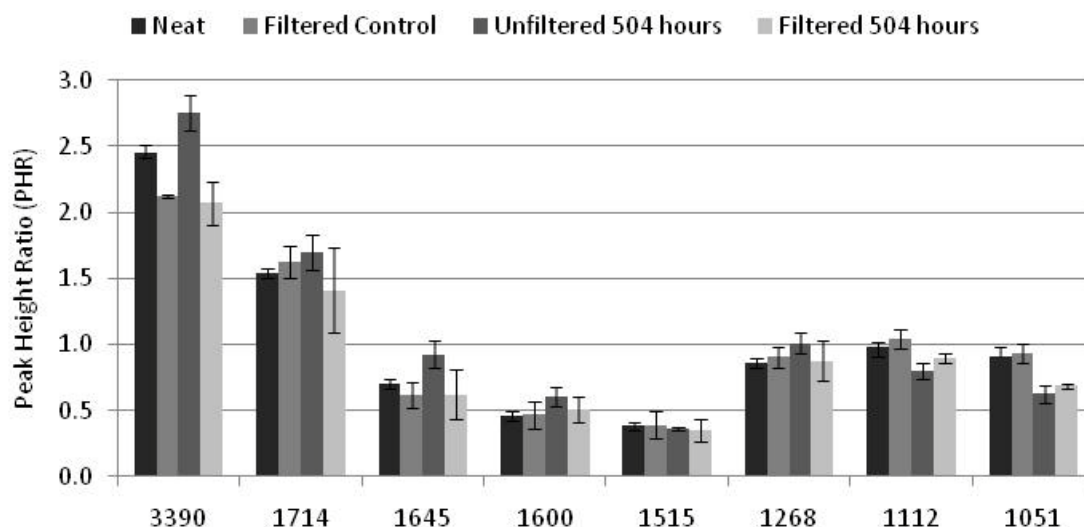


Figure 5.41 Calculated PHR for CCWF pyrolysis oil neat and filtered aged for 504 hours at 80 °C

In Figure 5.42 the PHRs for PCWT and when observing the graph there are no trends and when considering the large error bars there does not appear to be any trends that may be due to either noise in the spectra and/or there being no significant changes in the spectra. On difference that can be determined is the filtered control and filtered top after 504 hours of aging both have larger amounts of primary alcohols (1051 cm^{-1}) which suggest a change in the composition due to filtration. Overall it cannot be determined if there is any affect on the pyrolysis oil due to filtration.

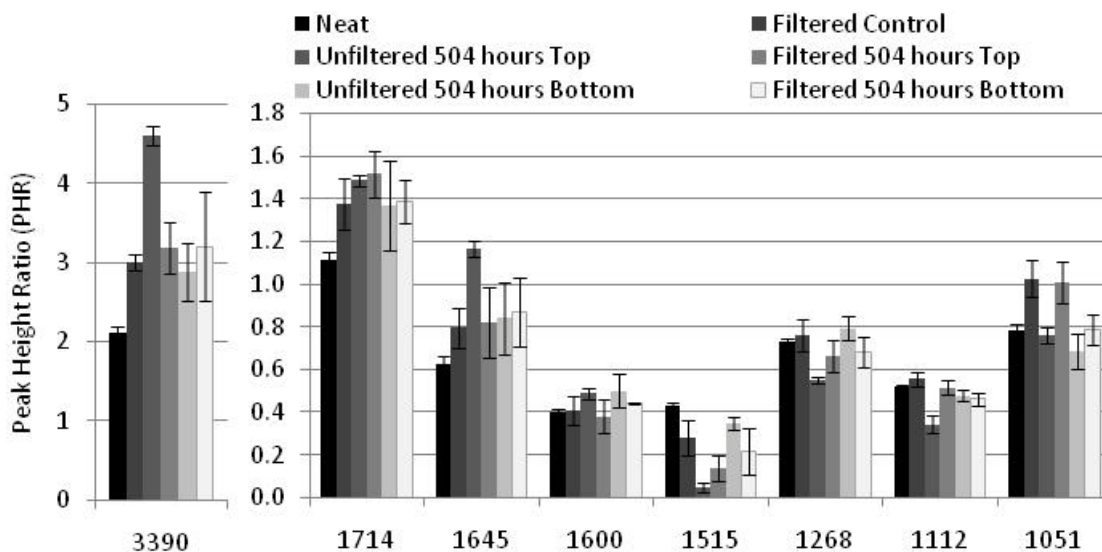


Figure 5.42 Calculated PHR for PCWT pyrolysis oil neat and filtered aged for 504 hours at 80 °C.

Figures 5.43 and 5.44 present the PHR data for the filtered and torn filter samples respectively compared to the unfiltered pyrolysis oil during aging where both the filtered and torn filter samples are single data points without error bars. With the data presented there appears to be an increase in the peaks at 1645 and 1600 cm⁻¹ and a decrease in 1112 and 1051 cm⁻¹ in the unfiltered samples that was also observed in the CCWF pyrolysis oil and the same changes were also observed in the filtered bottom phase. This suggests that the filtration did not effectively stop the reactions that are forming aromatic and/or carbonyl compounds. In addition there was little to no change in the torn filter samples, yet another difference from the filtered samples for an unknown reason.

It appears that the PCWF and CCWF pyrolysis oils, although different trees, have similar aging reactions, both showing increases in alkenes and conjugated ketones or aromatics (1645 and 1600 cm⁻¹) and decreases in primary and/or secondary alcohols or ethers (1112 and 1051 cm⁻¹).

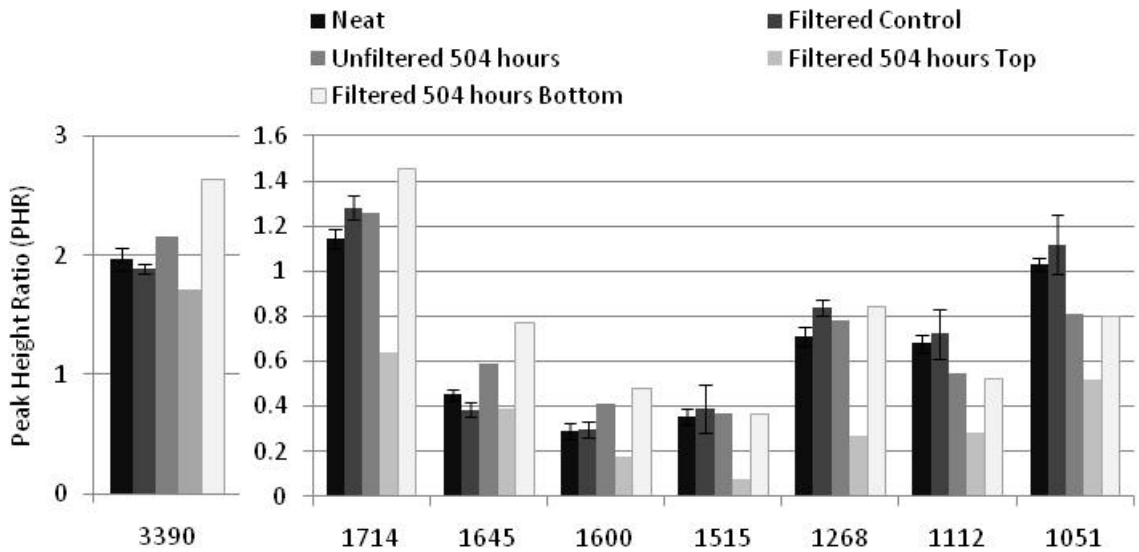


Figure 5.43 Calculated PHR for PCWF pyrolysis oil neat and filtered aged for 504 hours at 80 °C.

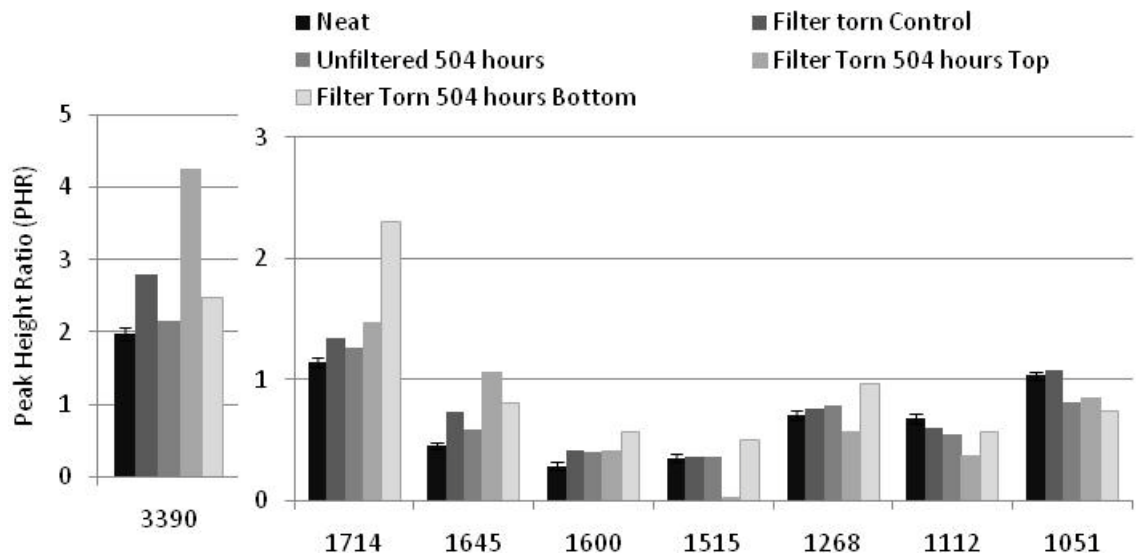


Figure 5.44 Calculated PHR for PCWF pyrolysis oil filter torn aged for 504 hours at 80 °C.

Calculated PHR for PBF pyrolysis oil during aging is presented in Figure 5.45 where the unfiltered top phase has a large increase in the OH stretch during aging that may be due to the increase in water content. In addition the unfiltered top phase also has

an increase in 1645 and 1600 cm^{-1} that decrease in the bottom phase showing a large difference in the two phases. There is also a decrease in the peaks at 1268, 1112 and 1051 cm^{-1} in the unfiltered top and bottom phases. This indicates there is a decrease overall in primary and/or secondary alcohols or ethers (1112 and 1051 cm^{-1}) and/or aromatic ethers or carboxylic acids but there is only an increase in the aromatics and ketone or carboxylic acids in the top phase (1645 and 1600 cm^{-1}). It would be expected that there would be a change in the bottom phase due to the large increase in molecular weight but on the other hand there is an increase in water content in the top phase. It could be possible that water, acids and ketones form in the top phase and a second set of products with high molecular weights are precipitate to the bottom phase but it is unclear what type of compound this would be.

Filtration does appear to have an effect on the PBF pyrolysis oil where the filtered bottom phase peaks do not appear to change significantly. In general there appears to be a common theme in the changes observed during aging regardless of the wood biomass used to produce the pyrolysis oil. It should be noted that the PBF had the largest changes which may have be related to the bark contents.

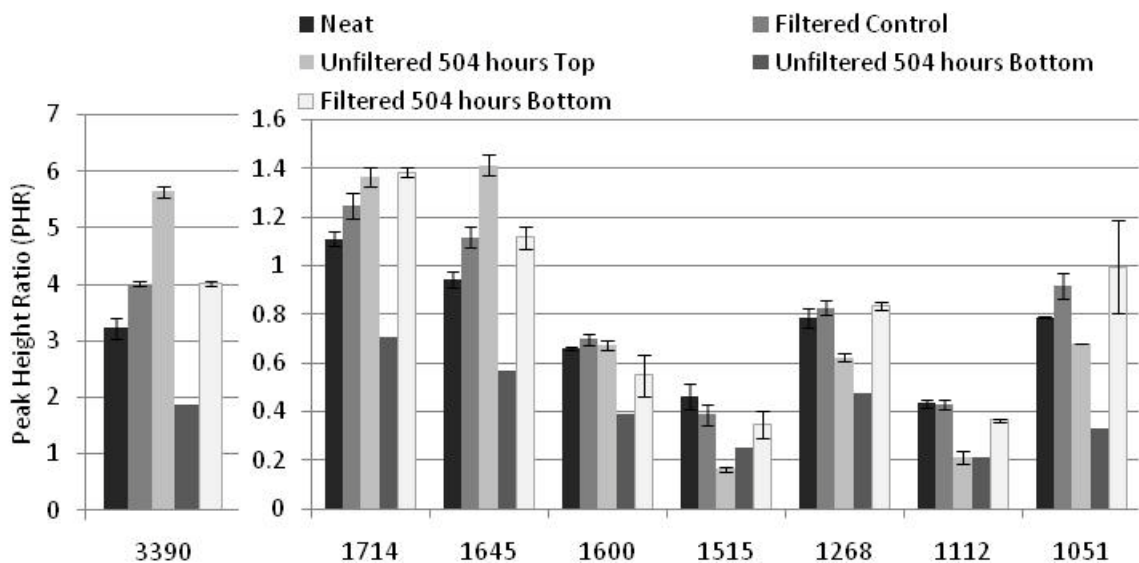


Figure 5.45 Calculated PHR for PBF pyrolysis oil neat and filtered aged for 504 hours at 80 °C

5.5.10 GC-MS

When examining Figure 5.46 for trends in aging, CCWF unfiltered and filtered samples had a large increase in 2,6-dimethoxy-phenol and filtered CCWF increase in 2-methoxy-4-methyl-phenol which was no observed in the unfiltered samples. In addition CCWF unfiltered decreased in phenol and several unidentified compounds that with filtration increased after 24 hours but then decreased more than the unfiltered samples did. There are so strong trends during aging and it does not appear that filtration prevented the aging after 504 hours, but may have slowed it within the first 24 h. Also, larger molecular weight compounds cannot be characterized using this method which results in the inability to characterize the produced high molecular weight components.

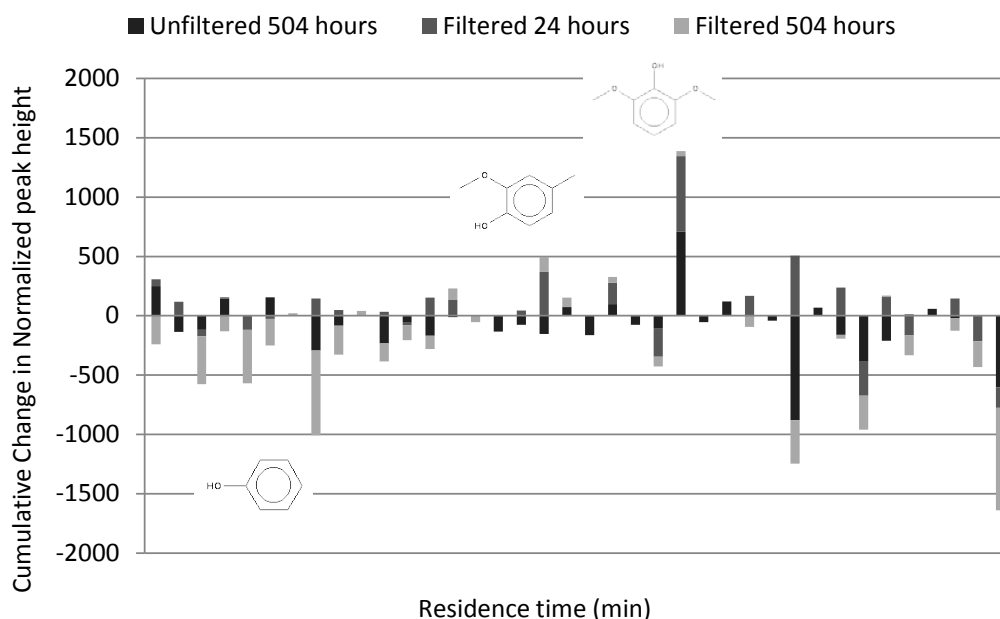


Figure 5.46 Cumulative changes in normalized GC/MS peak heights for CCWF unfiltered and filtered samples.

For PCWT unfiltered (Figure 5.47) most of the compounds are decreasing with aging and the only significant increase is 4-ethyl-2-methoxy-phenol. Identified compounds that decreased include 2-methoxy-phenol, 4-methoxy-3-methyl-phenol, 2-methoxy-4-vinylphenol and 2-methoxy-4-(1-propenyl)-Phenol (all displayed in Figure 5.48). It is difficult to determine a trend in what may be the reactants or products in the aging reactions as there are so few that could be identified and all of the components are phenolics substituted with ether functional groups. When comparing the filtered data to the unfiltered there are significant reductions to the changes indicating that the filtration did in fact retard the aging reactions in PCWT.

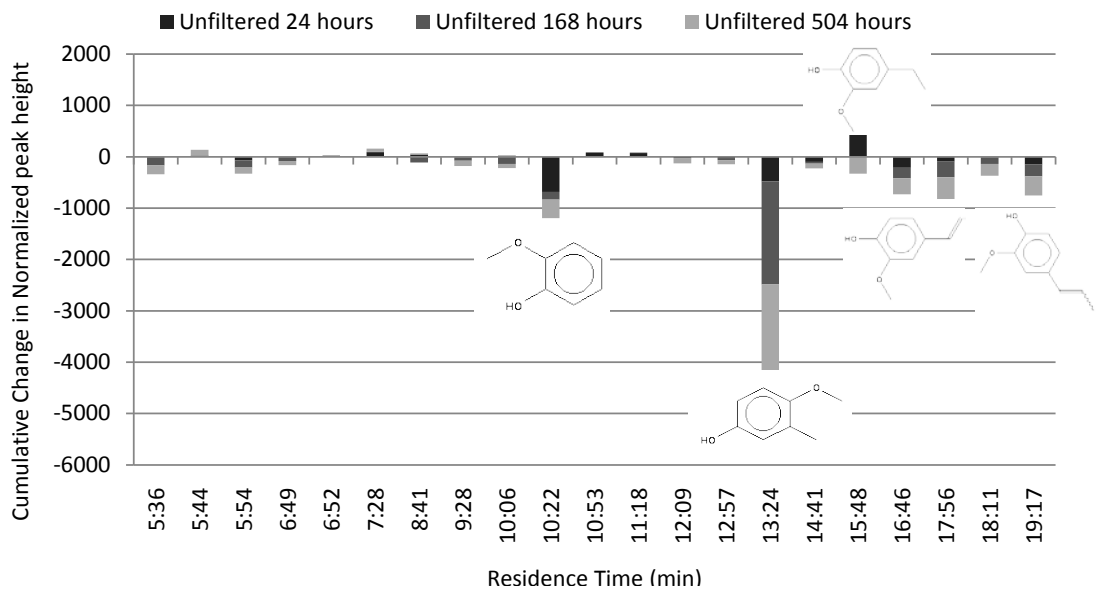


Figure 5.47 Cumulative changes in normalized GC/MS peak heights for PCWT unfiltered samples.

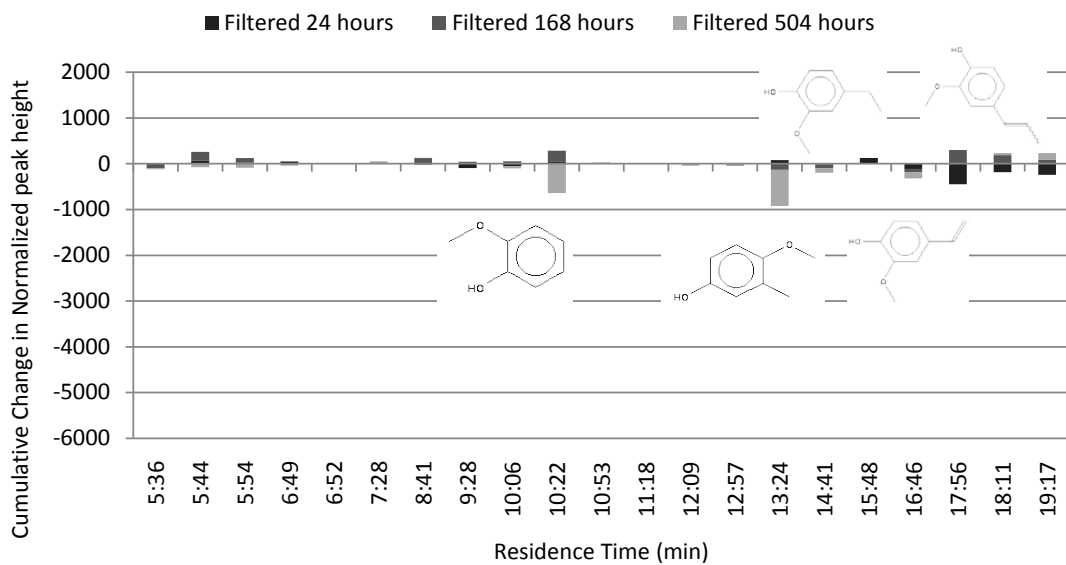


Figure 5.48 Cumulative changes in normalized GC/MS peak heights for PCWT filtered samples.

Figures 5.49 and 5.50 present the PCWF GC/MS data that show more increases when compare to the PCWT data. Compounds that increased in the unfiltered PCWF include mequinol, 4-ethyl-2-methoxy-phenol, and eugenol and there was an increased in

2-methoxy-4-methyl- phenol after 24 and 168 hours but decreased after 504 hours which may be due to sampling rather than a trend. When compared to the filtered and filter torn samples (Figure 6.35) there is a significant difference with not only a reduction in mequinol increase (10:23) but also now a reduction in 2-methoxy-4-methyl- phenol, 4-ethyl-2-methoxy-phenol, and eugenol. This demonstrates that the filtration did alter the aging reaction but rather than stabilize the pyrolysis oil is cause a separate reaction to occur which may lead to the large increase in viscosities and also account for the water content and molecular weight increases.

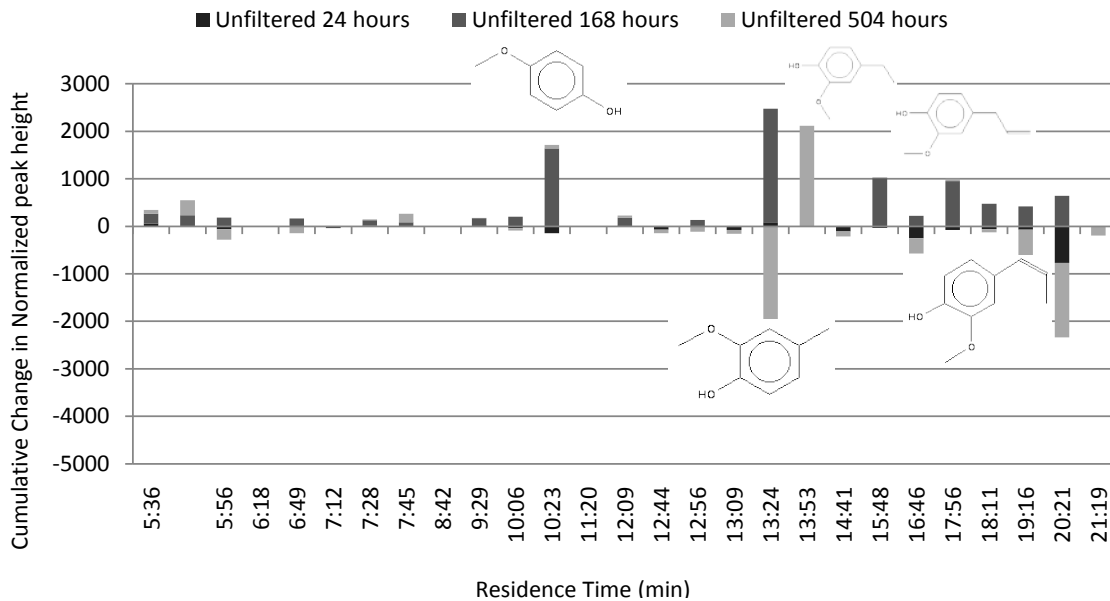


Figure 5.49 Cumulative changes in normalized GC/MS peak heights for PCWF unfiltered samples.

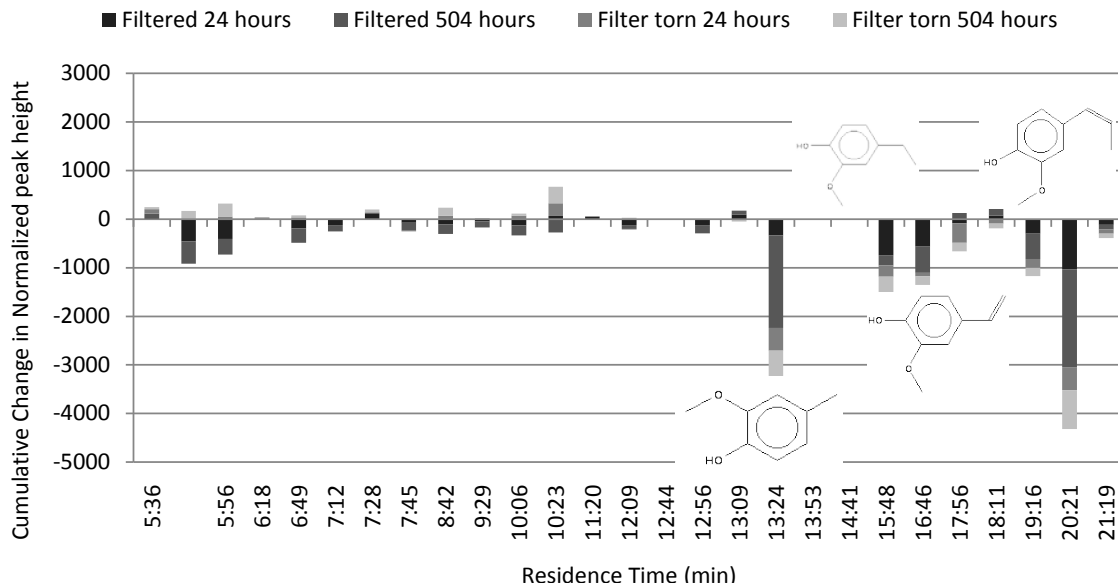


Figure 5.50 Cumulative changes in normalized peak heights for PCWF filtered GC/MS data.

PBF unfiltered and filtered GC/MS data analysis is presented in Figures 5.51 and 5.52 where there is an increase in compounds including 2-methoxy-phenol and 4-ethyl-2-methoxy-phenol, and decreases in 5-methyl-2-Furancarboxaldehyde, phenol, 2-methoxy-4-methyl-phenol, 2-Methoxy-4-vinylphenol and eugenol. When compared to filtered PBF the decrease in 5-methyl-2-Furancarboxaldehyde and phenol were reduced and the increase in 2-methoxy-phenol was replaced by a decrease. There does not appear to be a trend in what compounds were affected by the filtration and others not. In addition it does appear that the filtration did alter the aging reactions in some way but it cannot be determined how with the information provided.

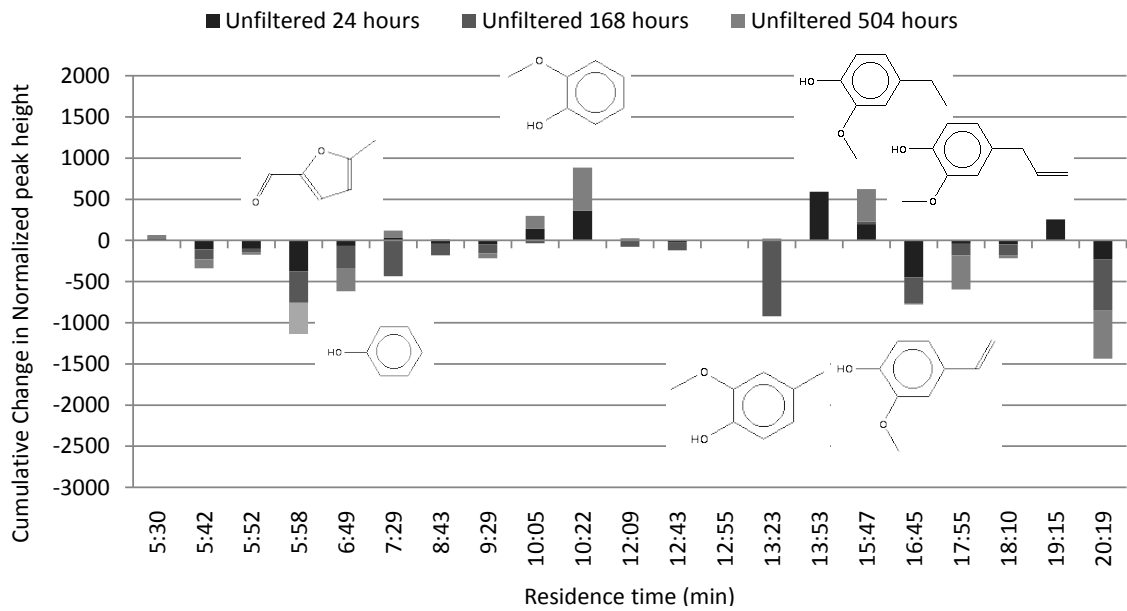


Figure 5.51 Cumulative changes in normalized GC/MS peak heights for PBF unfiltered samples.

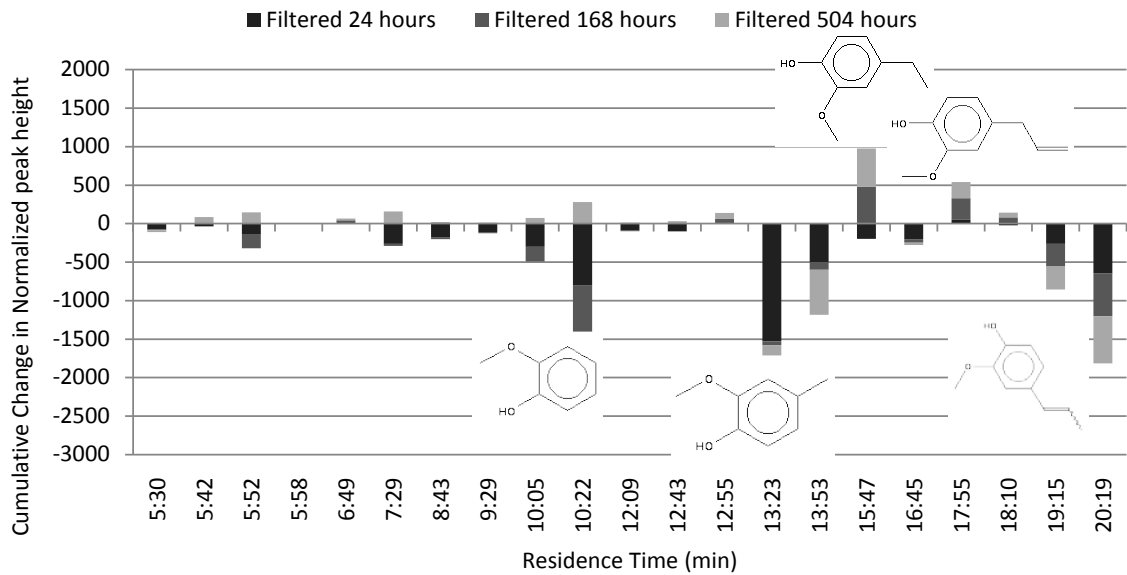


Figure 5.52 Cumulative changes in normalized GC/MS peak heights for PBF filtered samples.

5.5.11 Proposed Reactions

For all four pyrolysis oils, water content, viscosity and molecular weight increased during aging indicating one or more reactions are occurring that have water as a byproduct (condensation) and increase the average molecular weight (polymerizations). PCWT observed a decrease in pH which could be due to the formation of organic acids and the only change detected in IR analysis was an increase in alcohols (C-O st). GC/MS also detected a common theme of substituted phenolic compounds some of which had ether substituents, but there was no trend.

The most useful information in proposing potential reactions is the PHR information for CCWF, PCWF and PBF, all of which had increases in alkenes, aromatics and/or ketones (C=C or C=O bonds) and decreases in alcohols and/or ethers (C-O bonds).

Oxidation of alcohols typically use a reagent such as H_2CrO_4 or $\text{Na}_2\text{Cr}_2\text{O}_7$ and the oxidation of a secondary alcohol results in a ketone [Bruice].

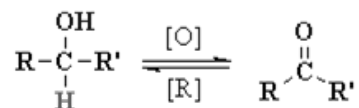


Figure 5.53 Oxidation of alcohols [Carey]

In the presences of strong oxidizing agents secondary alcohols will easily oxidized to produce ketones by acid dichromate at room temperature or slightly elevated. [March] Secondary alcohols in acetone will rapidly produce ketones with titration of Jones reagent, (a solution of chromic acid and sulfuric acid in water) [March].

It would be reasonable to have oxidation occur in pyrolysis oil if an oxidizing agent was present and given over 400 compounds are present, oxidation is possible.

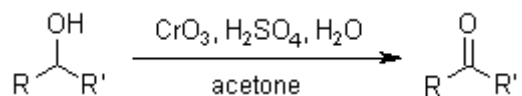


Figure 5.54 Jones Oxidation (o chem portal)

5.6 Conclusions

Four types of biomass produced pyrolysis oils were filtered and aged to determine if filtration of solids reduced the aging effects. Pine and cottonwood pyrolysis oils presented similar aging results before and after filtration demonstrating that many of the results during accelerated aging are not feedstock specific.

Nominal pH values remained stable for all the fractionated samples but decreased in PCWT, but may be related to the higher water content prior to aging and batch dependent. In addition, water content decreased after filtration and then increased for both the unfiltered and filtered samples. PCWT and PBF phase separated during aging and measured water contents were much lower for the bottom phase than the top with the water content of the top phase continuing to increase during aging.

Viscosity after filtration increased significantly for all of the pyrolysis oil samples studied and is thought to be related to the reduction in water content, a result of filter wetting and residue loss during filtration. During aging, both unfiltered and filtered samples increased in viscosity with the filtered samples having larger viscosities than the unfiltered samples throughout aging. In addition once PCWT and PBF phase separated, the viscosity decreased drastically due to the introduction of two separate layers. Molecular weight also increased during aging in all samples. In phase separated samples, the bottom phase had larger molecular weights that continued to increase during aging and the top phase molecular weight decreased to reach the initial (unaged) molecular weight of the sample.

ATR PHR showed that there was a general trend in the reactions occurring in the four pyrolysis oils during aging. All exhibited decreases in primary or secondary alcohols and/or ethers in addition to an increase in aromatics and ketones or carboxylic acids.

Using GC/MS analysis, it was determined that filtration does alter the aging reactions in PBF, PCWF and PCWT, but not CCWF. Changes in the normalized peak heights observed during aging were altered but not prevented suggesting that the removal char particulates may slow or prevent the original reaction(s) but also could allow for one or more additional reactions to proceed.

5.7 References

Agblevor, F.A.; Besler, S.; Evans, R.J. Inorganic Compounds in Biomass Feedstocks: Their Role in Char Formation and Effect on the Quality of Fast Pyrolysis Oils. In *TA Proceedings of the Biomass Pyrolysis Oil Properties and Combustion Meeting*, Milne Ed.; NREL, 1994, p. 77–89.

Agblevor, F.A.; Besler, S. Inorganic Compounds in Biomass Feedstocks. 1. Effect on the Quality of Fast Pyrolysis Oils. *Energy & Fuels* 1996, 10, 293-298.

Agblevor, F.A.; Scahill, J.; Johnson, D.K. Pyrolysis Char Catalyzed Destabilization of Biocrude Oils. *AIChE Symposium Series* 1998, 319, 94.

ASTM Standard E 203-01 Standard method for water using volumetric Karl Fischer titration, 396-405.

Ba, T.; Chaala, A.; Garcia-Perez, M.; Roy, C. Colloidal Properties of Pyrolysis oils Obtained by Vacuum Pyrolysis of Softwood Bark. Storage Stability. *Energy & Fuels* 2004, 18, 188-201.

Boucher, M.E.; Chaalab, A.; Roy, C. Pyrolysis oils obtained by vacuum pyrolysis of softwood bark as a liquid fuel for gas turbines. Part I: Properties of pyrolysis oil and its blends with methanol and a pyrolytic aqueous phase. *Biomass & Bioenergy* 2000, 19, 351-361.

Bridgewater, A.V. Renewable fuels and chemicals by thermal processing of biomass. *Chemical Engineering Journal* 2003, 91, 87–102.

Bridgewater, A.V. Biomass Fast Pyrolysis, A Review Paper. *Thermal Science* 2004, 8, 21-50.

Bruice, P.Y., Organic Chemistry, Fourth Edition. Prentice Hall, 2004.

Carey, F.A., Sundberg, R.J. Advanced Organic Chemistry, Fourth Edition. Part B: Reactions and Synthesis. Kluwer Academic/Plenum Publishers: New York, 2000; p. 332-339, 693-695.

Carey, F.A. Organic Chemistry, Fourth Edition; McGraw-Hill Companies, 2000; p. 590-593.

Chaala, A.; Ba, T.; Garcia-Perez, M.; Roy, C. Colloidal Properties of Pyrolysis oils Obtained by Vacuum Pyrolysis of Softwood Bark: Aging and Thermal Stability. *Energy & Fuels* 2004, 18, 1535-1542.

Czernik, S.; Johnson, D.; Black, S. Stability of Wood Fast Pyrolysis Oil. *Biomass & Bioenergy* 1994, 7, 187-192.

Czernik, S. Storage of Biomass Pyrolysis Oils. In *Proceedings of the Biomass Pyrolysis Oil Properties and Combustion Meeting*; Milne T.A., Ed.; NREL, 1994, p 67–76.

Diebold, J.P.; Czernik, S.; Scahill, J.W.; Philips, S.D.; Feik, C.J. Hot-gas filtration to remove char from pyrolysis vapours produced in the vortex reactor at NRE. In *Proceedings of the Biomass Pyrolysis Oil Properties and Combustion Meeting*; Milne T.A., Ed.; NREL, 1994, p 90–108.

Diebold, J.P.; Czernik, S. Additives To Lower and Stabilize the Viscosity of Pyrolysis Oils during Storage. *Energy & Fuels* 1997, 11, 1081-1091.

Diebold, J.P. A Review of the Chemical and Physical Mechanisms of Storage Stability of fast Pyrolysis Pyrolysis oils. Subcontractor Report for the National Renewable Energy Laboratory NREL/SR-570-27613; National Renewable Energy Laboratory: Golden, CO, 2000.

Elliot, D.C. Alkali and Char in Flash Pyrolysis Oils. *Biomass & Bioenergy* 1994, 7, 179-185.

Energy Information Administration (EIA). 2009. *Annual Energy Review 2008*. Washington, DC: US Department of Energy.

Fratini, E.; Bonini, M.; Oasmaa, A.; Solantausta, Y.; Teixeira, J.; Baglioni, P. SANS Analysis of the Microstructural Evolution during the Aging of Pyrolysis Oils from Biomass. *Langmuir* 2006, 22, 306-312.

Garcia-Perez, M.; Adams, T.T.; Goodrum, J.W.; Geller, D.P.; Das, K.C. Production and Fuel Properties of Pine Chip Pyrolysis oil/Biodiesel Blends. *Energy & Fuels* 2007, 21, 2363-2372.

Garcia-Perez, M.; Chaala, A.; Pakdel, H.; Kretschmer, D.; Rodrigue, D.; Roy, C. Multiphase Structure of Pyrolysis oils. *Energy & Fuels* 2006, 20, 364-375.

Hoekstra, E.; Hogendoorn, K.J.A.; Wang, X.; Westerhof, R.J.M.; Kersten, S.R.A.; van Swaaij, W.P.M.; Groeneveld, M.J. Fast Pyrolysis of Biomass in a Fluidized Bed Reactor: In Situ Filtering of the Vapors. *Industrial & Engineering Chemistry Research* 2009, 48, 4744-4756.

Kuptsov, A.H.; Zhizhin, G.N. Handbook of Fourier Transform Raman and Infrared Spectra of Polymers. Elsevier: New York, 1988; p 8, 10, 11.

Nakanishi, K.; Solomon, P.H. *Infrared Absorption Spectroscopy*. Holden Day: Oakland, 1977; p. 14, 19, 25,26, 31, 38-40.

Oasmaa, A.; Leppamaki, E.; Koponen, P.; Levander, J.; Tapola, E. *Physical Characterization of Biomass-Based Pyrolysis Liquids. Application of Standard Fuel Oil Analyses*. Technical Research Centre of Finland, VTT Publication 306, ESPOO 1997.

Oasmaa, A.; Peacocke, C.; *A guide to physical property characterisation of biomass-derived fast pyrolysis liquids*. Technical Research Centre of Finland, VTT Publication 450, ESPOO 2001.

Oasmaa, A.; Kuoppala, E. *Fast Pyrolysis of Forestry Residue. 3. Storage Stability of Liquid Fuel*. *Energy & Fuels* 2003, 17, 1075-1084.

Oasmaa, A.; Kuoppala, E.; Gust, S.; Solantausta, Y. *Fast Pyrolysis of Forestry Residue. 1. Effect of Extractives on Phase Separation of Pyrolysis Liquids*. *Energy & Fuels* 2003, 17, 1-12.

Paula, Yurkanis, Bruice, *Organic Chemistry*. Prentice Hall: New Jersey, 2001.

Pretsch, E.; Buhlmann, P.; Affolter, C. *Structure of Determination of Organic Compounds, Tables of Spectral Data*; Springer: New York, 2000; p. 245, 255, 263, 264, 286, 287, 291, 293.

Ringer, M.; Putsche, V.; Scahill, J. *Large Scale Pyrolysis Oil Production: A Technology Assessment and Economic Analysis*. *National Renewable Energy Laboratory*, Golden, CO, NREL/TP-510-37779, 2006.

Silverstien, R.M.; Webster, F.X. *Spectrometric Identification of Organic Compounds*; John Wiley & Sons Inc.: New Jersey, 1998; p. 82, 86, 87, 90-92, 94 95, 97.

Smith, M.B.; March, J. *March's Advances Organic Chemistry*; Wiley-Interscience; 2007.

CHAPTER VI

EFFECTS OF METHANOL ADDITION TO FRACTIONATED AND TOTAL PINE NEEDLE PYROLYSIS OIL DURING ACCELERATED AGING

6.1 Abstract

Pine needle total and fractionated pyrolysis oils were used to investigate the effects of methanol on the aging reactions during storage. Methanol was added to pine needle total [PNT] samples at 10 wt% and pine needle fractionated [PNF] samples were prepared with 5, 10 or 15 wt % methanol added. Unaltered and methanol-added samples were then aged at 80 °C for 24 and 504 hours. Characterization included pH, water content and viscosity measurements and attenuated total reflectance Fourier transform infrared (ATR-FTIR)] spectroscopy, gel permeation chromatography (GPC), and coupled gas chromatography-mass spectroscopy (GC/MS). Methanol addition was able to retard the effects of aging in the PNF samples but not in PNT which may be due to its high water content. Also, PNT appeared to have larger increases in molecular weight during aging. Addition of methanol to PNF reduced the molecular weight after 504 hours of aging and at 15 wt% prevented phase separation. In addition, GC/MS analyses indicated the formation of ester and/or aldehyde occurred with the addition of 15 wt% methanol during aging.

6.2 Introduction

Demand for alternative fuels continues to grow due to the rapid consumption of petroleum fuels, concerns for the environment [Boucher 2000 I] and high petroleum

prices [Jung 2008]. Due to these driving forces, there has been growing interest in biomass-derived fuels which provide advantages such as CO₂ neutrality and low concentrations of sulfur [Bridgwater thermal 2004]. Pyrolysis is the thermal decomposition of biomass in the absence of oxygen [Bridgwater 2003] and fast pyrolysis refers to short residence times for the gas phase with high heating rates and can result in higher yields (vs. slow pyrolysis) [Jung 2008].

Pyrolysis oil is also known as liquid smoke, pyrolysis oil, wood distillates, wood liquids, biofuel, biocrude oil, etc. [Bridgewater]. A large amount of the published research involves the fast pyrolysis of wood or wood wastes; feedstocks such as straw or bamboo [Jung 2008] or any other biomass including seeds, grasses, or agricultural residue can also be used to produce pyrolysis oil [Ingram 2008]. In addition, multiple reactor configurations such as fluidized bed, transport and circulating fluidized bed, ablative, rotating cone and vacuum reactors [Mohan 2006] have been shown to achieve liquid product yields as high as 70-80 wt% (based on dry biomass) [Czernik 2004]. Pyrolysis design variables include biomass water content, biomass particle size, reactor design, heat transfer rate and supply, temperature, vapor residence time, ash separation and liquid collection [Mohan 2006]. It has been proposed that pyrolysis oil could be used in boilers, turbines, sterling engines and diesel engines [Bridgewater 2004]. Some products from fast pyrolysis oil have been utilized in heat and power production, but their application as a transportation fuel is far more challenging [Bertoncini, 2006].

During pyrolysis complex biomass components (cellulose, hemicelluloses and lignin; ref) undergo a thermal decomposition leading to a micro-emulsion consisting of an aqueous phase of hemicellulose-derived components stabilizing lignin-derived macro-molecules through hydrogen bonding [Bridgwater 2003]. More than 400 chemical

compounds have been reported in pyrolysis oils [Diebold 2000] with water making up the largest percentage by weight followed by a poorly defined mixture of alcohols, acids, ketones, phenols, esters, sugars, furans, guaiacols and syringols [Diebold 2000]. These compounds are highly reactive and result in unusual properties [Bridgwater 2003] that create multiple barriers preventing direct use of pyrolysis oil as an alternative fuel including low pH, high solid content, a wide range of physical and chemical properties, instability during storage, and the lack of safety data [Oasmaa 2005].

One of these barriers is corrosion due to a pH values ranging 2.3-3.0 as a result of organic acids [Diebold 2000] and solids containing alkali metals entrained in the vapor during pyrolysis [Hoekstra 2009]. Pyrolysis oils have been found to corrode mild steel, aluminum and nickel based materials where stainless steel and various plastics are more resistant [Darmstadt 2004]. Corrosion increases with elevated temperature and/or water content [Darmstadt 2004] and when pyrolysis oil contains alkali metals corrosion occurs in gas turbine blades [Davidsson 2002] and pump and injection components [Czernick 2004]. Solids containing alkali metals, chlorides and sulfates within the pyrolysis oil can also result in fouling and plugging of orifices within boilers and turbines [Hoekstra 2009] and accelerate oxidation [Boucher 2000 I].

Instability is another significant barrier for pyrolysis oil usage in commercial applications. Due to high oxygen concentrations, pyrolysis oils are unstable during storage—often referred to as aging—that results in increased viscosity and water formation [Oasmaa 2004, Diebold 1997] and can lead to phase separation [Oasmaa 2004]. Additional changes over time and/or with elevated temperature include increased average molecular weight, increased heating value, and a decrease in volatile material such as aldehydes and ketones [Oasmaa 2004]. Reactive compounds during storage

polymerize are theorized to form larger molecules resulting in physical property changes [Diebold 1997]. It was proposed the aging reactions were primarily etherification and esterification between carbonyl, carboxyl and hydroxyl function groups [Diebold 1997].

To prevent the undesired aging, physical and chemical upgrading methods have been investigated including solvent addition [Diebold 1997, Boucher 2000, Oasmaa 2004, Shaddix 1999], emulsions with diesel fuel [Bridgwater 2004], deoxygenation over zeolite catalysts, and hydrotreating using a catalyst [Maggi 1994]. Emulsifying pyrolysis oil with diesel fuel is one of the simplest upgrading methods and requires the least amount of engine modification [Weerachanchai 2009]. Diesel fuel with up to 10 % pyrolysis oil and CANMET surfactant were successful in obtaining a stable, homogeneous emulsion [Weerachanchai 2009]. It was also suggested that the additives used for the stabilization of the emulsion would be dependent on the pyrolysis oil properties and feedstock [Weerachanchai 2009].

Various solvents investigated for addition to pyrolysis oil include methanol, acetone, ethanol, isopropanol, formic acid, and water [Diebold 97, Boucher 2000, Oasmaa 2004]. Polar solvents can homogenize pyrolysis oils and reduce the initial viscosity [Diebold 1997, Oasmaa 2004], flash point, and density [Oasmaa 2004]. In addition, mixing with alcohols improves the heating value [Oasmaa 2004, Weerachanchai 2009] and acidity [Weerachanchai 2009]. Solvents have been added to pyrolysis oil at concentrations up to 25 wt% before and after accelerated aging studies [Diebold 1997]. Methanol was determined to be the most effective solvent in reducing the aging effects [Diebold 1997, Oasmaa 2004]. Three mechanisms were proposed for solvent addition: physical dilution, molecular dilution, or solvent reaction with the pyrolysis oil preventing the original aging reaction(s) [Oasmaa 2004].

In one study, 10 wt% methanol added to hybrid poplar pyrolysis oil reduced the rate of viscosity increase (aging) by almost 20 % and was shown to not be acting solely by molecular dilution [Diebold 1997]. Unaltered pyrolysis oil increased in viscosity from 30 to 90 cP at 40 °C after 20.5 h of aging at 90 °C and the addition of methanol after 20.5 h of aging at 90 °C resulted in a viscosity lower than the initial unaltered pyrolysis oil. With methanol addition prior to aging, the viscosity was significant lower compared to when methanol was added prior to aging (17 cP vs. 25 cP at 40 °C) [Diebold 1997]. Methanol addition was tested both pre- and post-accelerated aging and reduced the viscosity of unaged pyrolysis oil prior to aging [Diebold 1997]. Pyrolysis oil and methanol samples were aged for 20.5 hours at 90 °C remained a lower viscosity when compared to the unaltered aged samples [Diebold 1997]. Methanol addition was found to delay, but not prevent, the formation of large aromatic molecules [Diebold 1997] and was most effective when added prior to storage/aging. GC/MS analysis revealed methanol addition decreased acetic acid concentration and increased methyl acetate concentration. It was theorized that the methanol reacted with oligomers creating non-reactive oligomers such that the (re)polymerization process is slowed [Diebold 1997].

A similar study—also with the addition of methanol at 10 wt %—with pyrolysis oil produced from mixed softwood species forestry residue (70 wt% fir, 28 wt% white spruce, 2 wt% larch) showed decreased viscosity with methanol addition [Boucher 2000]. Samples aged at room temperature for up to 262 days remained a single phase with a lower viscosity and molecular weight after aging as compared to the unaged, unaltered pyrolysis oil [Boucher 2000]. GC/MS analysis showed methylation had occurred in the pyrolysis oil samples aged in presence of methanol (higher concentration in methylstearate) [Boucher 2000].

In a separate study, ethanol, methanol and isopropanol were added at 5 and 10 wt% to pine sawdust and forestry residue derived pyrolysis oils [Oasmaa 2004]. Accelerated aging was conducted at 80 °C for 6 and 24 hours (correlating to 3-4 months and 1 year of room temperature storage, respectively) to test the stability [Oasmaa 2004]. Alcohol addition improved the homogeneity of the pyrolysis oils by enhancing solubility and decreasing the viscosity [Oasmaa 2004]. Methanol (10 wt%) addition reduced the viscosity increased by 20 % during aging [Oasmaa 2004]. It was determined that the addition of more than 10 wt % alcohol retards the aging reactions for 1 year for pyrolysis oil produced from forestry residue and pine sawdust and that methanol was the most effective of the alcohols [Oasmaa 2004]. Acetal formation of alcohols with aldehydes, ketones, and sugars was observed and esterification and acetalization were both suggested as reactions where methanol or ethanol protect the aldehyde and ketone functional groups [Oasmaa 2004].

In these three separate investigations involving different pyrolysis oil types demonstrated that solvent addition does retard the aging reactions. And while different degrees of aging retardation were observed for each study suggesting that the type of pyrolysis oil is related to the response, the overall conclusions is that methanol can be used as a universal retardant for aging in pyrolysis oils. Forestry residue and bark have been investigated as low cost feedstocks for pyrolysis oil demonstrating that the derived pyrolysis oils have different properties when compared to clear wood derived oils. An additional biomass of interesting within this group is pine needles which have a different composition when compared to heart wood with 7-8 times more extractives and higher hydroxy acid contents [Oasmaa 2003]. Also needles have additional chlorophyll and proteins resulting high concentrations of ash (0.1-0.2 wt %), alkali metals (400-1000

mg/kg), and nitrogen (0.1-0.4 wt %) [Oasmaa 2003]. Pyrolysis oil produced solely from pine needles was investigated in this study to examine accelerated aging characteristics and the effect of methanol addition (5, 10 and 15 wt%).

6.3 Methods and Materials

Feedstock: Plantation grown Loblollypine (*Pinus taeda*) trees were harvested, needles removed and dried to 10-15% moisture content (MC) in an oven (Despatch V series VREZ-19-ZE). Needle biomass was then ground (Bauer Bro. Co., 25 Hp, 1465 rpm) and screened resulting in particles between ~4-6 mm (Universal Vibrating Screener, Type S #1354).

Pyrolysis: MSU Forest Products Laboratory produced the pine needle pyrolysis oils using an auger pyrolysis reactor operated under vacuum at 400 °C, 25 °C (± 1 °C) at an average flow rate of 15-20 L/min. Fractionated oil collected refers to the exception of one condenser during oil collection where high concentrations of water are produced in addition to organic acids and during oil production the first condenser was not cooled. Total pyrolysis oil included all of the condenser products. Pyrolysis oil samples were stored at ~5 °C within 1 h of production to minimize aging reactions prior to experiments. Produced pyrolysis oil was dark in color with a pungent smell, multiple phases with a large concentration of solids and pyrolysis oil samples were aliquots from the same 1 L production batch.

Methanol addition: Methanol (99 %, McMaster Carr) was added to pine needle pyrolysis oils at 5, 10 and 15 wt% while stirring by batch and then divided into samples for aging.

Aging Conditions: Samples to be aged were prepared as 27 mL aliquots in 30 mL amber bottles with PTFE lined caps (in accordance to recommendations in Oasmaa, 2001). A convection oven was used to heat the samples at 80 °C for 24 and 504 hours and controls were stored at 5 °C to prevent aging. Aged bottle caps were retightened periodically to minimize weight loss and the initial and final weights were collected in addition to the characterizations. Triplicates were prepared for all samples including methanol added, controls and aged samples.

pH, Water Content and Density: pH was collected for the pyrolysis oil samples (AB15 Accumet Basic) with five point calibration with phosphate buffer solutions (2, 4, 7, 10, 12). Density was calculated using measured weight of known volumes. A Barnstead International Aquametry II Apparatus was used to perform Karl Fischer titration for water content determination with Hydranal Solvent CM (chloroform-methanol) and Hydranal Titrant 2E in accordance with ASTM E 203-01. A minimum of three measurements were collected and averaged to calculate the pH, water content and density and 95 % confidence intervals.

Viscosity: Step-flow tests were performed (TA Instruments AR 1500x rheometer) with 60 mm aluminum parallel plates and a Peltier plate to maintain the temperature at 40 °C. Shear rates were examined from 0.1 to 1000 Hz (1/s) using a stepped shear profile. Sample volumes were maximized in all runs with sample volumes ranging from 500 to 1200 μm , but dependant on the sample viscosity and gap distance. A minimum of 10 data points were averaged over a plateau region observed at higher shear rates (10-1000 1/s) to calculate an average viscosity and 95% confidence intervals.

Molecular Weight: Molecular weight (MW) was determined by gel permeation chromatography (GPC) using a nine point polystyrene calibration (162, 266, 486, 582,

891, 2780, 6480, 10261, 18200 MW standards, PSS Polymer Standards). GPC samples were prepared by diluting pyrolysis oil in tetrahydrofuran (THF, Optima grade, >95 wt%) to concentrations of 1-2 mg/mL, sonicating, and then filtering with 0.45 μm syringe filters. A custom-built GPC instrument was constructed with a Varian Star 9040 refractive index detector, Varian Mesopore guard column (50 x 4.6 mm ID), Varian Mesopore column (250 x 4.6 mm ID), Waters 610 Fluid Unit, and Waters 600 Controller operated at 0.3 mL/min and 50 μL samples. An internal standard ($M_w = 177,000$) was used to account for shifting retention time. Using the internal standard retention time, all calibration points were shifted to a common position and the calibration was then shifted to each sample internal standard position. Star WS and Waters Breeze software packages were used for data analysis and a minimum of 3 replicates per data point were conducted to obtain average values and 95 % confidence intervals.

FTIR Spectroscopy: Attenuated total reflectance Fourier transform infrared (ATR-FTIR) spectra were collected for liquid pyrolysis oil samples and diffuse reflectance infrared Fourier transform (DRIFT) spectra were collected for solids removed from top crust layers after preparation with 95% KBr powder using a Nicolet 6700 spectrometer (liquid nitrogen cooled MCT-A* detector, 4 cm^{-1} resolution, 256 scans). All ATR spectra were ATR corrected using Thermo Electron OMNIC software.

GC/MS Analysis: Samples were collected using a Varian 3600 gas chromatogram coupled with a Varian Saturn 2000 mass spectrometer (GC-MS; Varian Inc., Walnut Creek, CA) using a fused silica column Rtx-1MS (30 m \times 0.25 mm, film thickness 0.25 μm). The system was operated with an oven temperature 50-300 $^{\circ}\text{C}$, heating rate of 10 $^{\circ}\text{C}/\text{minute}$, helium carrier gas, 1.2 mL/min volumetric flow rate, and 250 $^{\circ}\text{C}$ detector temperature. Unknown compounds were identified by comparing spectra to the NIST

2005 organic compound database with MASPEC II 32 data system software. A GC/MS data analysis method was developed for peak height comparisons where all peak height data were normalized using sample concentration and aged samples were compared to the controls. One sample was analyzed by GC/MS for each sample condition (aging time and methanol concentration).

6.4 Results and Discussion

6.4.1 Aging

Weight loss during aging for pine needle fractionated [PNF] were below 0.5 wt% for the neat (0.36 wt%), 5 (0.48 wt%), 10 (0.36 wt%), and 15 (0.35 wt%) wt % methanol addition. Pine needle total [PNT] neat and 10 wt % methanol added observed weight loss of 0.34 and 0.36 % respectively. All of the aged samples formed a solid crust on the surface of the liquid sample, some of which visually had pieces of pine needle biomass and/or char in the crust. Crusts were removed from the samples prior to characterization and analyzed separately. Additional physical observations include phase separation prior to and after aging for PNF and PNT pyrolysis oils. After 24 h, PNF samples had a small amount of bottom phase and after 3 weeks of aging the bottom phase made up most of the sample and was indistinguishable from the crust layer. PNT had very little bottom phase present and the bottom layer volume, minus outliers, from small to large: without methanol >15 wt% MeOH > 5 wt% MeOH >10 wt% MeOH, indicating there may be a limit for amount of methanol added that is beneficiary.

Pictures showing the crust formation in the pine needle pyrolysis oil samples are presented in Figure 7.1. On the left the sample has visible texture on the surface due to needle like solids and on the right the crust is smooth without texture. Due to the visual

presences of char and/or biomass the top crust phase may have formed due to low density materials floating at the surface and during aging liquid solidified around these solids.

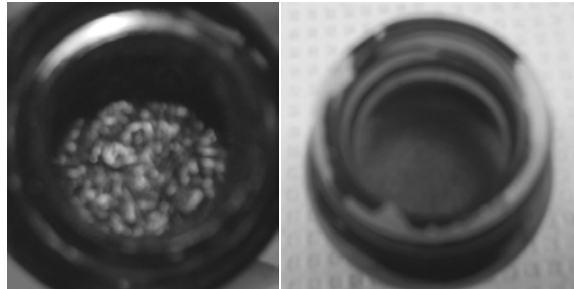


Figure 6.1 Photos of top crusts showing needle biomass or char particles creating highly texturized (left) or smooth crust (right).

6.4.2 pH

With the addition of methanol to PNF and PNT, the pH increased as a function of the weight percent added and the pH data is presented in Figure 7.2 with 95 % confidence intervals error bars. PNT pH is 9 % larger than the PNF oil and the unaltered PNT pH decreased 8 and 9 % after 24 and 504 h of aging respectively. With the addition of 10 wt% methanol increased the un-aged PNT oil pH by 10 % and remained constant (varied less than 1%) throughout aging. PNF unaltered samples observed a 7 and 12 % decrease in the pH after 24 and 504 h respectively and the addition of 5, 10 and 15 wt % methanol increased the pH by 5, 6, and 13 % respectively. Aged methanol added samples vary up to 8 % overall, which is very similar to the 7 and 12 % variation observed in the unaltered samples. Therefore, the addition of methanol increased the pH of the pyrolysis oils as a function of weight percent added prior to aging, but does not prevent or slow the pH variation during aging.

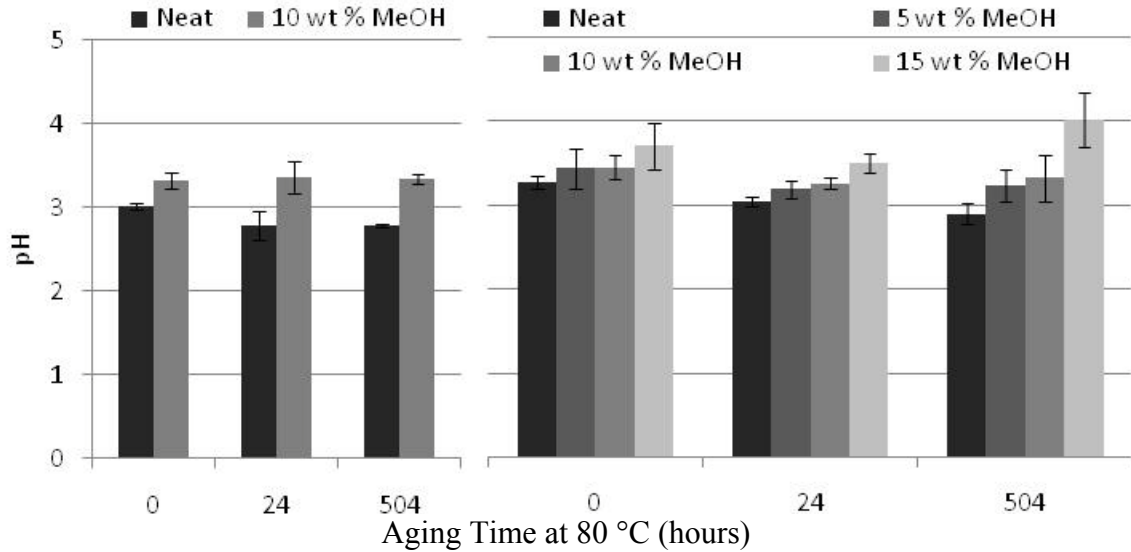


Figure 6.2 pH measurements for neat and 10 wt% methanol pine needle total [PNT, left] pyrolysis oil and neat and 5, 10 and 15 wt% methanol pine needle fractionated [PNF, right] pyrolysis oil aged up to 504 h at 80 °C.

6.4.3 Density

Neat PNT density (Figure 7.3, left) decreased during aging by 15 % and 16 % for 24 hours and 504 h (3 weeks) of aging, respectively. Addition of 10 wt % methanol initially decreased the PNT density by 15 % and then decreased by 7 % after 24 h and 10 % after 504 h of aging. PNT pyrolysis oil density is 4 % lower than the PNF oil. During aging, the density of unaltered PNF pyrolysis oil decreased by 15 % and 12 % for 24 h and 504 h respectively. Addition 5, 10 and 15 wt % methanol decreased the density by 22, 18 and 28 % respectively. Aged samples with methanol added reduced the variation of density during aging to 5, 2 and 13 % for 5, 10 and 15 wt % methanol added respectively. Thus the samples with 5 and 10 wt% methanol limited the reduction in density. Decreasing density could be due to the removal of the top crust phase that contains solids coated in potentially dense material similar in appearance to the bottom phase.

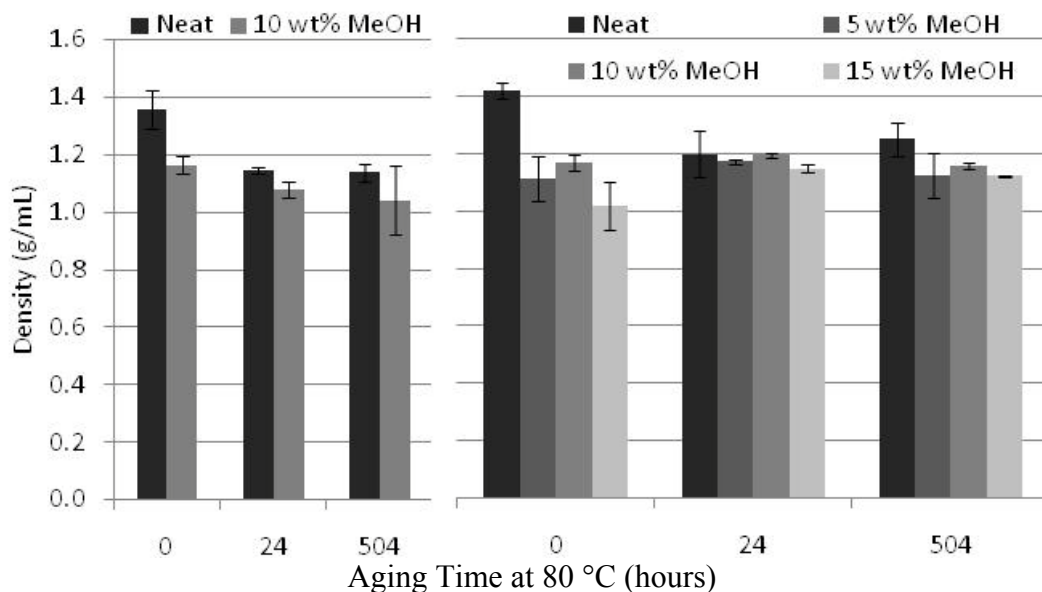


Figure 6.3 Calculated density for pine needle total [left] pyrolysis oil neat and 10 wt% methanol and pine needle fractionated [right] pyrolysis oil neat and 5, 10 and 15 wt% methanol aged up to 504 h at 80 °C.

6.4.4 Water Content

Water content measurements for PNT (left) and PNF (right) are presented in Figure 7.4. During aging the neat PNT water content increases 12 and 23 % after 24 h and 504 h, respectively. Addition of 10 wt % methanol reduced the water content by 17 % and during aging the water content increased by 17 and 30 % for 24 h and 504 h, respectively.

Comparing PNT to PNF, the water content is 50 % lower in PNF. Water content in neat PNF pyrolysis oil during aging decreased 3 % after 24 h and then increased 44 % after 504 h. With the addition of methanol the water content decreased by 23 and 37 % for the addition of 5, 15 wt% methanol respectively and increased 10 w% with the addition of 10 wt% methanol. It is unclear why the addition of 10 wt% methanol increased the water content when 5 and 15 wt% decreased. During aging the water content varied by 13, 18 and 21 % with the addition of 5, 10 and 15 wt % methanol

therefore the increase in water content due to aging was reduced by 13 , 26 and 23 % after 504 h respectively.

Methanol addition to PNF limited the increase in water content during aging but had no affect when added to PNT. This suggests that the water condensate in PNT inhibits the effectiveness of methanol addition either due to the high initial water content or additional components present in the water condensate.

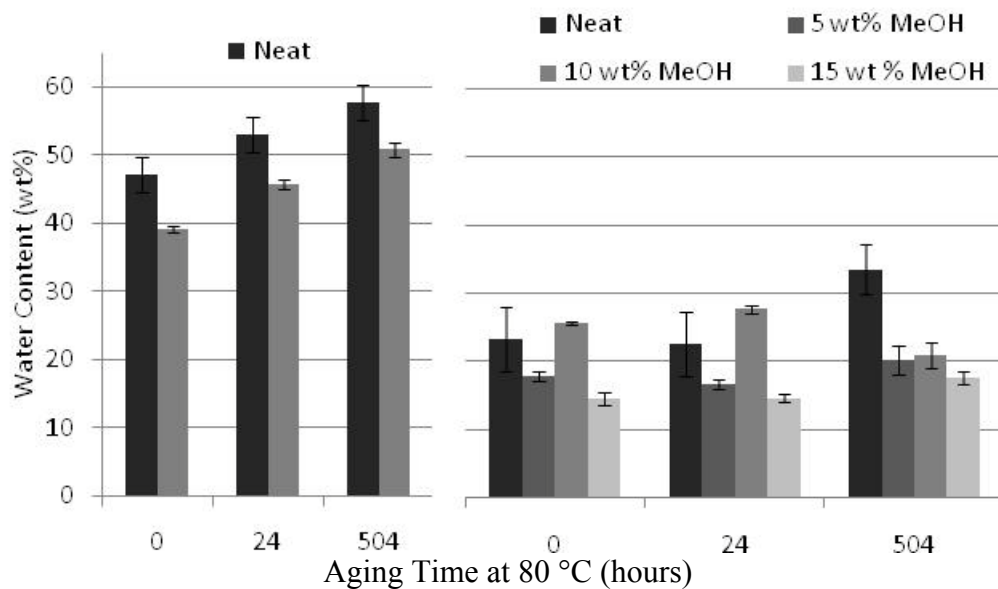


Figure 6.4 Water content for pine needle total [left] pyrolysis oil neat and 10 wt% methanol and pine needle fractionated [right] pyrolysis oil neat and 5, 10 and 15 wt% methanol aged up to 504 h at 80 °C.

6.4.5 Rheology

Pyrolysis oil viscosities were measured with and without the inclusion of the top crust (Figures 7.5, 7.6 and 7.7). PNT samples in Figure 7.5 have large error bars, most likely due to the combination of solids content, multiple phases and high water content making it difficult to obtain reproducible measurements. Considering the large 95% confidence intervals, there is no significant difference in the viscosities during aging

between the samples with or without added methanol. PNT aged samples (with or without the crust) have significantly smaller viscosities versus the unaged samples which is most likely due to the formation of a solid phase (crust) thus reducing the viscosity of the remaining (liquid) sample. Post aging the crust material was added back into the 10 wt% methanol added samples and the viscosity increased demonstrating the crust phase affects the rheological properties and may have dissolved into the liquid phase.

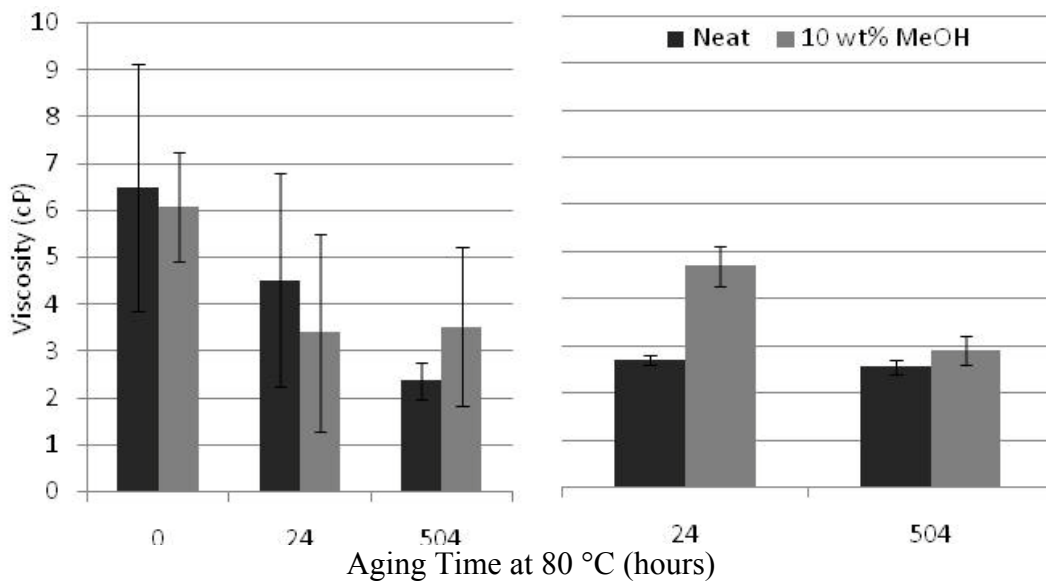


Figure 6.5 Viscosity for pine needle total pyrolysis oil neat and 10 wt% methanol without the solid crust [left] and including solid crust [right] aged up to 504 h at 80 °C.

PNF sample viscosities are presented in Figures 7.6 and 7.7 where the starting viscosity (130 cP) is 190 % larger than the PNT viscosity (7 cP). Over 504 h of aging the PNF samples viscosity increased significantly (by 600 %) to 909 cP. With the addition of methanol, the viscosity decreased by 23, 82 and 23 % for 5, 10 and 15 wt% methanol added samples, respectively. During aging the 5 wt% addition samples increased in viscosity by 94 % whereas the 10 and 15 wt% methanol samples decreased in viscosity

during aging. As observed in PNT samples the removal of the top crust layer is most likely the cause of the viscosity decrease. Also, all PNT including the 10 wt% methanol addition samples have significantly lower viscosities which may be related to the higher water contents.

Due to the removal of the crust phase it is difficult to determine definitively if the methanol addition had reduced the viscosity increase. There was not change observed in the PNT samples with or without the crust phase included. For PNF the methanol did reduce viscosity without the crust phase included showing methanol help to retard the aging and demonstrating as in the water content a difference between methanol addition in PNT and PNF.

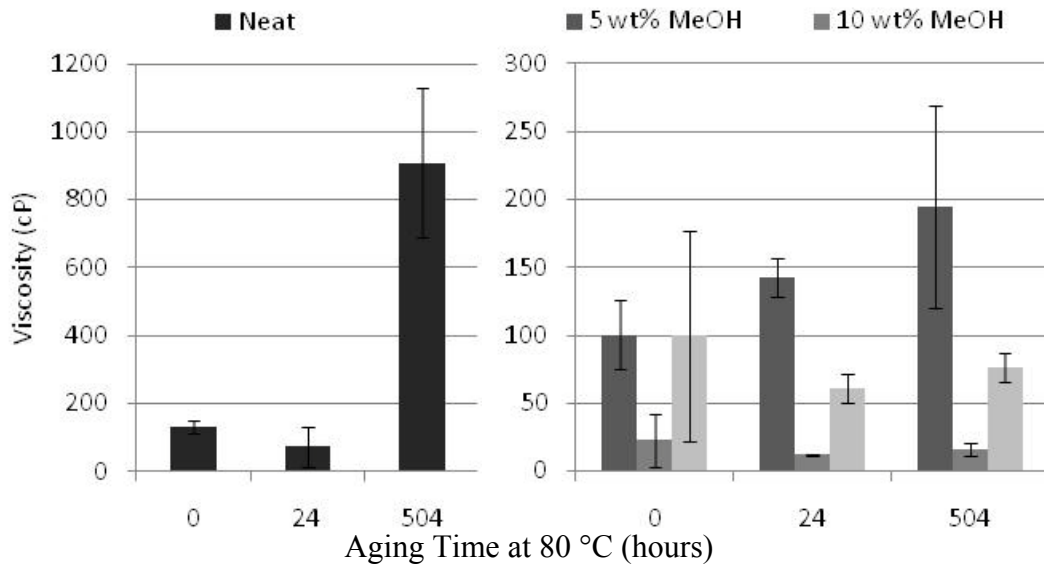


Figure 6.6 Viscosity for pine needle fractionated pyrolysis oil neat [left] and 5, 10 and 15 wt% methanol [right] without the solid crust aged up to 504 h (3 weeks) at 80 °C. *NOTE: Y axes have difference scales*

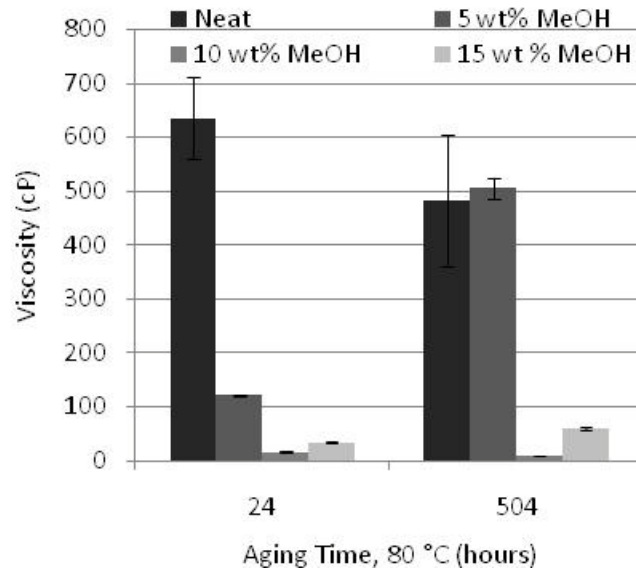


Figure 6.7 Viscosity for pine needle fractionated pyrolysis oil neat [left] and 5, 10 and 15 wt% methanol [right] including the solid crust aged up to 504 h (3 weeks) at 80 °C.

6.4.6 Gel Permeation Chromatography (GPC)

PNT pyrolysis oil phase separated into two phases prior to aging with weight average molecular weights (MW) of 407 and 664 Da for the top and bottom phases respectively (Figure 7.8). During aging, the MW in the bottom phase increased (as expected), but the top phase decreased. The crust phase had a molecular weight of 937 Da after 24 h, a higher MW than observed in the bottom phase. After 504 h, the bottom phase MW increased to 929 Da (40 %), the top phase decreased to 377 Da (7 %), and the crust phase decreased to 742 Da (21 %).

Methanol added to PNT (Figure 7.9) resulted in little to no change in the bottom phase MW prior to aging (>1 %) and 8 % decrease in the top phase MW. After 504 h the 10 wt% methanol top and bottom phase MWs were 386 and 998 Da respectively, a higher MW increase with methanol addition (14 and 7%). In addition the crust MW was 723

Da, a similar MW to the unaltered aged samples (2 %). As observed with the water content and rheology data, the addition of methanol did not prevent or retard the aging.

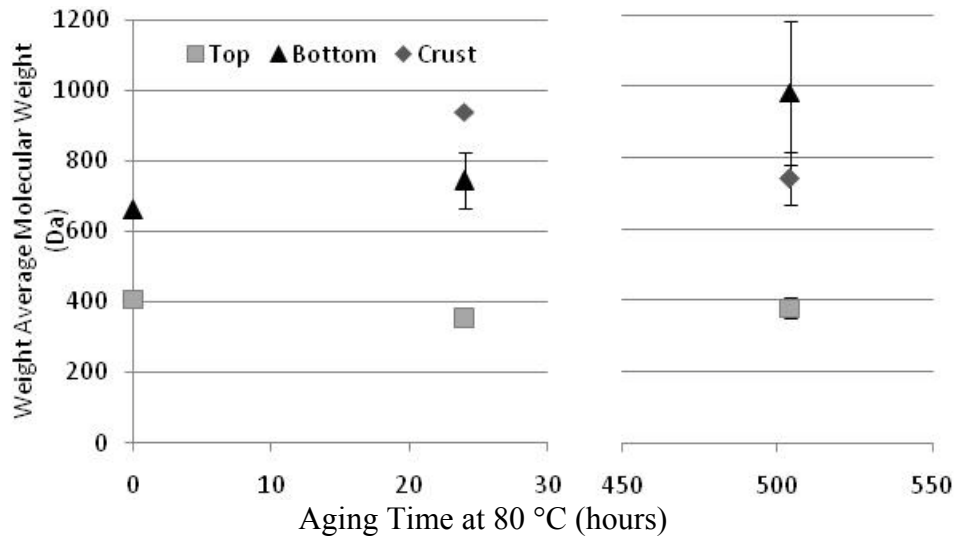


Figure 6.8 Weight average molecular weight (MW) for PNT pyrolysis oil aged up to 504 h at 80 °C presenting the top, bottom and crust phases.

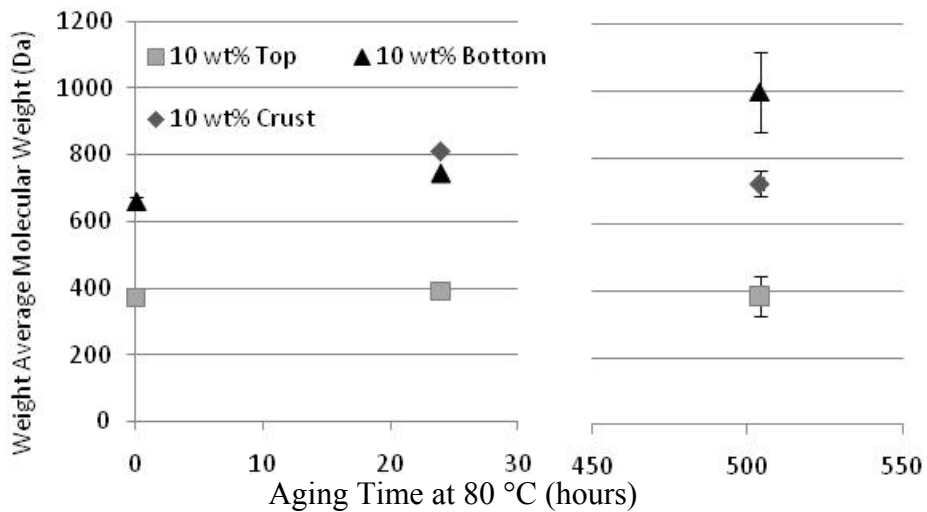


Figure 6.9 Weight average molecular weight (MW) for PNT 10 wt% methanol added pyrolysis oil aged up to 504 h at 80 °C presenting the top, bottom and crust phases.

Unaltered PNF molecular weight values are presented in Figure 7.10. Neat PNF had an initial MW of 552 Da that increased to 620 Da (11 % increase) accompanied with a crust of similar MW (638 Da) after 24 h of aging. After 504 h the bottom phase increased further to 732 Da (33 % total), the top phase decreased to 397 Da (28 % from neat) and the crust remained approximately the same at 651 (2 % increase).

Un-aged methanol added samples had MW values of 591, 484 and 622 Da for 5, 10 and 15 wt% methanol added, respectively. For 5 and 10 wt% methanol added the bottom phase increased by 24 and 44 % and the top phase decreased by 41 and 20 % respectively. Samples with 15 wt% methanol the top and bottom phases after 504 h have a smaller change with an 11 % increase in the bottom phase and 3 % decrease in the top phase. At this concentration (15 wt%) it appears the methanol is retarding the aging, resulting in a smaller increase in molecular weight and also allowing for the bottom phase to dissolve into the top phase making the sample more homogeneous.

For the top crust phase after 504 h of aging the molecular weights were within 1 % of the unaltered crust with 5 and 10 wt% methanol added but decreased with the addition of 15 wt% methanol (7 %). The crust phase appears to be unaffected throughout aging (± 2 % change between 24 and 504 hours) and also vary only 7% overall.

In addition when compared the PNT to the PNF there appears to be larger increase in MW over 504 h with MW values ~ 900 Da for PNT and only ~ 600 Da for PNF. This suggests the presence of the top phase with higher water content encourages the aging reactions resulting in higher MW in the bottom phase. This may also be the reason why methanol is not effective in retarding the aging reactions at the concentration of 10 wt%.

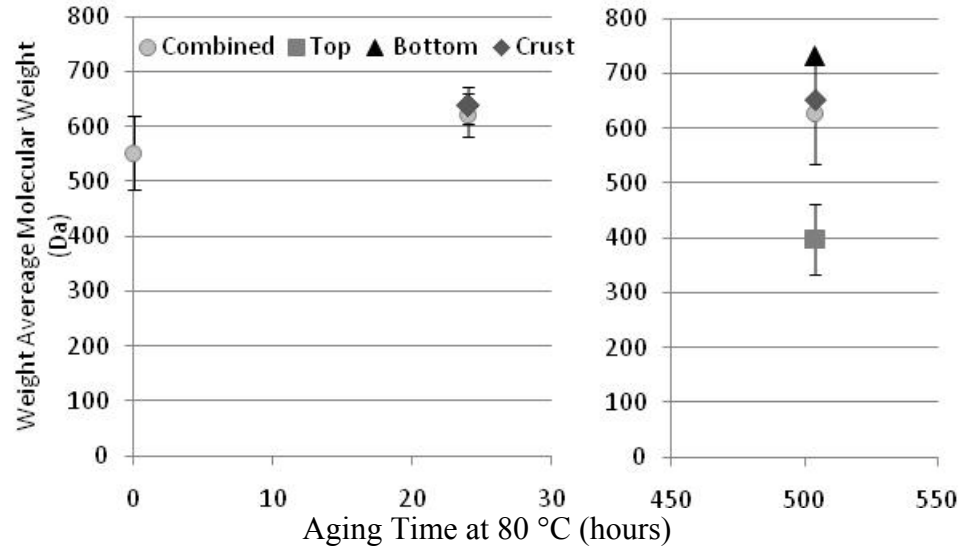


Figure 6.10 Weight average molecular weight (MW) for pine needle fractionated pyrolysis oil aged up to 504 h 80 °C with the single-phase and phase separated data (top, bottom, and crust) shown separately.

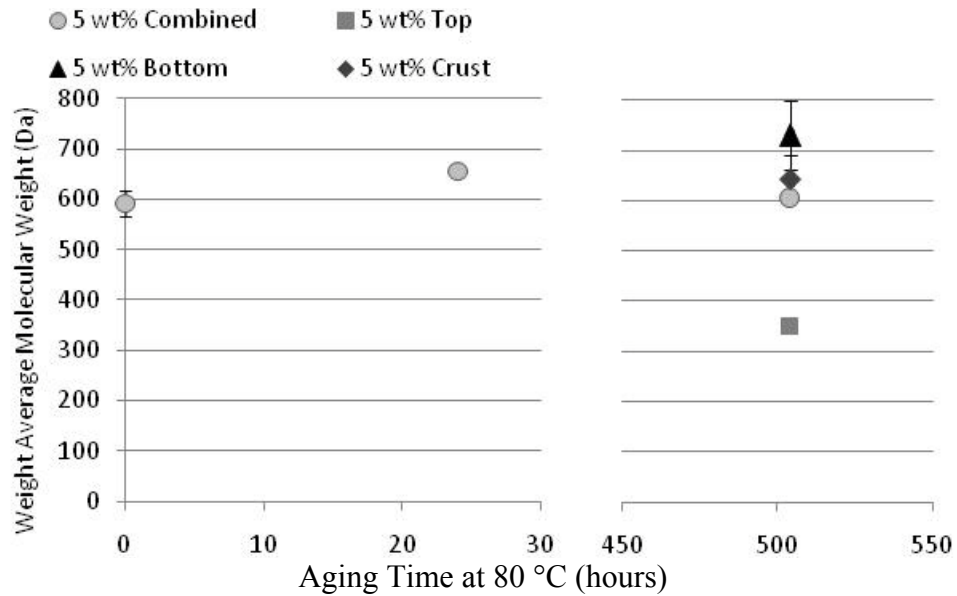


Figure 6.11 Weight average molecular weight (MW) for pine needle fractionated 5 wt% methanol added pyrolysis oil aged up to 504 h at 80 °C with the single-phase and phase separated data (top, bottom, and crust) shown separately.

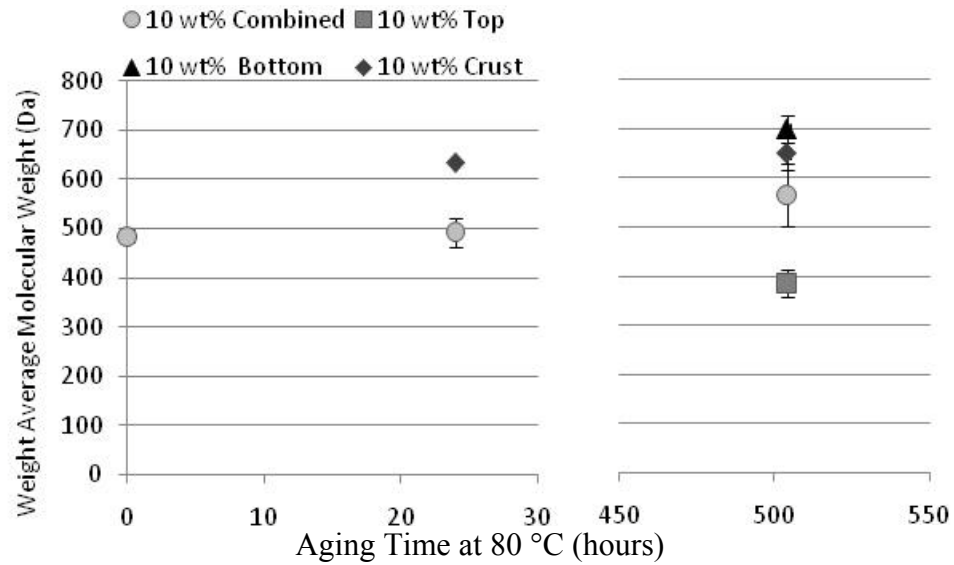


Figure 6.12 Weight average molecular weight (MW) for pine needle fractionated 10 wt% methanol added pyrolysis oil aged up to 504 h at 80 °C with the single-phase and phase separated data (top, bottom, and crust) shown separately.

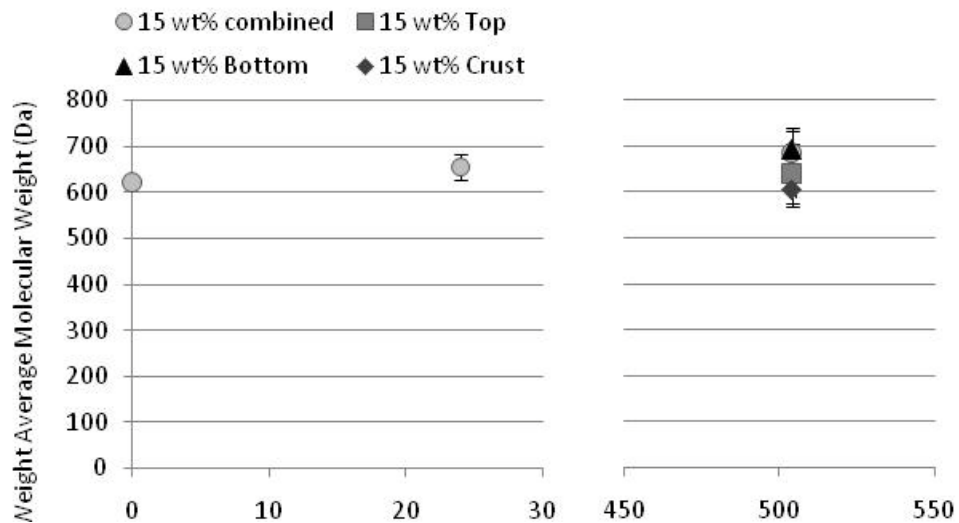


Figure 6.13 Weight average molecular weight (MW) for pine needle fractionated 15 wt% methanol added pyrolysis oil aged up to 504 h at 80 °C with the single-phase and phase separated data (top, bottom, and crust) shown separately.

6.4.7 ATR-FTIR: Qualitative Analysis of PNT vs. PNF

Figure 7.14 compares the ATR spectra for the total and fractionated pine needle derived pyrolysis oils in order to determine if there is a difference in the composition that may lead to higher molecular weights during aging. Two major differences can be observed at $\sim 1705\text{ cm}^{-1}$ for the carbonyl C=O stretch and at $\sim 1050\text{ cm}^{-1}$ for unsaturated primary alcohols [Silverstein]. Fractionated oil appears to have a higher concentration of primary alcohols and the shape of the carbonyl peaks are different due to presence of absence of additional functional groups present.

Peak fitting for the PNF (Figure 7.15) and PNT top and bottom phase (Figure 7.16) carbonyl regions ($1800\text{-}1540\text{ cm}^{-1}$) were conducted for better comparison. PNF contains three peaks at 1710 , 1643 and 1600 cm^{-1} identified as C=O stretch in an aliphatic or cyclic ketone and/or a carboxylic acid dimer ($1711\text{-}1708\text{ cm}^{-1}$) [Silverstein, Pretsch, Nakanishi], C=C stretch in alkenes and/or C=O stretch in a conjugated ketone ($1653\text{-}1644\text{ cm}^{-1}$) [Silverstein, Pretsch, Nakanishi] and C=C in aromatic hydrocarbons and/or skeletal stretching in heteraromatics ($1605\text{-}1599\text{ cm}^{-1}$) [Silverstein, Pretsch]. PNT top phase is very different from PNF with only two peaks located at 1714 and 1639 cm^{-1} cyclic ketone and/or a carboxylic acid dimer [Silverstein, Pretsch, Nakanishi] and C=C stretch in alkenes and/or C=O stretch in a conjugated ketone [Silverstein, Pretsch, Nakanishi] where the 1639 cm^{-1} peak is the dominant peak rather than the 1714 cm^{-1} peak. PNT bottom phase has three peaks all of which are very close to those in PNF which is in agreement with literature describing the bottom phase which similar characteristics of one phase pyrolysis oil. Both the PNF and PNT bottom samples have very similar peak fittings when compared to the PWTF-94 pyrolysis oil (Chapter 4) demonstrating a similar composition in pine pyrolysis oils.

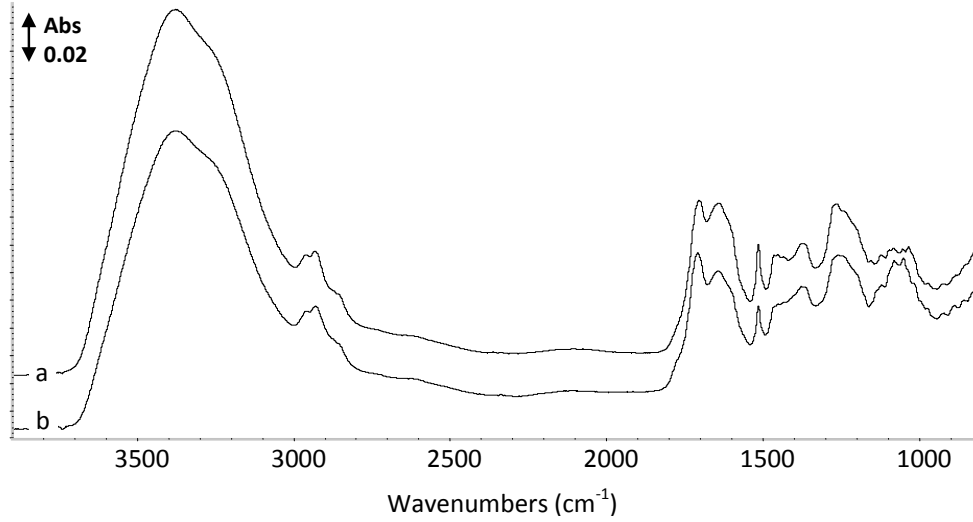


Figure 6.14 ATR comparison (common scale) of total (a) and fractionated (b) needle derived pyrolysis oils.

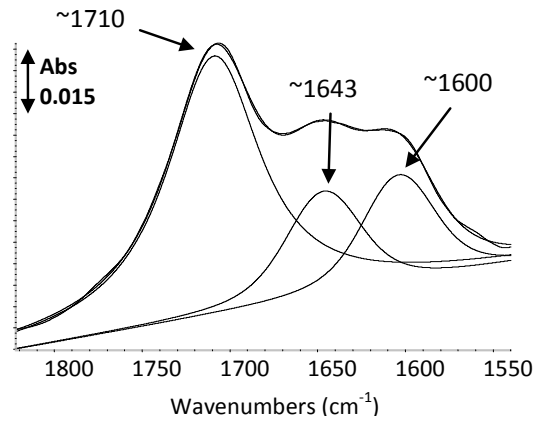


Figure 6.15 Peaks resolved for neat PNF carbonyl peak region

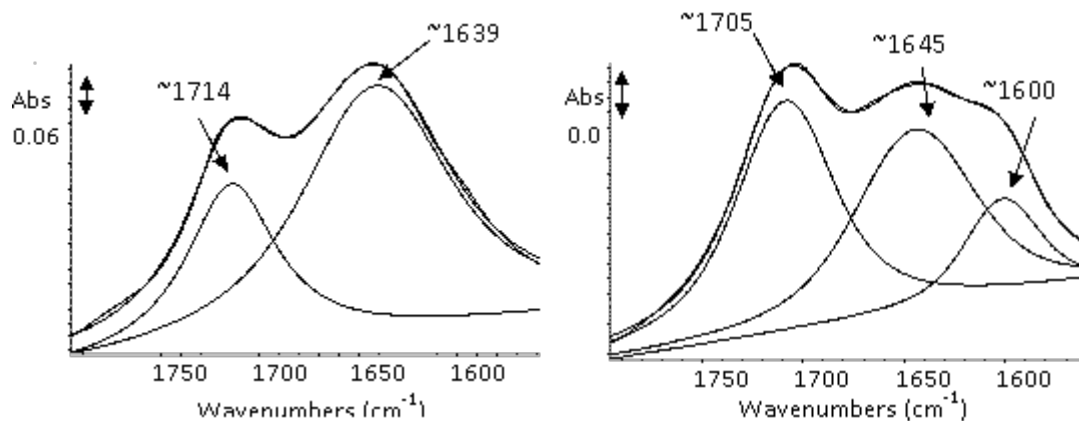


Figure 6.16 Peak fitting for the carbonyl region for neat PNW top (left) and bottom (right) phases.

6.4.8 Pyrolysis oil ATR-FTIR: Qualitative and Quantitative Analysis during aging

PNT samples prior to aging exhibited phase separation and therefore ATR spectra were collected for both phases separately. When the two phases were compared the top phase had only two dominant peaks; a large hydroxyl peak (3700-3000 cm^{-1} , OH st) and carbonyl peak (1800-1600 cm^{-1} , C=O st) with C-H st absent (3000-2800 cm^{-1}) and the bottom phase had a spectrum typical of pyrolysis oil. In addition it should be noted that the carbonyl peaks in the top and bottom phases are significantly different with different dominant peaks. During aging the top phase does not appear to change and the bottom phase has small variations in the carbonyl shape and possible decreases at C=C aromatic skeletal stretching (~ 1515) [Kuptsov, Silverstein] and carboxylic acid [Nakanishi, Silverstein] or =C-C-O stretch in an aromatic ether [Pretsch, Nakanishi, Silverstein, Kuptsov] (~ 1268 cm^{-1}). This suggests that the aging occurs in the bottom phase or products precipitate to the bottom phase where the only change is observed.

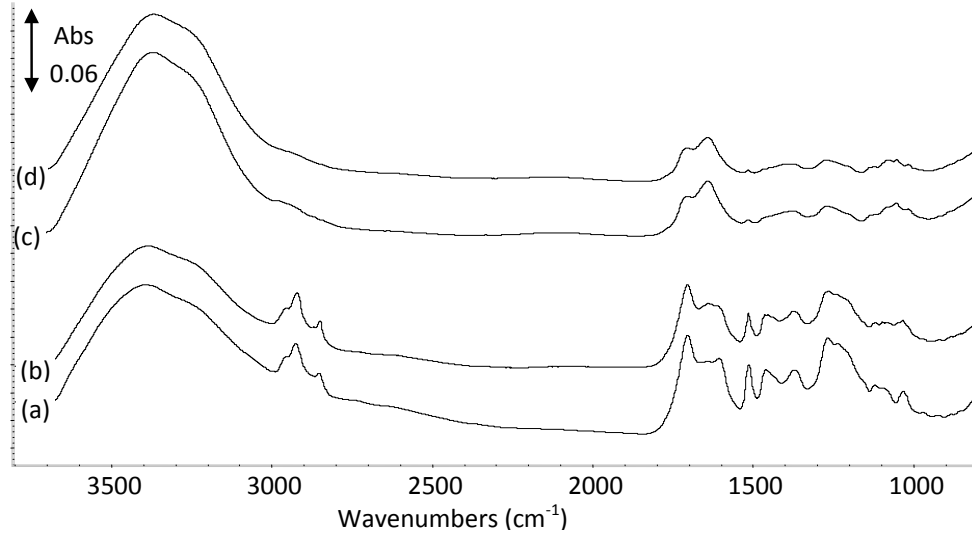


Figure 6.17 ATR spectra collected for PNT bottom phase neat (a) and aged (b) and top phase neat (c) and aged (d) for 504 h at 80 °C.

With the addition of 10 wt% methanol the top phase contains a larger amount of material including small peaks for the C-H stretch, methanol ($\sim 1018 \text{ cm}^{-1}$) and more definition to the peaks in the fingerprint region ($1800\text{-}850 \text{ cm}^{-1}$). There are still not changes in the top phase during aging and only a small change in the carbonyl peak during aging in the bottom phase.

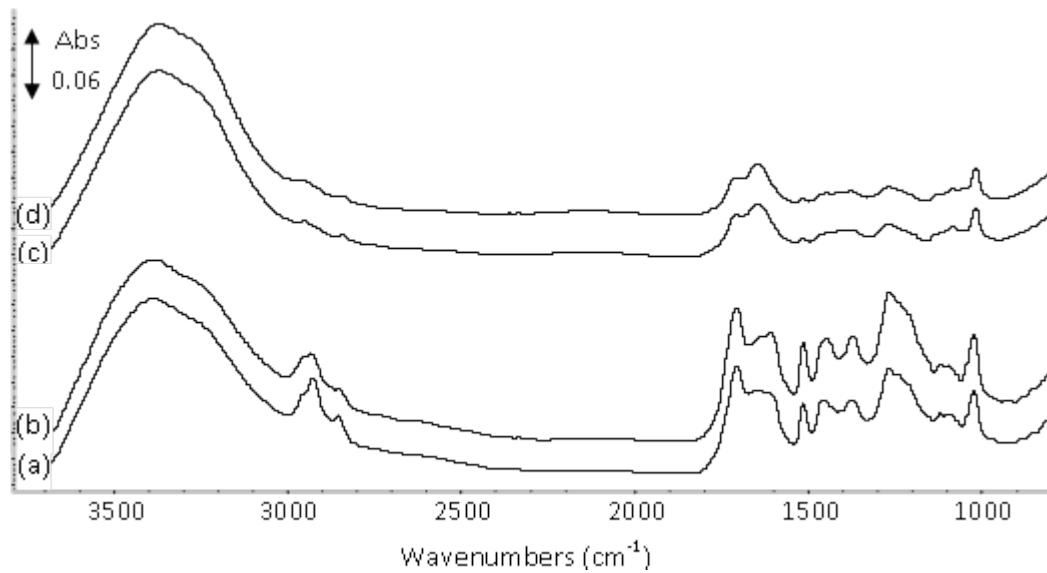


Figure 6.18 ATR spectra collected for PNT 10 wt% methanol added top phase un-aged (c) and aged (d) and bottom phase un-aged (a) and aged (b) for 504 h at 80 °C.

With the addition of 5 and 10 wt% methanol there was phase separation after 504 h which did not occur in the unaltered PNF samples during aging. This suggests that the methanol addition encouraged the phase separation rather than inhibiting it. Comparing the top phases of PNF and PNT, the top phase in PNF there are higher C-H stretch peaks present (3000-2800 cm^{-1}) and stronger fingerprint region peaks. Both top phases after 504 h of aging with 5 and 10 wt% methanol carbonyl peaks had a different shape, also observed in the aging of unaltered PNF. With the addition of 15 wt% methanol the samples were homogenized throughout aging, preventing the phase separation and after aging the spectra no peaks to appear to change significantly.

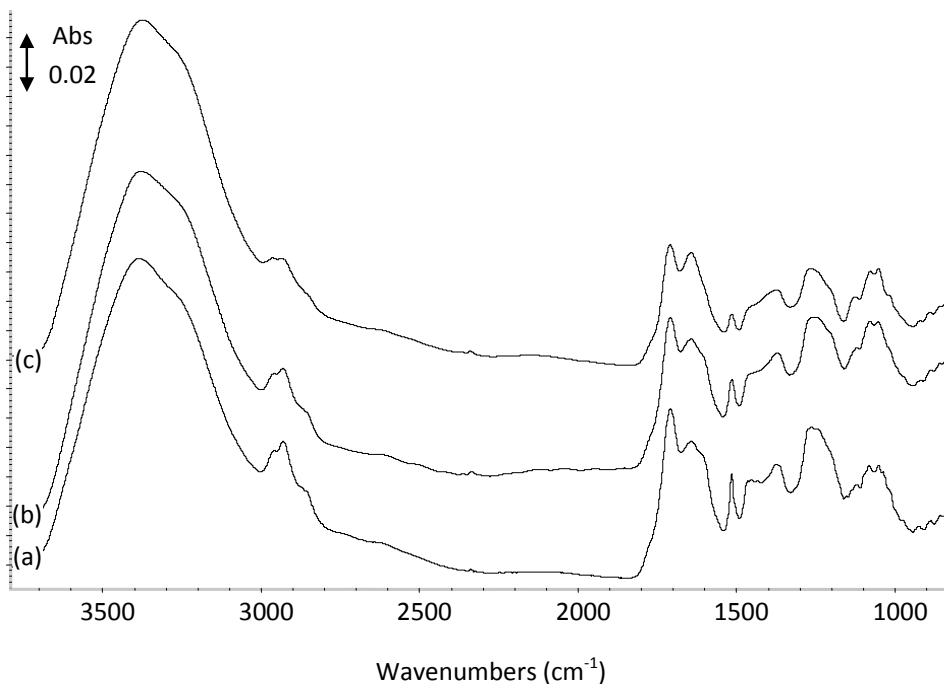


Figure 6.19 ATR spectra collected for PNF neat (a) and aged for 24 (b) and 504 (c) h at 80 °C.

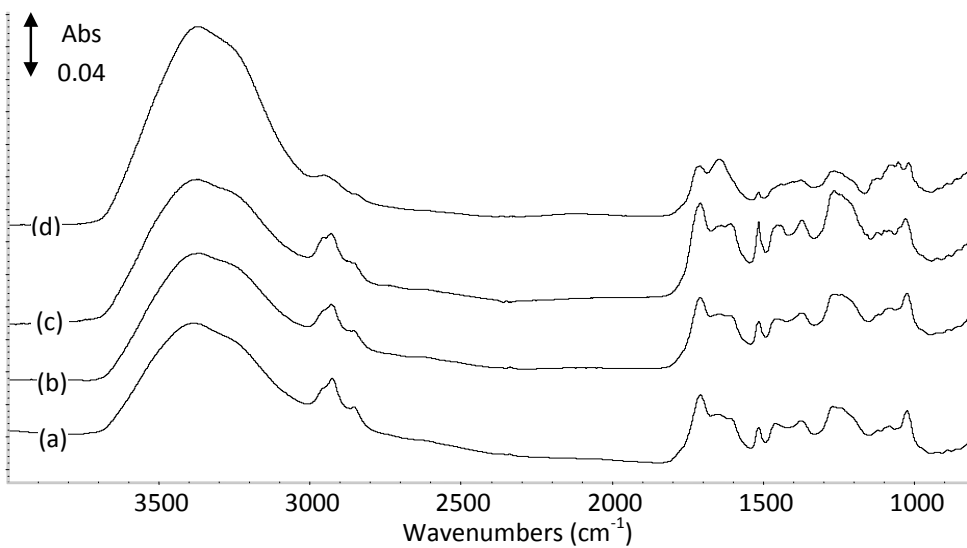


Figure 6.20 ATR spectra collected for PNF 5 wt% methanol added unaged (a) and aged for 24 (b) and 504 h [top (d), bottom (c)] at 80 °C.

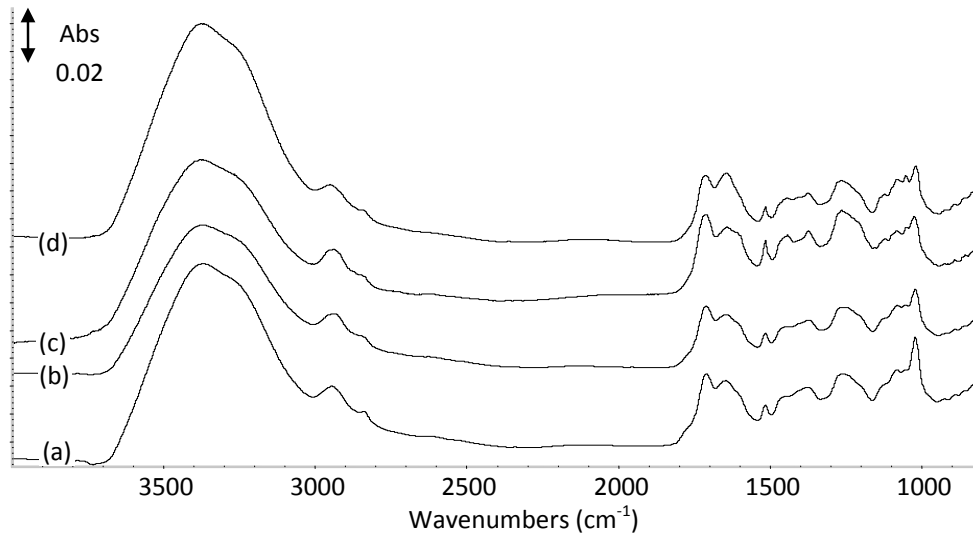


Figure 6.21 ATR spectra collected for PNF 10 wt% methanol added unaged (a) and aged for 24 (b) and 504 h [top (d), bottom (c)] at 80 °C.

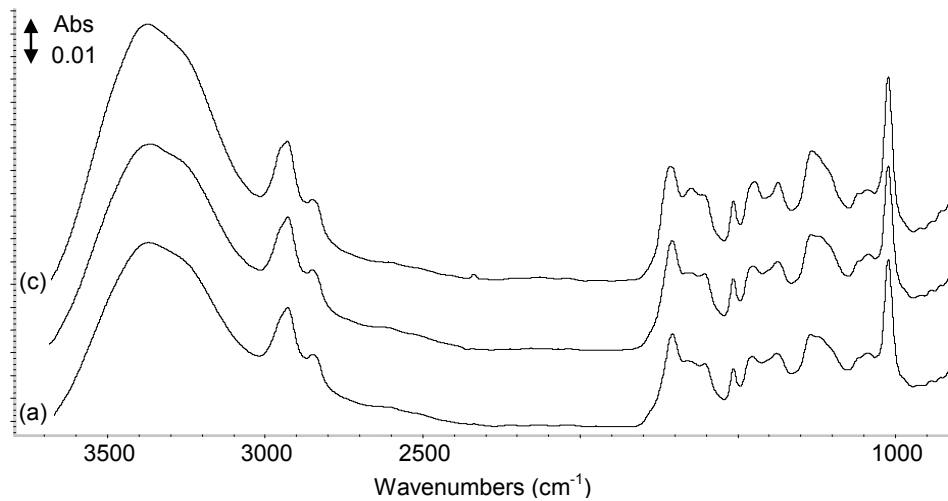


Figure 6.22 ATR spectra collected for PNF 15 wt% methanol added unaged (a) and aged for 24 (b) and 504 h (c) at 80 °C.

To compare the change in peaks during aging both peak height ratio (PHR) and peak fitting were conducted for PNT and PNF spectra. There was so significant change in any of the peak heights during aging but the PHRs do demonstrate the difference between the top and bottom phases for PNT (Figures 7.23 and 7.24). In Figure 7.23, the

right plot shows a significant increase in the peak at 1018 cm^{-1} in both top and bottom phases when methanol is added (primary alcohol C-O stretch) [Kuptsov, Silverstein, Nakanishi]. Also in Figure 7.23 (left), both bottom phases have an increase in the peak at 1268 cm^{-1} identified as =C-C-O stretch in an aromatic ether [Pretsch, Nakanishi, Silverstein, Kuptsov] and/or a carboxylic acid [Nakanishi, Silverstein]. There is an larger amounts of C=C stretch in alkenes and/or C=O stretch in a conjugated ketone [Silverstein, Pretsch, Nakanishi] in the top phases (1643 cm^{-1}) and an larger amounts of C=C aromatic skeletal stretching [Kuptsov, Silverstein] in the bottom phase (1513 cm^{-1}). There is no significant difference in the C=C in aromatic hydrocarbons and/or skeletal stretching in heteroaromatics at 1594 cm^{-1} [Silverstein, Pretsch]. The presence of aromatics in the bottom phase makes sense considering the molecular weight is much higher when compared to the top phase. Composition of the top and bottom phases are different but show no significant change during aging for any of the peaks suggesting that the molecular weight may be due to a polymerization where functional groups do not change but rather form a chain.

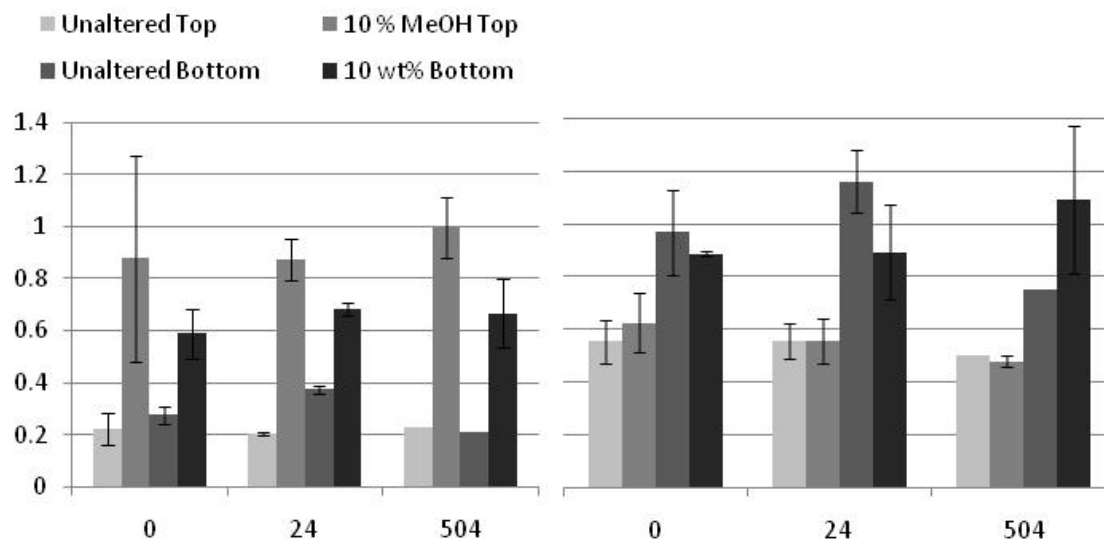


Figure 6.23 PHR for peak 1018 cm^{-1} (left) and 1268 cm^{-1} (right) comparing PNW top and bottom phases for unaltered and 10 wt% methanol added samples during aging up to 504 h at $80\text{ }^{\circ}\text{C}$.

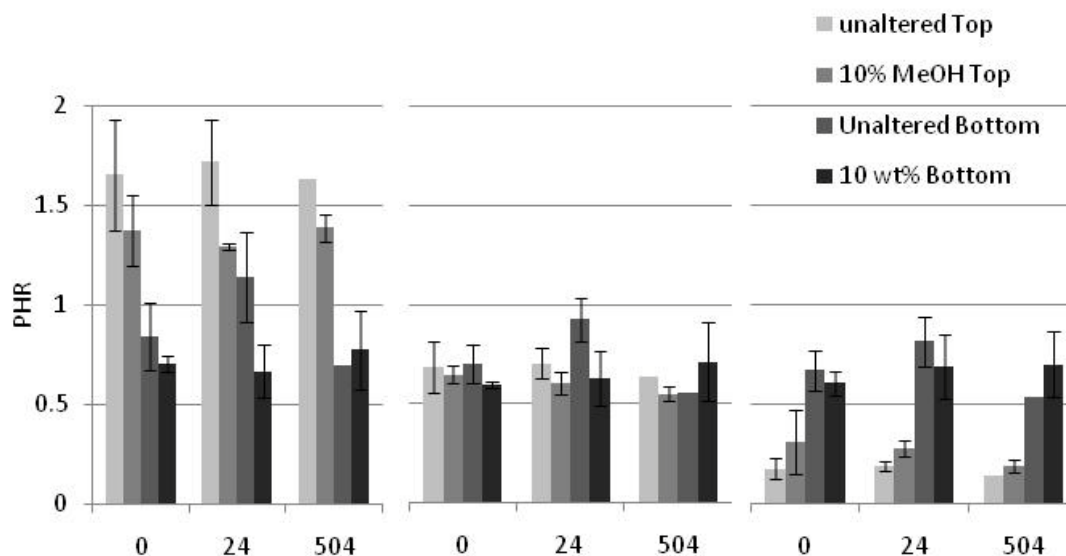


Figure 6.24 PHR for peak 1643 cm^{-1} (left), 1594 cm^{-1} (center) and 1513 cm^{-1} (right) comparing PNW top and bottom phases for unaltered and 10 wt% methanol samples during aging up to 504 h at $80\text{ }^{\circ}\text{C}$.

During peak fitting there was no visual difference in the peaks during aging. After 504 h of aging, the 5 and 10 wt% methanol samples phase separated resulting in carbonyl peaks similar to those of PNT samples.

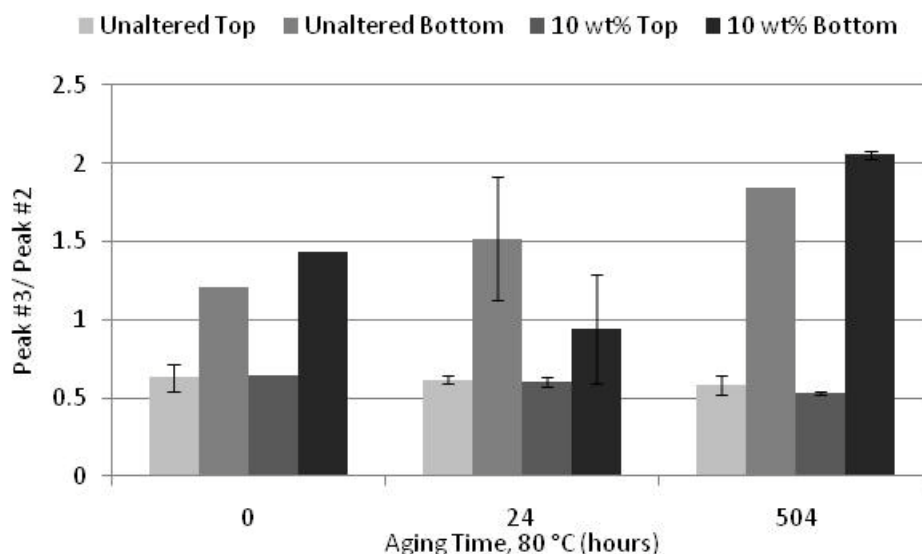


Figure 6.25 Ratios of peak heights from peak fitting #3/#2

There were also no trends or significant changes during aging of PNF pyrolysis oil and with the addition of methanol the PHR increased for the peak at 1018 cm^{-1} with increasing methanol percentage (Figure 7.26). There was no significant change in the peak heights within the peak fitting for peaks 1, 2 and 3 as observed in PNT samples. On the other hand for 15 wt% methanol added there was a significant change with the formation of a fourth peak located at $1730\text{-}1725\text{ cm}^{-1}$ after 504 h of aging (Figure 7.27). This peak is due to C=O stretch in aliphatic or aromatic aldehydes and/or α,β -unsaturated or aromatic esters [Pretsch, Nakanishis] suggesting that there is a formation of an aldehyde and/or ester functional groups in the presence of methanol at 15 wt%.

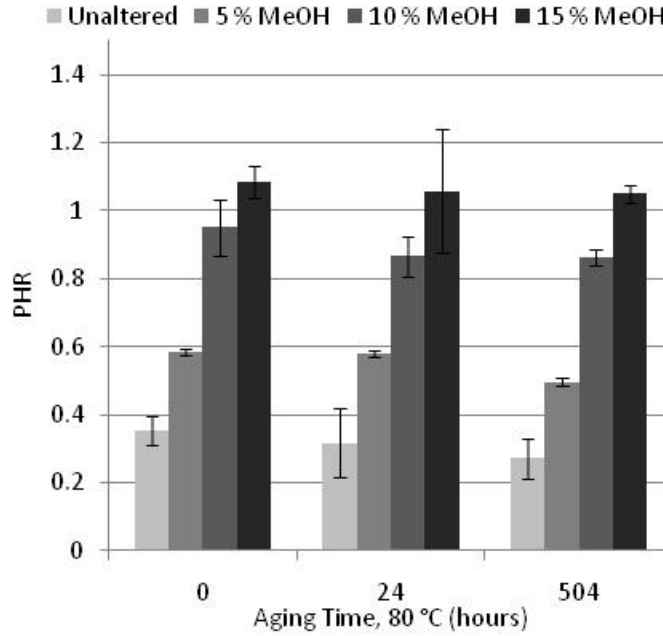


Figure 6.26 PHR for peak 1018 cm^{-1} comparing PNF unaltered, 5, 10 and 15 wt% methanol added samples during aging up to 504 h at $80 \text{ }^\circ\text{C}$.

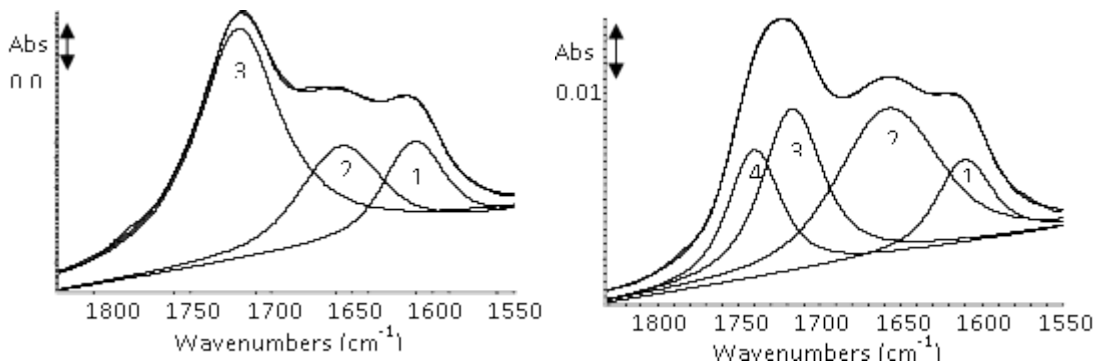


Figure 6.27 Peak fitting for PNF 15 wt% methanol added control (left) and aged for 504 h (right)

6.4.9 ATR-FTIR of Top Crust Phase

Crust top phases were characterized as removed prior to cleaning to determine if the coating of the solids were significantly different when compared to the pyrolysis oil.

In Figures 7.28 and 7.29 spectra for crust materials are displayed for PNT and PNF

samples respectively. In general the spectra look very similar to pyrolysis oil spectra with higher C-H stretch peaks ($3000-2800\text{ cm}^{-1}$). There also does not appear to be any significant difference between the crusts removed from unaltered samples and those with methanol added or a change during aging. This is in agreement with the GPC analysis where the molecular weight of the crust did not change significantly throughout aging.

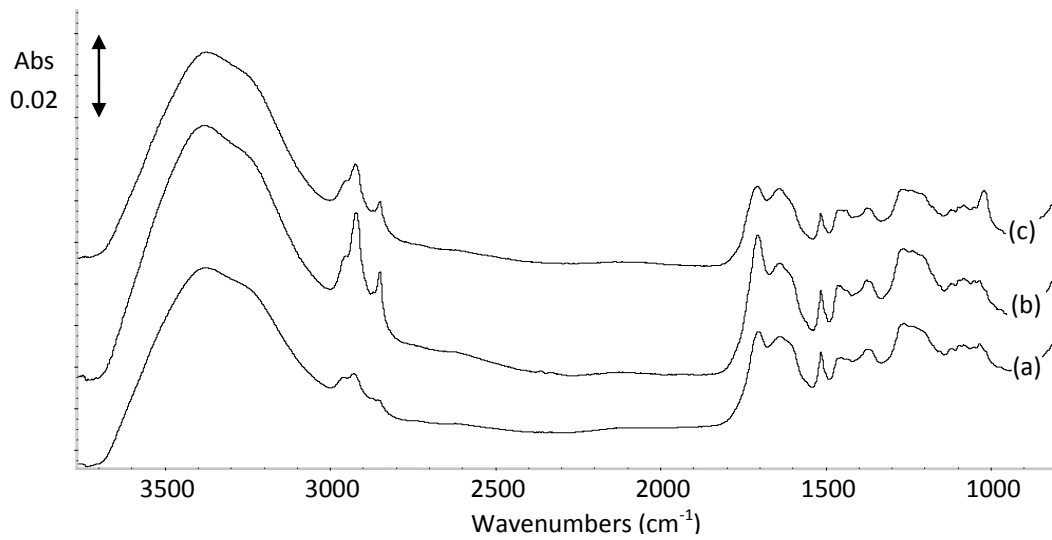


Figure 6.28 ATR spectra for PNT pyrolysis unaltered top crust after 24 (a) and 504 (b) hours and 10 wt% methanol after 504 h (c).

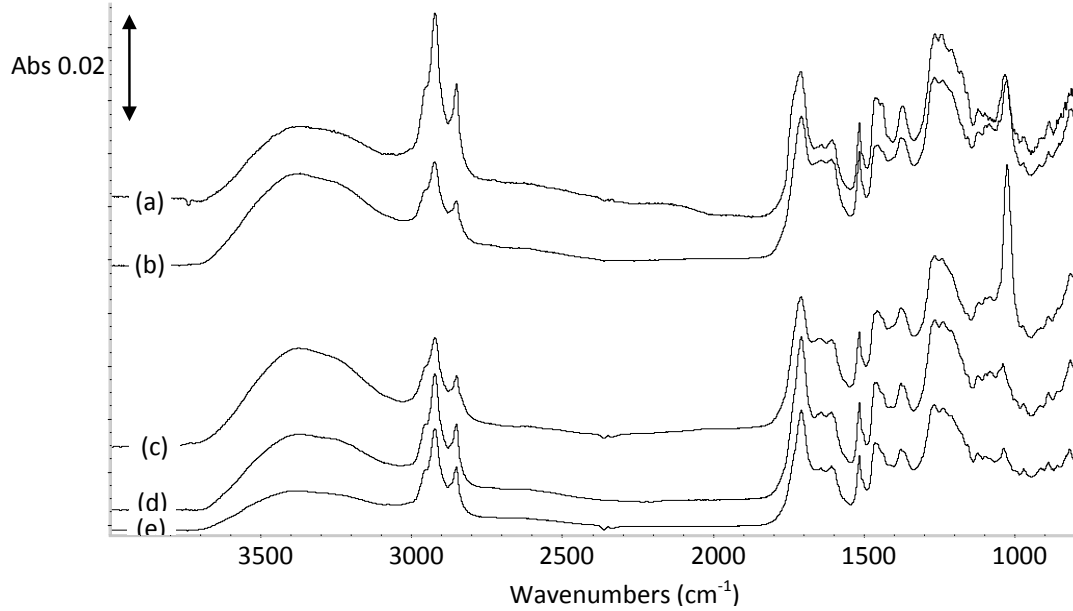


Figure 6.29 ATR spectra of unaltered PNF pyrolysis oil crust phase after aging for 24 (c, e) and 504 hours (d) and 5 wt% MeOH added crust phase after aging for 24 (b) and 504 (a) h.

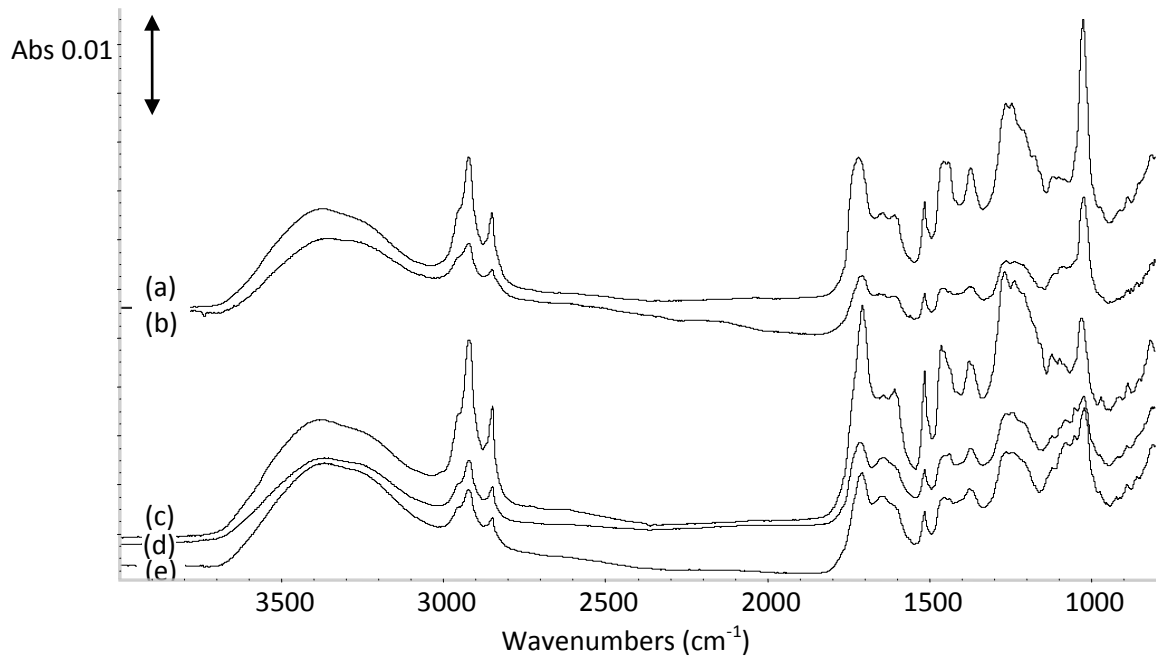


Figure 6.30 ATR spectra of pine needles fractionated pyrolysis oil 10 wt% MeOH added crust phase after aging for 24 (c, e) and 504 hours (d) and 15 wt% MeOH added crust phase after aging for 24 (b) and 504 (a) h.

Solids were removed from the top crusts by cleaning the pyrolysis oil residue with acetone and methanol and collecting the remaining solids. DRIFT spectra for the PNT (Figure 7.31) and PNF (Figure 7.32) cleaned solids are displayed and the spectra now look rather different from pyrolysis oil with stronger C-H stretch peaks, reduced primary alcohol and hydroxyl peaks (removal of liquids) and also a change in the general shape of the fingerprint region ($1800-900\text{ cm}^{-1}$). There does not appear to be any change in the solids during aging or with the addition of methanol either. It was theorized that the solids were either needle biomass or char entrained during pyrolysis. When comparing the solid spectra to those of needle biomass and char in Figure 7.33 they do not appear to be one or the other but perhaps a combination. It is unclear why the solids have the strong C-H stretch peaks because the biomass and char do not have this. This may be due to either residual pyrolysis oil on the solids or perhaps surface reaction occurred during aging changing increasing the C-H stretch.

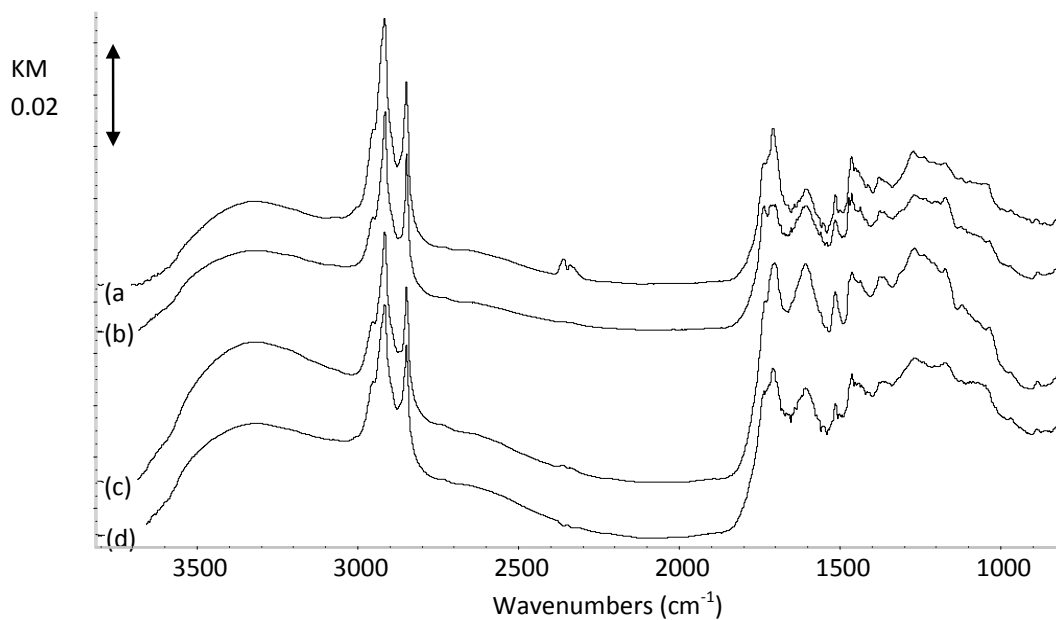


Figure 6.31 DRIFT spectra for the crust solids for unaltered pine needle pyrolysis oil aged for 24 h (d) and 504 h (c) and 10 wt% MeOH added pyrolysis oil samples aged for 24 h (a) and 504 h (b) at 80 °C.

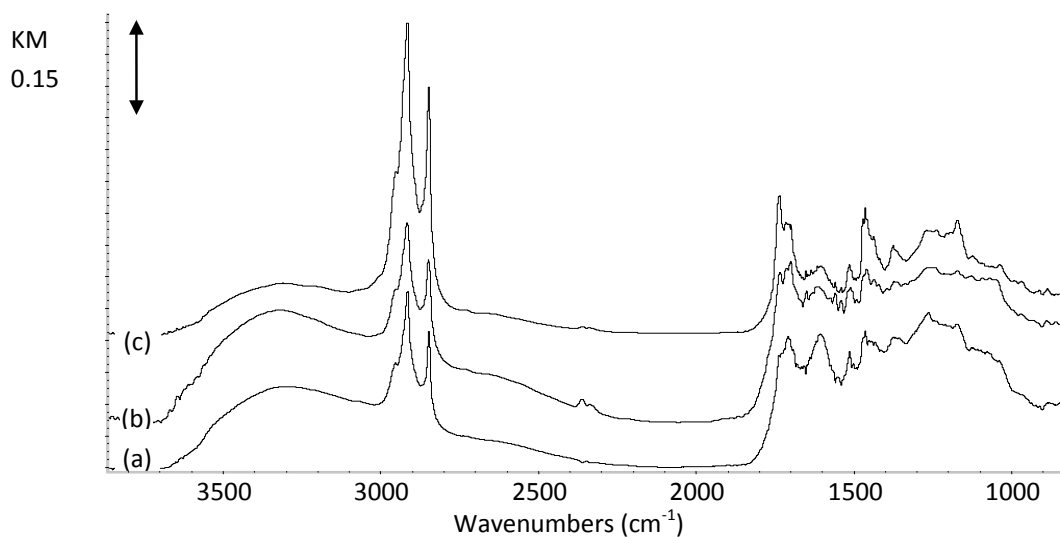


Figure 6.32 DRIFT spectra for the crust solids for PNF unaltered aged for 504 h (a), and 10 wt% methanol added aged for 24 h (b) and 5 wt% methanol added aged for 504 h (c).

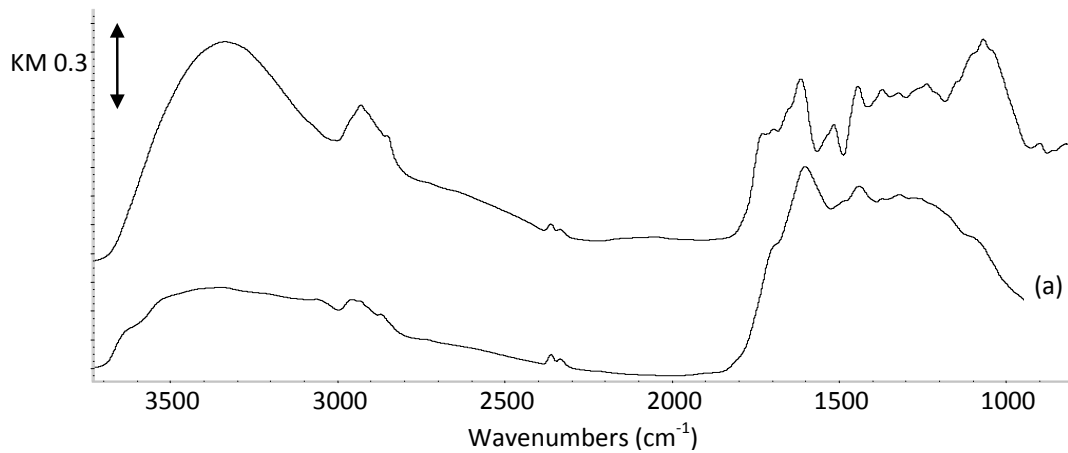


Figure 6.33 DRIFT spectra for the pine needle char (a) and pine needle biomass (b).

6.4.10 GC-MS data

Figure 7.34 displays the changes in height of ion 91 (the dominant ion in many of the largest peaks) during aging and identified compounds for each peak. For both unaltered and 10 wt% addition PNT, the majority of the peaks decreased during aging which may be due to chemical changes in higher molecular weight compounds that cannot be analyzed with GC/MS or the inability to get a representative sample with the phase separation. Methanol addition does appear to slow the decrease in compounds as shown by a larger normalized peak for the 10 wt% MeOH sample than the neat sample after 24 h of aging.

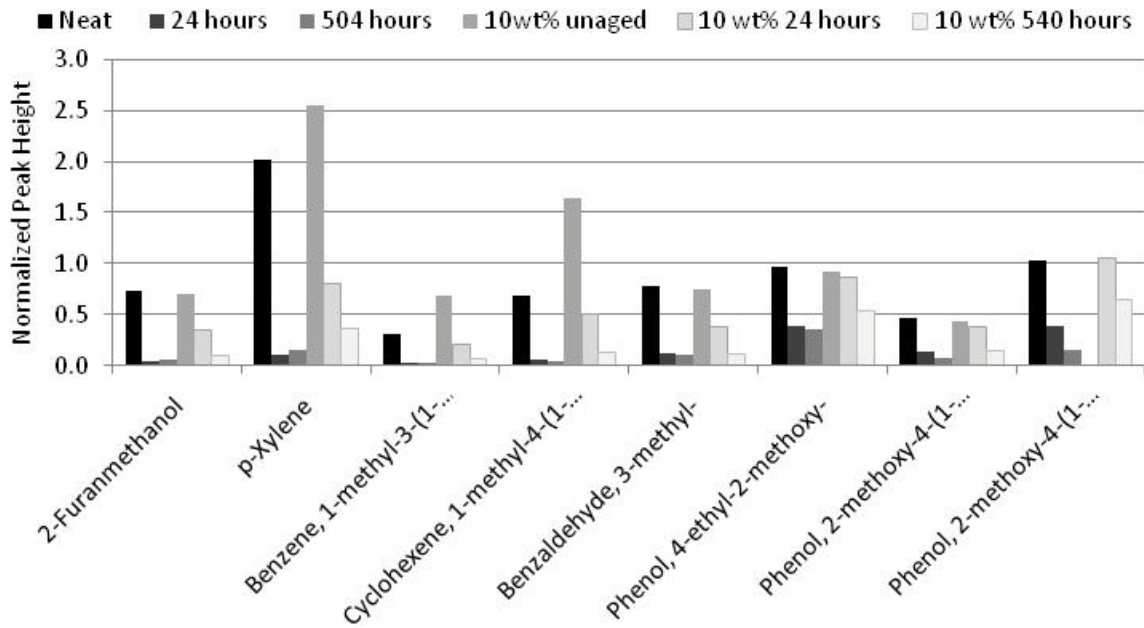


Figure 6.34 GC-MS analysis of ion 91 for unaltered and 10 wt% added PNT during aging

In Figure 34 ion 90 is examined and shows that with methanol there is an increase in 2-methylphenol, 5-methylphenol and 1,2benzendiol and suggests that a new reaction is occurring within the pyrolysis oil due to the methanol addition.

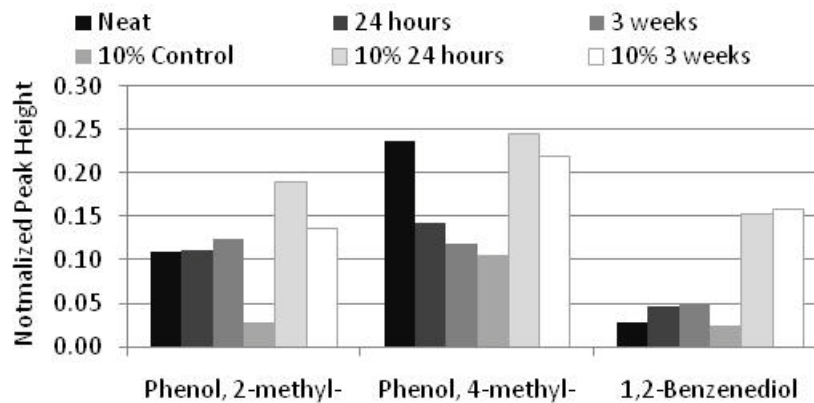


Figure 6.35 GC-MS analysis of ion 90 for unaltered and 10 wt% added PNT during aging

An overall comparison of the PNT unaltered and 10 wt% methanol added samples during aging are presented as changes in normalized height after 24 h and 504 h of aging (Figure 7.36). During aging, most of the compounds decrease in PNT unaltered pyrolysis oil excluding 3-methyl-1,2-cyclopentanedione, 4-methyl-1,2-Benzenediol, and 2-methoxy-4-(1-propenyl)-phenol. With the addition of methanol there is an increase during aging in 2-methyl-phenol, 4-methyl-phenol, 2-methoxy-phenol, and 2-methoxy-4-methyl-phenol. Methanol could either be creating new reactions or may be increasing the solubility of the two phases, allowing for better sampling and thus for certain compositional increases to be observed.

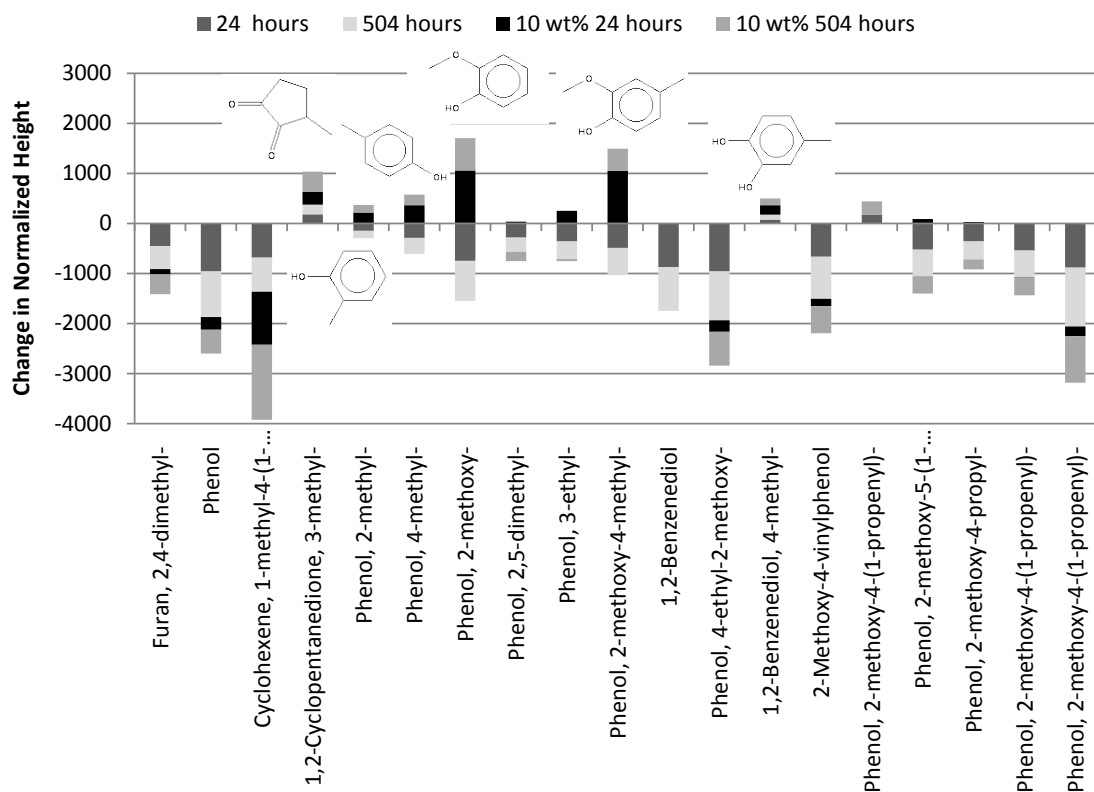


Figure 6.36 Changes in normalized heights from control samples for PNT unaltered and 10 wt% methanol added samples aged at 80 °C for 24 and 504 h.

When comparing the changes in normalized heights in PNT to that of PNF (Figures 7.37 and 37.38 there are much large changes occurring in the PNT samples yet again suggesting that the top phase compounds accelerate the aging. In PNF the largest change is a decrease in 1-methyl-4-(1-methylethenyl)-(S)-cyclohexene, which occurs in all samples regardless of methanol addition. Rather than a decrease in the changes due to methanol addition the 10 and 15 wt% methanol added samples exhibited larger changes.

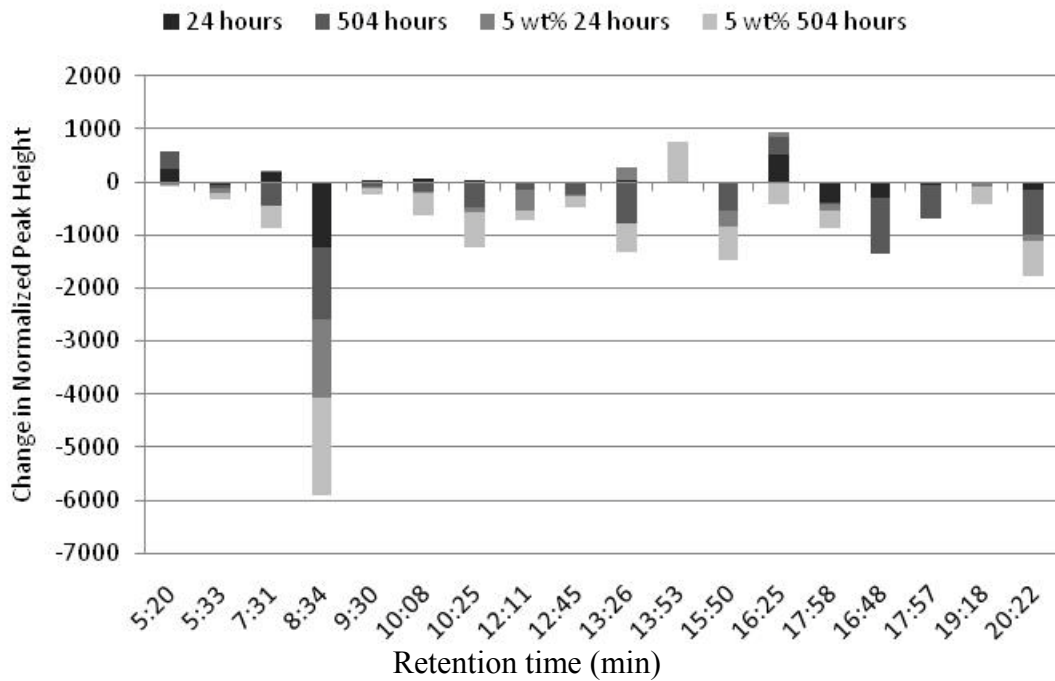


Figure 6.37 Changes in normalized heights from control samples for PNF unaltered and 5 wt% methanol added samples aged at 80 °C for 24 and 504 h.

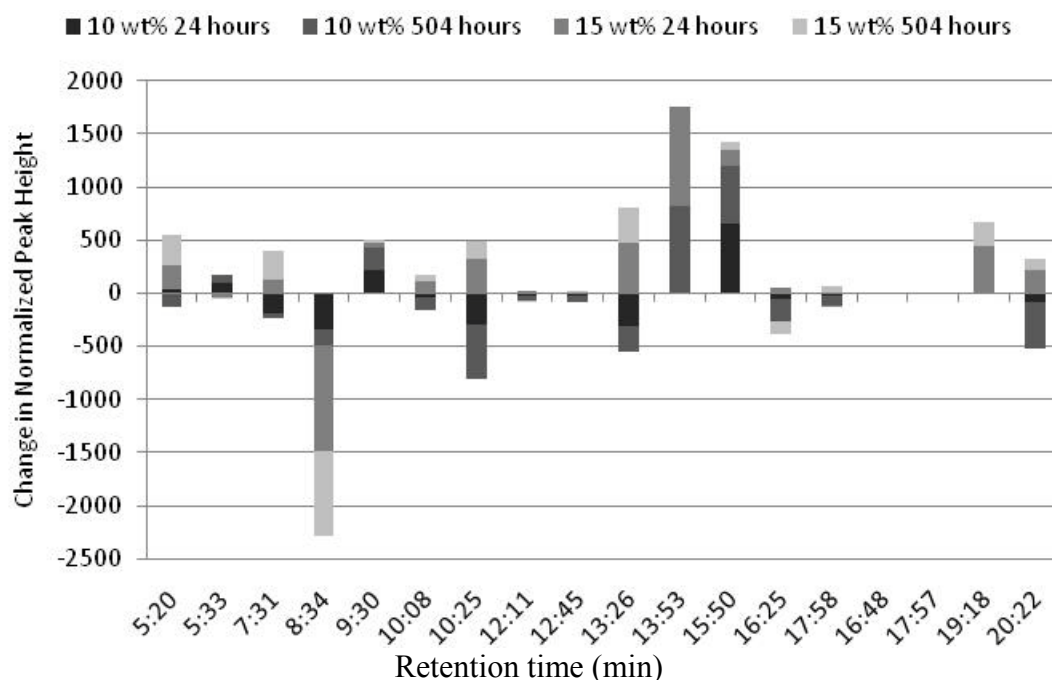


Figure 6.38 Changes in normalized heights from control samples for 10 and 15 wt% methanol added samples aged at 80 °C for 24 and 504 hours.

6.4.11 Proposed Reactions

Providing that FTIR analysis and GC/MS analysis did reveal a lot of information about the chemical change in the pyrolysis oils it is difficult to propose specific reactions that may be occurring. Organic acids may be produced resulting in the decrease in pH and water content formation could be the result of a condensation reaction. An increase in molecular weight suggests a polymerization such as polycondensation.

6.4.12 Conclusions

The use of pine needles as the sole feedstock produces a unique pyrolysis oil that phase separates into three phases (crust, top, bottom) during aging at 80 °C. Removal of the crust phase prior to characterization resulted in a decrease in the density and viscosity of the residual liquid sample, making it difficult to monitor the true progression of the overall aging process. When comparing PNT to PNF, PNT has a larger initial MWs and

also larger increases in MW suggesting that the aging reaction is related to the top phase which contains larger amounts of water. In addition, methanol was able to retard aging in PNF but not in PNT which may be related to the high water content in PNT.

Due to the crust removal, viscosity measurements could not be used as an accurate indicator for aging, instead molecular weight and water content was used to determine if aging occurred. Unaltered and 10 wt% methanol PNT samples exhibited an increase in molecular weight in the bottom phase and a decrease in the top phase. PNF unaltered samples also exhibited an increase in molecular smaller when compared to PNT. This is another indication that top phase plays a role in the aging reactions where reaction products may precipitate from the top phase into the bottom phase, reducing the molecular weight in the top phase.

ATR analysis was not able to determine changed in the functional groups during aging but was able to show the difference between the PNT top and bottom phases. PNT bottom phase and PNF are similar in composition containing higher amounts of ether/ketone and aromatic and the top phase contains more alkene/ketones. The presences of the alkenes and/or ketones in the top phase result in the higher aging affects observed.

GC/MS results indicated formation of ester and/or aldehyde with the addition of 15 wt% methanol during aging. Addition of methanol reduced the molecular weight after 504 hours with increasing percentage and 15 wt% resulted in no phase separation and very little increase in the molecular weight. To prevent phase separation and retard the aging 15 wt% methanol is suggested.

6.4.13 References

Bertoncini, B.; Durand, E.; Charon, N.; Espinat D.; Quignard, A. Distillation and multidimensional GC analysis of a biomass pyrolysis oil. *Prepr. Pap.-American Chemical Sociert, Divison of Petroleum Chemistry* 2006, 51, 376.

Boucher, M.E.; Chaala, A.; Roya, C. Pyrolysis oils obtained by vacuum pyrolysis of softwood bark as a liquid fuel for gas turbines. Part I: Properties of pyrolysis oil and its blends with methanol and a pyrolytic aqueous phase. *Biomass & Bioenergy* 2000, 19, 337-350.

Boucher, M.E.; Chaalab, A.; Roy, C. Pyrolysis oils obtained by vacuum pyrolysis of softwood bark as a liquid fuel for gas turbines. Part I: Properties of pyrolysis oil and its blends with methanol and a pyrolytic aqueous phase. *Biomass & Bioenergy* 2000, 19, 351-361.

Bridgewater, A.V. Biomass Fast Pyrolysis. *Thermal Science* 2004, 8, 21-50.

Bridgewater, A.V. Renewable fuels and chemicals by thermal processing of biomass. *Chemical Engineering Journal* 2003, 91, 87-102.

Czernik, S. Bridgewater, A.V. Overview of Applications of Biomass Fast Pyrolysis Oil. *Energy & Fuels* 2004, 18, 590-598.

Darmstadt, H.; Garcia-Perez, M.; Adnot, A.; Chaala, A.; Kretschmer, D.; Roy, C. Corrosion of Metals by Pyrolysis oil Obtained by Vacuum Pyrolysis of Softwood Bark Residues. An X-ray Photoelectron Spectroscopy and Auger Electron Spectroscopy Study. *Energy & Fuels* 2004, 18, 1291-1301.

Davidsson, K.O.; Stojkova, B.J; Pettersson, J.B.C. Alkali Emission from Birchwood Particles during Rapid Pyrolysis. *Energy & Fuels* 2002, 16, 1033-1039.

Diebold, J.P. A Review of the Chemical and Physical Mechanisms of Storage Stability of fast Pyrolysis Pyrolysis oils. Subcontractor Report for the National Renewable Energy Laboratory NREL/SR-570-27613; National Renewable Energy Laboratory: Golden, CO, 2000.

Diebold, J.P.; Czernik, S. Additives To Lower and Stabilize the Viscosity of Pyrolysis Oils during Storage. *Energy & Fuels* 1997, 11, 1081-1091.

Diebold, J.P.; Milne, T.A.; Czernik, S.; Oasmaa, A.; Bridgewater, A.V.; Cuevas, A.; Gust, S.; Huffman, D.; Piskorz, J. Proposed Specifications for Various Grades of Pyrolysis Oils. In *Developments in Thermochemical Biomass Conversion*; Bridgewater,

A.V., Boocock, D.G.B., Ed.; Blackie Academic & Professional: New York, 1997; Vol. 1; p. 433-447.

Hoekstra, E.; Hogendoorn, K.J.A.; Wang, X.; Westerhof, R.J.M.; Kersten, S.R.A.; van Swaaij, W.P.M.; Groeneveld, M.J. Fast Pyrolysis of Biomass in a Fluidized Bed Reactor: In Situ Filtering of the Vapors. *Industrial and Engineering Chemistry Research* 2009, 48, 4744-4756.

Ingram, L.; Mohan, D.; Bricka, M.; Steele, P.; Strobel, D.; Crocker, D.; Mitchell, B.; Mohammad, J.; Cantrell, K.; Pittman C.U. Pyrolysis of Wood and Bark in an Auger Reactor: Physical Properties and Chemical Analysis of the Produced Pyrolysis oils. *Energy & Fuels* 2008, 22, 614-625.

Kuptsov, A.H.; Zhizhin, G.N. Handbook of Fourier Transform Raman and Infrared Spectra of Polymers. Elsevier: New York, 1988.

Maggi, R.; Delmon, B. Characterization and Upgrading of Pyrolysis oils Produced by Rapid Thermal Processing. *Biomass & Bioenergy* 1994, 7, 245-249.

Mohan, D.; Pittman, C.U; Steele, P.H. Pyrolysis of Wood/Biomass for Pyrolysis oil: A Critical Review” *Energy & Fuels* 2006, 20, 848-889.

Nakanishi, K.; Solomon, P.H. Infrared Absorption Spectroscopy. Holden Day: Oakland, 1977; p. 14, 19, 25,26, 31, 38-40.

Oasmaa, A.; Kuoppala, E.; Selin, J.; Gust, S.; Solantausta, Y. Fast Pyrolysis of Forestry Residue and Pine. 4. Improvement of the Product Quality by Solvent Addition. *Energy & Fuels* 2004, 18, 1578-1583.

Oasmaa, A.; Peacocke, C.; Gust, S.; Meier, D.; McLellan, R. Norms and Standards for Pyrolysis Liquids. End-User Requirements and Specifications. *Energy & Fuels* 2005, 19, 2155-2163.

Oasmaa, A.; Kuoppala, E.; Gust, S.; Solantausta, Y. Fast Pyrolysis of Forestry Residue. 1. Effect of Extractives on Phase Separation of Pyrolysis Liquids. *Energy & Fuels* 2003, 17, 1-12.

Oasmaa, A.; Kuoppala, E.; Solantausta, Y. Fast Pyrolysis of Forestry Residue. 2. Physicochemical Composition of Product Liquid. *Energy & Fuels* 2003, 17, 433-443.

Pretsch, E.; Buhlmann, P.; Affolter, C. Structure of Determination of Organic Compounds, Tables of Spectral Data; Springer: New York, 2000; p. 245, 255, 263, 264, 286, 287, 291, 293.

Silverstien, R.M.; Webster, F.X. Spectrometric Identification of Organic Compounds; John Wiley & Sons Inc.: New Jersey, 1998; p. 82, 86, 87, 90-92, 94 95, 97.

Jung, S.; Kang, B.; Kim, J. Production of pyrolysis oil from rice straw and bamboo sawdust under various reaction conditions in a fast pyrolysis plant equipped with a fluidized bed and a char separation system. *Journal of Analytical and Applied Pyrolysis* 2008, 82, 240-247.

Weerachanchai, P.; Tangsathitkulchai, C.; Tangsathitkulchai, M. Phase behaviors and fuel properties of pyrolysis oil-diesel-alcohol blends. *World Academy of Science, Engineering and Technology* 2009, 56, 387-393.

CHAPTER VII

RHEOLOGICAL EFFECTS OF CHAR, SAND, AND SILICA ADDITION TO COTTONWOOD PYROLYSIS OIL

7.1 Abstract

Cottonwood whole tree total [CWTT] and cottonwood bark total [CBT] pyrolysis oil samples were used to investigate the rheological effects of added solids to pyrolysis oil. Particles added included ground char produced along with the pyrolysis oils, white quartz sand, fumed silica and silica packing. All particles were added to 10 mL of pyrolysis oil to obtain 3.5, 1.75, and 0.875 vol% samples. Rheological data was then collected for forward and reverse stepped shear experiments over the range 0.1 to 1000 1/s. It was determined that char addition resulted in elevated viscosities as compared to the neat pyrolysis oil. In addition, both neat and altered pyrolysis oil samples displayed positive and negative viscosity hysteresis effects which were most noticeable in the cottonwood whole tree total pyrolysis oil samples.

7.2 Introduction

Pyrolysis oil is a complex, multiphase fluid with a network structure of oligomers and non-polar oligomeric micelles [Garcia-Perez, 2006, 364-375] comprised of 300+ components [Ringer] with 15-50 wt% water [Bridgewater 2003] and highly reactive species including alcohols, aldehydes, carboxylic acids, carbohydrates and ketones [Oasmaa 2003 1075-1084]. It has also been described as a microemulsion where an

aqueous phase of (holocellulose-derived) stabilizes and a discontinuous phase (pyrolytic lignin macromolecules) through hydrogen bonding [Bridgewater 2003 ChJ].

Due to the wide range of components and multiple phases, pyrolysis oil can have a wide range of properties that hinders the direct application of pyrolysis oil as a fuel [Garcia-Perez, 2006, 364-375, Ba, 2004] including instability during storage, phase separation, deposition of waxy materials on pipe walls, and filtration problems [Garcia-Perez 2006] and alkali metal compounds from entrained char particulates [Davidson 2002]. Entrained char particles result in plugging of fuel nozzles [Garcia-Perez 2006] and it has been shown that these deposits plugged 0.8 mm diameter holes in a fuel injector even after preheating pyrolysis oil to 90 °C [Rossi 1994]. In addition, particle growth was observed in recirculation loops and was attributed to polymerization reactions and particle agglomeration [Chaalal 2004].

Char particulates entrained during pyrolysis and condensed with the liquid can be removed by including cyclones and hot gas filtration into the reactor system prior to condensation and was shown to slow aging [Diebold 1997]. In direct contrast, the addition of char to pyrolysis oil has been shown to accelerate aging [Agblevor 1998]. Alkali metals in char particulates have been proposed as catalysts for aging reactions [Ringer 2006, Diebold NREL 2000].

Pyrolysis oil has been reported to typically display Newtonian behavior. However, during phase separation (that has been observed in forestry residue oil) the bottom phase (80-90 wt%) remained Newtonian but the top phase (10-20 wt%) was slightly non-Newtonian at low temperatures and became Newtonian when heated [Oasmaa 2004, Oasmaa VTT 2001]. In lignin rich phase separation the top phase also

has lower water content and density but higher heating value and solids content [Oasmaa 2001].

Strong interlocking or irregular shaped particles can cause non-Newtonian behavior in fluids. Traces of water can collect at the interface between particles and hold them together by interfacial forces (a water bridge). When shear force is applied, the water bridge can be torn apart resulting in lower viscosity [Nielsen 1997].

With the addition of rigid filler, a Newtonian fluid can exhibit non-Newtonian behavior. Concentrated suspensions can have pseudoplastic or plastic behavior when the matrix fluid is Newtonian [Nielsen 1997]. Also when solids aggregate in a fluid and a shear stress is applied, the break-up of weak agglomerates in a shear field can be a major cause of decreased viscosity [Nielsen 1997]. At high shear rates, both plastic and pseudoplastic materials commonly have constant viscosity and appear Newtonian [Nielsen 1997]. Agglomeration in pyrolysis oil is typically caused by condensation of alkali onto char particles thus forming a liquid layer and allowing the particles to agglomerate [Davidson 2002].

With the presences of multiple phases and particulates, pyrolysis oil could easily display non-Newtonian behavior. Filtration after condensation (Chapters 5) did not prevent the expected age-related increases in molecular weight or water content and suggests the viscosity increase observed is cause by a separate mechanism then water content and molecular weight increases. With that in mind it may also be possible that the addition of char to pyrolysis oil does not induce chemical aging but rather a physical change, such as agglomeration. Cottonwood whole tree total [CWTT] and cottonwood bark total [CBT] pyrolysis oils were investigate to determine the influence of char and other solids on rheological properties prior to aging.

7.3 Methods and Materials

Feedstock: Cottonwood trees were harvested and separated into heart wood, bark and leaf biomass, or bole wood (bark, limbs and wood) and leaf. Biomass was dried to 10-15% moisture content (MC) in an oven (Despatch V series VREZ-19-ZE). Heart wood and bole wood biomass was then chipped (separately) to 1-2 inch chips (Carthage Machine Inc., Model 39 chipper, 1470 rpm). Leaves were added to the (dried and chipped) bole wood to reproduce the cottonwood whole tree biomass composition. Whole tree biomass was then ground (Bauer Bro. Co., 25 Hp, 1465 rpm) and screened resulting in ~4 to 6 mm particles (Universal Vibrating Screener, Type S #1354). Separated bark biomass was ground separately and screened. Prior to pyrolysis all biomass was dried to 1-2 % MC.

Pyrolysis: MSU Forest Products Laboratory produced the cottonwood bark and whole tree pyrolysis oils with an auger pyrolysis reactor operated under vacuum at 400 °C with an average flow rate of 15-20 L/min, and the gas product was condensed using four serial water condensers maintained at 25 °C (± 1 °C). Both pyrolysis oil samples were produced as total oil which includes the products of all of the condensers. Pyrolysis oil samples were stored at ~5 °C within 1 hr of production to minimize aging. Total pyrolysis oils were produced as dark, pungent smelling, opaque liquid which phase separated due to high concentrations of water.

Solids Addition: Char added to the pyrolysis oil was obtained from the production of the pyrolysis oil from whole tree and bark biomass and prepared by grinding in a motor and pestle. Sigma-Aldrich white quartz sand (MW = 60.08 g/mol) was purchased and used as purchased with particle sizes ranging 50-70 mesh size (0.212 to 0.3 mm). Fumed silica with a particle size of 0.014 μm and silica packing with particle size of 5

μm were both purchased from Sigma-Aldrich and used 'as is'. Density was determined by weighing a known volume of the material. The weight of particles added was calculated using the measured densities to obtain 3.5, 1.75, and 0.875 vol% for each particle type. Pyrolysis oil samples were allowed to warm to room temperature, separated into 10 mL aliquots, and the particles were slowly added to the oil with gentle mixing using a magnetic stirrer.

Particle Size Distribution Analysis: Micrographs of both chars and sand were taken for the unfiltered and filtered pyrolysis oil before and after aging using an Olympus BX51 microscope. Particle size distribution (PSD) analyses were conducted with Image-Pro Plus software.

Rheology: Step-flow tests were performed using a TA Instruments AR 1500x rheometer with 60 mm aluminum parallel plates and a Peltier plate to maintain the temperature at 40 °C. Shear rate was varied over the range of 0.1 to 1000 Hz (1/s), in both forward and reverse directions. Sample volumes were maximized but ranged from 1000 to 1200 μm depending upon the sample viscosity and gap distance. A minimum of 10 data points were averaged over a plateau region observed at higher shear rates (10-1000 1/s) to calculate an average viscosity and 95% confidence intervals.

ATR-FTIR: Attenuated total reflectance Fourier transform infrared (ATR-FTIR) spectra were collected using a Nicolet 6700 spectrometer (liquid nitrogen cooled MCT-A* detector, 4 cm^{-1} resolution, 256 scans) with Pike Veemax IITM accessory set to a 60-degree incident angle and ZnSe 60-degree ATR crystal. All ATR spectra were ATR corrected using Thermo Electron OMNIC software prior to analysis.

7.4 Results and Discussion

Pyrolysis oils that were used for this investigation included cottonwood whole tree total [CWTT] and cottonwood bark total [CBT]. Total pyrolysis oils typically have higher water content (vs. fractionated oils) and so also have a greater tendency to exhibit phase separation. The CWTT and CBT samples in this study had 'as produced' water contents of 29 and 40 wt%, respectively, and phase separated prior to aging.

7.4.1 Particle Analysis

Silica packing and fumed silica are reported by the manufacturer with 5 μm and 0.014 μm average particle diameters, respectively, and are not expected to have a large variation in particle size. Sand has a nominal range of particle diameter between 0.368-0.27 mm. Native (as produced) char particle distributions were unknown; therefore, a particle size analysis based on multiple optical micrographs per sample was conducted. Particle size distributions (PSD) based on the major and minor axes for ground cottonwood whole tree char and bark char are presented in Figures 3 and 4, respectively. Both the CBT and CWTT char PSD look similar with the majority of particles measuring $<20 \mu\text{m}$ indicates there were no measurable differences in char size between the bark and whole tree biomass samples after grinding which was expected. CWTT and CBT major axes maximums occurred at 8 μm with number ratios of 0.32 and 0.30, respectively. The minor axis maximum was at 6 μm for both CWTT and CBT with identical number ratios of 0.28. In addition, for both char samples the major and minor axes number ratios are similar and point to spherical particle shapes.

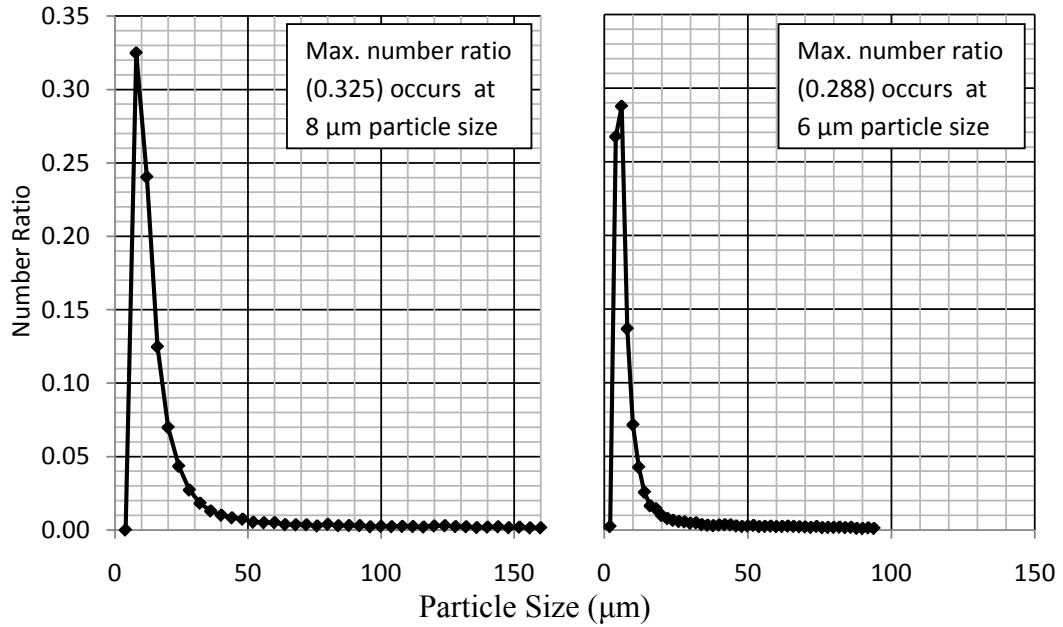


Figure 7.1 Particle size distributions for CWTT char showing the major (left) and minor (right) axes.

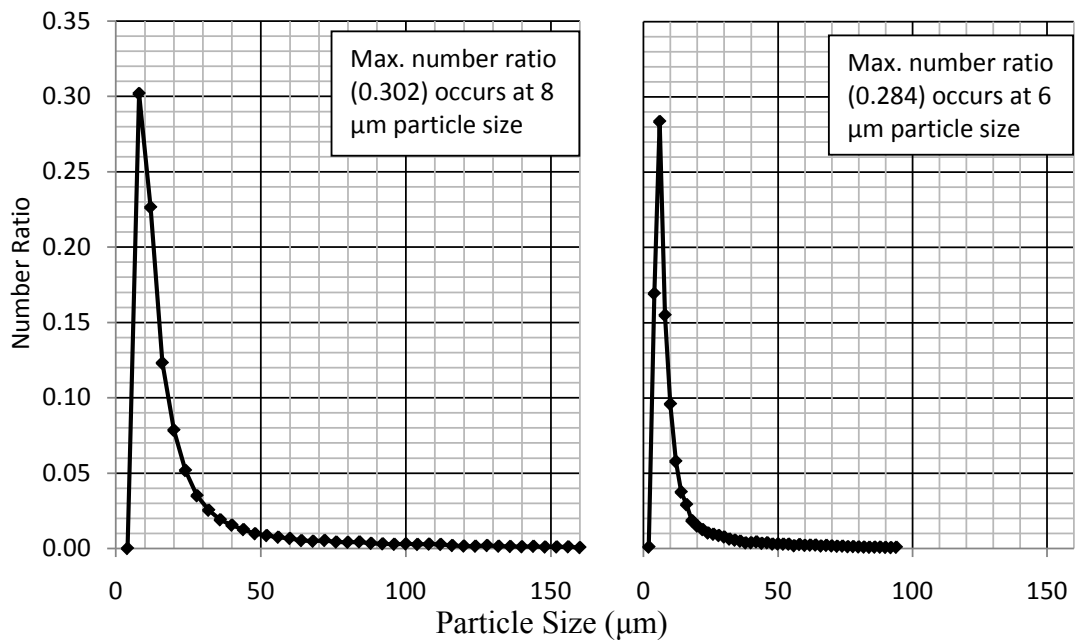


Figure 7.2 Particle size distributions for CBT char showing the major (left) and minor (right) axes.

A PSD was also measured for the sand sample (Figure 5) and the largest number ratios occurred at 400 and 315 μm for the major and minor axes, respectively. Both the shape of the major and minor axes distributions are Gaussian and the major axis had a slightly broader distribution with particle diameters ranging from 200-600 μm . In addition, the major and minor axes particle sizes overlap the expected values of 270-368 μm but a broader particle diameter range was measured than was reported by the manufacturer.

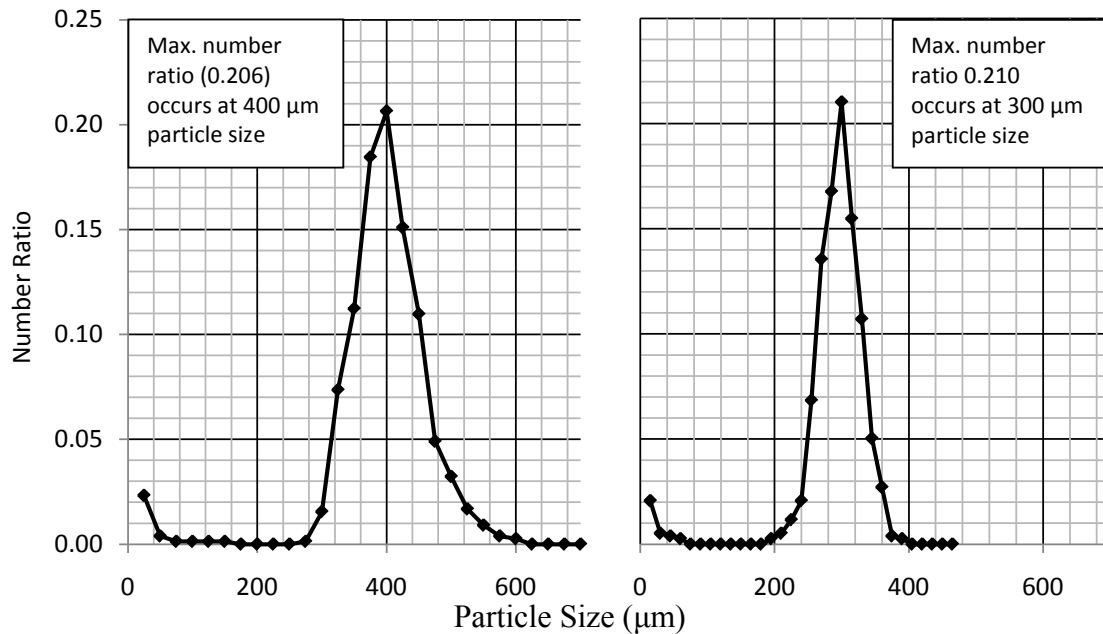


Figure 7.3 Particle size distributions for sand showing the major (left) and minor (right) axes.

7.4.2 Particle Addition

Pyrolysis oil and particle densities used in the particle addition study were measured and are displayed in Table 8.1. Calculated weight and volume percentages for each sample are also shown; solids content ranged from 0.5-5.5 % (v/v) for CWTT and 0.7-4.3 % (v/v) for CBT.

Table 7.1 Calculated weight and volume percentages for sand, char, fumed silica, and silica packing that were added to cottonwood whole tree total [CWTT] and cottonwood whole tree total [CBT] pyrolysis oils.

CWTT ($\rho = 1.55845$ g/mL)	wt%	vol %	CBT ($\rho = 1.3518$ g/mL)	wt%	vol%
Sand ($\rho = 1.79$ g/mL)	5.43%	4.76%	Sand ($\rho = 1.79$ g/mL)	4.45%	3.40%
	2.78%	2.43%		2.15%	1.63%
	1.33%	1.16%		1.09%	0.83%
Char ($\rho = 0.249$ g/mL)	0.66%	3.98%	Char ($\rho = 0.247$ g/mL)	0.81%	4.28%
	0.50%	3.07%		0.32%	1.72%
	0.21%	1.29%		0.17%	0.92%
Silica Packing ($\rho = 0.3706$ g/mL)	1.36%	5.49%	Silica Packing ($\rho = 0.3706$ g/mL)	0.77%	2.76%
	0.54%	2.24%		0.46%	1.64%
	0.23%	0.96%		0.25%	0.92%
Fumed Silica ($\rho = 0.051$ g/mL)	0.13%	3.89%	Fumed Silica ($\rho = 0.051$ g/mL)	0.12%	3.20%
	0.02%	0.51%		0.07%	1.77%
	0.04%	1.13%		0.03%	0.69%

7.4.3 Rheology: Cottonwood Whole Tree Total [CWTT]

In general all of the pyrolysis oil samples have non-Newtonian, shear thinning behavior and the addition of solids to the pyrolysis oil samples had varying effect.

Average viscosity values, collected over the 100-1000 1/s (plateau) shear rate range, are displayed in Table 8.2 for CWTT pyrolysis oil. When comparing the entire forward and reverse step-shear data, the reverse (decreasing shear) average viscosities are generally larger when compared to the forward average viscosities indicating hysteresis effects during testing.

Addition of fumed silica at 0.51 vol % increased the average viscosity the most by 110 % (forward) to 125 % (reverse) and the smallest change occurred with the addition of silica packing at 0.96 vol % which *reduced* the average viscosity by 24.4 % (forward)

and 25 % (reverse). The largest changes in the average viscosity occurred when the smallest (fumed silica, 0.014 μm) and largest (char, $\sim 6\text{-}8 \mu\text{m}$) particles were added.

It would be expected that the larger the concentration of particles would be the larger viscosity increase, but this was not the case. A lack of trends between particle volume percent and average viscosity may be due to particle agglomeration. When aliquots were removed for shear testing, the particles were not evenly distributed. It has previously been reported that oil-coated char particles agglomerate in pyrolysis oil [ref] and agglomeration could contribute to the results presented.

Table 7.2 Average viscosities (as measured between 100-1000 1/s for both increasing and decreasing shear) of cottonwood whole tree total [CWTT] pyrolysis oil with added char, sand, silica packing, and fumed silica.

Sample Name	Particle % (v/v)	Increasing Shear		Decreasing Shear	
		Avg. Viscosity (cP)	95% CI	Avg. Viscosity (cP)	95% CI
Neat	0.00	12.63	0.98	13.92	1.08
	0.51	26.55	0.57	31.32	2.45
	1.13	10.68	0.97	12.07	1.07
Fumed Silica	3.89	12.42	1.11	13.25	1.02
	0.96	9.56	1.15	10.44	0.91
	2.24	12.16	0.96	13.55	1.05
Silica Packing	5.49	11.37	1.19	12.29	0.99
	1.29	10.83	1.01	13.39	1.26
	3.07	9.25	1.07	9.54	0.80
Char	3.98	24.09	0.79	26.72	1.85
	1.16	11.63	0.89	13.24	1.10
	2.43	19.22	1.39	20.69	1.68
CWTT sand	4.76	12.16	0.99	13.02	1.09

Rheology data for CWTT with added char is presented in Figure 8.4 with the forward stepped shear test on the left and the reverse on the right. Neat and char-added samples all have similar starting viscosity (2100-2600 cP), curve shape, and (with the exception of the highest char concentration, 3.98 %v/v) inflection point where the

viscosity plateaus at approximately 10 cP. The 3.98 %v/v char sample plateaus earlier at approximately 25 cP. In contrast, the reverse shear rate data show two important features. First, while the samples showed nearly identical viscosity at lower shear rates (0.1-50 1/s), as the shear was increased above ~50 1/s, there was a distinct viscosity difference between the highest solids content sample tested (3.98 %v/v) and the remainder of the samples. Second, hysteresis is present so that after the samples were sheared that rheological history affected the viscosity, at least for some period of time. Curiously, at a given shear rate the reverse shear viscosities are lower than the forward values for all of the CWTT samples with the exception of the highest solids content sample tested (3.98 %v/v). Hysteresis may be due to the alignment of particles during the forward shear or the breaking of agglomerations in the pyrolysis oil which could explain the decrease in viscosity in the reverse shear. The 3.07 %v/v sample showed a greater viscosity decrease in the reverse experiment than the neat and 1.29 %v/v samples. Only one rheology test was conducted on each sample, so there is a possibility that the 3.98 %v/v data set was an anomaly.

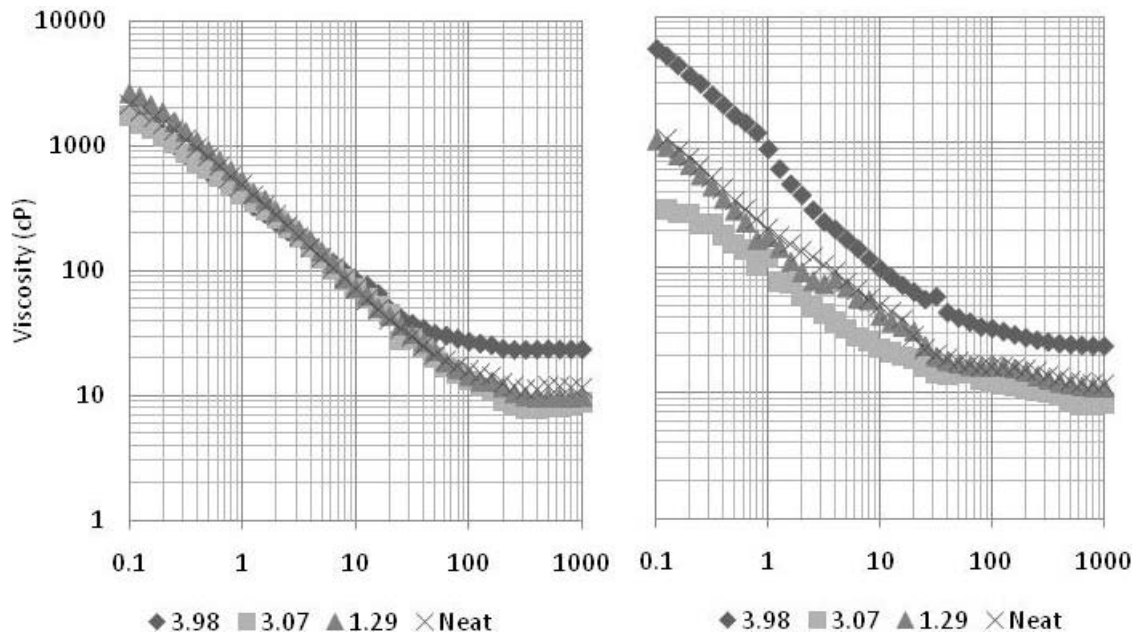


Figure 7.4 Step-shear rheology data for cottonwood whole tree total [CWTT] pyrolysis oil. Neat (as produced) and char added (3.98, 3.07, and 1.29 %v/v) samples were tested from 0.1 to 1000 1/s [left] and then from 1000 to 0.1 1/s [right].

Sand addition (Figure 8.5) did not have a large impact on the rheology. There was an observed change only for the 2.43 vol % sand added CWTT sample which increased by 51.2 % in the plateau region. Hysteresis was observed in the 2.43 and 1.16 vol % sand-addition samples. Over the shear rates tested, the 2.43 vol % sample viscosity ranged from ranging 14 to 52 % higher than the neat curve, and the 1.16 vol % sample viscosity was 7 to 100 % lower than the neat sample viscosity. The 4.76 vol % sample showed a similar step-shear trace and average viscosity as the neat pyrolysis oil.

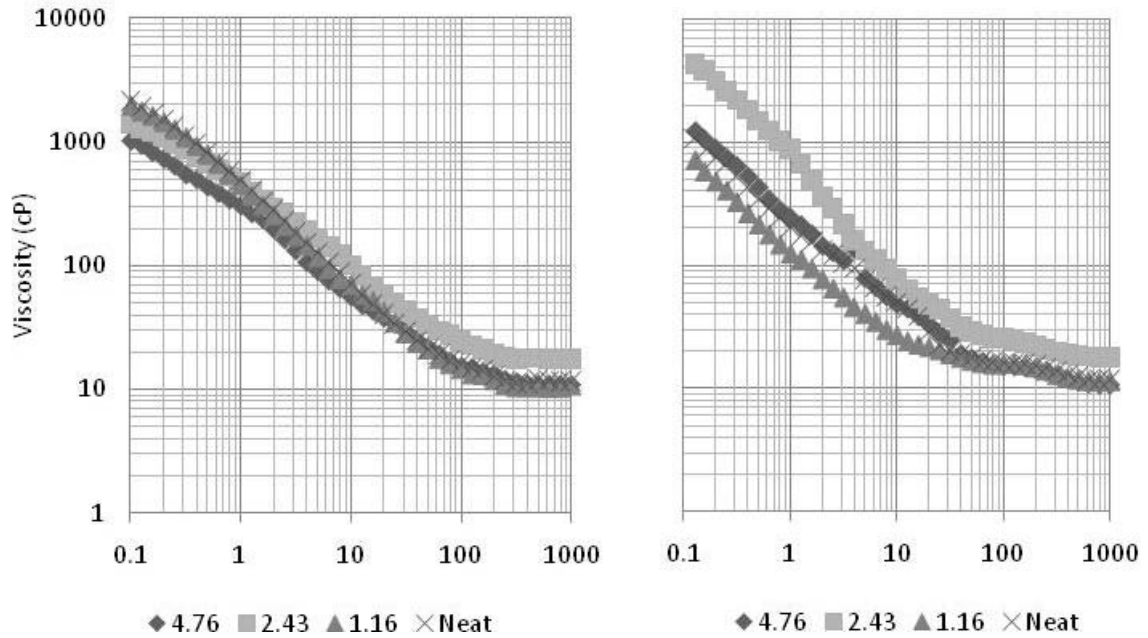


Figure 7.5 Rheology from 0.1 to 1000 1/s [left] and 1000 to 0.1 1/s [right] for cottonwood whole tree total [CWTT] pyrolysis oil neat and with 4.76, 2.43, and 1.16 v/v% of added sand.

Addition of fumed silica to CWTT pyrolysis oil (Figure 8.6) resulted initially in no change until the shear rate range of 10 to 1000 1/s where the 0.51 vol % fumed silica viscosity increased above that for neat pyrolysis oil. In addition, hysteresis was also observed in the 0.51 vol % sample in the reverse, elevating the viscosity by 120 to 400 %.

Comparing the rheology data for the silica packing addition in Figure 8.7 there is little to no difference in the shape, trend or value of the shear curves during the forward stepped flow. There is a smaller hysteresis effect during the reverse flow where the samples did not separate until the second half of the stepped shear rate between 10 and 0.1 1/s compared to the hysteresis observed in the char, sand and fumed silica samples where the curves were separated initially.

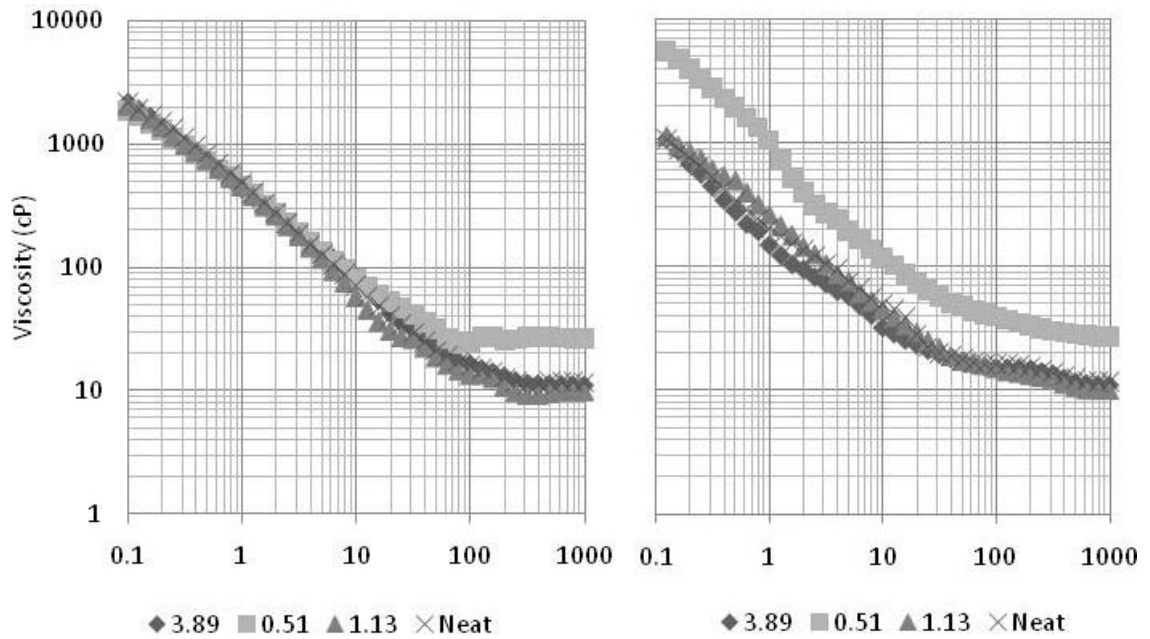


Figure 7.6 Rheology from 0.1 to 1000 1/s [left] and 1000 to 0.1 1/s [right] for cottonwood whole tree total [CWTT] pyrolysis oil neat and 3.89, 0.51 and 1.13 v/v% of fumed silica added.

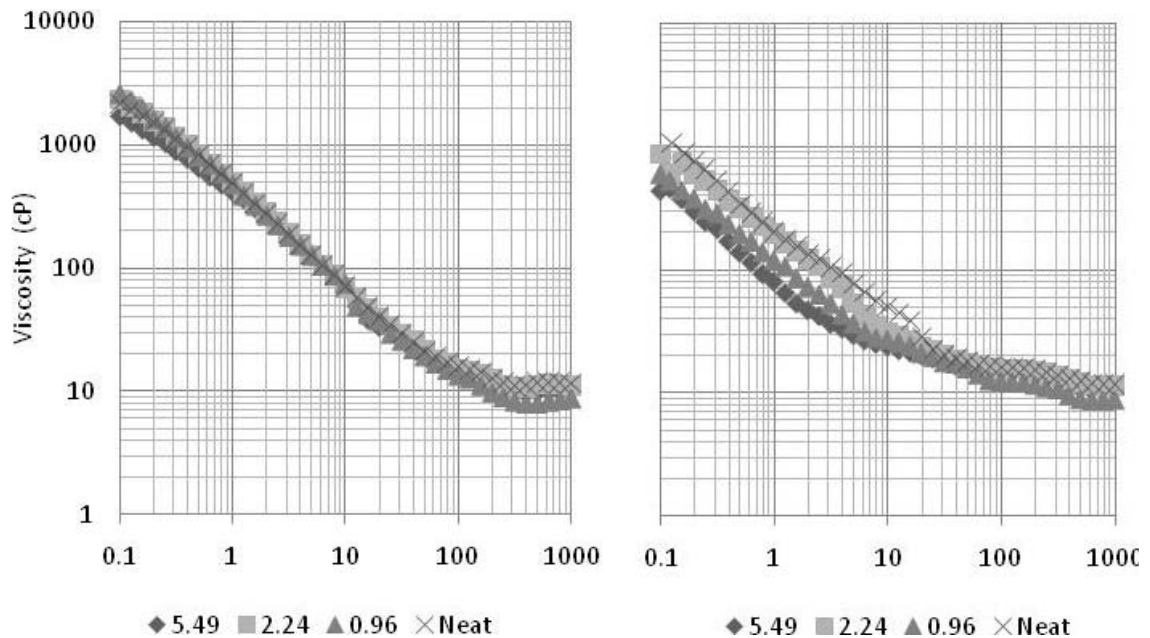


Figure 7.7 Rheology from 0.1 to 1000 1/s [left] and 1000 to 0.1 1/s [right] for cottonwood whole tree total [CWTT] pyrolysis oil neat and 5.49, 2.24 and 0.96 % by volume of silica packing added.

7.4.4 Rheology: Cottonwood Bark Total [CBT]

A rheology overview of the char, sand and silica particles addition to cottonwood bark total [CBT] pyrolysis oil is displayed in Table 8.3 providing the particle volume % and the average viscosity for the forward and reverse shear rate between 0.1 and 1000 1/s. CBT viscosities are much lower than the CWTT oil discussed in the previous section. All the particle added samples exhibited an increase in average viscosity except the 2.76 vol% silica packing. Addition of 1.72 vol% char to CBT resulted in the largest change in viscosity with a 64 % increase forward and 190 % increase in reverse. As stated previously it was expected that the higher the volume percent of particles the larger the increase in viscosity, but this was not observed for CBT either and may be due to agglomeration of particles in the pyrolysis oil or poor mixing in the samples prior to the viscosity measurements. These data suggest that the particle composition has the most significant impact versus particle size and other factors. Similarly for the sand addition the largest increase in viscosity was for the middle volume percent, 1.63 vol%, by 97 % forward and 84 % in reverse. Fumed silica and silica packing had the largest viscosity increases for volume percentages of 1.77 and 0.92 with increased of 75 and 125 % forward shear rates and 130 and 210 % in reverse respectively.

Table 7.3 Average viscosity overview for cottonwood bark total [CBT] pyrolysis oil shear increasing (0.1 to 1000 1/s) and shear decreasing (1000 to 0.1 1/s) with char, sand, silica packing and fumed silica added.

Sample Name	Particle % (v/v)	Increasing Shear		Decreasing Shear	
		Average (cP)	95% CI	Average (cP)	95% CI
Neat	0.00	3.03	0.21	3.28	0.35
Fumed Silica	0.69	4.77	0.57	5.96	1.32
	1.77	5.29	0.67	7.69	1.21
	3.20	3.72	0.25	4.36	0.58
Silica Packing	0.92	6.80	0.70	10.18	1.60
	1.64	3.64	0.36	3.48	0.15
	2.76	2.92	0.17	2.99	0.19
Char	0.92	3.42	0.22	3.69	0.49
	1.72	4.95	0.87	9.54	0.80
	4.28	3.24	0.27	3.69	0.38
CWTT sand	0.83	4.53	0.71	4.80	0.60
	1.63	5.95	0.68	7.06	1.23
	3.40	3.08	0.20	3.26	0.22

The stepped flow data for cottonwood bark total [CBT] pyrolysis data resulted in larger variance in the viscosity data as compared to the cottonwood whole tree total [CWTT] oil samples. In addition CBT samples appear to dip down and curve upwards at the high shear rates between 100 and 1000 1/s rather than begin a plateau region as in

CWTT. With the addition of ground char there was some deviation from the neat rheological curve, but there is no trend the samples followed relating to the char addition. Also, both sets of pyrolysis oils had phase separation but due to the larger amount of water in PBT it may have been more difficult to collect consistent rheology data for.

Addition of fumed silica and silica packing had little to no effect on the forward shear testing of the CBT oils (Figures 8.8 and 8.9, respectively). There was some hysteresis observed, most obviously with the silica packing samples where there was separation of the viscosity curves. Both samples with sand (Figure 8.10) and fumed silica (Figure 8.11) added show little to no hysteresis effects in the reverse shear and is interesting since these materials represent the extremes of the particle sizes studied. It should be noted that data has been collected so far for single samples and thus oddities, such as the neat reverse shear CBT pyrolysis oil curve, may be represent errors in sample preparation or data collection rather than significant findings for that sample.

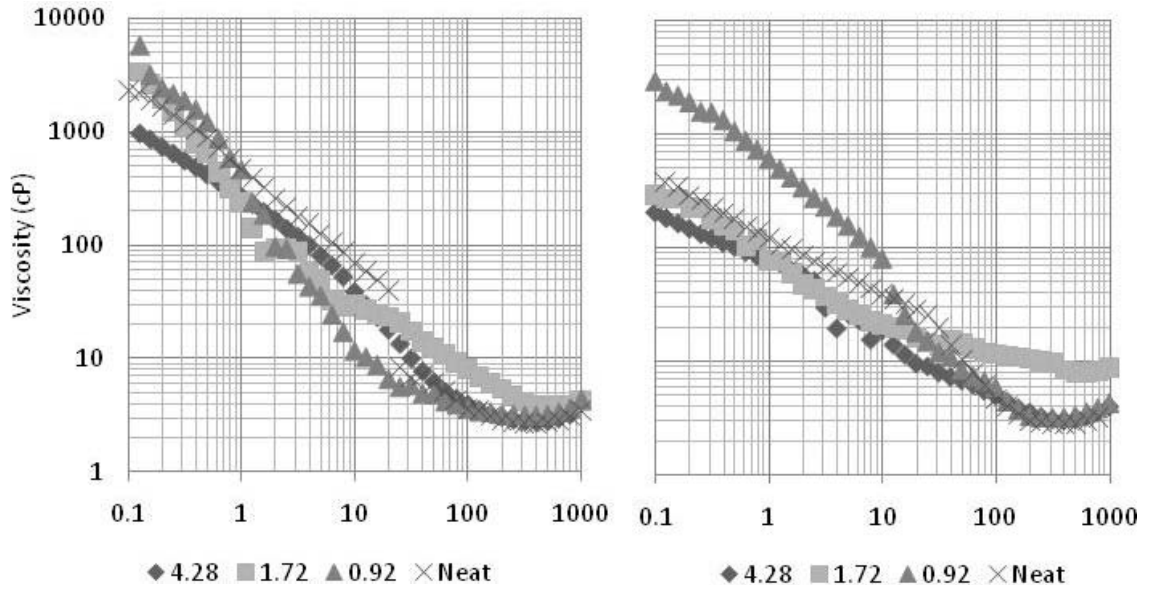


Figure 7.8 Rheology from 0.1 to 1000 1/s [left] and 1000 to 0.1 1/s [right] for cottonwood bark total [CBT] pyrolysis oil neat and 4.28, 1.72 and 0.92 % by volume of char added.

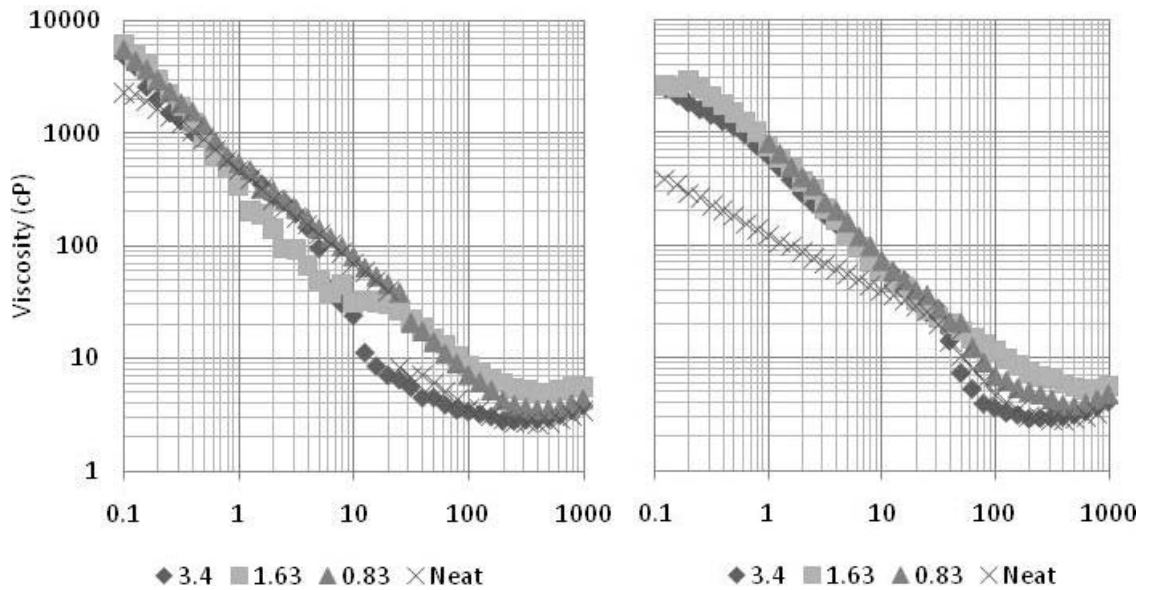


Figure 7.9 Rheology from 0.1 to 1000 1/s [left] and 1000 to 0.1 1/s [right] for cottonwood bark total [CBT] pyrolysis oil neat and 3.4, 1.63 and 0.83 % by volume of sand added.

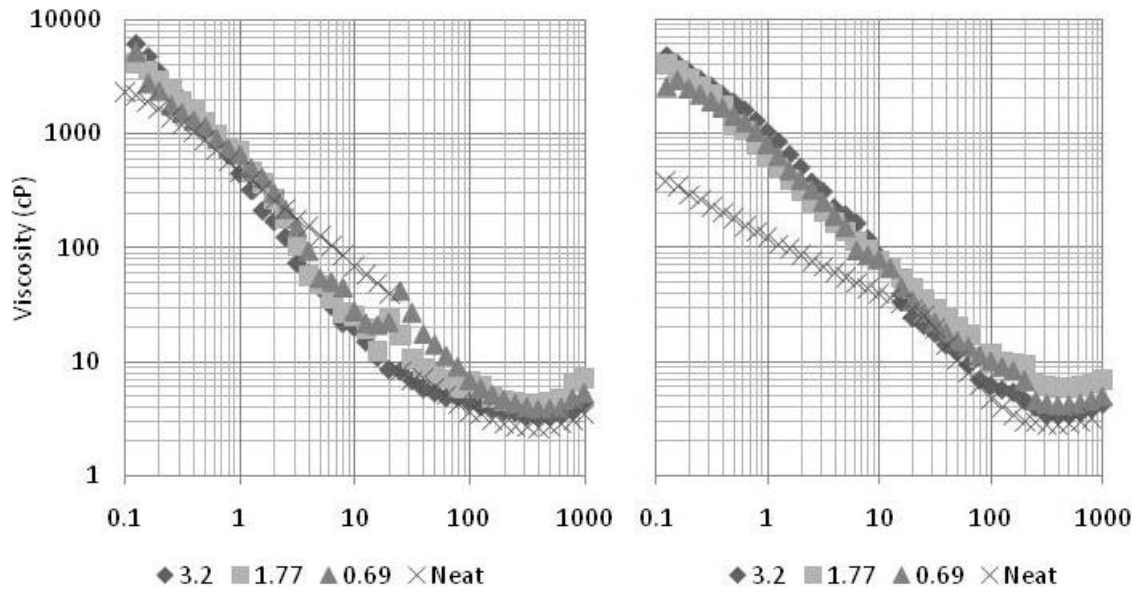


Figure 7.10 Rheology from 0.1 to 1000 1/s [left] and 1000 to 0.1 1/s [right] for cottonwood bark total [CBT] pyrolysis oil neat and 3.2, 1.77 and 0.69 % by volume of fumed silica added.

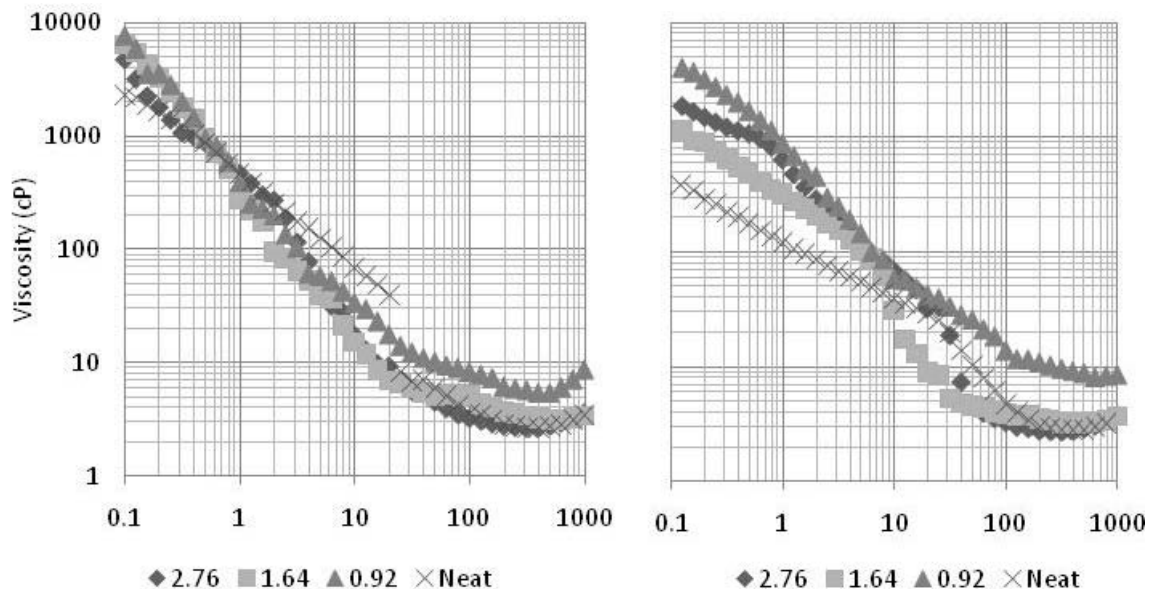


Figure 7.11 Rheology from 0.1 to 1000 1/s [left] and 1000 to 0.1 1/s [right] for cottonwood bark total [CBT] pyrolysis oil neat and 2.76, 1.64 and 0.92 % by volume of silica packing added.

7.4.5 ATR-FTIR Spectroscopy

To verify that the addition of char, sand, and silica particles did not cause chemical changes in the pyrolysis ATR-FTIR spectra were collected and presented in Figures 8.12 and 8.13. Spectra for cottonwood clear wood total [CCWT] neat (a) and the highest solid density samples studied for char (b), sand (c), silica packing (d), and fumed silica (e) are shown. There were no significant differences observed between the spectra of the solids-added samples as compared to the neat CWTT sample.

Cottonwood bark total [CBT] pyrolysis oil spectra (Figure 15) compare neat (a) and the highest concentration of added char (b), sand (c), silica packing (d), and fumed silica (e). There are no significant differences when comparing the solid added spectra to the neat pyrolysis oil sample. There is a slight difference in the silica packing spectra at $\sim 1050\text{ cm}^{-1}$ which is typically identified as a primary alcohol [Kuptsov, Silverstein, Nakanishi].

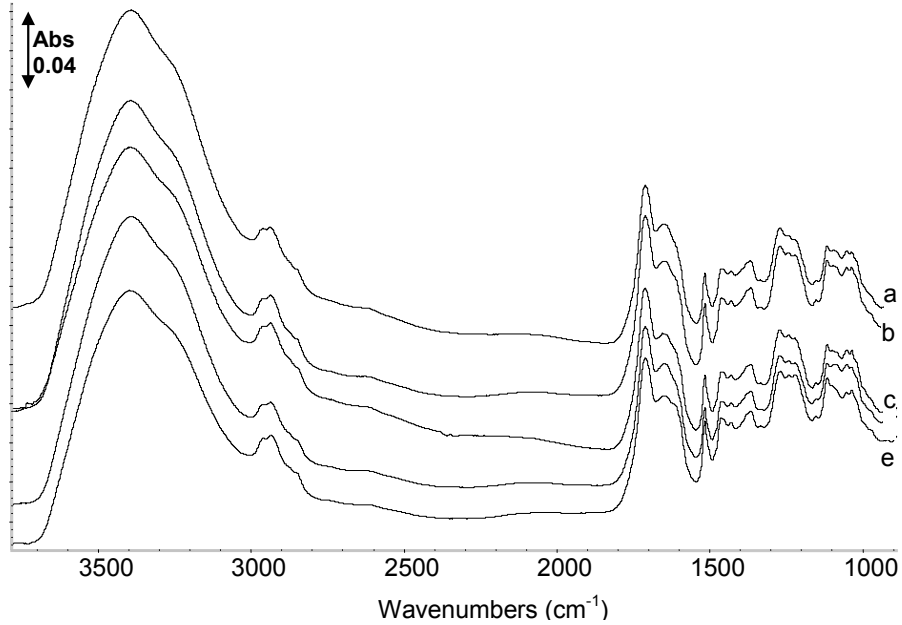


Figure 7.12 ATR-FTIR spectra of cottonwood whole tree total [CWTT] pyrolysis oil: neat (a), sand (b, 4.76 % v/v), char (c, 3.98 % v/v), silica packing (d, 5.49 % v/v), and fumed silica (e, 3.89 % v/v).

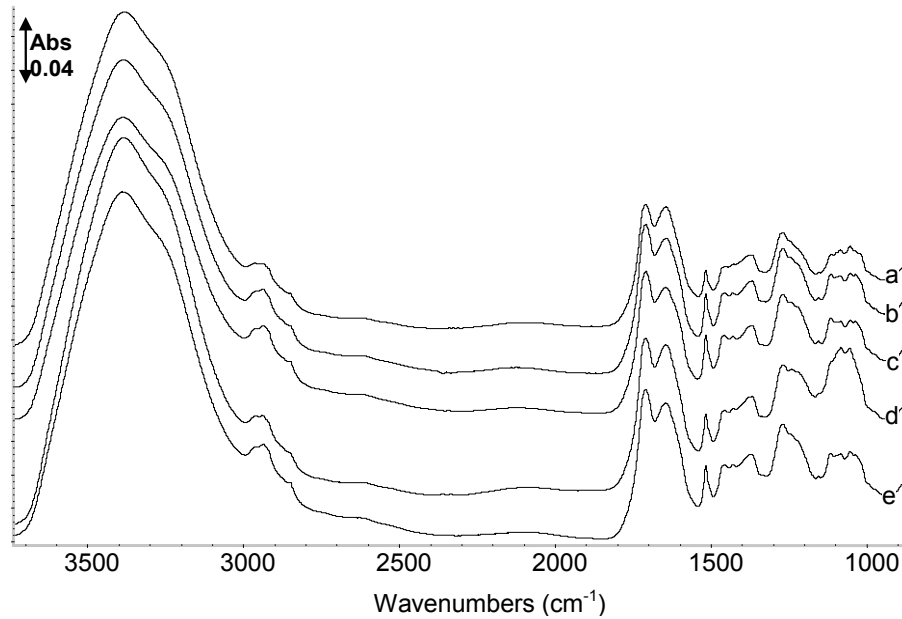


Figure 7.13 ATR-FTIR spectra of cottonwood bark total [CBT] pyrolysis oil: neat (a), sand (b, 3.4 % v/v), char (c, 4.28 % v/v), silica packing (d, 2.76 % v/v), and fumed silica (e, 3.2 % v/v).

7.5 Conclusions

Addition of particles to cottonwood whole tree total and cottonwood bark total pyrolysis oils along with rheological studies provided some insight into the physical behavior of pyrolysis oil. Char addition resulted in elevated viscosities as compared to the neat pyrolysis oil. Also, it was shown that the pyrolysis oil does have positive and negative viscosity hysteresis effects that were most noticeable in the cottonwood whole tree total pyrolysis oil samples. Hysteresis in these samples did not appear to be dependent on particle size, at least for the particle sizes and volume percentages studied. The ATR-FTIR spectra indicated there were no significant chemical changes in the pyrolysis oil due to the solids addition. Overall it was shown that the addition of a range of particle sizes do not have a significant effect on the rheology of pyrolysis oil at the low concentrations investigated. Hysteresis effects were observed in both neat and solid added samples where the solids did appear to amplify the effect. With the rheology data from this study, it is reasonable to propose that char fines remaining after hot gas filtration in concentration less than ~5 vol % do not affect the initial viscosity significantly.

7.6 References

Agblevor, F.A.; Besler, S. Inorganic Compounds in Biomass Feedstocks. 1. Effect on the Quality of Fast Pyrolysis Oils. *Energy & Fuels* 1996, 10, 293-298.

Agblevor, F.A.; Scahill, J.; Johnson, D.K. Pyrolysis Char Catalyzed Destabilization of Biocrude Oils. *AIChE Symposium Series* 1998, 319, 94.

Ba, T.; Chaala, A.; Garcia-Perez, M.; Roy, C. Colloidal Properties of Pyrolysis oils Obtained by Vacuum Pyrolysis of Softwood Bark. Storage Stability. *Energy & Fuels* 2004, 18, 188-201.

Boucher, M.E.; Chaala, A.; Roy, C. Pyrolysis oils obtained by vacuum pyrolysis of softwood bark as a liquid fuel for gas turbines. Part I: Properties of pyrolysis oil and its blends with methanol and a pyrolytic aqueous phase. *Biomass & Bioenergy* 2000, 19, 337-350

Chaala, A.; Ba, T.; Garcia-Perez, M.; Roy, C. Colloidal Properties of Pyrolysis oils Obtained by Vacuum Pyrolysis of Softwood Bark: Aging and Thermal Stability. *Energy & Fuels* 2004, 18, 1535-1542.

Davidsson, K.O.; Stojkova, B. J.; ettersson, J. B. C. Alkali Emission from Birchwood Particles during Rapid Pyrolysis. *Energy & Fuels* 2002, 16, 1033-1039

Diebold, J.P.; Czernik, S. Additives To Lower and Stabilize the Viscosity of Pyrolysis Oils during Storage. *Energy & Fuels* 1997, 11, 1081-1091.

Energy Information Administration (EIA). 2009. *Annual Energy Review 2008*. Washington, DC: US Department of Energy.

Elliot, D.C. Water, Alkali and Char in Flash Pyrolysis Oil. *Biomass & Bioenergy* 1994, 7, 79-185.

Garcia-Perez, M.; Chaala, A.; Pakdel, H.; Kretschmer, D.; Rodrigue, D.; Roy, C. Multiphase Structure of Pyrolysis oils. *Energy & Fuels* 2006, 20, 364-375.

Kuptsov, A.H.; Zhizhin, G.N. Handbook of Fourier Transform Raman and Infrared Spectra of Polymers. Elsevier: New York, 1988; p 8, 10, 11.

Nakanishi, K.; Solomon, P.H. Infrared Absorption Spectroscopy. Holden Day: Oakland, 1977; p. 14, 19, 25,26, 31, 38-40.

Nielsen, L.E., Polymer Rheology, Marcel Dekker, Inc.: New York, 1977.

Oasmaa, A.; Kuoppala, E.; Selin, J.; Gust, S.; Solantausta, Y. Fast Pyrolysis of Forestry Residue and Pine. 4. Improvement of the Product Quality by Solvent Addition. *Energy & Fuels* 2004, 18, 1578-1583.

Oasmaa, A.; Peacocke, C.; A guide to physical property characterisation of biomass-derived fast pyrolysis liquids. Technical Research Centre of Finland, VTT Publication 450, ESPOO 2001.

Oasmaa, A.; Kuoppala, E.; Gust, S.; Solantausta, Y. Fast Pyrolysis of Forestry Residue. 1. Effect of Extractives on Phase Separation of Pyrolysis Liquids. *Energy & Fuels* 2003, 17, 1-12.

Rossi, C. *Proceedings of Biomass Pyrolysis Oil Properties and Combustion Meeting*, CO, Sept 26-28, 1994; p 321-328.

Silverstien, R.M.; Webster, F.X. *Spectrometric Identification of Organic Compounds*; John Wiley & Sons Inc.: New Jersey, 1998; p. 82, 86, 87, 90-92, 94 95, 97.

CHAPTER VIII

CONCLUSIONS AND RECOMMENDATIONS

8.1 Conclusions

8.1.1 General

FTIR analysis indicated that leaf and bark biomass contains more aromatic compounds than clear wood and whole tree biomass while char contains more aromatic, alcohol, ether and/or ester containing compounds. When comparing neat pyrolysis oils produced from pine and cottonwood, there were differences in the pH, density, and viscosity depending on the part(s) of the tree used. Pine and cottonwood pyrolysis oils presented similar aging results before and after filtration demonstrating that many of the results during accelerated aging are not feedstock specific. Preliminary comparisons of (i) pine and cottonwood feedstocks and (ii) total pyrolysis oil, fractionated pyrolysis oil, and water condensate suggest that the incorporation of bark and/or leaves/needles alters the chemical composition and properties of the pyrolysis oil and could lead to large difference between these materials during aging.

It was found that the presence forestry residue (bark needles and/or leaves) in the biomass affects the water content of unaged pyrolysis oil while the tree species, at least for cottonwood and pine), had no impact. Pyrolysis oil collection (total, fractionated, water condensate) was shown to plays a large role where the total oil containing the water condensate affects all of the properties with the largest impact on viscosity and initial molecular weight. GC/MS analysis showed a presence of phenolic and aromatic ether

compounds in PWTF, PCWT, PCWF, PBF and CCWF pyrolysis oils showing similarities between cottonwood and pine pyrolysis oil and between.

PCWT and PBF phase separated during aging and measured water contents were much lower for the bottom phase than the top with the water content of the top phase continuing to increase during aging which may be due to the presence of the water condensate in PCWT and bark derivatives in PBF.

Pine and cottonwood pyrolysis oil viscosity after 24 hours of aging did not show a significant correlation where molecular weight was significantly affected by aging (24 h). After 504 hours of aging all of the properties (pH, water, viscosity and MW) were shown to be significantly affected by aging.

8.1.2 Filtration

In an initial 2-step serial filtration study, filtration was shown to prevent the viscosity increase demonstrated in the unfiltered sample during aging for PWTF pyrolysis oil. However, further investigation of serial filtration (using a 2-step process) in PBF and CCWF and (a 3-step process) in PCWT and PCWF oils showed filtration caused decreased water contents and also increased the initial (unaged) sample viscosities. In this second filtration study, filtration did not prevent the viscosity increase during aging.

Viscosity after filtration increased significantly for all of the pyrolysis oil samples studied and is thought to be related to the reduction in water content, a result of filter wetting and residue loss during filtration. During aging, both unfiltered and filtered samples increased in viscosity with the filtered samples having larger viscosities than the unfiltered samples throughout aging. In addition once PCWT and PBF phase separated,

the viscosity decreased drastically due to the introduction of two separate layers with very different properties. Molecular weight also increased during aging in all samples. In phase separated samples, the bottom phase had larger molecular weights—that continued to increase during aging—and the top phase molecular weight decreased to reach the initial (unaged) molecular weight of the sample.

Etherification during aging was determined by GC-MS and FTIR in the PWTF pyrolysis oil. Both aromatic ethers and phenolic compounds were formed in both the filtered and unfiltered pyrolysis oil samples. In the second filtration study, ATR-FTIR PHR showed that there was a general trend in the reactions occurring in PCWT, PCWF, PBF and CCWF oils during aging. All exhibited decreases in primary or secondary alcohols and/or ethers in addition to an increase in aromatics and ketones or carboxylic acids. Using GC/MS analysis, it was determined that filtration does alter the aging reactions by moderating in composition within PBF, PCWF and PCWT, but not CCWF. This suggests that the removal of the solids (along with the material coating the solids) may prevent one reaction but also could allow for other reactions to proceed.

8.1.3 Methanol Addition

The use of pine needles as the sole feedstock produces a unique pyrolysis oil that separates into three phases after accelerated aging. Removal of the crust decreased the density and viscosity of the remaining liquid preventing viscosity from being used to reliably monitor aging. In addition, PNT appeared to have a larger MW increase due to aging compared to PNF.

Methanol addition was able to retard the aging reactions in PNF but not in PNT, perhaps due to the high concentration of water in PNT. Addition of methanol to PNF

reduced the molecular weight after 504 hours and the 15 wt% methanol added sample resulted in no phase separation and very little increase in MW. With the addition of 15 wt % methanol, GC/MS results indicated formation of ester and/or aldehyde during aging.

8.1.4 Solids Addition

Addition of particles to cottonwood whole tree total and cottonwood bark total pyrolysis oils along with rheological studies demonstrated that char addition will elevate viscosities prior to aging, but not to the extent that is observed in aging. In addition, pyrolysis oil displayed positive and negative viscosity hysteresis effects that were most noticeable in the cottonwood whole tree total pyrolysis oil samples. Given the collected data hysteresis did not appear to be dependent on particle size in the pyrolysis oils investigated.

8.2 Recommendations

8.2.1 General

Pine needle-derived pyrolysis oil presented unique properties resulting in three phases after accelerated aging. Having three phases is not ideal for the use of pyrolysis oil. So, oil produced solely from needle biomass is not likely viable as a fuel source.

8.2.2 Filtration

Filtration of condensed pyrolysis oil proved difficult and inefficient. In addition water and material loss during filtration increase the initial viscosity in the second filtration study which is undesirable. If filtration of condensed pyrolysis oil is to be

research further it may be of interest to elevate the temperature of the pyrolysis oil during filtration to aid in filtration and reduce the amount of material lost.

To investigate the effect of solids on pyrolysis oil instability, the reactor configuration should be altered to compare cyclone and hot gas filtered pyrolysis oils to oils without any solids removed during production. At the very least a crude filtration should be conducted with newly produced hot pyrolysis oil to remove the largest of the particles. In addition, *in situ* hot gas filtration technology should also be investigated further and perhaps used in conjunction with post-reactor liquid filtrations.

8.2.3 Methanol Addition

Due to the highly unique properties of the needle-derived pyrolysis oil, this study should be expanded to incorporate additional pyrolysis oil samples for comparison. For needle-derived fractionated pyrolysis oil, 15 wt% methanol was determined to be effective in preventing phase separation and aging effects but the required percentage may be dependent upon the specific pyrolysis oil sample.

8.2.4 Solids Addition

Further investigation could examine higher concentrations of solids. Also, the addition of char could be investigated with and without grinding and also before and after aging to determine if the char particles change in shape or composition over during accelerated aging.

An applied shear could potentially assist in reducing viscosities observed in pyrolysis oils, but further investigation at various temperatures should be conducted for comparison. In addition, it is currently unknown how long the hysteresis effect lasts and should also be investigated.

APPENDIX A
PYROLYSIS OIL PROCEDURES

A.1 Working with Pyrolysis Oil General

Pyrolysis oil, commonly known as pyrolysis oil is unstable at room temperature, contains 200+ compounds, is fairly viscous, phase separates, has a low pH of 2-3, contains char particles and is air sensitive. Due to all of these properties working with pyrolysis oil can be extremely challenging. It is important to always work in a vented hood due to the strong scent of the pyrolysis oil and to avoid any potential hazards. In addition protecting hands, eyes and skin are also important.

All pyrolysis oil is stored in a refrigerator to prevent aging which is accelerated by heat. In order to work with a pyrolysis oil sample it must first warm to room temperature which allows for multiple phases to mix more readily and the viscosity decreases at room temperature. If phases are analyzed separately, which is highly recommended, the pyrolysis oil should be used cold when the phases are well defined. Phases will start to mix and become unclear rather quickly (less than 5 minutes for 4 mL vials).

Due to the viscosity and particulates the pyrolysis oil does not easily draw into a needle or syringe therefore when transferring to jars, bottles, etc. it is best to use a beaker with a spout or a graduate cylinder. If needed, a 14 gauge stainless steel needle or large works best with a glass syringe. Also keep in mind that pyrolysis oil coats all glassware and anything it comes in contact with. When measuring out samples minimizing the glassware size reduced the amount of sample that is lost during sample preparation.

Due to organic acids, high water content and alkali metals in pyrolysis oil it is highly corrosive and therefore only stainless steel and glass should be used. If needed PTFE or PP have been tested to use with pyrolysis oil (PTFE lined caps, PP centrifuge tubes) and can be used.

A.2 Accelerated Aging of Pyrolysis Oil

1. Remove the pyrolysis oil sample of interest from the refrigerator and allowed to warm up to room temperature (minimum of 15 minutes, longer for larger samples).
2. Shake the bottle or jar until the pyrolysis oil is mixed thoroughly. Check to make sure the bottom viscous layer is no longer visible on the bottom of the bottle.
3. Label the sample jars accordingly with chemical and water resistant labels
4. Using a graduate cylinder measure 27 mL of pyrolysis oil for every 30 mL glass jar with PTFE lined lids. This ratio is suggested by Oasmaa 2001 where 90 mL of pyrolysis oil was aged in 100 mL air tight glass jars [Oasmaa 2001]. The reduction of headspace is ideal where the pyrolysis oil aging can increase in the presence of air [Oasmaa 2001].
5. Weight the pyrolysis oil filled jars with the cap on and record the initial weight
6. Tightened the lids to the jars well prior to aging to prevent mass loss
7. Placed the jars in the oven at the desired temperature in a metal or glass pan/dish.
8. Tighten the jar lids multiple times within the first 24 hrs and then periodically through the aging period
9. When the aging time is complete, remove the jars from the oven and immediately cool them in an ice water bath for 15 minutes to stop the ageing reactions.
10. Dry the outside of the jars and then weigh them, recording the final weight.
11. The samples are then placed in the refrigerator until further analysis

A.3 Filtration Methods for Pyrolysis Oil

A.3.1 Filters Tested

In Table A.1 the different filtration methods available for pyrolysis oil are displayed including the pore size. The two meshes are made of 316 stainless steel (SS), the frits are glass and the filters are vacuum filters unless specified otherwise.

Table A.1 The different filtration methods available including pore size.

Name	Pore Size (μm)
Medium SS Mesh	1183
Fine SS Mesh	84
Whatman 41 filter	20-25
Medium Glass Frit	10-15
Whatman 40 filter	8
Fine Glass Frit	4-5.5
Whatman 5 filter	>2.5
VWR filter (28321-009)	1
Centrifuge Filter (0.45)	0.45
Centrifuge Filter (0.20)	0.20

A.3.2 Results From Filtration Testing

Medium wire mesh: All of the pyrolysis oil samples underwent a crude filtration using the medium wire mesh. The only pyrolysis oil sample that was not included in the crude filtration was the pine needles fractionated pyrolysis oil sample which contained a large amount of “chunks” in the pyrolysis oil and does not flow freely.

Fine wire mesh: The pyrolysis oil is too viscous for the fine wire mesh to flow through, especially the fractionated pyrolysis oils. In addition the pores are too large to use the mesh with vacuum.

Glass frits: The 30 mL frits were ordered in two porosity sizes; medium and fine. The medium frit worked with the pine clear wood fractionated [PCWF-91] pyrolysis oil but took some time to filter 50 mL (~20-30 minutes). The fine glass frit did not work well with the pyrolysis oil and after one hour very little had been filtered. In addition the vacuum began to pull off the volatile materials from the filtered pyrolysis oil and made it bubble.

A.3.3 Volumes After Crude Filtration

Table A.2 displays the volumes of the cottonwood and pine pyrolysis oils after crude filtration which removed the largest solids from the pyrolysis oil.

Table A.2 Volumes (mL) of the cottonwood and pine pyrolysis oils after crude filtration.

Cottonwood Clear Wood			Pine Clear Wood		
Name	Aqueous	Total	Name	Aqueous	Total
CCWF		550	PCWF		900
CCWW	450	700	PCWW		900
CCW-WF	450	450	PCW-WF	500	650
Cottonwood Whole Tree			Pine Whole Tree		
Name	Aqueous	Total	Name	Aqueous	Total
CWTF		450	PWTF*	0	350
CWTW	500	700	PWTW	500	500
CWT-WF	625	625	PWT-WF	450	550
Cottonwood Bark			Pine Bark		
Name	Aqueous	Total	Name	Aqueous	Total
CBF		400	PBF		750
CBW		600	PBW		200
CB-WF	500	500	PB-WF		850
Cottonwood Leaves			Pine Needles		
Name	Aqueous	Total	Name	Aqueous	Total
CLF		350	PNF	-	not filtered
CLW	500	550	PNW	200	500
CL-WF		500	PN-WF1	300	400
			PN-WF2	500	1000

A.3.4 Vacuum Filtration

Vacuum filtration can be used for a pre-filtration, a standalone filtration or multiple steps in a serial filtration.

1. Attach a Buchner funnel to an Erlenmeyer vacuum flask with the use of a rubber stopper and attach the flask to a vacuum source. The smaller the flask the less pyrolysis oil that will be lost due to glassware coating.
2. Dry a filter in the oven for a minimum of 5 minutes at 80 °C (to remove any moisture from filter)

3. Weigh filter and record dry weight. Do this immediately after removing the filter from the oven because the filters begin to gain moisture from the air quickly.
4. Place filter in the Buchner clean funnel
5. Pour 10-20 mL of the pyrolysis oil onto the surface of the filter and spread it around using a stainless steel spatula, coating the entire surface.
6. Once the filter is wetted pour an additional 15-20 mL of pyrolysis oil onto the filter moving it around with the spatula. Be careful not to put too much pyrolysis oil on the filter at one time or it will saturate the filter. If the pyrolysis oil has a high concentration of char particles reduce the volume of pyrolysis oil added.
7. Filter approximately 50 -75 mL of pyrolysis oil per vacuum filter unless filtration is fast and the filter appears clean.
8. To replace the filter, remove vacuum pressure from the Erlenmeyer vacuum flask and remove the pyrolysis oil coated filter with stainless steel forceps.
9. Weigh the wet filter, record the wet weight and place it in a labeled glass petri dish.
10. The wet filter should be stored in the refrigerator until the solids are removed.
11. Repeats steps 1-10 until the pyrolysis oil sample is filtered.
12. To remove the filtered pyrolysis oil from the Erlenmeyer vacuum flask remove the Buchner funnel and stopper.
13. Invert the flask and allow the pyrolysis oil to drain into a second bottle or jar with the use of a ring stand. The use of a stainless steel spatula can be used to scrape the inside of the flask to recover the pyrolysis oil.

A.3.5 Centrifuge Filter Preparation

1. Label the centrifuge test tubes and caps with a number or labeling scheme.
2. Weigh the dry, clean weights of the whole centrifuge tube, just the filter insert and just the test tube (with cap).
3. Add the neat or previously filtered pyrolysis oil to the filtration insert 5-15 mL per test tube
4. Weigh the total weight of the pyrolysis oil filled test tube
5. Pair test tubes of similar weight. Weights of pairs must be within 1 g of each other. If needed remove or add pyrolysis oil to a test tube to balance the pair
6. Parafilm around the caps of the centrifuge test tubes to prevent leakage

A.3.6 Centrifugation

Centrifuge: Eppendorf 5810 R with swing buckets

The centrifuge filters cannot be operated above 2500 rpm without tearing.

1. Turn the centrifuge on with the switch at the right side of the instrument as well as the power button on the front display
2. When the open button turns blue, press it to open the lid of the centrifuge.
3. Place the test tubes in the swing buckets making sure to balance the pairs in opposite positions across the rotor
4. Close the lid of the centrifuge and hold the lid and allow it to latch shut
5. Set the desired time by pressing the time button and adjusting it using the up and down arrow buttons. The rpm setting is adjusted in the same fashion.
6. Test the balance of the samples by running the centrifuge at 1000 rpm for 1 minutes. If the centrifuge does not shake or produce an error message proceed
7. Set the 2500 rpm for 5-10 minutes

8. When the run is complete the centrifuge will beep and the open button will turn blue
9. Open the lid and check the centrifuge test tube. If the pyrolysis oil is completely filtered remove all of the test tubes. Repeat step 7 if the pyrolysis oil is not fully filtered.
10. To shut the centrifuge down, close the lid and press the power button on the front display as well as the power button on the right of the instrument

A.3.7 Cleaning Inside the Centrifuge

In the case of a leaking centrifuge tube or for routine cleaning of the centrifuge, the swing bucket inserts and metal swing buckets can be removed from the interior of the centrifuge to be cleaned. It is recommended to clean the accessories with warm soapy water. The swing bucket inserts taken apart making it easier to clean the inside and bottom.

A.3.8 Centrifuge Filter Separation

Recovering filtered pyrolysis oil and solids

1. After centrifugation, if there is liquid on top of the filter, pipette it from the top of filter without removing any solids from the surface of the filter.
2. Tare the weight of a vial or jar and transfer the liquid to a labeled clean vial or jar. Measure the weight of the unfiltered liquid.
3. Remove the filter insert and weigh it wet on a tared weigh boat.
4. Put the filter into a clean test tube and label it.
5. Weigh the test tube, cap and filtered pyrolysis oil.

6. Remove the filtered liquid at the bottom of the test tube using a pipette and/or a stainless steel spatula and put it into a jar or vial to save.
7. Weigh the test tube and cap with the remaining pyrolysis oil residue.
8. Rinse the filter insert and filter with methanol to remove the solids in the clean test tube.
9. Collect the solids and methanol mixture in a jar or vial.
10. Sonicate the filter insert in methanol until the methanol is clear.
11. Dry the filter in the vacuum oven for a minimum of 30 minutes at 80 °C and weigh the dry filter.
12. Calculate the percentage of solids removed from the pyrolysis oil

A.3.9 Pyrolysis Oil Centrifuge Test Tube Cleaning

The pyrolysis oil typically coats the inside of the test tubes. To re-use the test tubes:

1. Make sure NOT to use acetone in the plastic centrifuge test tubes. These test tubes are made of polypropylene and will be damaged if acetone is used.
2. Clean the pyrolysis oil from the test tube and cap with soap and warm water.
3. Fill the test tube with a polar solvent (such as MeOH) and sonicate it for 15-30 minutes.
4. Empty the solvent and dispose of it properly.
5. Rinse with the same solvent. If solvent is still tinted repeat the sonication.
6. Rinse the test tubes with and allow the test tubes to dry and put them away.

A.4 pH Adjustment of Pyrolysis Oil

Dry KOH pellets were used to adjust the pH of neat pyrolysis oil

1. Measure the initial weight of a clean, dry beaker
2. Pour the desired amount of adjusted pyrolysis oil into a beaker
3. Measure the pyrolysis oil + beaker weight (do not tare the weight of the beaker)
4. Measure the pH of the pyrolysis oil for an a starting point
5. Add a magnetic stir bar and place on a magnetic stirrer
6. Turn the stirrer to a setting where the pyrolysis oil moves and mixes well
7. Add several KOH pellets and allow to mix for 2-5 minutes making sure the pellets mix into the pyrolysis oil
8. Weight the pyrolysis oil with the added KOH and record the new weight
9. Measure the pH of the pyrolysis oil
10. Repeat steps 7-9 until the pyrolysis oil is at the desired pH
11. *NOTE: When adjusting to higher pH values such as 7 or 9 the addition of the solid KOH pellets increase the viscosity, the mixture becomes difficult to stir and the pyrolysis oil becomes almost solid.

A.5 pH Measurements

Two pH meters: SevenEasy™ pH Meter S20 and manufactured by Mettler Toledo and AB15 Accument Basic manufactured by Fischer Scientific.

pH Buffer solutions: nominal values of 2, 4, 7, 10 and 12

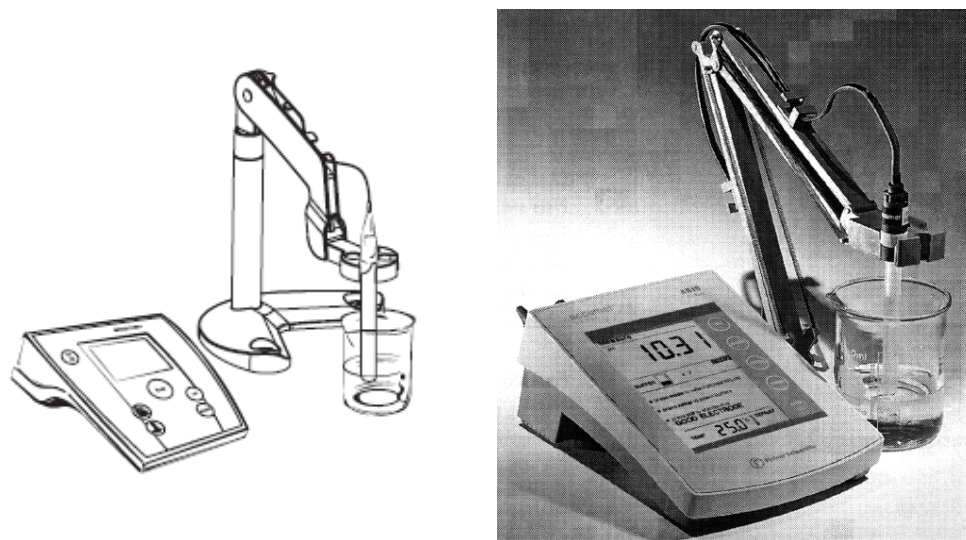


Figure A.1 pH meter set-ups SevenEasy (left)[seveneasy manual] and Accument Basic (right) [accument basic manual]

A.5.2 SevenEasy pH Meter:

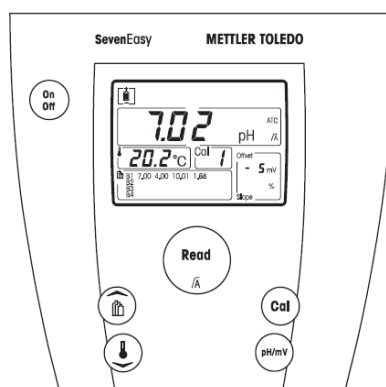


Figure A.2 The keypad representation of the SevenEasy pH meter.

1.5.3 SevenEasy Setup

The SevenEasy pH meter allows for 1-, 2- and 3-point calibrations. If the calibration is selected from the 4 fixed groups defined in the meter, the buffers are automatically recognized during calibration (auto buffer recognition).


The 4 fixed buffer group options:

B1: (25 °C) 7.00 4.00 10.01 1.68

B2: (25 °C) 7.00 4.01 9.21 2.00 11.00

B3: (20 °C) 7.00 4.00 9.00 2.00 12.00

B4: (25 °C) 6.86 4.01 9.18 1.68

To select the buffer group Press the  key, the selected buffer group will blink. Use up and down arrow keys to select a different buffer group. Press the read button to select the desired buffer group.

1.5.4 SevenEasy Calibration

1. Place the electrode in a calibration buffer and press calibration (CAL) button on the keypad.
2. The SevenEasy pH meter will automatically read the endpoints when calibrating.
3. To manually endpoint the calibration, press the read button.
4. At the endpoint the meter displays the pH buffer value, and shows the electrode offset.
5. Press the read button to return to sample measurement
6. Use distilled water to rinse the electrode.
7. Repeat steps 1-6 for the second and third buffer solutions
8. It is best to repeat the calibration if the slope is not 95-105% as displayed in Figure 3.




4 Electrode condition		
		
slope: 95-105 % offset: \pm (0-15) mV Electrode is in good condition	slope: 90-94 % offset: \pm (15-35) mV Electrode needs cleaning	slope: 85-89 % offset: \pm (>35) mV Electrode is faulty

Figure A.3 The SevenEasy pH slope display.

A.5.5 Accument Basic pH Meter

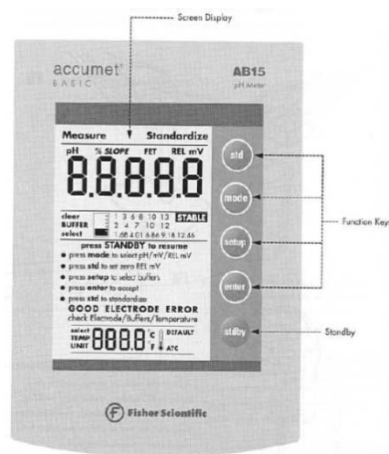



Figure A.4 The keypad representation of the Accument Basic pH meter.

1. Press the setup key twice followed by the enter key to clear any existing calibration
2. Place the electrode in a pH buffer and press the standard (std) button
3. The selected buffer group will display for a moment
4. Press the std button again to start the calibration and the meter will automatically recognize the buffer and it will display it on the screen
5. The STABLE icon will appear and the meter will return to the measure screen
6. Clean the electrode with distilled water
7. Repeat steps 2-6 for up to 5 buffer solutions

8. After the second buffer the meter will display the slope for the calibration. The electrode should be within 90-102 % for a good electrode.
9. If Electrode Error is displayed the slope is outside of this range. Press the enter key to return to the measure screen and repeat the calibration until the slope is within range.

A.5.6 Pyrolysis Oil pH Measurement

1. Allow the pyrolysis oil to warm to room temperature (temperature will affect the pH measurement)
2. Prior to measurement mix/ shake the sample thoroughly (if pyrolysis oil is very viscous then try to stir with a spatula)
3. Place the electrode into the middle of the pyrolysis oil sample. Do not push the electrode to the bottom of the sample where it can be coated with the bottom sludge phase.
4. Allow for the pH measurement to stabilize one a number indicated by  by SevenEasy or by STABLE on the Accumet Basic.
5. Record the measurement and remove the electrode.
6. Rinse the electrode with methanol until there not longer is pyrolysis oil present. Then rinse the electrode with distilled water.
7. Repeat steps 1-6 for additional samples.

The pH meter should be calibrated frequently as recommended by Oasmaa 2001 for pyrolysis oil measurements, typically every 30 minutes. In addition the pH measurement must be collected immediately after the sample is mixed.

A.6 Pyrolysis Oil Water Content

Hydranal Solvent CM (chloroform-methanol) and Hydranal Titrant 2 or 2E.

A.6.1 Procedure for Water Content (Aquameyry Apparatus II & ASTM E 203-01)

1. Fill the burette with Karl Fisher Reagent (KFR) [Hydranal Titrant]
2. Add 50 mL (or until the end of the meter is submerged) of solvent to the vessel through the sample port along with stir bar [Hydranal Solvent-CM].
3. Zero the KFR by adding KFR from the burette to the jar until the color of the solvent changes from clear to a dark brown and remains that way. The needle on the meter will go to 4.4 in the KF (red) zone [do not rely solely on the meter it can be highly inaccurate].
4. Refill the burette with KFR to read zero
5. Fill a syringe with 25 to 50 mg of distilled water and weigh the initial weight (W_i)
6. Inject the water into the vessel through the port (the color will change to a yellow)
7. Re-weigh the syringe and record the final weight (W_f)
8. Calculate the weight of the water ($W_i - W_f$)
9. Slowly add KFR titrant to the vessel until the liquid is dark brown again and the meter reads 4.4 in the KF zone. It important to titrate to the same point everytime.
10. Record the amount of KFR titrant used (mL).
11. Discard the contents of the vessel into the waste jar and clean the vessel with acetone.

Repeat Steps 1-12 for a second water sample and pyrolysis oil samples

A.6.2 Notes

1. The glassware piece that connected to the top of the titrant bottle is very fragile and care should be taken when replacing the tyrant.
2. The solvent contains Chloroform so use caution when using it
3. Make sure the work space is vented and on
4. Clean the vessel between each sample: empty vessel contents into a waste bottle and clean with acetone.
5. The two water samples must be done for every session samples are measured (even if morning and afternoon sessions)
6. A minimum of two sets of data should be collected for each pyrolysis oil sample and averaged.

A.6.3 Calculations

F- KFR water equivalence (mg/mL)

A- KF titrant required for the titration of the sample (mL)

S- weight of sample used (g)

(average the 2 measurements)

(the 0.1 is a combination of the *100 for percentage and /1000 for the conversion of g to mg)

A.7 Pyrolysis Oil Viscosity Determination by Rheology



Figure A.5 AR 1500 ex rheometer (TA Instruments)

Peltier Plate temperature range of -20 to 200 C with a temperature accuracy of +/- 0.1 C platinum resistance thermometer sensor at the cent of the plate ensures accurate temperature measurement and control

A.7.2 Instrument Startup and Calibrations

Rheometer: AR 1500ex with AR instrument control software and TA data analysis software with peltier plate. When the instrument has been turned off, the following steps should be followed to turn it on before use:

1. Turn on the computer. (There is no password for the computer so just press 'Enter'.)
2. Turn on the compressor by pressing the green button on the front.
3. Open the valve connecting the compressor to the rheometer. (It will make a hissing noise as you open it.)
4. Once the valve is open, make sure the gauge reads 30 psi. If it does not, then adjust the pressure using the black knob on the front of the compressor. To do this, pull out on the knob and move it accordingly. When the pressure is properly adjusted, push the knob in locking it in place.
5. Plug in the power cord to the pump. Make sure the pump is completely submerged in distilled water. Distilled water should be added to the bath if it is not.
6. Turn on the rheometer using the switch on the back left of the instrument. Allow for the instrument to initialize.
7. Open the control software, AR Instrument Control.
8. Attach the geometry (e.g., parallel plate) to the instrument. This is done by sliding the geometry on to drive shaft without pushing upward and turning the knob at the top clockwise. If the geometry was previously created select the file by Geometry>open. (If monthly calibrations need to be performed, including the instrument inertia calibration must be conducted prior to attaching the geometry.)

The system is now setup and ready for calibration. There are both monthly and daily calibrations required ensuring the instrument is collecting accurate data. Note that the temperature should be adjusted to the desired temperature before the zero gap is

performed. If during usage of the instrument the temperature needs to be changed, the zero gap needs to be performed after every temperature change.

Calibration procedures are explained in full in the attached copy of TA Instruments' "Introductory Guide to Using an AR Series Rheometer". A brief listing of the steps involved for monthly and daily calibrations is given below as well as the instructions.

A.7.2.1 Monthly Calibrations

Instrument Inertia, Geometry Inertia, Bearing Friction Correction, Rotational Mapping, and Zero Gap.

A.7.2.2 Daily Calibrations

Geometry Inertia, Rotational Mapping, and Zero Gap.

Table A.3 Rheometer Calibration Schedule

Instrument Inertia	Monthly Recommendation: Keep a log of this value
Geometry Inertia	Once during the geometry setup Verification of value is recommended daily, but not required
Bearing Friction Correction	Monthly Recommendation: Keep a log of this value
Rotational Mapping	Once daily (if same geometry) Every time the geometry is changed
Zero Gap	Every time geometry is removed or replaced

A.7.2.3 Instrument Inertia

Determine the instrument inertia by selecting *Options>Instrument>Inertia* and press the ‘*Calibrate*’ button. The value for the instrument should not change by more than 15% of the original Inertia value. If you notice a continual drift of this value, check the quality of the air used, as it could be indicative of a poor quality supply. If the problem persists, contact the instrument service department.

A.7.2.4 Geometry Inertia

The value of the inertia for each measuring system differs because they all have been uniquely engineered and have different masses. It is important to calibrate the inertia value for every geometry, particularly if high frequency oscillations are being used, or if low viscosity fluids are being measured.

Calibrate the geometry inertia by pressing the ‘*Calibrate*’ button that is found in the Geometry Page *>Settings>Inertia: Calibrate*.

A.7.2.5 Bearing Friction Correction

An air bearing is used to set the drive shaft afloat and provide virtually friction free application of torque to the sample. However, there will always be some residual friction. With most test materials, this is insignificant, but in about 1% of low viscosity samples, this inherent friction causes inaccuracies in the final rheological data. To overcome this, the software has an air bearing friction correction that should be activated.

NOTE: Ensure that the Instrument and Geometry inertia has been calibrated before determining the ‘bearing friction correction’ value.

go to *Options>Instrument>Miscellaneous*, check the ‘*bearing friction correction*’ box and press the ‘*Calibrate*’ button.

This value is unique for each air bearing assembly and rheometer model. An acceptable range for this value is $\sim 0.5-1.1 \mu\text{Nm}/(\text{rad/s})$. This value should be within $\sim 20\%$ of the original BFC value.

A.7.2.6 Rotational Mapping

Due to the micron-level tolerances needed to make an air bearing work, any bearing will have small variations in torque behavior around one complete revolution of the shaft. They are consistent over time unless changes occur in the air bearing.

By combining the absolute angular position data from the optical encoder with microprocessor control of the motor, these small variations can be mapped automatically and stored in memory for subsequent real-time corrections in the test. To create a map, the software rotates the drive shaft at a fixed speed, monitoring the torque required to maintain this speed through a full 360° of rotation. This results in a very wide operating range of the bearing without operator intervention - a confidence check in bearing performance.

Perform a rotational mapping on the geometry when the test procedure will be applying either a flow or transient (Creep or Stress Relaxation) mode of deformation. Begin the rotational mapping by pressing the icon or go to *Instrument > Rotational Mapping*. Select either the number of iterations or mapping type within the icon dialog window.

The number of points in the map and the speed of rotation used are dependent upon the mapping type used. When mapping the geometry, the recommended settings are 'one' iteration and 'standard' type.

A.7.2.7 Zero the Geometry Gap

Choose the zero gap icon , or select *Instrument>Gap>Zero Gap* and follow the directions on screen.

NOTE: The upper geometry should be at the testing temperature before zeroing the gap. This will account for the change in dimensions due to the coefficient of thermal expansion of the testing geometry/system.

A.7.3 Software

In the AR Instrument control software there are four tabs across the top, AR-1500EX (instrument page), 60mm Al Plate (geometry page), Flow Procedure, and Last Data Collected.

The AR-1500EX instrument page is used to adjust the instrument settings, including the set temperature and the gap distance. There are four columns labeled parameters, actual value, required value and units. To change the settings for one of the parameters double click on the value in the required value column, enter the desired value into the pop-up window and click ok. The instrument will adjust the value to new set value and the actual value will change.

The 60mm Al Plate geometry page must be set-up when the geometry is first used. Otherwise, the only time the geometry page is needed is during calibration when the geometry inertia is calibrated.

The Flow Procedure page is the most important page because it is where the data collection method is determined. The Flow Procedure page contains three sections: Conditioning Step, Stepped Flow Step, and Post Experiment Step. Under the Conditioning Step section there are three tabs: Settings, Advanced, and General. For

most studies the Settings tab is the only one that needs to be used. The temperature needs to be set and for pyrolysis oil a 2 minute (0:02:00) equilibration is used.

For the Stepped Flow Step there are four tabs: Test, Step Termination, Advanced, and General. Most of the conditions are determined in the Test tab. The first option is a drop down menu of all of the possible functions that can be used. For pyrolysis oil, the stepped flow function is best but the peak hold function can be used as well. The stepped flow function varies shear rate and measures the viscosity over a specified shear rate interval. The peak hold function holds the shear rate constant and measures the viscosity over a specified time. The following settings are the standard parameters used for pyrolysis oil samples.

Stepped Flow

Ramp: Shear Rate

From: 10 to 1000

Mode: Log

Points per decade: 10

Temperature: 40 °C

Constant time: 0:00:30

Average last x seconds: 0:00:15

Under the Step Termination tab, conditions can be set to stop the data collection. For pyrolysis oil, it is a good idea to set the maximum torque to 1500 $\mu\text{N}\cdot\text{m}$, which is the maximum torque of the machine. This will ensure that when the instrument reaches the maximum torque the data collection will stop and the instrument will not be damaged. The Advanced and General tabs under the Stepped Flow Step are not typically used.

The last tab, which shows the last data set, will automatically open when the data collection starts, and allows for the measurements to be observed in real time.

A.7.4 Pyrolysis Oil Sample Application

Ideally a 2 mL disposable glass pipette would be used to dispense the pyrolysis oil onto the Peltier plate in order to attempt to keep the sample volume and ultimately the gap distance constant. Due to the nature of pyrolysis oil this is not always possible especially for highly viscous (aged) samples that do not easily pipette. In some cases the end of a glass pipette can be carefully scored and broken to create a larger opening to pipette viscous pyrolysis oil. If the pyrolysis oil is not able to be pipetted, then it can be poured directly onto the Peltier plate. This should be the last option due to the volume added being an unknown, which will cause the gap distance to vary greatly.

To prevent particles in the pyrolysis oil from interfering with the viscosity measurements, the sample volume should be maximized in order to maximize the gap distance. (essentially, you want to ensure the gap distance is greater than the particle diameters.) In order to maximize gap distance in 'typical' pyrolysis oil samples, a minimum of 3 full pipettes (~ 6 mL) should be dispensed onto the Peltier plate.

Pipette the pyrolysis oil samples onto the center of the Peltier plate. If the sample is off center then it becomes more difficult for the sample to uniformly cover the entire gap between the two plates. The more viscous the sample, the easier it is to apply a larger volume; for pyrolysis oil, 3-4 full pipettes (~ 6-8 mL) can easily be applied. For low viscosity fluids, a large volume will most likely flow off of the Peltier plate. For low viscosity liquids, 2 pipette volumes can be added to the Peltier plate and while bringing the top 60mm plate down to narrow the gap distance add the third pipette. Once the top

plate makes contact with the sample, surface tension will help to keep the sample from flowing off of the plate. If the sample has flowed off the plate, then bring the plate into contact with the sample and then raise the upper plate to a higher gap distance. This will pull the sample under the plate. Then the area around the edge of the plate can be cleaned and then the gap distance can be adjusted so the sample fills the entire gap between the two plates.

The area around the two plates should always be cleaned before data collection begins. The sample cannot be on the top 60 mm plate. Also, make sure that there are no voids (that the gap is completely filled) all around the edge of the sample.

A.7.5 Data Collection

There is a green arrow or 'play' button at the top left of the software screen. When the sample and flow procedure are set up this can be pressed to start the data collection. A pop-up screen will appear asking for the Sample Name, File Name, and where the file will be saved. In addition, the density of the sample material can be entered. If the density is unknown, then set the density is equal to 1 g/cm³. There is also a section where experimental notes can be entered.

While the instrument is collecting data, make sure not to bump the instrument or the countertop where it is located. The instrument is very sensitive to vibrations and if the counter or instrument is bumped during data collection it could result in oscillations or noise in the data.

A.7.6 Saving Data and Data Analysis

In order to analyze the data in other programs (such as Microsoft Excel), the data must be exported into a text file. Open the Data Analysis software and then open the

desired file. The data will not automatically show on the screen. To view the tabulated data click the table icon button along the top and to view a graph click on the graph icons along the top. To export the data as a text file, open the file in the data analysis software and then go to file, export as text.

A.7.7 Cleaning

After each sample is run, the parallel plate and Peltier plate must be cleaned thoroughly to ensure there is no contamination between samples.

A.7.8 Instrument Shutdown

After the last sample has been cleaned the instrument can be shut down by following the procedure below.

1. Remove the geometry by holding the geometry in place (locking the bearing helps with this) and then unscrewing it at the top of the instrument.
2. Close the control software, AR Instrument Control.
3. Unplug the power cord to the pump.
4. Turn off the rheometer using the switch on the back left of the instrument.
5. Turn on/off the compressor by pressing the green button on the front.
6. Close the valve connecting the compressor to the rheometer. (It will make a hissing noise.)
7. Turn off the computer.

Make sure that the area (instrument, countertop, and floor) has been cleaned.

There should be no pyrolysis oil on any surface. The geometry must be put away in the cabinet.

A.7.9 Troubleshooting

A.7.9.1 Oscillations in the Data

If the data for either a stepped flow or peak hold experiment have oscillations or variation, it may be due to bubbles or voids in the sample. If voids are observed during or at the end of the data collection, it should be noted and the sample should be run again.

A.7.9.2 Decrease in Viscosity When Shear Rate is Increased

If the viscosity of a sample decreases as the shear rate increases or decreases, then the fluid is exhibiting a non-Newtonian behavior. With non-Newtonian behavior, the viscosity cannot be determined using rheology. There are several changes to the experimental procedure that may change the viscosity behavior of pyrolysis oil (so that it behaves as a Newtonian fluid).

1. Elevate the temperature to 50 °C. By increasing the temperature, pyrolysis oil tends to act more Newtonian for all shear rates.
2. Increase the gap, which also increases the sample volume. If the gap distance is too small, then particles in the pyrolysis oil may be interfering with the measurement and causing the pyrolysis oil to appear to be non-Newtonian.

A.8 PolySEL Pyrolysis Oil GPC

A.8.1 Sample Preparation

1. Dissolve the Sample: The mobile phase in the PolySEL pyrolysis oil GPC system is Optima THF. Therefore, samples prepared in Optima THF by and allowed to stand for a minimum of 4 hours (preferable 24 hours to make sure the sample is completely in solution). Sample concentration is 2-3 mg of pyrolysis oil per 1 mL.

- a) Label a 4 mL vial for a given sample and tare the weight on the scale. Make sure the sample is at room temperature.
 - b) For one phase samples mix the sample well by shaking. For highly viscous samples use a stainless steel spatula to stir the sample. Use a glass puppet or stainless steel spatula to measure out 8-12 mg of sample in the vial and record the weight.
 - c) For two phase samples prepare two vials, pipet the top phase for the first sample and use a stainless steel spatula for the bottom phase.
 - d) Pour Optima THF into a clean beaker and have an empty beaker for waste.
 - e) Rinse a glass syringe (with a stainless steel needle) three times with THF to ensure that there are no contaminants (depositing the THF into the waste beaker).
 - f) Add 4 mL of THF to each vial using the cleaned syringe.
 - g) Parafilm around the cap of the vial. Parafilm also needs to be wrapped around the label to prevent bleeding and removal during sonication. Store the sample for 4-24 hours.
 - h) After 4-24 hours sonicate the samples for a minimum of 15-30 minutes (or until the pyrolysis oil is completely dissolved in the THF). Bottom phase samples or samples aged for long periods of time require more sonication.
2. Filtration: Use a 0.45 μm or 0.20 μm syringe filter to filter the sample into a 1mL GPC snap vial. (Note: a new syringe filter should be used for each sample to avoid contamination. The syringe filters are expensive so only filter sample you intend on running.)

- a) Pour Optima THF into a clean beaker and have an empty beaker for waste.
 - b) Rinse a glass syringe (with a stainless steel needle) three times with THF to ensure it is clean.
 - c) Use the glass syringe to extract 1 mL of pyrolysis oil dissolved in THF
 - d) Remove the needle from syringe holding the plunger in place to prevent loss of liquid and replace the needle with a syringe filter.
 - e) Push the sample through the filter into a new 1 mL GPC sample vial.
 - f) Make sure there are no particulates in the filtered solution and snap the top into place. Make sure to label the 1 mL vial with the sample name, size of syringe filter and the date.
3. Between samples rinse the syringe three times with clean THF, each time putting the washing into a waste beaker. Replace the needle after each sample.
 4. After the sample is prepared use a 250 μ L syringe and add 1-2 small drops of concentrated (50 mg/mL) PS 1 polystyrene standard (177,000 Da) to each sample. The internal standard is used to account for the shifting retention times and pressure differences in the pyrolysis oil GPC system.

A.8.2 GPC Instrumentation

The PolySEL pyrolysis oil GPC system is a custom-built instrument comprised of a Varian Star 9040 refractive index detector, Waters 610 Fluid Unit, Waters 600 Controller, Varian guard column, and Varian Mesopore 250 x 4.6 mm ID column. Data analyses are performed using Star WS software and Waters Breeze software. The GPC

instrument should always be running in recycle mode at 0.1 mL/min to prevent the columns from drying out.

A.8.3 Data Collection

1. The GPC system should be ramped up to 0.4 mL/min by stepping up the flow 0.01 ml/min at a time. Press the up arrow button to select the flow rate and then enter in the desired number using the number keys followed by the enter button.
2. Move the exit tube from the detector from the recycle position in the Erlenmeyer flask reservoir to the waste Erlenmeyer flask.
3. Purge the system for a minimum of 15 minutes at 0.4 mL/min by selecting the purge button on the detector. Stop the purge by selecting the purge button a second time (make sure the green light turns off).
4. Ramp the flow rate down from 0.4 mL/min to 0.3 mL/min by using the up arrow button and entering in the desired number and selecting enter.
5. Allow the system to equilibrate for a minimum of 15-30 minutes. Select “resume plot” in the Star software located on the left immediately above the plot. This will show real-time data collection. The system is at equilibrium when the plot line is flat without an incline or bumps.
6. Using a 250 μ L syringe and inject 50 μ L of Optima THF into the injector in the load position.
7. Press the start button in the Star software, located on the top left of the screen. Wait for the previous trace to clear and then move the injector from load to inject. The software will collect data for the set amount of time

(typically 14-15 minutes). During data collection the Star software will read “data acquisition” in green to the right of the start button.

8. When the software has completed there will no longer be “data acquisition” and the full trace will be presented. The THF “blank” trace should be flat with the exception of a negative peak at ~ 12 minutes indicating the end of the sample injection.
9. Move the injector back to the load position and remove the syringe.
10. Rinse the syringe with clean THF three times, each time putting the THF into a waste beaker.
11. Repeat steps 6-10 for desired samples.

A.8.4 Exporting Data in Star/Importing Data in Breeze

The data collected from the pyrolysis oil GPC instrument is collected as a Varian data file and requires conversion to the .AIA format in the Star program.

1. Select the Star software toolbar at the top of the screen.
2. Select Varian to AIA
3. Select the file that requires converting (can only select one at a time) and press OK
4. Enter where to save the file and press OK
5. Repeat steps 2-4 or to convert more files or press Exit

Before importing the data into the Waters Breeze software for analysis first view the data files, and remove the period from each default name by renaming it. The Breeze software does not recognize the data files with a period in the name.

Example: 16005.AIA change to: 16005AIA

Once the data files are renamed save the files on the Waters GPC computer in the folder my documents/cdn within a folder named for the data collection date.

1. Open the Breeze software (if not open already).
2. Go to *File, Change User/Project* and select the project “*Bio-oil*”, select *OK* and allow for the software to change to the project file.
3. On the left tool bar select *find data* (a circular button).
4. Along the sub-toolbar select the channels tab, which will display the pyrolysis oil database.
5. To import new data select *Database* in the main toolbar at the top of the screen and then *import data*.
6. Select the desired data files by browsing in my documents and click *OK*
7. A new window will open displaying the selected files and the file names do not import with the files. Use the drop down menu for each sample to delineate the type of file it is. For standards- *narrow standard* and for samples- *broad unknown*, save the changes using the save icon or by going to file and save then click *OK*.
8. The newly imported data will not appear until the *update* button along the top of the screen is clicked.
9. Once the new data is present under the channels tab each sample needs to be renamed. To identify each sample the date and time stamp is displayed for each sample and using the order the samples were collected each can be named from recorded notes. Select a given file, right click and select *alter sample*. A new window will open where the same name can be

entered. Enter the sample name, press *enter* and then click the save icon.

Close the window and do the same for all of the new samples.

A.8.5 GPC Calibration

Nine polystyrene standards are used to calibrate the Pyrolysis oil GPC system periodically (every 1-2 weeks). The polystyrene information is presented in Table A.4. The standards are prepared using the sample preparation procedure described in A.8.1 including the addition of the PS1 internal standard. The internal standard is prepared using the same procedure but the concentration is increased to 50 mg/mL. The standard samples are run by the same procedure as described in Data Collection and should not be run in sequential order but rather in random.

Table A.4 Polystyrene standard data including weight average, number average and point average molecular weights and polydispersiy (PDI).

Standard Name	Mw (D)	Mn (D)	Mp (D)	PDI
PS 4	18200	17900	18200	1.02
PS 5	10261	9590	9890	1.07
PS 6	6480	6240	6520	1.04
PS 7	2780	2620	2770	1.06
PS 8	891	807	890	1.10
PS 9	582	498	474	1.11
PS 10	486	392	370	1.24
PS266	226			
PS126	126			

After the standard data has been collected:

1. Export and import the data using the Export/Import procedure described above (A.8.4).
2. When rename the data files in the new window enter the standard name and make sure “narrow standard” is selected.

3. In the new window go to *Edit* in the tool bar at the top and select *Components*, which will bring up a third window. In the components editor window Click on *Current Sample* tab at the bottom of components editor window
4. Select the *Moments* tab
5. Enter the Mw, into the correct cells (Table A.4).
6. After the information is entered, click *OK*.
7. Click save in the alter sample window and *OK*. In order for the changes to be updated the *update* button must be selected.
8. Repeat Steps 3-8 for all of the standards.
9. Select the standard files and right click on the selected files and select *Review*. The window will change from the viewing the channels to the review window.
10. Before integrating the main standard peak the internal standard PS1 peak position must be recorded (the smaller peak at the left).
11. For the small internal standard peak, use the cursor and left click on the left side of the peak, drag under the peak and connect to the right of the peak. A red line will appear under the peak and the peak position will be labeled at the apex. The red baseline should be straight and follow the same trend as the overall baseline. The slope of the line can be altered by moving the ends of the line.
12. Record the PS1 peak position for each PS standard.
13. After the PS1 peak position is recorded the integration can be cleared by going to *Edit* (in the main toolbar at the top) and selecting *clear integration*.
NOTE: in the same dropdown menu it also has *clear calibration*. BE VERY

CAREFUL not to select clear calibration because it cannot be recovered and have to be redone.

14. To integrate the standard main peak using the same method described in step 12 for the larger peak to the right. Record the position of the peak.
15. Click the 7th button from the left on the upper tool bar (calibrate button).
16. Repeat the integration [steps 15 and 16] for all nine of the standards.
17. To save the calibration, go to *file, save* and select *Calibration* or *All*.
18. Open the calibration by going to *window* in the main toolbar and selecting *calibration*. It can also be accessed by pressing
19. Check to make sure that the calibration looks reasonable (the points are all on the calibration line). The previous calibration will still be present and will be entered as manual points.
20. The previous calibration can be deleted or select the ignore check box to not include the calibration. If the part or all of the previous calibration curve will be used then it must be shifted to the new PS1 peak position.
21. To account for the shifting retention times due to pressure each standard position will be manually shifted to one PS1 position. Shift all PS1 peaks to the PS1 peak of PS10 and record the shift value. Then calculate the new peak positions of each standard.
22. To manually shift the new calibration points they must be entered manually. At the base of the calibration data click in the first blank row and duplicate one of the new calibration points by entering the position and molecular weight.
23. Repeat for each calibration point.

24. Once the data points are entered in manually edit the peak positions with the shifted positions and save the calibration.
25. The calibration is now ready for data analysis

A.8.6 Data Analysis

For each sample the calibration must be shifted to the position of the sample PS1 peak to account for any shift in the retention time.

1. Export and import the data using the Export/Import procedure described above.
2. Once imported, go to the Find Data button in the left column of the Breeze software. The data is imported without a file name but the date and time collected is preserved.
3. Rename the data files by right clicking on an individual file and selecting alter sample. A new window will open and using recorded notes enter the standard name and make sure “broad unknown” is selected.
4. After the information is entered, click “Ok”.
5. Click save in the alter sample window and OK. In order for the changes to be updated the update button must be selected.
6. Repeat Steps 3-5 for all of the samples.
7. Highlight the standard files and right click on the selected files and select Review.
8. Before integrating the sample peak the internal standard PS1 peak position must be recorded (the smaller peak at the left) for each sample.

9. Using the cursor, left click on the left side of the peak, drag under the peak and connect to the right of the peak. A red line will appear under the peak and the peak position will be labeled at the apex. The red baseline should be straight and following the same trend as the overall baseline. The slope of the line can be altered by moving the ends of the line.
10. Record the PS1 peak position for each sample.
11. After the PS1 peak position is recorded go to Edit and clear integration to remove the integration of the PS1 Peak.
12. To integrate the sample use the same method described in step 9.
13. Go to window, calibration.
14. Open the most recent calibration file in excel and calculate the shift required to bring the calibration PS1 position to the sample PS1 position.
15. Enter the shift into excel.
16. Use the peak positions calculated in excel to edit the calibration curve peak positions in Breeze. Once the calibration is shifted save the calibration by file, save and calibration.
17. Return to the sample analysis window by going to window and XX.
18. Click the Xth button [insert image] from the left on the upper tool bar (calibrate button) insert image [if cursor is hovered it will say XX].
19. Click the XX tab at the base of the XX window to view the sample data.
20. Right click in the window and select copy. The data can then be pasted into an excel file where the sample name needs to be entered.
21. Repeat the calibration shift and sample integration [steps 7-20] for all of the samples.

A.8.7 Routine Maintenance

Daily- Purge the system at 0.45 mL/ min for a minimum of 15 minutes in the morning, refill the THF reservoir at the end of the day

Weekly- Replace the frit insert with a cleaned/ sonicated replacement

Monthly- Run Polystyrene standards and recalibrate system

A.9 FTIR- Transmission, ATR and DRIFT

The transmission FTIR (T-FTIR) spectra were collected of pyrolysis oil smears on KBr crystals using a Nicolet 6700 spectrometer (DTGS detector, 4 cm^{-1} resolution, 128 scans). DRIFT spectra of the filtered pyrolysis oil solids were collected after preparation with 95% KBr powder (MCT-A* detector, 4 cm^{-1} resolution, 256 scans). ATR spectra were collected on ZnSe 60° single bounce ATR crystal (MCT-A* detector, 4 cm^{-1} resolution, 256 scans).

On a Thermo Electron corporation Nicolet 6700 FT-IR with a helium-neon laser, mercury-cadmium-telluride (MCT) detector or deuterated triglycine sulfate (DTGS) detector, with Pike VeeMax II for external reflectance or attenuated total reflectance spectroscopy, Pike EasyDiff for diffused reflectance infrared Fourier transform spectroscopy, or Thermo Electron universal sample holder for transmission spectroscopy using Omnic 8.1.10 software (copyright 1992-2009, Thermo Fisher Scientific Inc.).

A.9.1 FTIR Maintenance

A.9.1.1 Clearing air line

1. Check the sink for glassware and provide ear plugs for everyone in the lab
(loud process)

2. On the wall behind the Waters GPC, close the yellow handled valve on the compressed airline.
3. Open the red handled valve at the base of the airline (this will begin the purge).
4. Loosen the screws at the base of the two filters to the right of the yellow handled valve. Air will exit from the base of the filter release pressure.
5. Compressed air, with any moisture accumulation in the drip leg will exit into the sink.
6. Watch the air flow into the sink and wait for the air to be clear of moisture (when moisture is present it will appear hazy)
7. Once there is no longer moisture in the airline close everything in reverse starting with the filters followed by the red handled valve.
8. Open on the yellow handled valve and check to make sure that 30 psi is being provided to the FTIR instrument. Adjust the flow meter to adjust the flow if required.

A.9.1.2 Instrument Alignment

FTIR instrument should be aligned every 2-3 weeks. Prior to alignment clear the air line (A.9.2.1), put the transmission accessory in place and allow for 10-20 minutes for the chamber to purge with dry air. Also add liquid nitrogen to cool the MCT detector (A.9.3.1).

1. Close the Omnic software
2. Open the Bench Diagnostics program by going to the start menu, Thermo Scientific Omnic and Bench Diagnostics.

3. Test the power, laser, source, electronics and detector by clicking on the square buttons across the top of the window. For each button the program will go to a new screen and display green check marks when the test has passed. Return to the main window.
4. Select the *Performance Test* button. At the top of the new screen two buttons indicate the two detectors (Top: DTGS, Bottom: MCT).
5. Select the top button for the DTGS detector. In the new screen select run test. Omnic will open and with a window prompt. Select the *transmission* accessory. Make sure to not have a sample or standard in the transmission accessory.
6. Omnic will automatically run the test and once done will report either a pass or fail in the *Bench Diagnostics* window. When finished click the return button to return to *Performance Test* screen and Omnic will close automatically.
7. Repeat steps 5 and 6 for the MCT detector.
8. Once the Performance tests have been conducted for both detectors select *Advanced Tests*. Select *Signal to Noise test* in the new screen. Omnic will open and automatically run the test. The results of the test (pass or fail) will be displayed in the Bench Diagnostics screen. After the signal to noise test Bench Diagnostics can be closed.
9. Open Omnic and collect a spectrum for one of the standard cards (PTFE or PE) following the procedure for transmission data collection (A.9.2.2).
10. Compare the collected spectra to the library spectra under *Analyze, Library Manager* and search for PTFE or PE in the libraries.

A.9.1.3 KBr Crystal Cleaning Procedure

It should not be assumed the transmission crystals are thoroughly cleaned at any time. Always clean the crystals prior to use. Following the procedure is imperative; if the crystals are not cleaned properly residual sample can appear in later samples.

1. Wipe both sides of the crystal with a methanol soaked cotton ball
2. Over a beaker spray both sides of the crystal with methanol. Spray both sides completely twice.
3. Dry the crystal with the nitrogen gun (Do not drop the crystal, it will break!
Hold your hand under the crystal to prevent it from falling)
4. The crystal is ready to be used.
5. This procedure should be carried out before each sample and between samples in addition to at the end of use

A.9.2 FTIR: Transmission

A.9.2.1 Pyrolysis Oil Sample Preparation

The sample preparation will depend on the properties of the pyrolysis oil, but either way the water must be removed from the sample before the spectrum is collected in transmission mode. Otherwise water peaks will obstruct the majority of the spectrum.

1. Before the pyrolysis oil can be applied make sure it has been allowed to warm to room temperature and mixed thoroughly
2. Using a cleaned KBr crystal apply a small amount of pyrolysis oil using a disposable glass pipette (follow the cleaning procedure to clean the crystal)
3. If the pyrolysis oil is a liquid it can be applied by a drop or two. If the pyrolysis oil is viscous put the pipette into the pyrolysis oil, mix it and then

apply a small amount by smearing it on the crystal. Always try and apply the pyrolysis oil in the center of the crystal.

4. If there is a large amount of pyrolysis oil it may be helpful to remove some with a second pipette
5. Place the crystal in a labeled petri dish and put in vacuum for a minimum of 15 min
6. Take the crystals out of the oven and carefully using a spatula smear the sample on the crystal, removing most of sample to create a semi-clear thin layer of pyrolysis oil on the crystal
7. Replace the crystal in the vacuum oven for an additional 15-30 minutes. The sample and crystal should be in the oven until the pyrolysis oil no longer flows when the crystal is vertical.

A.9.2.2 Data Collection

1. Prior to any FTIR data collection always clear the airline according to the procedure
2. Open the Omnic Software and select collect along the top menu and experimental setup.
3. Select open at the bottom of the experimental setup window
4. Select the transmission file where all of the settings are saved
5. On the tab of the experimental setup window
6. If the transmission accessory has been in place for an extended period of time then open and close the sliding window at the top and then allow a few minutes to pass (~2-6 min). Otherwise put the transmission accessory into

place, close the chamber and allow for a minimum of 20 minutes for evacuation.

7. Collect the background by opening the experimental setup and selecting collect background before every sample, save and close the experimental setup window.
8. Select collect and collect background. Open the collected background to the open window when prompted. Save the background.
9. Open the experimental setup window and select the “Use specific background file:” option, browse and open the background just collected and save.
10. Once the background is saved, place the sample into position by opening the sliding window, orienting the sample holder facing right and slide the holder into the groves. Make sure to push the holder all the way down, making it flush with the transmission accessory. Close the sliding window and wait 3-4 minutes.
11. After 3-4 minutes select collect and collect sample. Enter the sample name when prompted. Observe the spectrum during data collection and stop the collection when the water peaks are no longer present and the CO₂ peak is a minimum.
12. When prompted select “Add to Window” if the spectrum is satisfactory or “More Scans” if the water peaks are still present.
13. Once the spectrum is collected and saved the sample can be removed from the chamber and a new sample put in place.
14. The crystal with the sample should then be cleaned according to the cleaning procedure.

A.9.3 Attenuate Total Reflectance (ATR)

A.9.3.1 ATR: Filling the Liquid Nitrogen MCT Detector Dewar

1. Liquid nitrogen is used to cool the MCT detector and the filling port is located on the left side of the instrument and the circular lid closest to the front.
2. Open the lid, remove the black plug and place the funnel (metal stem only for liquid nitrogen) into where the black plug was removed.
3. Pour liquid nitrogen into the funnel, filling it once and then allow the instrument to cool several minutes (2-5).
4. Gently pour liquid nitrogen into the funnel until it over flows, indicated by bubbling at the base of the funnel and crackling.
5. Once nitrogen does not visible exit the hole, remove the funnel and carefully replace the black plug.
6. Do not close the lid forcibly to prevent damage but rather gently close the lid allowing it to rest on top of the rubber gasket.
7. Once rubber gasket is up to room temperature, press lid into place.

A.9.3.2 ATR: Start-up

1. Make sure that the air line has been purged prior to using the instrument.
2. Cool the MCT detector by filling the reservoir with liquid nitrogen (see previous procedure)
3. With the ATR accessory in place insert the B screen to the left of the accessory to reduce the signal to a useable level [single should be below a max of 8]

4. If the ATR accessory is not in place open the main chamber, carefully remove the transmission or DRIFT accessory and replace it with the ATR accessory, connecting the air line to the back of the chamber. Make sure to slide the two earpieces into the entrance and exit positions to seal the accessory. [NOTE: undergrads should ask a graduate student for help with this task].
5. Allow for a minimum of 20 minutes to purge the accessory.
6. Carefully place the ZnSe ATR crystal into place and check to make sure the angle is set to 60 °C. Wait a minimum of 6 minutes before using the apparatus allowing for the evacuation of the ATR accessory.

A.9.3.3 Collecting Data

1. Open the OMNIC software
2. In the toolbar go to Collect and experimental set-up or use the experimental set-up button. A new window will open.
3. Select Open at the bottom of the Experimental Set-up window. Go to My Documents/CDN/FTIR and select the MCT autogain file [parameters].
4. Under the collect tab under, under the background handling section click on either collect background before every sample.
5. Proceed to the bench tab in the window and check to make sure that the MCT detector is selected, the source is IR and that a signal is visible in the left part of the window.
6. Before closing the experimental set-up window select Save at the bottom.
7. Collect a background by going to collect, collect background, selecting the button along the top or by hitting Ctrl + B.

8. Add the background to a new or existing window.
9. Save the background by going to file, save and selecting the folder created with the date of collection. A new background should be collected every 30 min or when required.
10. Open the experimental setup window and select “Use specific background file:” and open the recently collected background. Click Save and then Ok.
11. Dispense a drop of pyrolysis oil onto the small red spec on the ZnSe crystal.
12. Collect a sample by going to collect, collect sample, selecting the collect sample button or Ctrl+S
13. You will be prompted to name the same.
14. Once collected add the sample to a new or existing window. Check the carbonyl region ($1800-1600\text{ cm}^{-1}$) for noise or interference. This is indicated by bumps or dips in the spectrum rather than a smooth curve. If the spectrum is smooth then the crystal can be cleaned using cotton balls and methanol and the next sample spectrum can be collected.
15. When noise is visible in a sample, collect the sample again and collect the background immediately after.
16. Go to experimental set-up and in the collect tab select “collect background after every sample”
17. Close the experimental set-up and collect the sample
18. After the 128 scans have been collected a pop-up window will to collect the background
19. Clean the crystal, make sure it is dry and then select ok

20. The sample will then be adjusted using the new background and added to the window
21. A new background then needs to be collected: experimental set-up and in the collect tab select “collect background before every sample”
22. Once the background is collected, add it to the window and then save it (file, save).
23. Open the experimental set-up window and browse for the recently collected background under “Use specific background file:”.
24. Additional samples can then be collected using the new background (starting at Step 11)

A.9.4 Diffused Reflectance Infrared Fourier Transform (DRIFT) Spectroscopy:

Samples prepared for DRIFTS by creating a 5% sample, 95% KBr powder mixture. DRIFT Sample Prep

1. First 0.005 g of sample weighed out, then 0.095 g of KBr weighed out and both crushed and mixed together before being placed in tube for storage
2. First metal “cup” contains pure KBr which has to be crushed and placed inside the cup by means of a razorblade chopping up the pieces very small and making a smooth surface for the laser to bounce off of.
3. The second metal “cup” contains the prepared sample, put in the metal cup in similar fashion as the KBr in the first one
4. Both are placed in a holder and this is snapped onto a metal bar inside the FTIR

5. The holder is pulled back until stops and the FTIR hood is closed and 25 min must be waited before background can be taken
6. Once background taken, the top of the hood is opened and the holder is pushed forward until stopped and the top is closed and 3-8 min must be waited until sample can be taken
7. Once finished the KBr background stays put, the sample is placed back into its proper tubing, and another sample is prepared

APPENDIX B

PRELIMINARY INVESTIGATION OF COTTONWOOD PYROLYSIS OIL

B.1 Methods and Materials

Pyrolysis: Cottonwood clear wood (lumber) biomass was ground and screened to particle sizes between 20 mesh and 4 mm and dried to 10% MC. MSU Forest Products Laboratory auger pyrolysis reactor produced the oil operating at 450 °C under vacuum 01/12/09 from cottonwood clear wood biomass. All condenser products were collected and the pyrolysis oil was stored at 5 °C. The oil yield was 49 % with 21 % char. Phase separation was observed in the pyrolysis oil with an aqueous top phase and a thick “sludge” bottom phase.

Aging Conditions: Cottonwood clear wood total [CCWT] oil was prepared as 27 mL samples in 30 mL jars to minimize the headspace and reaction with oxygen [Oasmaa VVT 450 2001]. Controls were stored at 5 °C and aged samples were heated in a Thermo electron conduction oven at 80 °C for up to 7 days. The initial and final weights were recorded to account for volatile loss.

Physical Properties: Water content measurements were collected by Karl Fischer titration and pH was measured using the Mettler Toledo SevenEasy pH meter S20 calibrated with three phosphate buffer solutions.

Viscosity: Viscosity measurements were collected using size 4 and 10 viscosity tubes (name of type of tube) which required samples of ~1mL and ~6.5mL respectively. A sample was placed in the viscosity tube and then in a 40°C bath and allowed to warm up for 10 minutes in the size 4 tube and 20 minutes for the size 100 tube. Kinematic viscosities were determined by multiplying the time in seconds by the calibration constant for the viscometer tubes.

Molecular Weight Determination (GPC): Gel permeation chromatography (GPC) samples were prepared 5-6 mg per 1 mL of tetrahydrofuran (THF) and filtered with a

0.45 µm syringe filter. Samples were analyzed on the MSU Forestry Products laboratory Waters 600E instrument with a refractive index detector. A five point calibration was conducted using polystyrene standards (162, 580, 1050, 1930, and 3070 Da). Column operated at 1 mL/min, 20µL sample injection and 28 minutes allotted for each sample.

FTIR Spectroscopy: Pyrolysis oil smears were prepared on KBR crystals to collect transmission Fourier transform infrared (T-FTIR) spectra using a Nicolet 6700 spectrometer (DTGS detector, 4 cm⁻¹ resolution, 128 scans). The smears were dried in a vacuum oven for up to 1 hour to remove water from the sample.

B.2 Results and Discussion

B.2.1 Elemental Analysis

The elemental analysis of the neat cottonwood clear wood total [CCWT] pyrolysis oil is presented in Table 1. The R% represented the remaining content other than carbon, hydrogen and nitrogen. It is assumed most is oxygen, therefore 67.3 wt% of the oil contains oxygen, followed by 25 wt % carbon, 7.5 wt % hydrogen and 0.2 wt % nitrogen.

Table B.1 Elemental composition of neat cottonwood clear wood total pyrolysis oil

C (wt%)	H (wt%)	N (wt%)	R (wt%)
25.0	7.5	0.2	67.3

B.2.2 pH and Acid Value

pH and acid value were measured for the neat and aged pyrolysis oil samples and are presented in Figure B.1. Both the acid value and pH increased after one day of aging at 80 °C but then decreased between 1 day and 7 days. Only single data points were

collected therefore variation in the samples including phase separation or poor mixing may affect the measurements greatly. Although no trend can be ascertained the data does demonstrate the low pH of the oil in addition to the high acid value (mg) which are behind the corrosive nature of pyrolysis oil.

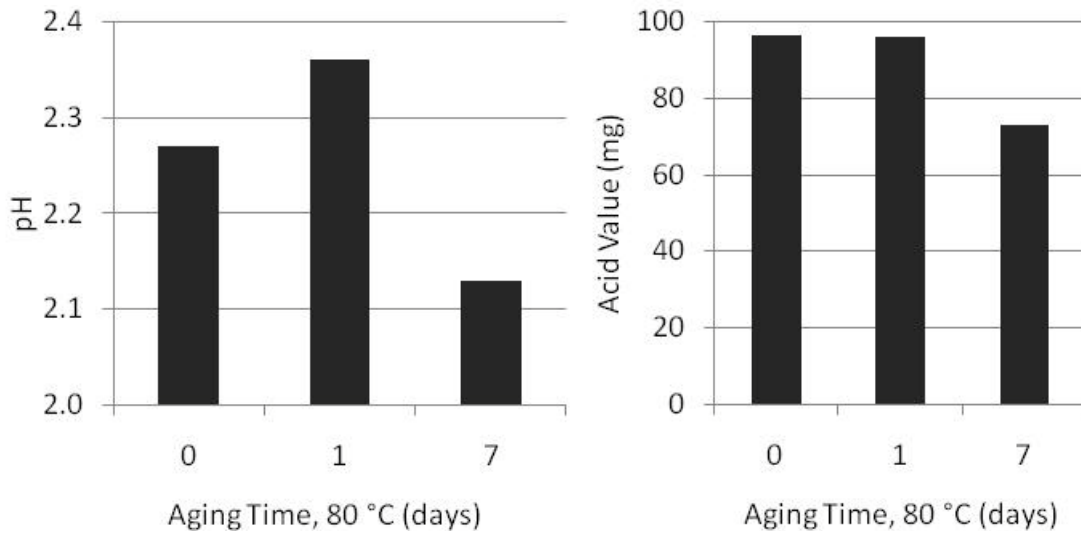


Figure B.1 pH and acid value for cottonwood clear wood pyrolysis oil neat and aged up to 7 days at 80 °C.

B.2.3 Water Content

Water content measurements are presented in Figures B.2 and B.3. Figure B.2 presents the comparison of water content measurements in two laboratories and the variability of the measurements. The measurements collected in Forestry Products are single data points where the PolySEL measurements are multiple points presented with 95 % confidence interval (CI) error bars. When comparing the two sets of data there is a significant difference in the values and also the trend. The forestry products data has a significant 66 % decrease in the water content after 7 days where the PolySEL data indicates a 23 % decrease after 7 days. Also when compared to day 1 and day 2 the

PolySEL data indicates a slight increase after 7 days. The variation in the data can be attributed to the phase separation in the samples, poor mixing and human error in Karl Fischer titration.

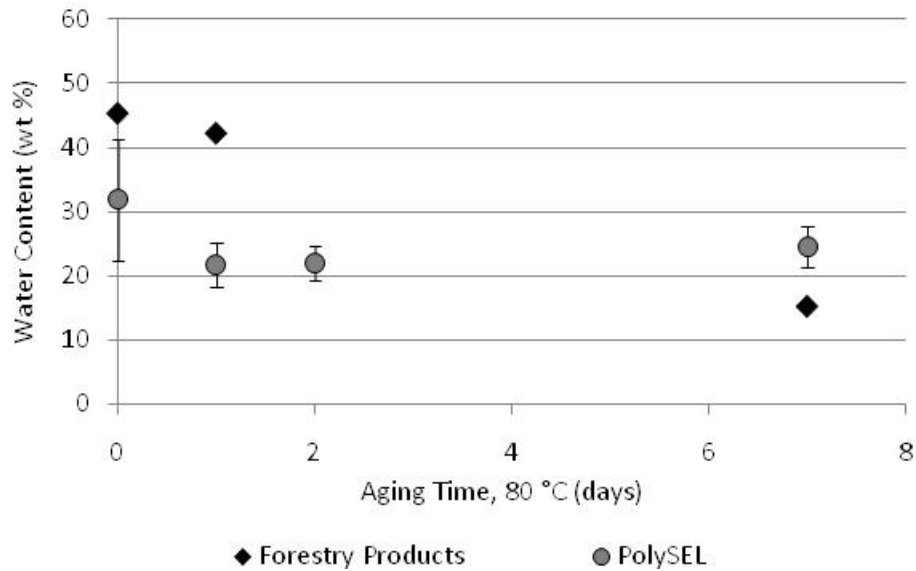


Figure B.2 Water Content for cottonwood clear wood pyrolysis oil neat and aged up to 7 days at 80 °C.

Figure B.3 presents the water content comparison of the top and bottom phases to the mixed pyrolysis oil (data collected by PolySEL). The Mixed and bottom phase have almost identical water contents which is unexpected when compared to the very different water content of the top phase. This indicates that the mixed pyrolysis oil may have been poorly mixed and the bottom phase dominated the samples. Figure 3 also demonstrates the significant difference in water content in the top phase.

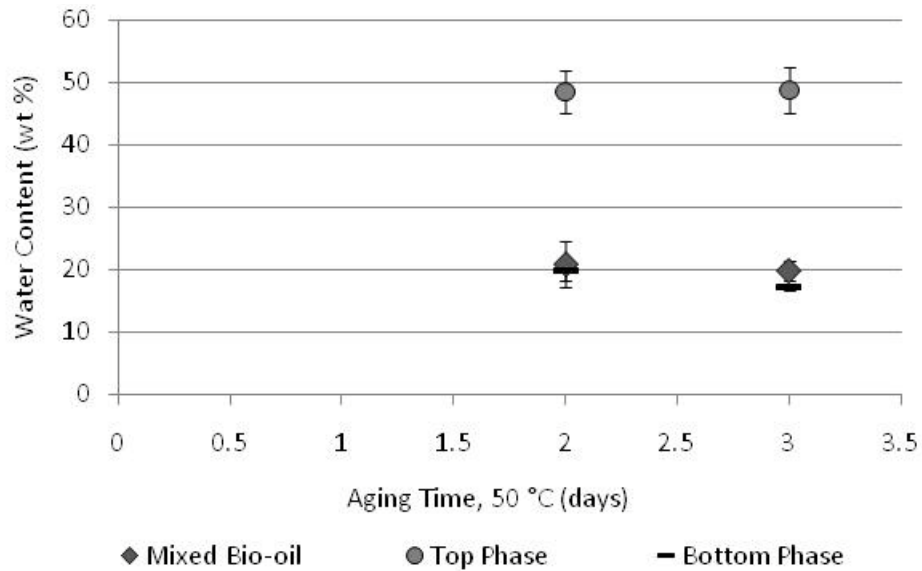


Figure B.3 Water Content for cottonwood clear wood pyrolysis oil neat and aged up to 7 days at 80 °C comparing the top and bottom phase with the mixed oil.

B.2.4 Viscosity

Figure 4 presented the viscosity measurements for the CCWT neat and aged oil at 80 C for 7 days. There is a potential decrease in viscosity over aging but without addition points the data is inconclusive. In addition the phase separation and char particles in the oil may have caused error in the measurements.

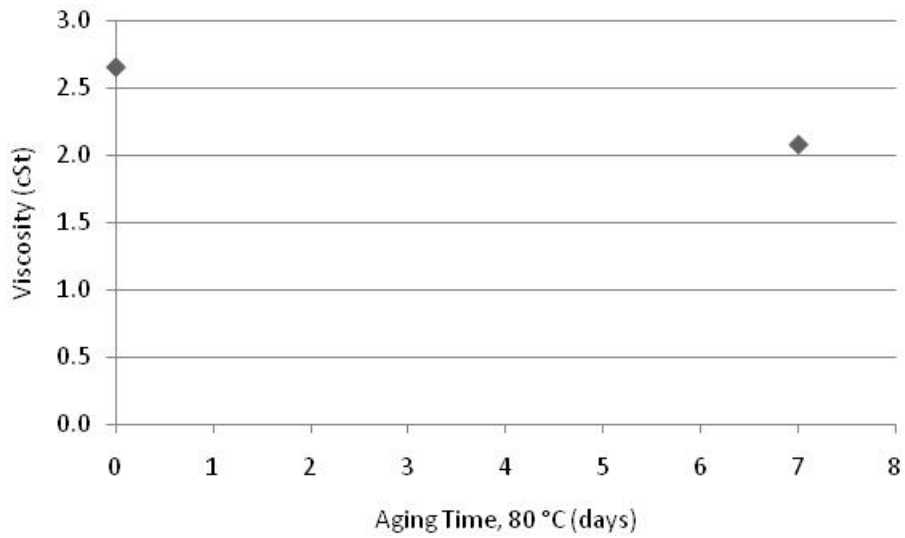


Figure B.4 Viscosity measurements for CCWT oil neat and aged for 7 days at 80 °C.

2.2.5 FTIR Spectroscopy

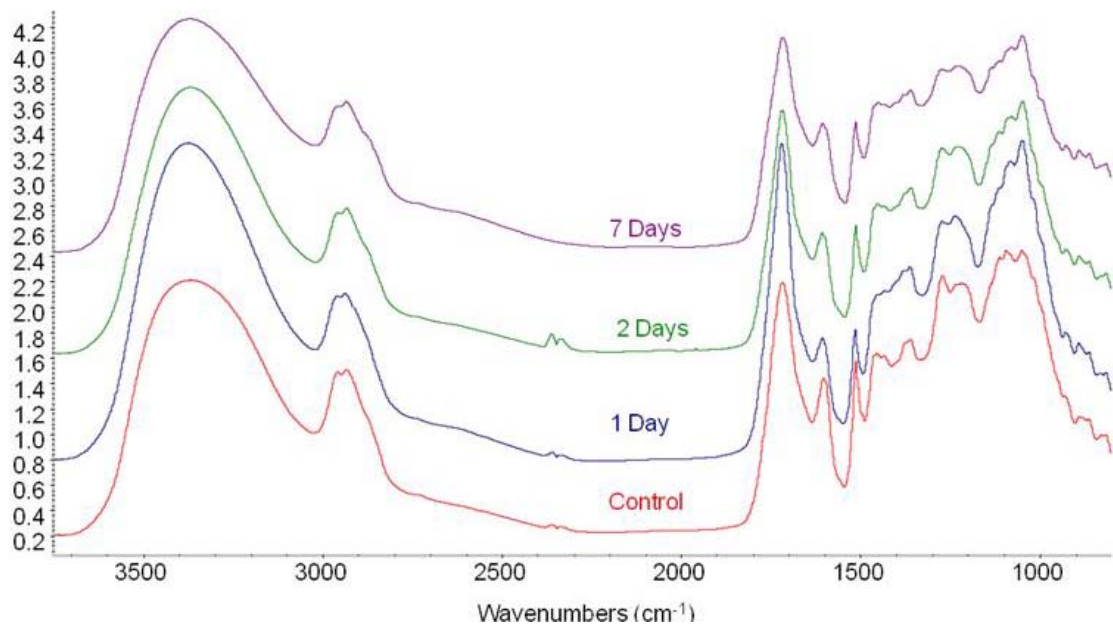


Figure B.5 Transmission FTIR spectra collected for CCWT oil neat and aged at 80 °C up to 7 days.

B.2.6 Gel Permeation Chromatography

CCWT pyrolysis oil weight averaged molecular weight [M_w] is presented as a function of aging time. GPC analysis displays an increase in the average molecular weight over the course of the 7-day aging. The M_w increase is due to the appearance of a higher MW component as evidenced by the development of a bi-modal distribution which can be observed in the GPC traces presented. An increase in molecular weight has been previously reported to coincide with viscosity and water content increase.

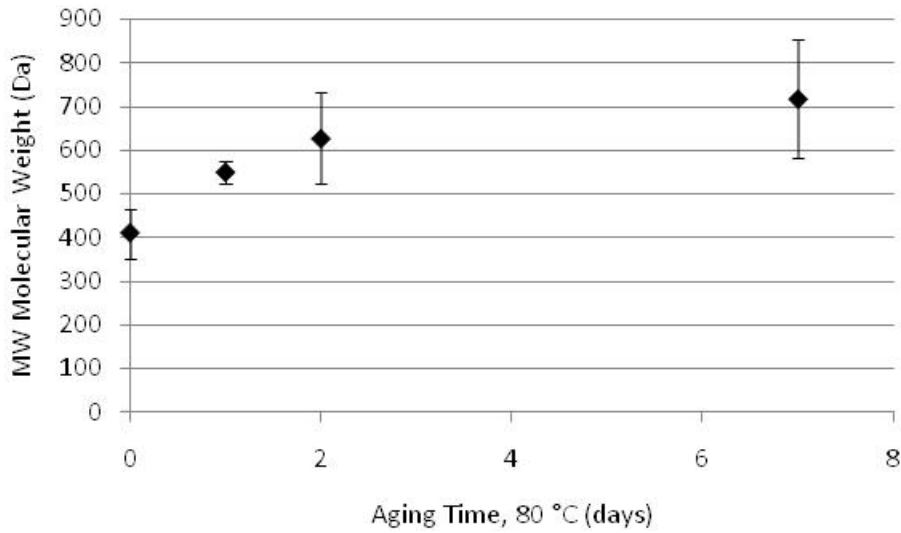


Figure B.6 Weight averaged molecular weight $\langle MW \rangle$ of cottonwood clear wood pyrolysis oil was found to increase during aging at 80 °C.

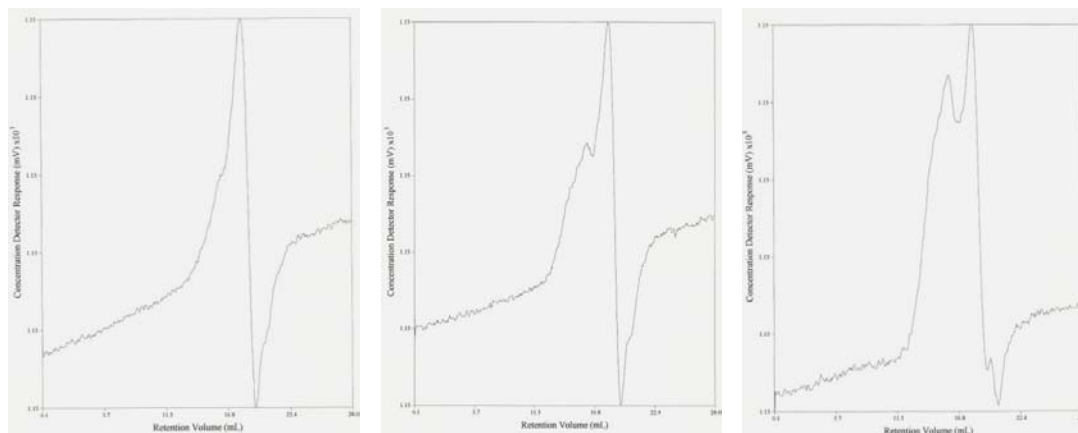


Figure B.7 GPC traces displaying the progression during aging and the formation of the bi-modal distribution

B.2.7 GC-MS

Qualitative and quantitative GC/MS analysis of the aged cottonwood clear wood pyrolysis oil samples was performed. The quantitative results were calculated based on a calibration curve of 32 target compounds and 6 internal standards and compared to a custom GC/MS library. The qualitative results were calculated using the 6 internal standards and compared to three GC/MS libraries.

In Table 1 the top five target compounds from the qualitative GC/MS data are displayed for the neat cottonwood clear wood pyrolysis oil sample and the cottonwood clear wood pyrolysis oil aged for 7 days at 80 °C. According to the GC/MS results, the concentration of 1,2- benzenediol increased from 16% to 23% of the sample as the pyrolysis oil was aged for 7 days at 80 °C. For these sample samples, the concentrations of levoglucosan and phenol decreased during aging. There are no trends in the GC/MS data that point to specific reactions or changes in the pyrolysis oil as it ages.

Due to the nature of the qualitative analysis, only the concentrations of the 32 target compounds can be determined, not the concentrations for all of the compounds in the pyrolysis oil. The increase in molecular weight that is displayed in the GPC analysis

can not be confirmed by GC/MS because it does not encompass all of the chemical compounds in the pyrolysis oil samples.

Table B.2 Top five target compounds identified in the quantitative GC/MS data analysis for cottonwood clear wood pyrolysis oil aged at 80°C for 0 and 7 days.

Cottonwood clear wood pyrolysis oil <i>Aging conditions:</i> 80°C, 0 d	Conc. (ug/mL)	% of sample	MW (Da)	Chemical Formula
1,2-benzenediol	4037.52	16.957	110.11	C ₆ H ₆ O ₂
oleic acid	186.04	0.781	282.46	C ₁₈ H ₃₄ O ₂
levoglucosan	168.05	0.706	162.14	C ₆ H ₁₀ O ₅
phenol	152.21	0.639	94.11	C ₆ H ₆ O
2-methoxy-4-methyl phenol	93.76	0.394	138.16	C ₈ H ₁₀ O ₂

Table B.3 Top five target compounds identified in the quantitative GC/MS data analysis for cottonwood clear wood pyrolysis oil aged at 80°C for 0 and 7 days.

Cottonwood clear wood pyrolysis oil <i>Aging conditions:</i> 80°C, 7 d	Conc. (ug/mL)	% of sample	MW (Da)	Chemical Formula
1,2-benzenediol	4780.86	23.208	110.11	C ₆ H ₆ O ₂
phenol	52.81	0.256	94.11	C ₆ H ₆ O
3-methyl-1,2-cyclopentanedione	41.21	0.200	112.13	C ₆ H ₈ O ₂
levoglucosan	39.28	0.191	162.14	C ₆ H ₁₀ O ₅
2-methoxyphenol	26.56	0.129	124.14	C ₇ H ₈ O ₂

Pyrolysis oil solids characterization will be conducted for all aging studies by removing the solids using centrifugation filtration. Light microscopy will be used to analyze the collected particulates and aspect ratios and maximum lengths will be measured. A comparison of the mass and particle size distributions of pyrolysis oil solids

will be made to identify possible connections between the solids content and feedstock/biomass and age parameters. The isolated solids will also be examined with Fourier transform infrared (FTIR) to characterize the particulate surface chemistry. The biomass will be characterized by elemental analysis and Fourier transform infrared (FTIR). The chemical composition of the biomass will also be determined by solvent extraction.

APPENDIX C

KOH ADDITION TO PINE PYROLYSIS OIL

C.1 Materials and Methods

Pyrolysis: Pine clear wood (lumber) biomass was dried to 10% MC, ground and screened to particle sizes ranging from 20 mesh to 4mm. Pyrolysis oil samples were produced by the auger pyrolysis reactor MSU Forest Products Laboratory operated at 450 °C under vacuum.

pH adjustment: Pine clear wood fractionated [PCWF] pyrolysis oil received 03/20/09 and the pH was adjusted with dry KOH pellets at room temperature while stirred to nominal pH values of 5, 7 and 9.

Aging: Three samples of ~27 mL were prepared for each pH value in 30 mL amber jars lined with PTFE. Samples were aged at 80°C in a conduction oven 7 and 14 days and controls were stored at 5 °C. The initial and final weights were recorded.

Physical Characteristic: Mettler Toledo SevenEasy pH meter S20 was used to measure the pH using a three point calibration and phosphate buffer solutions. Karl Fischer titration was collected using the Barnstead International Aquametry II Apparatus in accordance to ASTM E 203-01 with Hydranal Solvent CM (chloroform-methanol) and Hydranal Titrant 2E.

FTIR: Transmission Fourier transform infrared (T-FTIR) spectra were collected using KBr crystals with pyrolysis oil smears and a Nicolet 6700 spectrometer (DTGS detector, 4 cm⁻¹ resolution, 128 scans).

C.2 Results and Discussion

C.2.1 Physical Observations

Notable increase in viscosity due to KOH addition was observed especially for pH values of 7 & 9). It is theorized the addition of dry KOH added without a fluid carrier

increased the viscosity to the point where the magnetic stir bars stopped working. The samples then had to be stirred by hand using a spatula.

C.2.2 pH Adjustment

Table C.1 presents the weights of the pyrolysis oil, added KOH pellets and the % of KOH added.

Table C.1 The weights of pine clear wood fractionated pyrolysis oil and KOH added.

	Adjusted pH		
	5	7	9
Pyrolysis oil (g)	115.8	117.23	114.56
KOH (g)	7.2	10.5	14.8
Wt % KOH	5.8	8.2	11.4

C.2.3 Aging

Below in Table C.2 the initial weights, final weights and % change in weight are displayed for the controls and pH adjusted samples during aging. All of the samples stayed under 0.3 % weight loss during storage and aging

Table C.2 Initial and final weights and calculated % change in weight for PCWF pyrolysis oil controls and aged samples at 80 °C for 7 and 14 days.

Aging Time (days)	Initial Weight (g)	Final Weight (g)	% Change
Control(~pH 2)			
0	84.2415	84.1535	-
7	85.0597	84.8907	0.20%
14	85.7394	85.5452	0.23%
pH 5			
0	84.5139	84.84291	-
7	85.0180	84.8393	0.21%
14	85.2042	84.9533	0.29%
pH 7			
0	84.9007	84.8122	-
7	85.1221	84.9461	0.21%
14	85.0963	84.8582	0.28%
pH 9			
0	85.4090	85.3264	-
7	86.2899	86.126	0.19%
14	85.8013	85.5851	0.25%

C.2.4 pH Measurements

Figure C.1 presents the measured values of pH for the neat and adjusted samples stored at 5 °C and aged at 80 °C for 7 and 14 days. 95 % confidence intervals are presented as error bars and indicate the low error in the pH measurements. The pH of the unadjusted pyrolysis does not change during aging. The un-aged samples increase due to the addition of KOH and then decrease during aging. The decrease in pH during aging is greater for the oil adjusted to nominal pH value of 9. The decrease in pH may be due to poor mixing during the KOH addition prior to the initial pH measurement or due to a reaction reducing the pH.

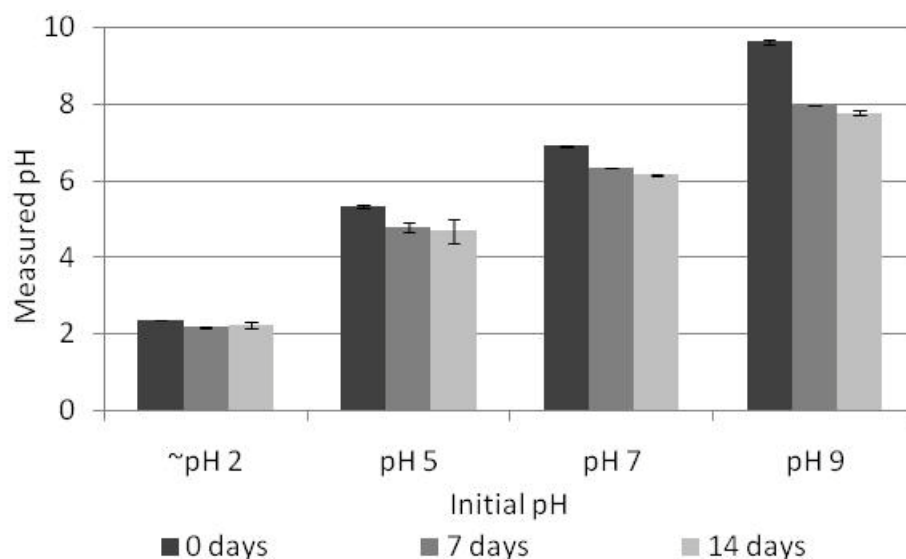


Figure C.1 Measured pH of neat and pH adjusted pyrolysis oils stored at 5 °C and aged at 80 °C for 7 and 14 days.

C.2.5 Water Content

The water content measured for the neat (~pH 2) and adjusted oil samples controls and aged at 80 °C for 7 and 14 days is provided in Figure C.2. The un-aged samples display an increase in water content due to the pH adjustment and then increases further after aging 7 and 14 days. The water content for pH 7 aged for 14 days and both aged samples for pH 9 were not able to be measured due to the samples not dissolving in the solvent during the Karl Fischer titration.

The combination of increased water content and pH due to the adjustment suggests that the KOH disassociates in the pyrolysis oil and is reacting with the oil to produce water and producing an acid resulting in an increased pH. After the initial pH adjustment an additional reaction occurs that reduced the pH and increased the water content of the pyrolysis oil.

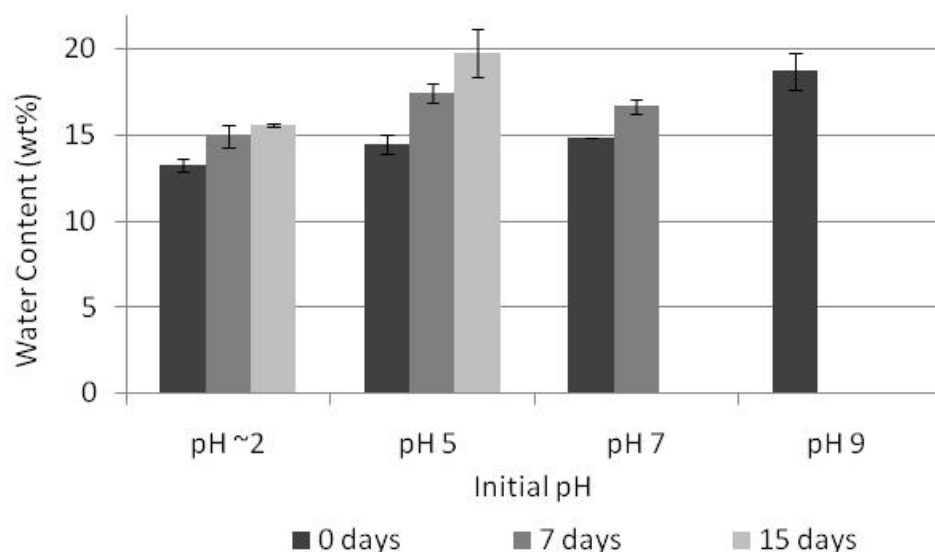


Figure C.2 Water Content for neat and pH adjusted pyrolysis oils stored at 5 °C and aged at 80 °C for 7 and 14 days.

C.2.6 Transmission FTIR

Figure C.3 presents the spectral comparison of neat and pH adjusted PCWF pyrolysis oil un-aged. There is a significant change where the carbonyl peak at ~ 1700 cm^{-1} decreases and a second peak at 1600 cm^{-1} increases. In addition there is an increase in the peaks at 1050 and 1400 cm^{-1} . Carbonyl peak shift from ~ 1700 to 1640 indicates the formation of carboxylate anion expected from the neutralization of the acid group upon KOH addition. In addition the presence of the peak at 1400 verifies the presence of the carboxylate anion. The peak at 1050 can be identified as a primary alcohol.

The decrease in pH upon the pH adjustment in addition to the increase in water content indicate a reaction occurring with the pyrolysis oil and the KOH. The KOH disassociates in the oil samples and then reacts resulting in the carboxylate anion and primary alcohols. .

With the reaction resulting in the water increase and primary alcohol this could potentially simulate the addition of alcohol which has been shown to slow the aging reactions.

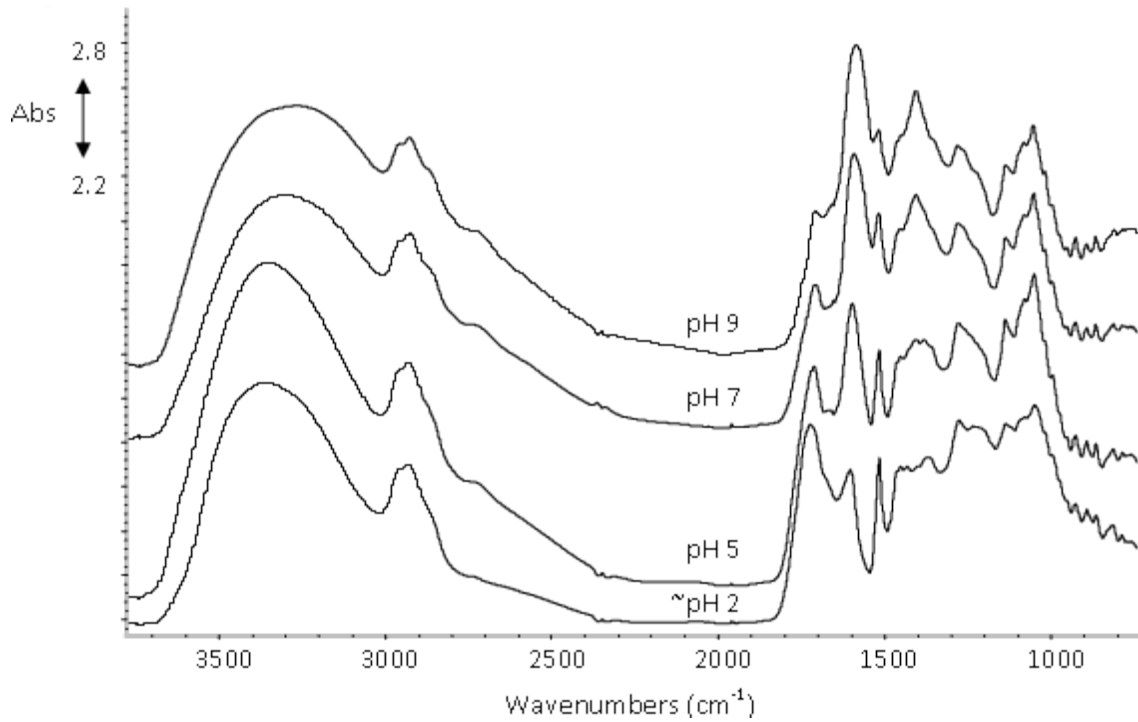


Figure C.3 Transmission spectral comparison of unaged control (~pH2) and pH adjusted PCWF pyrolysis oil samples.

Figure C.4 presents PCWF pyrolysis oil pH adjusted to a nominal value of 5 unaged and aged at 80 °C for 7 and 14 days. On visual inspection there is a shift in the carbonyl peak at ~1700 cm⁻¹ in addition to a change in shape and formation of a shoulder.

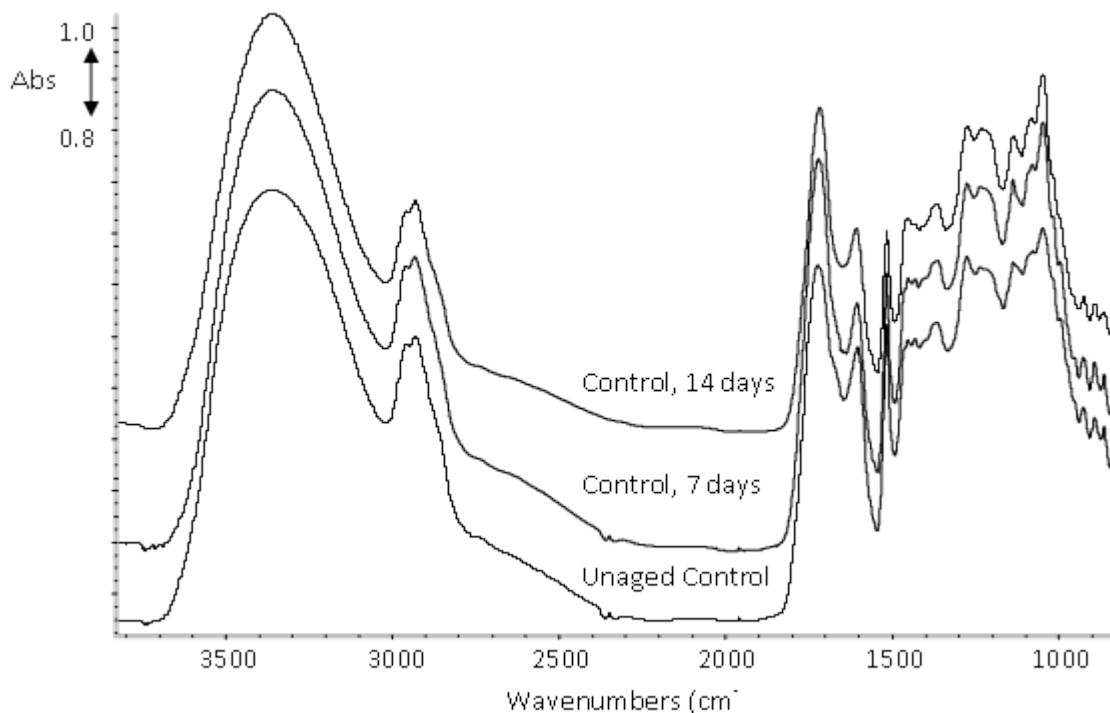


Figure C.4 PCWF pyrolysis oil neat aged at 80 °C for 7 and 14 days.

PCWF pyrolysis oil adjusted to nominal value of 7 is presented in Figure C.5 for un-aged and aged at 80 °C for 7 and 14 days. Visually there appears to be an increase in the carbonyl peak at ~1700, primary alcohol peak at ~1050 and also the phenolic peak at ~1200. There may also be a change in the peak at ~1600 due to aromatic skeletal vibrations.

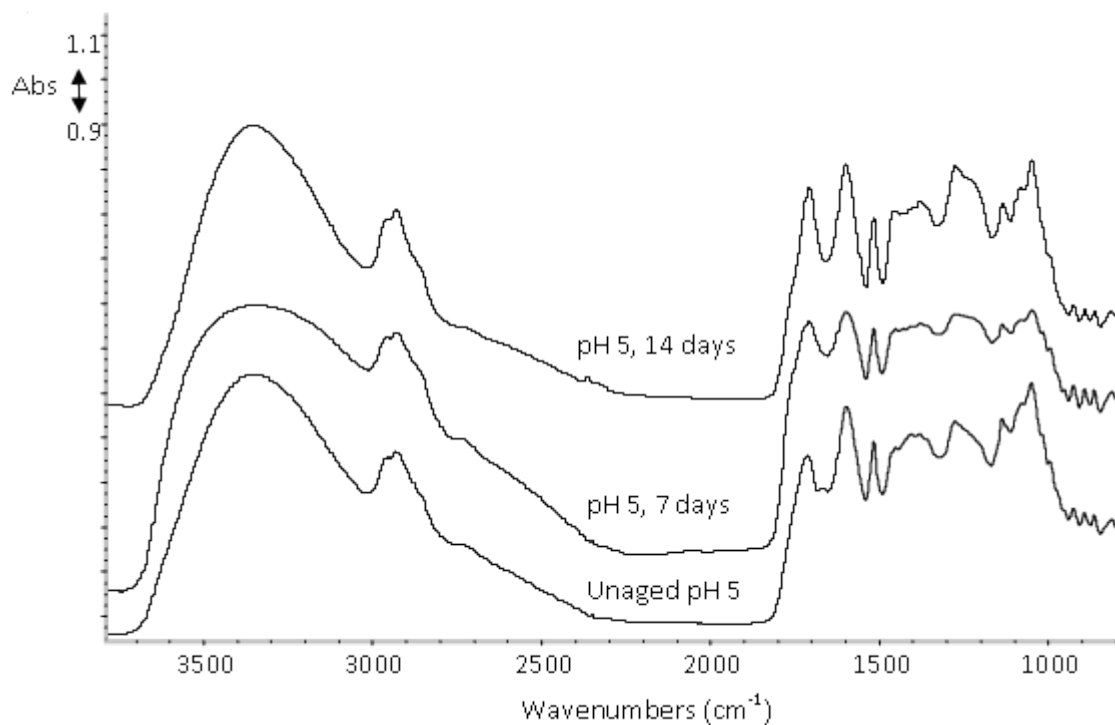


Figure C.5 PCWF pyrolysis oil pH adjusted to 5 and aged at 80 °C for 7 and 14 days.

Figure C.6 displays the PCWF pyrolysis oil samples adjusted to pH of 9, un-aged and aged at 80 °C for 7 and 14 days. Visual spectral comparison indicates a potential increase in the peak at ~1600 representing aromatic skeletal vibrations. There may also be an increase in the peak at ~1400.

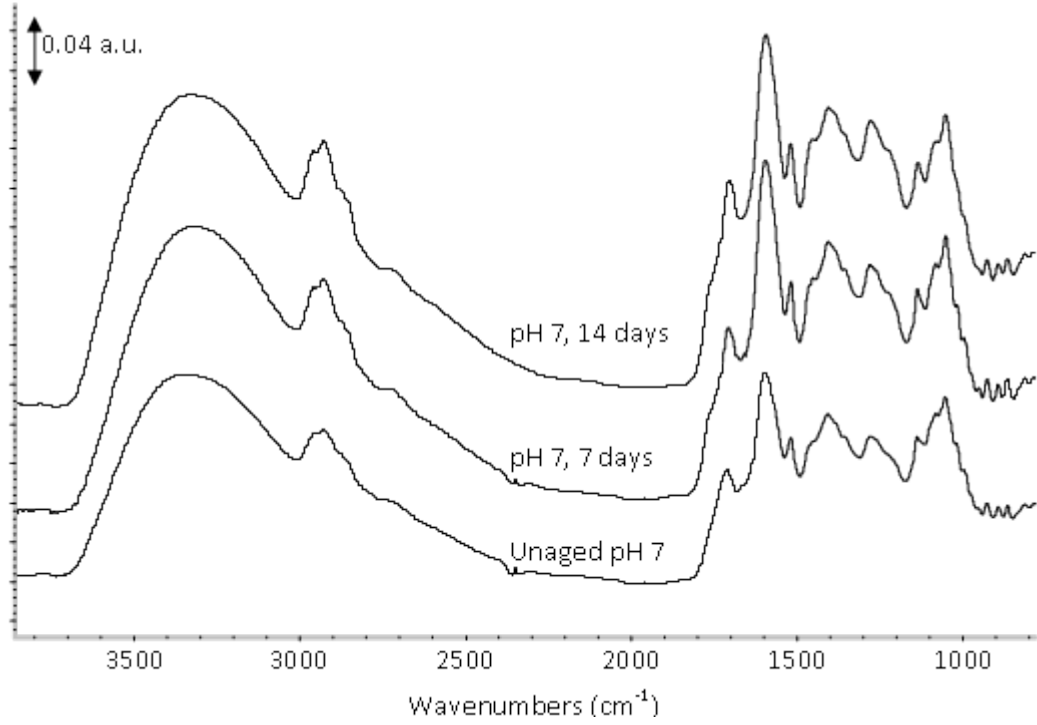


Figure C.6 PCWF pyrolysis oil pH adjusted to 7 and aged at 80 °C for 7 and 14 days.

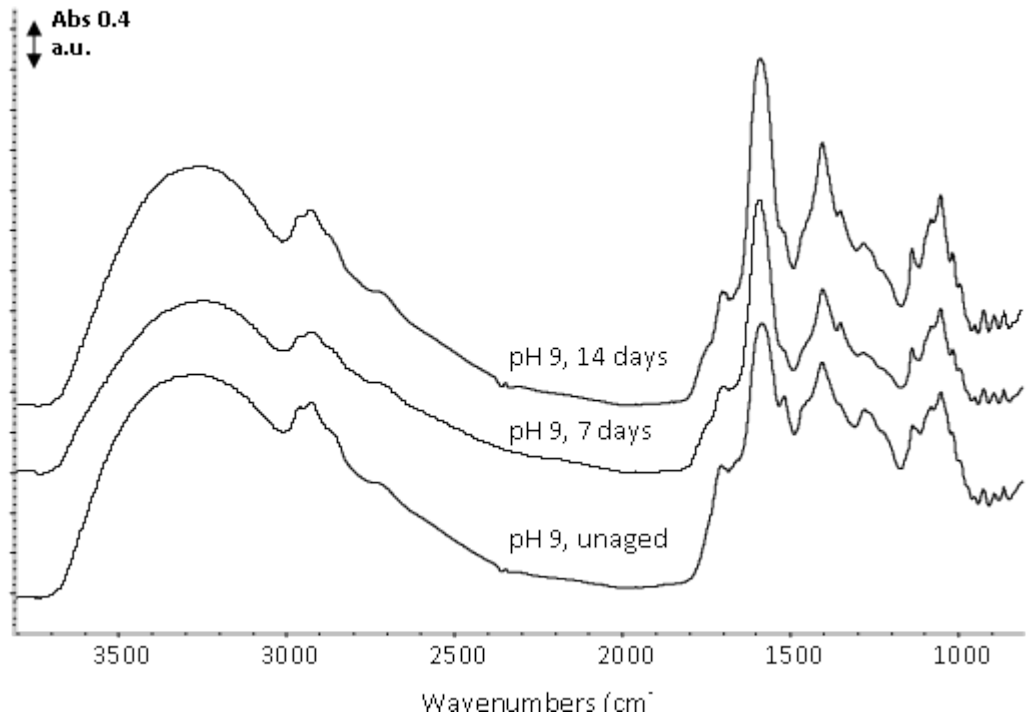


Figure C.7 PCWF pyrolysis oil adjusted to pH 9 and aged at 80 °C for 7 and 14 days.

pH adjusted pyrolysis oil was no soluble in tetrahydrofuran (THF) and therefore gel permeation chromatography (GPC) and gas chromatography coupled with mass spectroscopy could not be conducted to investigate the molecular weight and chemical composition further. Therefore it is difficult to determine if the pH adjustment retarded changed or stopped the aging reactions.

C.3 Conclusions

The pH of the pyrolysis oil was adjusted with dry KOH which resulted in the increase in the pH, water content and acid value. In addition the pH adjustment formed carboxylate anion and primary alcohols.

C.4 References

Oasmaa, A., Peacocke, C., Gust, S., Meier, D., McLellan, R., "Norms and Standards for Pyrolysis Liquids. End-User Requirements and Specifications" Energy & Fuels 2005, 19, 2155-2163

APPENDIX D

CONTROLLED POLYMERIZATION OF PINE PYROLYSIS OIL

D.1 Materials and Methods

D.1.1 Controlled Polymerization #1

Three 5 g samples of pine clear wood fractionated [PWCF] pyrolysis oil received 12-08 were prepared in test tubes with septa. The samples were then polymerized them with the following method:

D.1.1.1 Sample number, catalyst

1. stannous octanoate 0.3031g
2. p-toluic acid 0.1023g
3. AlCl₃ 0.1045g

D.1.1.2 Conditions

1. 0.5 h at room temp under N₂ purge
2. Ramp to 135 °C under N₂ purge (~15 min.)
3. 2 h at 135C under N₂ purge
4. Ramp to 170 °C under vacuum (~15 min.) and injected catalysts dissolved in toluene
5. 16h at 170 °C under vacuum
6. Quenched to room temp by using an ice bath

The polymerized pyrolysis oil samples solidified during the reaction and appeared black, glassy and possibly crystalline. The samples were removed from the test tubes with a metal spatula. The FTIR spectra were collected using the method of DRIFTS.

D.1.2 Controlled Polymerization #2

Twelve 5 g samples of pine clear wood fractionated [PCWF] pyrolysis oil received 12-08 were prepared in test tubes with septa. The samples were then polymerized them with the following method:

D.1.2.1 Sample number, catalyst

1-3 with stannous octanoate “polymerized”

4-6 without catalyst “polymerized”

7-9 with stannous octanoate at ~24 °C (ambient for 24 hours)

10-12 with stannous octanoate at 5 °C (refrigerated)

D.1.2.2 Conditions (Samples 1-6)

1. 0.5 h at room temp under N₂ purge
2. Ramp to 135 °C under N₂ purge (~15 min.)
3. 2 h at 135C under N₂ purge
4. Ramp to 170 °C under vacuum (~15 min.) and injected catalysts dissolved in toluene
5. 16h at 170 °C under vacuum
6. Quenched to room temp by using an ice bath

Samples 7-12 were inverted and sonicated briefly after the addition of the catalyst to ensure it was mixed well. The room temperature samples [7-9] were at room temperature from 10:00 am (the start of the reaction) to 8:45 am the following day. Sample 1-6 were cooled in an ice bath and stored in the refrigerator until removed from the test tubes. Samples 5 and 6 were “sticky” solids where samples 1-4 were solids.

D.2 Results and Discussion

D.2.1 Pyrolysis Oil Controlled Polymerization #1

Figure D.1 displays the DRIFTS spectra of the polymer pyrolysis oils #2 and #3 collected are compared to pine clear wood fractionated [PCWF] neat pyrolysis oil (12-08) collected by transmission FTIR. Despite the large change in the physical properties of the polymer pyrolysis oils (solid and possibly crystalline) the majority of the peaks in the spectra are comparable to those in the neat liquid pyrolysis oil sample. The largest difference in the polymer pyrolysis oils are the shifts and broadening in the hydroxyl band as well as peaks in the overtone-combination region indicating aromatics. In addition there is a change in the shape of the C-H peak and the carbonyl peak. There is also a major change in the peak at $\sim 1050\text{ cm}^{-1}$ which is due to primary alcohols.

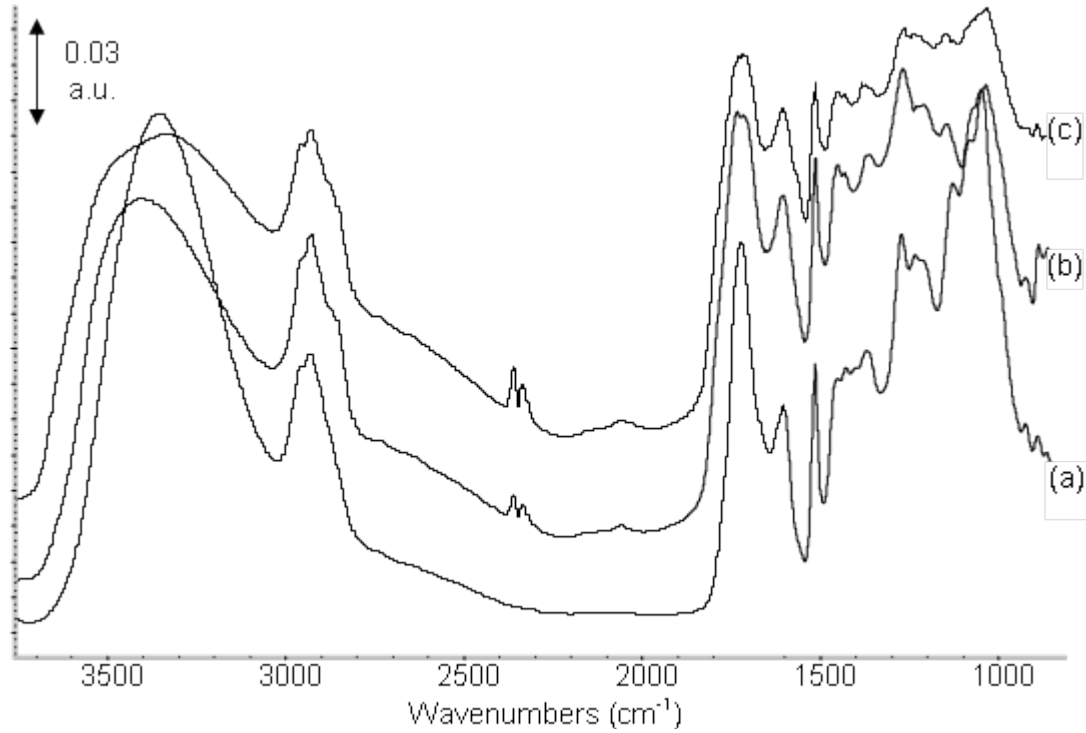


Figure D.1 FTIR spectral comparison of neat pine clear wood fractionated [PCWF] pyrolysis oil (a) and PCWF polymerized pyrolysis oil with p-toluic acid catalyst (b) and AlCl₃ catalyst (c).

Figure D.2 displays the spectral comparison of the fingerprint region of samples 2 and 3 with the neat pine clear wood fractionated [PCWF] pyrolysis oil received 12-08 (common scale).

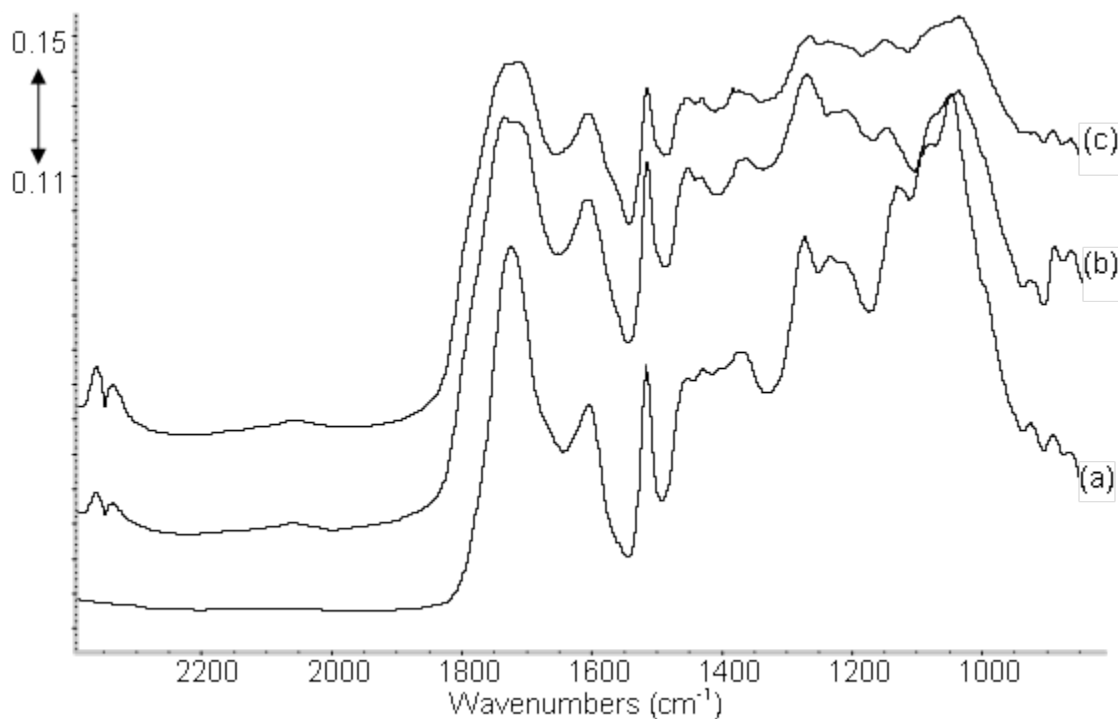


Figure D.2 Spectral comparison in the fingerprint region of neat pine clear wood fractionated [PCWF] pyrolysis oil (a) and PCWF polymerized pyrolysis oil with p-toluic acid catalyst (b) and AlCl_3 catalyst (c).

D.2.2 Pyrolysis Oil Controlled Polymerization #2

D.2.2.1 Physical Observations

The polymerized samples [1-6] regardless of catalyst solidified during the reaction. The samples with catalyst at room temperature [7-9] and in the refrigerator [10-12] did not solidify.

D.2.2.2 FTIR and DRIFT

In Figure D.3 the FTIR spectrum of neat Pine Clear Wood Fractionated [PCWF] (a) is compared to the DRIFT spectra of the “polymerized” of PCWF without catalyst (b-d) and catalyzed with stannous octanoate (e, f). All of the polymerized pyrolysis oil samples have differences when compared to the neat pyrolysis oil. Catalyzed samples (e,

f) appear to have two peaks in the hydroxyl band where the pyrolysis oil without catalysis does not but the shape appears to be different than the neat pyrolysis oil. In addition all polymerized pyrolysis oil samples (b-e) have a change in the C-H peak shape possible with the addition of a second peak.

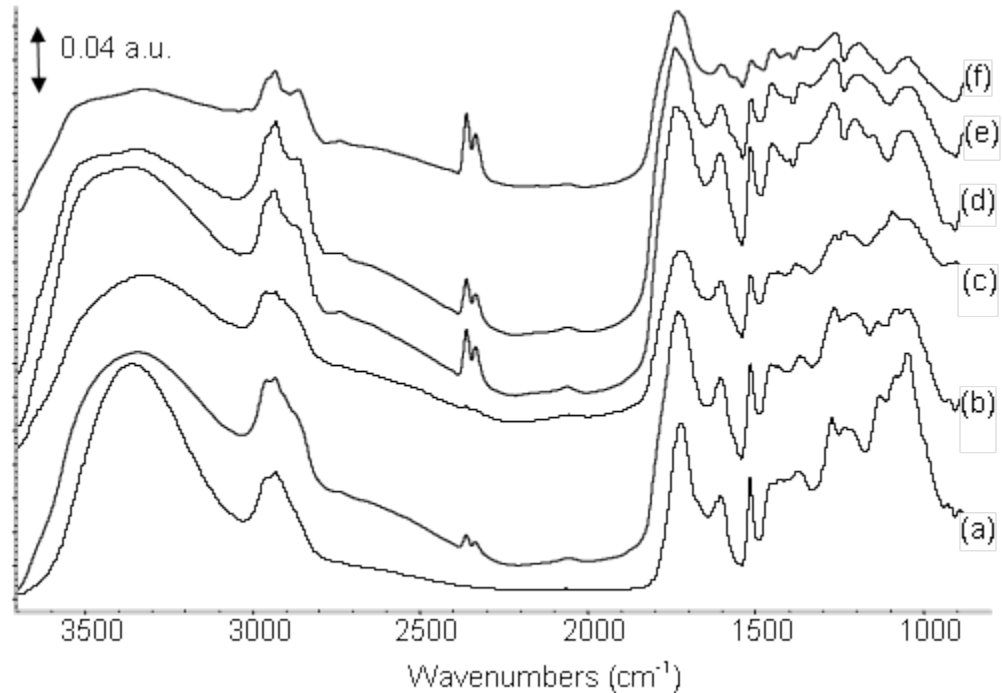


Figure D.3 FTIR transmission spectrum of neat Pine Clear Wood Fractionated [PCWF] (a) compared to the DRIFT spectra of the “polymerized” pyrolysis oil samples of PCWF without catalyst (b-d) and with stannous octanoate catalyst (e, f).

In Figure D.4 the fingerprint region for the FTIR spectrum of neat PCWF is compared to the DRIFTS spectra of the “polymerized” of PCWF “polymerized” without catalyst (b-d) and catalyzed with stannous octanoate (e, f). When comparing the neat PCWF to the catalyzed samples (e, f) there appears to be a shift in the dominant peak from $\sim 1050\text{ cm}^{-1}$ to a carbonyl peak at $\sim 1700\text{ cm}^{-1}$. Also, there are two main peaks in the neat sample between 1500 and 1100 cm^{-1} that evolve into many smaller peaks (~ 4 peaks).

Overall the changes in the pyrolysis oil samples are larger when compared to accelerated aging in pyrolysis oil at 80 °C with sealed jars.

When examining the samples polymerized without catalyst in Figure D.4 (b-d) the change from the neat pyrolysis oil is not as apparent as those observed in the catalyzed samples (e, f). There also appears to be a shift in the dominant peak and it may be possible that the same reaction occurs in both sets and the catalyst encourages the reaction to proceed, making the changes more pronounce in the catalyzed samples.

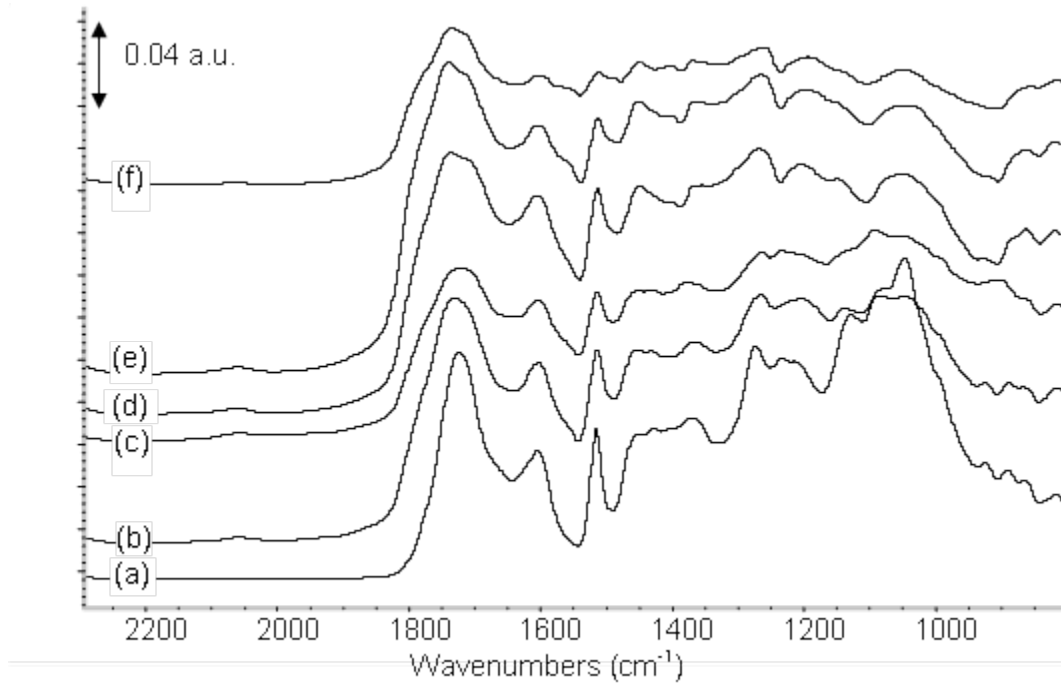


Figure D.4 Fingerprint region of the FTIR transmission spectrum of neat Pine Clear Wood Fractionated [PCWF] (a) compared to the DRIFT spectra of the “polymerized” pyrolysis oil samples of PCWF without catalyst (b-d) and with stannous octanoate catalyst (e, f).

Figure D.5 displays the FTIR spectra of the neat PCWF pyrolysis oil compared to the “polymer” pyrolysis oils 7-9 (stored at ambient temperature with catalyst) at common scale. In the initial comparison of the spectra the main difference is that the hydroxyl

band broadens in the “polymer” pyrolysis oil spectra. Also there is the formation of a shoulder to the right of the C-H peak at approximately 2850 cm^{-1} and the development of a weak peak in the overtone region at $\sim 2050\text{ cm}^{-1}$. This shows that with catalyst without heat there is a reaction occurring.

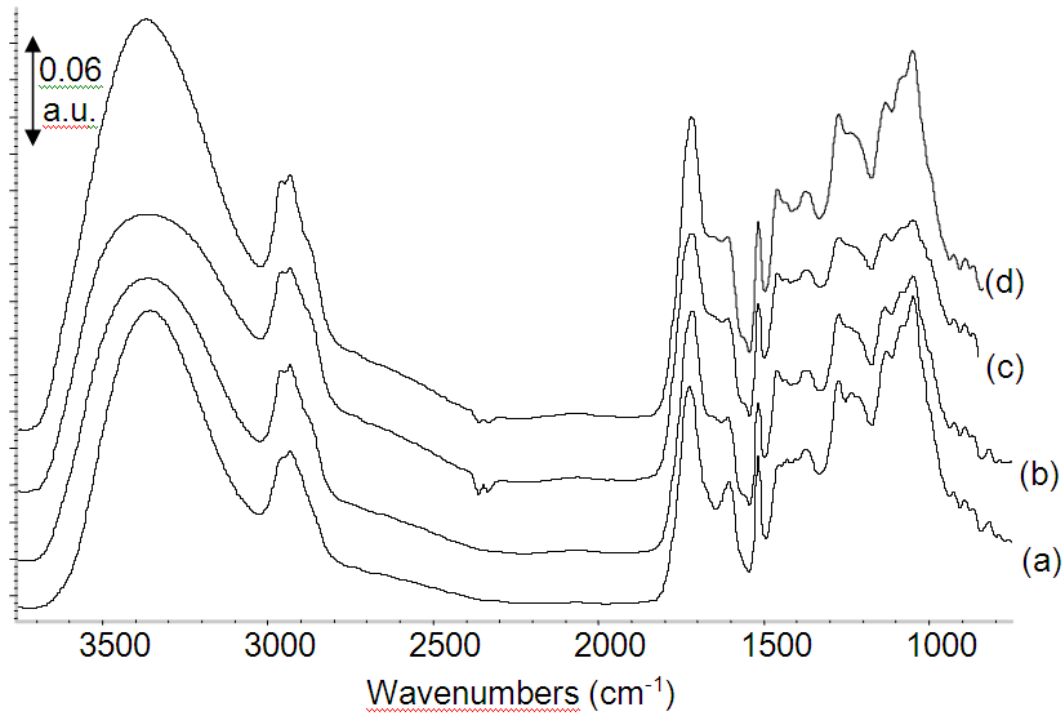


Figure D.5 FTIR spectral comparison of neat pine clear wood fractionated [PCWF] (a) and polymerized samples 7 (b), 8 (c), and 9 (d) of PCWF at $\sim 21\text{ }^{\circ}\text{C}$ (room temperature) and stannous octanoate catalyst.

In Figure D.6 the fingerprint region of the FTIR spectrum of Neat Pine Clear Wood Fractionated (PCWF) received 12-08 compared to the “polymerized” samples [7, 8, and 9] of PCWF at $\sim 21\text{ }^{\circ}\text{C}$ (room temperature) with the addition of stannous octanoate [catalyst] is displayed at common scale. When examining the fingerprint region of the spectra there are several differences from the neat pyrolysis oil. First there is a shift in the carbonyl band from $\sim 1725\text{ cm}^{-1}$ to $\sim 1717\text{ cm}^{-1}$ in all of the polymer pyrolysis oil

samples. Also there is a shoulder development at $\sim 1650\text{ cm}^{-1}$ as well as a small peak formation at $\sim 1650\text{ cm}^{-1}$.

The change in the pyrolysis oil at room temperature is unexpected within 24 hours because even when aging pyrolysis oil at an elevated temperature changes are not always displayed. This demonstrates that the catalyst is having an effect on the possible polymerization reactions that are occurring.

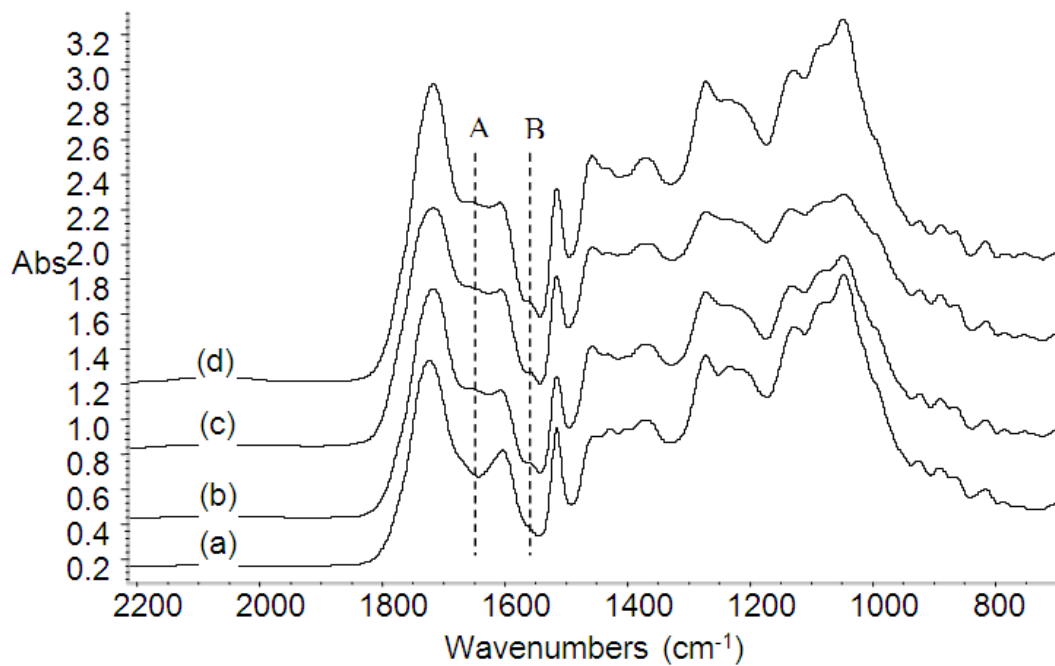


Figure D.6 The Fingerprint region of neat pine clear wood fractionated [PCWF] (a) and polymerized samples 7 (b), 8 (c), and 9 (d) of PCWF at $\sim 21\text{ }^{\circ}\text{C}$ (room temperature) and stannous octanoate catalyst.

Figure D.7 displays the FTIR spectrum of Neat Pine Clear Wood Fractionated (PCWF) received 12-08 compared to the “polymerized” samples [10,11, and 12] of PCWF at $5\text{ }^{\circ}\text{C}$ (refrigerated) with the addition of stannous octanoate [catalyst] at common scale. When examining the four spectra there are no obvious differences between the neat sample and the catalyzed samples that were stored in the refrigerator. When the

spectra are examined closer the only difference that can be found is a small shoulder at $\sim 1550\text{ cm}^{-1}$. It is worth nothing that there are no peaks (weak or strong) in the overtone region where there are weak peaks present in the other spectra including the samples stored at room temperature.

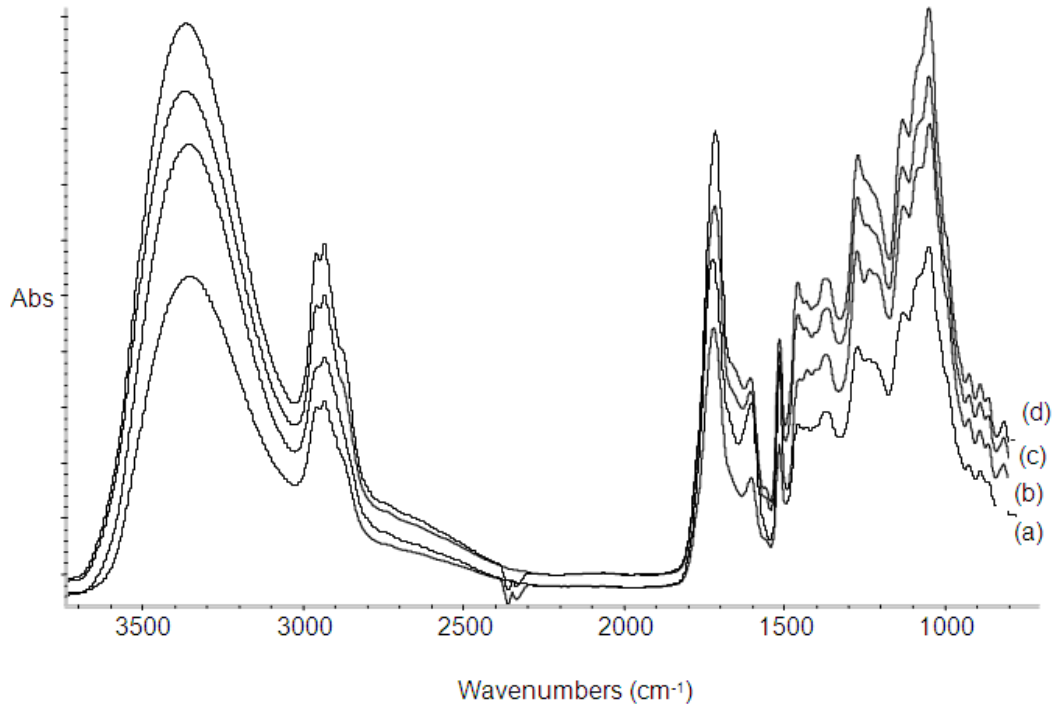


Figure D.7 Spectral comparison of neat pine clear wood fractionated [PCWF] (b) to the polymerized samples 10 (d),11 (a), and 12 (c) of PCWF at 5 °C with the addition of stannous octanoate catalyst.

During polymerization the vapors removed by vacuum during throughout the heating was collected in a liquid nitrogen trap and the collected condensate spectra is presented in Figure D.8. When compared to the neat and polymerized samples the condensate has a very different spectrum. Two major are a strong carbonyl peak at 1723 cm^{-1} and different set of peaks between $1500\text{ and }1000\text{ cm}^{-1}$. A peak at 1045 cm^{-1} is

stands out in this region. In addition there is a shift in the hydroxyl peak when compared to

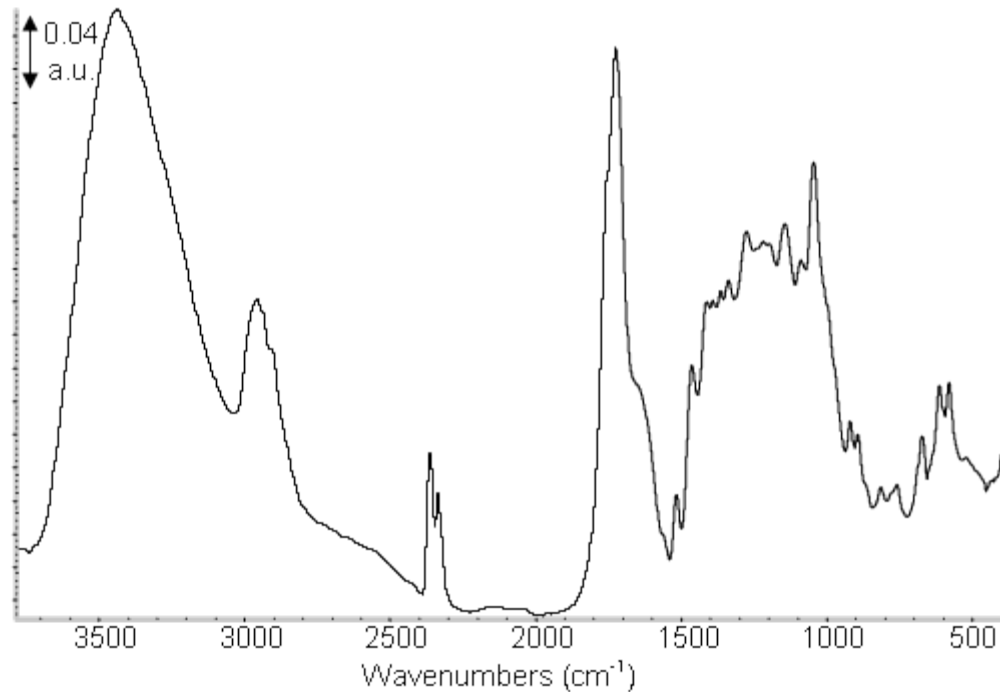


Figure D.8 FTIR spectrum of the collected condensate during the controlled polymerization run #2 by a liquid nitrogen vacuum trap.

D.2.2.3 Calorimetry

Caloric value was determined for several of the polymerized samples in addition the unaltered PCWF pyrolysis oil and the results are presented in Figure D.9. For all of the samples polymerized at elevated temperatures with and without catalyst increased the caloric value by 42 to 56 %. Samples stored at 24 and 5 °C did not demonstrate a significant change indicating that the increase in caloric value is related to the elevated temperatures during polymerization. It is unclear if the increase in caloric value is due to the removal of water and other low volatile material during polymerization.

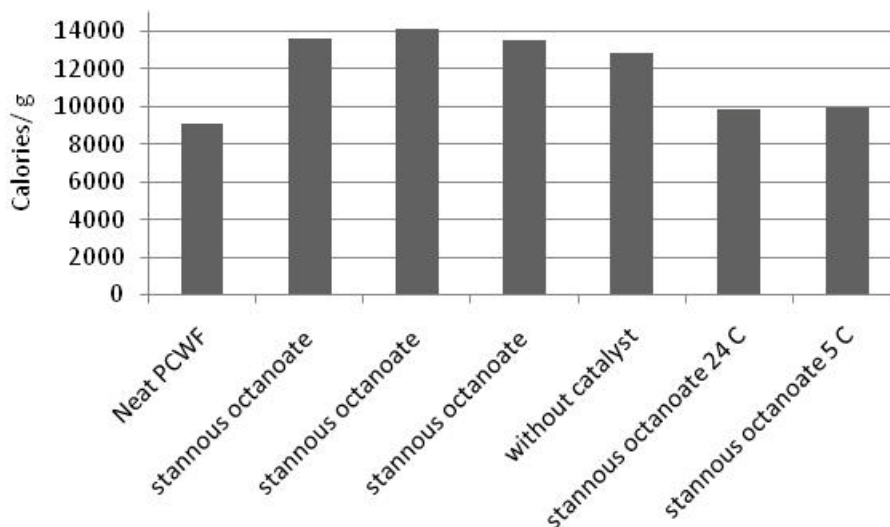


Figure D.9 Calorimetry data for polymerized pyrolysis oil

D.2.2.4 Gel Permeation Chromatography

Molecular weight was determined by Gel Permeation Chromatography (GPC) and the average weight average molecular weights are presented in Figure D.10. Most of the polymerized pyrolysis oil samples were not completely soluble in THF and therefore the molecular weight values are not completely representative of the final result.

Polymerization without catalyst demonstrates the largest molecular weight increase and also was completely soluble in THF. Without catalyst there is a 500 % increase in molecular weight after polymerization. It may be possible that the molecular weight with catalyst is higher than the sample without catalyst but it could not be determined using the current method.

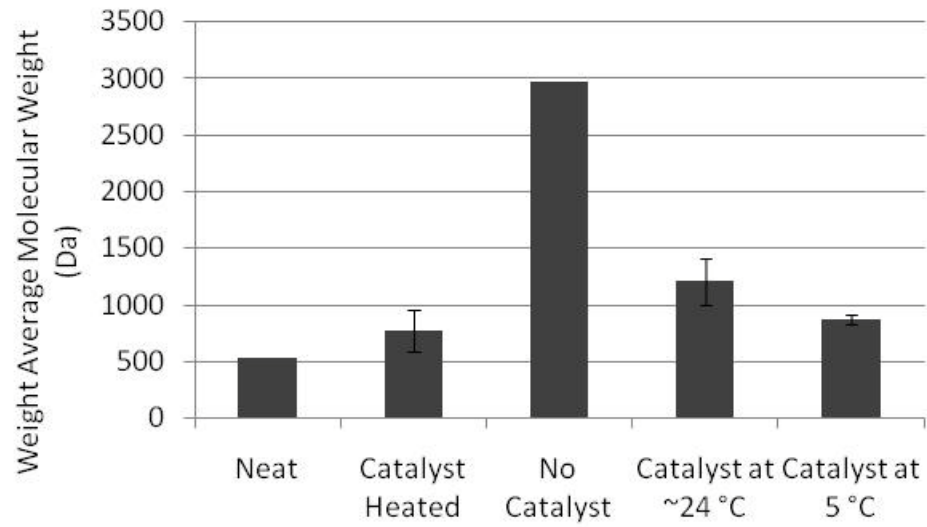


Figure D.10 Molecular weight for soluble portions of polymerized pyrolysis oils

D.3 References

Nakanishi, K. and Solomon, P.H. "Infrared Absorption Spectroscopy second edition" 1977 Holden-Day Inc. Oakland, CA.

Pretsch, E., Buhlmann, P., and Affolter, C. "Structure Determination of Organic Compounds. Tables of Spectral Data." 2000, Springer New York, New York.

A.L. Morales-Cruz et al., Applied Surface Science, 2005, 241 , 371–383. [379]

Silverstein, R.M., Webster, F.X. "Spectrometric Identification of Organic Compounds. Sixth Edition." John Wiley & Sons, Inc. 1998, USA.

APPENDIX E

XRF DATA FOR PINE AND COTTONWOOD BIOMASS AND CHAR

E.1 Method

A Spectro Xepos with a aluminum backscattering filter, Co filter, Highly ordered pyrolytic graphite filter, and Mo filter. A Pd anode x-ray tube, silicon drift detector, software is X-Lab Pro. Standard is proprietary.

E.2 Results and Discussion

As previously discussed, in addition to silica alkali metals such as Na, K, Mg, P and Ca can be found in pyrolysis oil [McKendry 2002]. Elements detected using X-ray fluorescence (XRF) are presented in Figures 3 and 4 for cottonwood and pine, respectively, and include only the most abundant elements (above 1 atomic %) since 38 elements were detected (most at concentrations on the order of parts per million). In both cottonwood and pine there are higher concentrations of Si, Na, Ca, K, Mg and P in the char as compared to the biomass which is in agreement with previous studies describing alkali metals concentrated in char.

Cottonwood bark and leaf biomass have higher CaO content in addition to the leaf biomass have larger SiO₂ when compared to heart wood. Cottonwood bark and leaf char increase further in concentration for both CaO and SiO₂ and the presence of the bark and leaves in the whole tree char increase the CaO and SiO₂ noticeably. Similarly, the pine needle biomass has more SiO₂ when compared to heart wood and the needle char increase by SiO₂. In addition the needles char also has almost 3% of both CaO and K₂O.

When comparing the two tree types, cottonwood biomass and char have larger percentages of the alkali metals than pine biomass and char, specifically SiO₂ and CaO. Pine bark contains less CaO than cottonwood bark, and the pine needles contain a much

larger concentration of K_2O than the cottonwood leaves. In addition to the graphed data cottonwood leaves were the only feedstock that included more than 1% SO_3 .

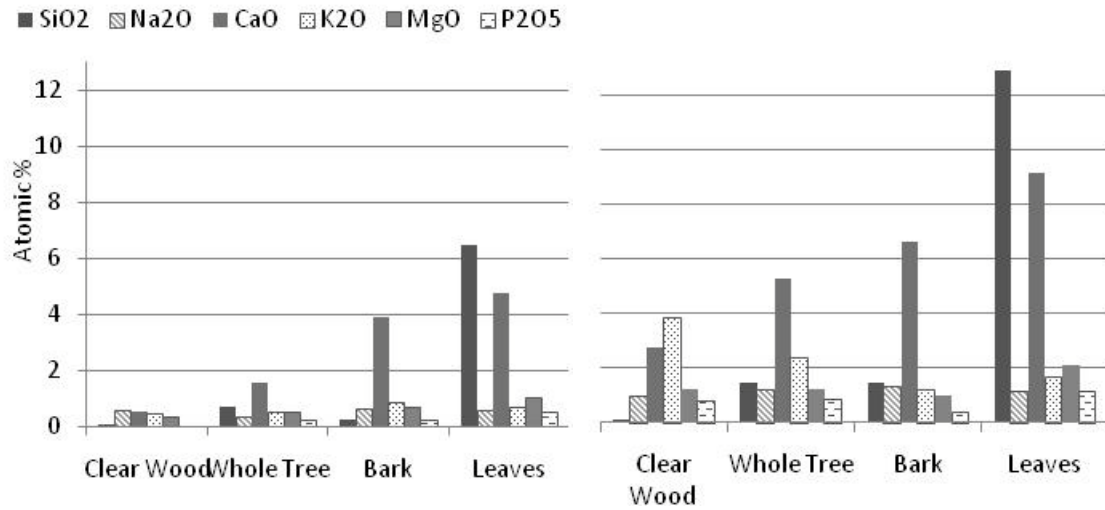


Figure E.1 XRF data for cottonwood biomass (left) and char (right) showing SiO₂, Na₂O, CaO, K₂O, MgO and P₂O₅ atomic percentages.

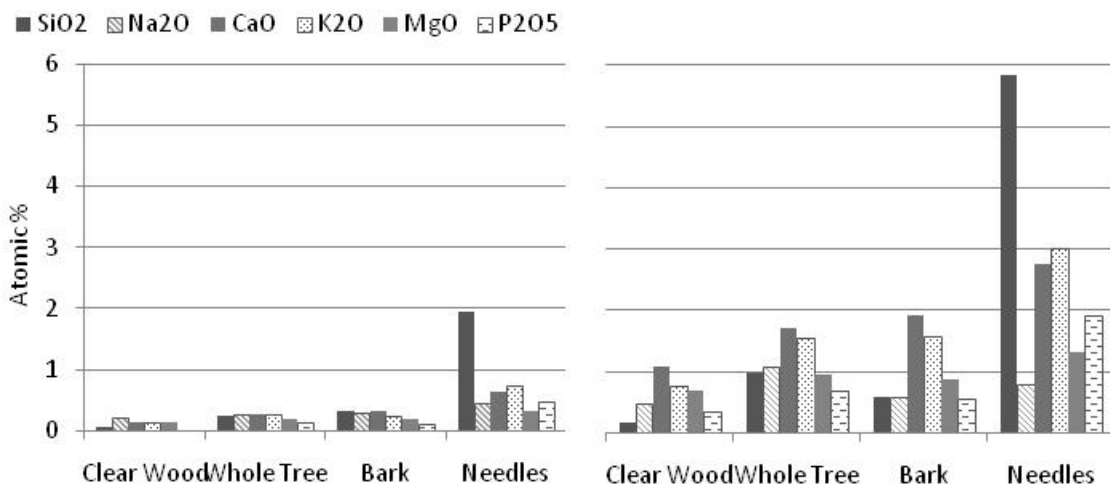


Figure E.2 XRF data for pine biomass (left) and char (right) showing SiO₂, Na₂O, CaO, K₂O, MgO and P₂O₅ atomic percentages.

APPENDIX F
INVESTIGATION INTO THE EFFECT OF PYROLYSIS OIL CONTACT WITH
POLYMER MATERIALS

F.1 Abstract

Pyrolysis oil, or more commonly described as bio-oil, can be derived for a wide variety of materials. Bio-oil derived from wood biomass is produced with a low pH of approximately 2 to 3. This property makes the bio-oil highly corrosive and can cause serious problems during storage, transportation and use of bio-oil. Previously, materials have been tested for storage and transportation capability during a corrosion study¹. If the material does not lose mass during the exposure to bio-oil at varied temperatures, it is considered to be resistant to corrosion. This does not take into account the surface interactions between the material and bio-oil where the material may be degraded or the physical properties altered. Two polymer materials were tested for the effects of corrosion on the surface chemistry and the physical properties. These materials were polypropylene (PP) and polyvinyl chloride (PVC). PP is especially important because it is used to manufacture a large variety of lab supplies including test tubes and PVC is a common piping material².

In order to test the materials, the samples were submerged in bio-oil at room temperature for three weeks. The samples exposed to bio-oil were washed with methanol prior to recording the initial and final weight of the materials. A physical and chemical characterization was then conducted for the samples stored in bio-oil and compared to characterizations obtained from the raw material (controls). For each set of material, tensile testing was conducted in accordance with ASTM standard. Selected fracture surfaces were examined by scanning electron microscopy (SEM) for each material and the surface chemistry was examined using X-ray Photon Spectroscopy (XPS). In addition, the pH of the bio-oil was measured and recorded before and after storage.

There was no statistically significant change in the weight of the polymers after bio-oil treatment or the pH of the bio-oil. The bio-oil had no significant effect on the mechanical properties of the polymers. The acidic nature of the bio-oil may have roughened the surface the polymers and it is most likely the polymer absorbed a mineral containing silicon and oxygen from the bio-oil. The PVC specimens also lost oxygen bonded to carbon due to the bio-oil treatment.

F.2 Introduction

Bio-oil, can encompass a wide group of oils produced using the method of pyrolysis. Pyrolysis is a thermal decomposition of a material in the absence of oxygen. This investigation was focused on bio-oil produced from the pyrolysis of wood biomass, specifically pine. When produced, bio-oil has a low pH (~2) which is due to the 8-10 wt % of volatile acids such as formic acid and acetic acid¹. With the presence of various acids and a high content of water which can exceed 30 wt%, the bio-oil can be very corrosive especially at elevated temperatures¹. Corrosion can cause failure during processing or storage, which is undesirable and can be costly.

Taking into account the abundance of lignocellulose materials, a functional group found in bio-oils, and the commercial values of polypropylene (PP) and polyvinyl chloride (PVC) it is reasonable to examine these materials as potential materials for bio-oil storage. The two test materials are favorably chosen based on if they would be affected by organic materials (especially acids), industrial development and cost. A reason to explore PP and PVC is because rigid polymer foams represent a group of lightweight materials currently used in a wide variety of industries, such as packaging, building, and insulation. These applications are limited due to the inferior strength, poor

surface quality, and low thermal and dimensional stability of the materials⁸. PP has many advantages, such as simple synthesis process, low cost, easy forming, and excellent overall properties. However, it also has limited application due to its high shrinkage rate, especially at low temperature. It has been reported that PVC material can be corroded by bio-oil, where the functional groups of PVC and organic lignocellulose in bio-oil may have proton donor/acceptor interactions⁷. For example, the carboxylic groups of the bio-oils and α hydrogen of PVC can react, or the hydroxyl groups of bio-oil and chlorine of PVC can react⁷.

Chemical resistivity tests on a wide variety of materials in bio-oil were previously conducted by Oasmaa et al. at VTT Technical Research Centre of Finland¹. Within this study “test rods” were submerged into glass bottles of bio-oil produced from hardwood at different temperatures ranging from room temperature to 80 °C. The material was stored in the bio-oil for up to 6 weeks. The specimens were then removed after storage, cleaned with ethanol, and weighed to determine the change in mass. Due to little to no weight loss, it was determined that polymers such as polytetrafluoroethylene (PTFE), high density polyethylene (HDPE) and polypropylene (PP) were very resistant to the bio-oil. In addition it was determined that AISI 316 stainless steel was more chemically resistant to the bio-oil when compared to AISI 304¹.

Figure F.1 displays the tensile strength and breaking extension ratio data collected in Hu et. al. during the thermal degradation of PP for 0, 10, and 20 days. It was determined that after 20 days there was no significant change in the mechanical properties. In addition, the study also included the determination of the surface chemistry using XPS and utilized SEM to observe any surface changes. The XPS analysis of the raw PP included three C 1s peaks, where the aged PP sample contained four C 1s peaks.

The formation of the fourth peak in addition to changes in the original three peaks indicated the PP underwent a thermal oxidation during the aging.

Time, day	0	10	20
Tensile strength, MPa	39.68	38.01	38.74
Breaking extension ratio, %	84	51.40	74.31

Figure F.1 Table 2 from Hu, 2006 displaying the tensile strength and breaking extension ration of PP after thermal degradation of 0, 10, and 20 days²⁰.

Previous research demonstrated that polypropylene (PP) can undergo hydrolytic aging in the presence of solutions with pH values of 6, 7 and 8 over a course of several months¹⁵. XPS was utilized to observe this degradation and a change in surface chemistry. The XPS analysis was focused on the evolution of oxygen in the polypropylene, which is the main impurity. From the data obtained in the aging study it was determine that the PP underwent oxidation (loss of an electron), where the polymer formed bonds with the ions in the surrounding solution. This was determined through the comparison of the C1s and O1s peaks¹⁵.

A second investigation into the natural aging of PP at room temperature when exposed to ambient light demonstrated that as the PP ages, the oxidation leads to the formation of double bonded oxygen, and the formation of bonds such as C=O, O-C=O¹⁸.

F.3 Experimental Set-up

F.3.1 Polymer Materials

Ten dog bone specimens were prepared for each material (PP and PVC) in accordance with ASTM standards D 638-03. Five samples of each material were used for tensile test as a control (untreated) and a second set of five samples were submerged

in bio-oil and tested. Each set of samples were washed with methanol and weighed prior to being submerged in bio-oil held in a glass Pyrex dish. Each set of material was held in a separate dish. Approximately 800 mL of pine bio-oil was used for each glass dish. The specimens were stored in separate pyrex dishes of the same bio-oil for up to three weeks to prevent cross contamination. Small pieces of each material were cut and stored in 30 mL jars with bio-oil to be used for the XPS analysis. After the three weeks, the specimens were taken out of the bio-oils, washed with methanol and the final weight recorded. Tensile testing was then conducted for the control and the treated specimens. Apart from the mechanical properties, the surface and fractured surface of select specimens was investigated through Scanning Electron Microscopy (SEM), and the surface chemistry was investigated by X-ray Photon Spectroscopy (XPS). In addition, the pH of the bio-oil was measured prior to and after the material treatment.

For each material there was five specimens allowing for replication in case of premature failures or flaws in the specimens. All the specimens (control and treated) were cut from the material in the same direction using a band saw to cut 1 in x 8 in strips. The dog bone shape was then created using a router and a guide in the standard shape required for the ASTM standard. An example of the dog bone shape as well as the visual appearance of the PP and PVC specimens are displayed in Figure F.2.

According to the ASTM standard, 10 specimens should be conducted when isotropic. This investigation is to compare a control material to a treated material where the isotropic nature does not play a role in the material testing. It should be noted that to completely investigate the mechanical properties of either material, additional testing would be required.

Due to difficulty in the acquisition of stainless steel 304 as well as the planning and cutting of the stainless steel 304L the planned stainless steel specimens were not treated with bio-oil nor was the neat material tested in anyway.



Figure F.2 The visual appearance of neat PVC (top) and PP (bottom)

F.3.2 Bio-oil Treatment

The bio-oil; procured from Forestry Products; was produced from pelletized pine biomass by the process of pyrolysis. The pyrolysis reactor is an auger reactor operated at 400 °C without purge or vacuum. The bio-oil sample was fractionated which refers to the exclusion of the second condenser which has a large percentage of water and organic acids. The bio-oil was then stored at approximately 5 °C in a refrigerator until the polymer treatment.

Five specimens of the PP and PVC were submerged in the pine bio-oil at room temperature for three weeks. The two sets of specimens were treated in separate glass Pyrex dishes to prevent any cross contamination. The ends of the dog bones were supported by glass microscope slides to prevent the specimens from resting on the bottom of the dish, which would prevent even contact of the dog bone with the bio-oil. In addition the polypropylene floated in the bio-oil. To ensure that the specimens remained

F.3.3 Tension testing

Standard test for tensile properties of plastics cover the determination of the tensile properties of plastics. The testing is done in the form of standard dumbbell-shaped (or “dog bone”) test specimens when tested under defined conditions of pretreatment, temperature, humidity, and testing machine speed. The Instron model 5869 and 5800 controller for the tensile test were used for the tensile testing. The polymer specimen dimensions were 0.12 ± 0.01 inch thick, 0.49 ± 0.03 inch wide and 3.2 ± 0.02 inch long. The speed of testing (inch/min) was determined as 3 inch/min based on Table 1 of ASTM Standard D 638-03. The tests were conducted for a total of ten specimens for polypropylene (PP) and Polyvinyl chloride (PVC) [5 control, 5 treated each]. The ASTM standard⁴ recommends that tests should be conducted at $23 \pm 2^\circ\text{C}$ [$73.4 \pm 3.6^\circ\text{F}$] and $50 \pm 5\%$ relative humidity so the tensile testing was conducted at room temperature. The elastic modulus, yield strength, ultimate tensile strength, and elongation to failure were calculated from the collected data, and the control and treated specimens were compared.

The mechanical properties were calculated from the obtained data by below equations⁶.

- Elastic modulus (ksi): $\text{initial stress change (lbf/in}^2) / \text{initial strain (\%)} * (100\%/1) * (1\text{ksi} * \text{in}^2 / 1000 \text{lbf})$
- Ultimate Tensile Strength (ksi): $\text{Maximun stress (lbf/ in}^2) * (1\text{ksi} * \text{in}^2 / 1000 \text{lbf})$
- Tensile strength at failure (ksi): $\text{failure tensile strength lbf} * (1\text{ksi} / 1000 \text{lbf})$
- Elongation to Failure (%): $\text{The final elongated length (in.)} / \text{original length (in.)} * 100(\%)$

F.3.4 Scanning Electron Microscopy (SEM)

The EVO 50 Carl Zeiss and the Joel JSM 6500F Scanning Electron Microscopes were used for the PVC and PP respectively for the Scanning Electron Microscopy (SEM) analysis. Two specimens were observed per material (PP and PVC) using SEM; a control specimen and a bio-oil treated specimen. Both sets of materials require coating prior to entering the SEM chamber due to the non-conductive properties. These specimens were coated with gold palladium (60% Au, 40% palladium) by sputtering for approximately 30 seconds which is equivalent to approximately 7 nm. To prevent charge effects in the chamber, the specimens were attached to the stub using carbon tape which was brought up the side of the sample to make contact with the surface of the specimen.

F.3.5 X-ray Photon Spectroscopy (XPS)

X-ray Photon Spectroscopy (XPS) was used to determination the surface chemistry of the two sets of polymer specimens. The Phi 1600 XPS Electron Scanning Chemical Analysis Instrument was used in conjunction with PHI surface analysis software version 3.0 (data collection) and analysis software CasaXPS. Initially a survey scan was conducted to detect the elements present and to calculate the atomic percentages. In addition a high resolution scans were conducted for the elements present in the survey scan. From the high resolution scan the data was then peak fitted for the determination of bonding for each element. In order to calculate the 95% confidence intervals for the data, three spots were analyzed for each specimen and the average, standard deviation, and 95% confidence intervals were calculated.

F.4 Results and Discussion

F.4.1 Bio-oil- pH

The pH of the bio-oil was measured using SevenEasy™ pH Meter S20 manufactured by Mettler Toledo which was calibrated using a three point calibration and phosphate buffer solutions with pH values of 4,7, and 10. The pH of the bio-oil was measured in triplicates to ensure the measurements were replicable. Figure F.3 displays the comparison of the average pH values for the control bio-oil stored in the refrigerator at 5 °C and the bio-oil that the PP and PVC were stored in at room temperature for three weeks. The error bars represent the 95% confidence intervals (95% CI) for each set of data.

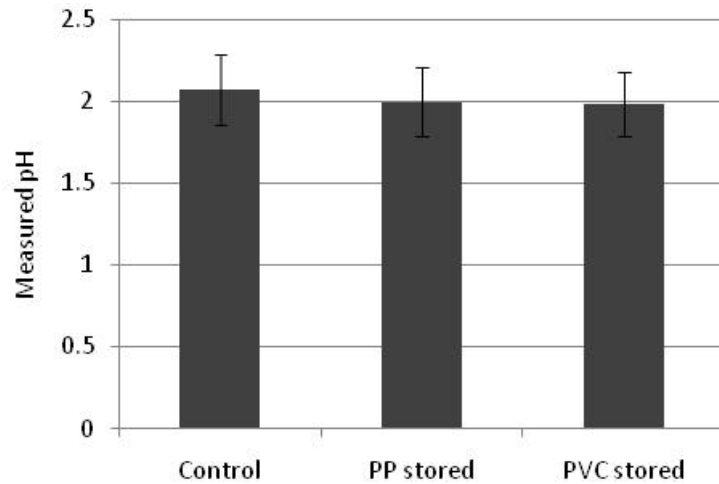


Figure F.3 Measured pH values of the control bio-oil and the bio-oil PP and PVC were stored in.

F.4.2 Bio-oil Treatment

When the specimens were removed from the bio-oil many of them had oily residue stuck to the surface at parts. In addition there were some pieces of biomass derived solids floating in the bio-oil. The specimens were washed with methanol until

the methanol was clear. A Kimwipe was then used to wash the specimens a second time and then dry them. The specimens were placed under vacuum for approximately 15 minutes to remove any residual solvent prior to weighing. The final weights were then measured.

When the two set of polymers were removed from the bio-oil there were several large pieces of chunks floating in the bio-oil which may be either biomass that was not pyrolyzed or char particles from the pyrolysis. When the specimens were removed from the bio-oil there was also oily globs attached to the surface that would not easily wash. The PP was stained to a distinct yellow where the PVC did not appear to have any visual change. The comparison of the control PP compared to the stained PP due to the bio-oil treatment is displayed in Figure F.4.

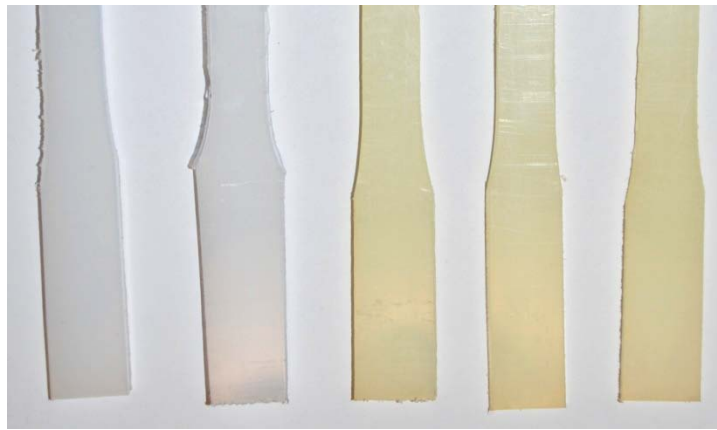


Figure F.4 Visual comparison of neat PP (left) to bio-oil treated PP (right).

In Figure F.5 the measured initial and final weights are displayed as a column graph for the polypropylene (PP) and polyvinyl chloride (PVC) with 95% CI error bars. When comparing the average change in weight for both sets of data there appears to be little to no change in the PVC specimens and a small decrease in weight in the PP

specimens. When comparing data and considering the 95% confidence intervals it the 95% CI encompass the initial and final average weights and therefore there small changed observed is not statistically significant. Therefore statistically there is no change in the weights due to the bio-oil treatment.

The previous corrosion study with bio-oil also determined that PP was very resistant to bio-oil corrosion due to no significant change in the weight in addition to polytetrafluoroethylene (PTFE) and high density polyethylene (HDPE)¹.

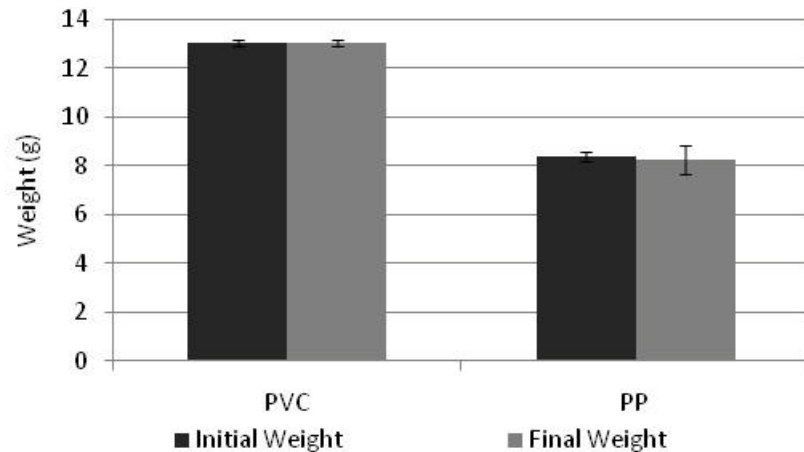


Figure F.5 Measured initial and final weights for the bio-oil treated PP and PVC specimens with 95% CI error bars.

F.4.3 Tensile Testing: PP

Initial characterization included visual observations of the general surface and fracture surface of each specimen prior to SEM analysis. When comparing PP and PVC, the PP specimens had a larger percent elongation for both control and bio-oil treated specimens, which indicates the material ductility. In contrast, the PVC specimens displayed a more brittle fracture for both the control and bio-oil treated specimens.

In Figure F.6 a visual comparison of the tensile test specimens for the control and bio-oil treated polypropylene is displayed. The PP specimens elongated during the tensile test and had a relatively ductile fracture due to the narrowing and elongation of the specimens. Also, many of the specimens curled at the fracture surface. Overall there is obvious difference in the fracture of the material other than the yellowing of PP after the bio-oil treatment.

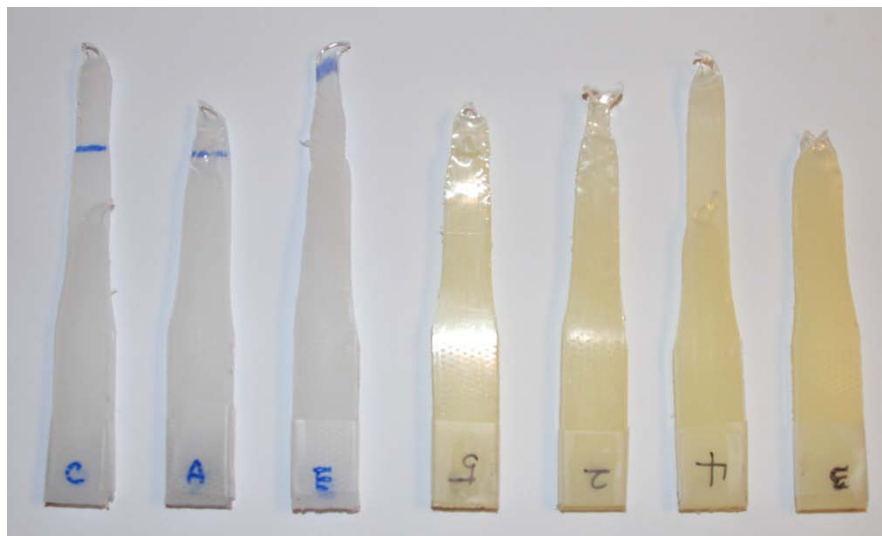


Figure F.6 Tensile testing specimens of the neat PP (left) and bio-oil treated PP (right).

In Table F.1, the mechanical properties calculated from the tensile testing data for the control PP are displayed including the average values, standard deviations and 95% confidence intervals. An outlier test was conducted using the Grubb's Test²⁴ for all properties. For the elongation to failure data it was determined that sample D with a value of 196.79 % was a significant outlier. Therefore this data point was excluded from the calculations for the average, standard deviation and 95% confidence interval. The average values for the Elastic modulus, tensile strength at failure, ultimate tensile strength

and elongation to failure were calculated to be 19.20 ksi, 0.96 ksi, 1.21 kis and 98.62 % respectively.

Table F.1 Calculated mechanical properties for the control polypropylene specimens including the average, standard deviation and 95% CI.

PP: Control	Elastic Modulus(ksi)	Tensile Strength at Failure (ksi)	Ultimate Tensile Strength(ksi)	Elongation to Failure (%)
A	18.24	0.93	1.32	96.74
B	18.92	0.92	1.43	96.66
C	19.15	0.96	1.41	97.08
D	20.00	1.00	1.47	196.79*
E	19.71	1.01	1.44	104.00
Average	19.20	0.96	1.41	98.62
Std Dev	0.69	0.04	0.06	3.59
95% CI	0.60	0.04	0.05	3.52

* indicates a significant outlier which is not included in calculations

In Table F.2, the mechanical properties calculated from the tensile testing data for the bio-oil treated PP are displayed including the average values, standard deviations and 95% confidence intervals. The Grubb's Test was also conducted for all of the properties to identify any outliers. The ultimate tensile strength (UTS) for sample 1 was determined to be a significant outlier and therefore was not used in calculations. The average values for the Elastic modulus, tensile strength at failure, ultimate tensile strength and elongation to failure were calculated to be 18.70 ksi, 0.95 ksi, 1.49 kis and 94.04 % respectively.

When comparing the mechanical properties in Tables F.1 to those of the bio-oil treated specimens in Table F.2 there a slight increase in the ultimate tensile strength and a small decrease in the elongation to failure %. When comparing the averages as well as the 95% CI for the UTS there is no statistical significant difference observed due to the overlap of the 95% confidence intervals.

Table F.2 Tensile test results from the collected data the bio-oil treated polypropylene specimens.

PP: Bio-oil treated	Elastic Modulus(ksi)	Tensile Strength at Failure (ksi)	Ultimate Tensile Strength(ksi)	Elongation to Failure (%)
1	11.25	0.51	0.81*	71.93
2	19.25	0.93	1.43	132.04
3	19.73	0.99	1.44	84.06
4	20.30	1.01	1.45	86.56
5	22.99	1.31	1.64	95.60
Average	18.70	0.95	1.49	94.04
Std Dev	4.41	0.29	0.10	22.86
95% CI	3.87	0.25	0.10	20.04

* indicates a significant outlier which is not included in calculations

Table F.3 displays the average mechanical properties for the control and bio-oil treated PP specimens. The percent reduction of each property is also presented. Table F.3 demonstrates the small increase in the UTS as well as the small decrease in the elongation to failure. Unfortunately these changes are not statistically significant. Figure F.7 displays the UTS and tensile strength at failure with 95% CI error bars. This Figure gives a good visual representation of how the 95% CI encompass the averages of the control and bio-oil treated properties and therefore show no change in the mechanical properties.

Table F.3 Comparison of the mechanical properties of the control and bio-oil treated polypropylene.

Treatment	Elastic Modulus (ksi)	Tensile Strength at Failure (ksi)	Ultimate Tensile Strength (ksi)	Elongation to Failure (%)
Control (Avg.)	19.2	0.96	1.41	98.62
Bio-oil (Avg.)	18.7	0.95	1.49	94.04
% Change	-2.6%	-1.0%	5.7%	-4.6%

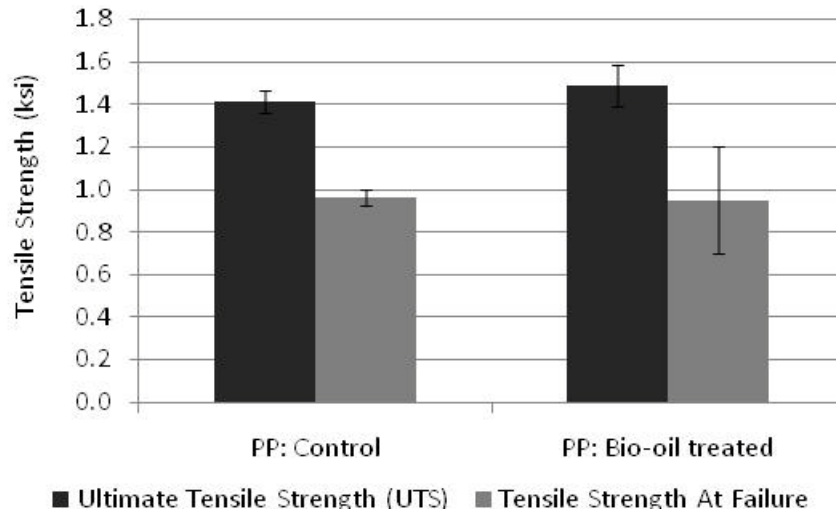


Figure F.7 Ultimate Tensile Strength (UTS) and Tensile strength at Failure displayed for PP control and bio-oil treated averages including 95% CI error bars.

As discussed in Figure F.1, the thermal degradation of PP at 120 °C for 20 days resulted in a 2.4 % decrease in tensile strength and 11.5 % decrease in elongation to failure²⁰. For the bio-oil treated PP a 1.0 % decrease in tensile strength at failure, 5.7 % increase in ultimate tensile strength and 4.6 % decrease in elongation to failure was observed. These observed changes are less than those observed in the thermal degradation of PP (Figure F.1). From the data presented in Figure F.1 (Hu, 2006), it was concluded that the thermal oxidation aging did not affect the mechanical properties significantly. This also supports the conclusion that the effect of bio-oil was

F.4.4 Tensile Testing: PVC

In Figure F.8 a visual comparison of the tensile test specimens for the control and bio-oil treated polyvinyl chloride is displayed. Both sets of specimens display a relative brittle fracture where there was a low percentage of elongation and a jagged fractured surface. Overall there is no significant difference in the specimens.

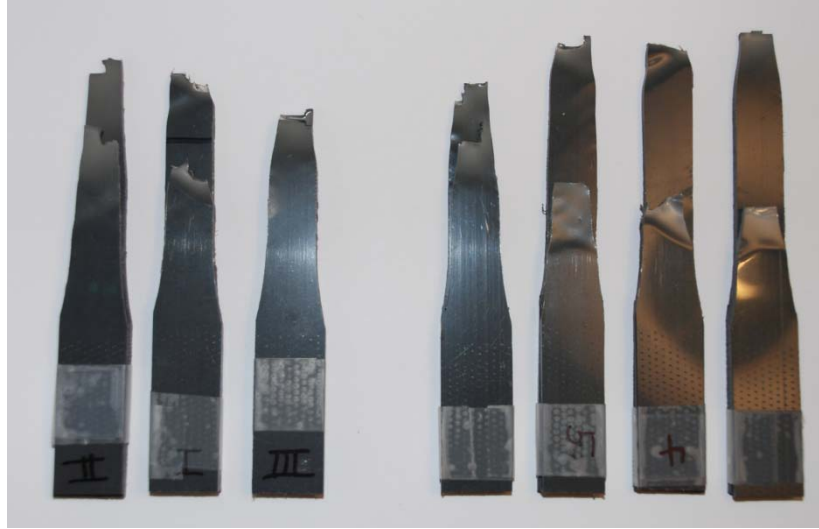


Figure F.8 Tensile testing specimens of the neat PVC

Table F.4 displays the average mechanical properties for the control PVC specimens including the average, standard deviation and 95% confidence interval. There are no significant outliers in the data. The average values for the Elastic modulus, tensile strength at failure, ultimate tensile strength and elongation to failure were calculated to be 167.76 ksi, 6.37 ksi, 9.11 ksi and 26.72 % respectively.

Table F.4 Tensile test results from the collected data the control polyvinyl chloride specimens

PVC: Control	Elastic Modulus(ksi)	Tensile Strength at Failure (ksi)	Ultimate Tensile Strength(ksi)	Elongation to Failure (%)
I	166.96	6.58	9.07	13.16
II	169.30	6.01	9.15	37.80
III	167.31	6.21	9.15	24.13
IV	166.83	6.23	9.13	35.39
V	168.42	6.80	9.07	23.11
Average	167.76	6.37	9.11	26.72
Std Dev	1.06	0.32	0.04	10.02
95% CI	0.93	0.28	0.03	8.78

Table F.5 displays the average mechanical properties for the control PVC specimens including the average, standard deviation and 95% confidence interval. No significant outliers were found when conducting the Grubb's Test. The average values for the Elastic modulus, tensile strength at failure, ultimate tensile strength and elongation to failure were calculated to be 165.71 ksi, 6.01 ksi, 8.98 ksi and 22.91 % respectively.

When comparing the mechanical properties of the control PVC in Table F.4 to the bio-oil treated PVC properties in Table F.5 there was a 1.2% decrease in the elastic modulus, a 5.7% decrease in tensile strength at failure, a 1.4% decrease in ultimate tensile strength, and a 14.3 % decrease in elongation to failure. The summary of the percent reduction of the mechanical properties is displayed in Table F.6. When comparing these values and considering the 95% confidence intervals there is not statistically significant change in the mechanical properties due to the overlap of the 95% CI and the averages.

Table F.5 Tensile test results from the collected data the bio-oil treated polyvinyl chloride specimens.

PVC: Bio-oil treated	Elastic Modulus(ksi)	Tensile Strength at Failure (ksi)	Ultimate Tensile Strength(ksi)	Elongation to Failure (%)
1	162.58	6.04	8.83	18.85
2	164.82	5.80	8.92	24.73
3	169.24	5.80	8.96	22.76
4	168.64	6.38	9.12	19.66
5	163.27	6.02	9.09	28.54
Average	165.71	6.01	8.98	22.91
Std Dev	3.07	0.24	0.12	3.94
95% CI	2.69	0.21	0.10	3.45

Table F.6 Comparison of the mechanical properties of the control and bio-oil treated polyvinyl chloride.

Treatment	Elastic Modulus (ksi)	Tensile Strength at Failure (ksi)	Ultimate Tensile Strength(ksi)	Elongation to Failure (%)
Control (Ave.)	167.76	6.37	9.11	26.72
Bio-oil (Ave.)	165.71	6.01	8.98	22.91
% Change	-1.2%	-5.7%	-1.4%	-14.3%

In Figure F.9 the comparison of the ultimate tensile strength and tensile strength at failure are visually compared for the control and bio-oil treated bio-oil specimen data including 95% CI error bars. Figure F.9 allows for a visual representation of the 95% CI overlap demonstrating there is no statistically difference between the mechanical properties for the two sets of specimens.

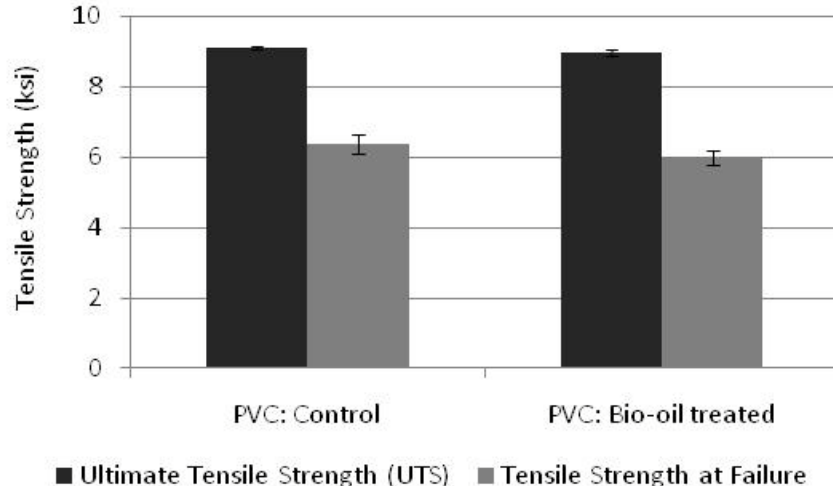


Figure F.9 Ultimate Tensile Strength (UTS) and Tensile strength at Failure displayed for PVC control and bio-oil treated averages including 95% CI error bars.

F.4.5 SEM: PP

One specimen from the control and bio-oil treated PP were chosen for SEM analysis. Figure F.10 displays the comparison of the control and bio-oil treated PP at the surface of the tensile specimens at 500 x and 10 kx. In Image (b) there are cracks present on the surface of the specimen where in image (a) there is no cracking observed. In addition the surface of the bio-oil treated specimen in image (d) has a rough surface where image (c) does not have as much. These differences could be due to the exposure to bio-oil or due to the tensile testing. In order to determine what caused the difference in the surface addition material would need to be compared that did not undergo tensile testing. In addition multiply specimens would need to be examined.

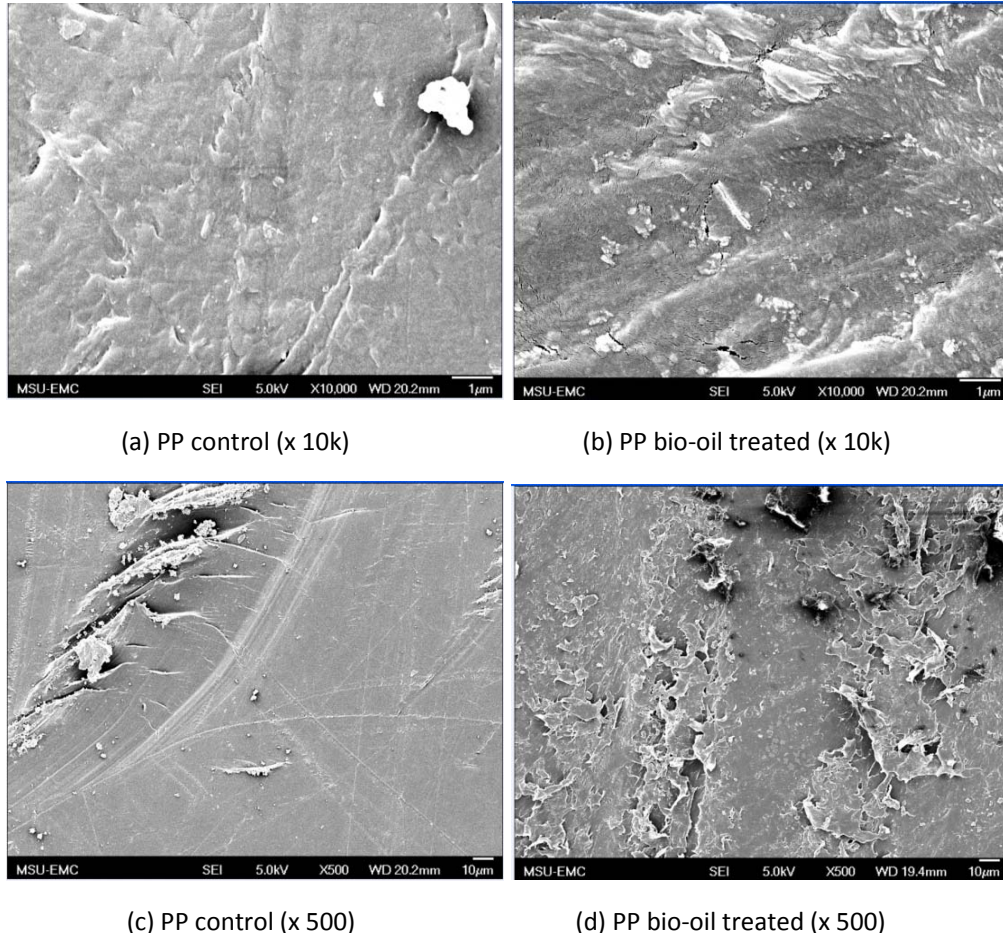


Figure F.10 SEM images for general surfaces of PP control and PP bio-oil treated (a) PP control (x 10k), (b) PP bio-oil treated (x 10k), (c) PP control (x 500), (d) PP bio-oil treated (x 500)

Figure F.11 (Hu, 2006) displays the change of a PP surface by 105 days of thermal degradation at 120 °C. The thermal degradation of the PP in Figure F.11 resulted in grooves and cracking of the surface at 5 kx. When comparing the bio-oil treated PP at 10 kx in Figure F.10 there are no linear grooves in the surface but some cracking. The thermal degradation for 105 days in Figure F.11 caused deep grooves and more cracks on the surface of PP. The thermal degradation of the PP appears to be have affected the PP more than the bio-oil. In order to get a better comparison PP should be treated for the

same time period (105 days) and the SEM images should be at the same magnification (5 kx).

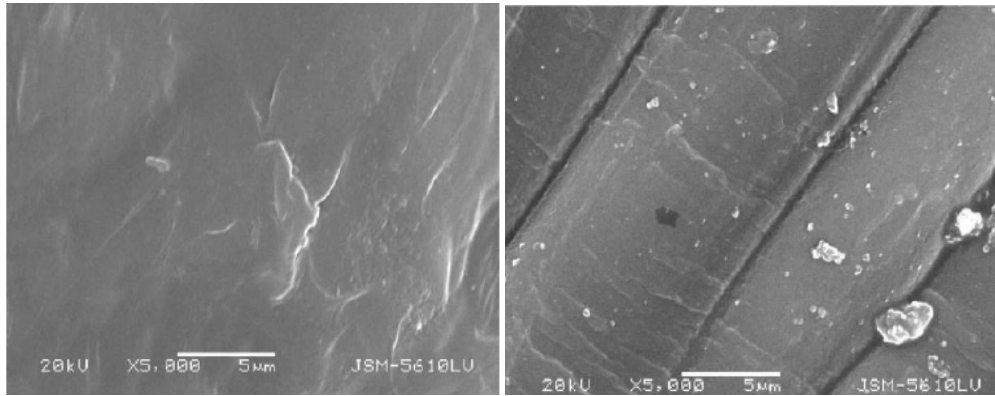


Figure F.11 SEM images for general surfaces on PP control and PP thermally degraded Left PP control (x 5000), Right PP thermally degraded (x 5000) [from Hu, 2006 , PP after thermal degradation of 105 days²⁰].

Figure F.12 displays the comparison of the control and bio-oil treated PP at the fractured surface of the tensile specimens at 200-250 x and 1.5 kx. When comparing images (a) and (b) there does not appear to be any significant difference where fracture surfaces look similar. In addition there are ripples observed in both images which are due to the elongation during tensile testing followed by contracting after the failure of the sample. When comparing images (c) and (d), it is difficult to compare the two images due to image (d) have very little of fractured surface visible.

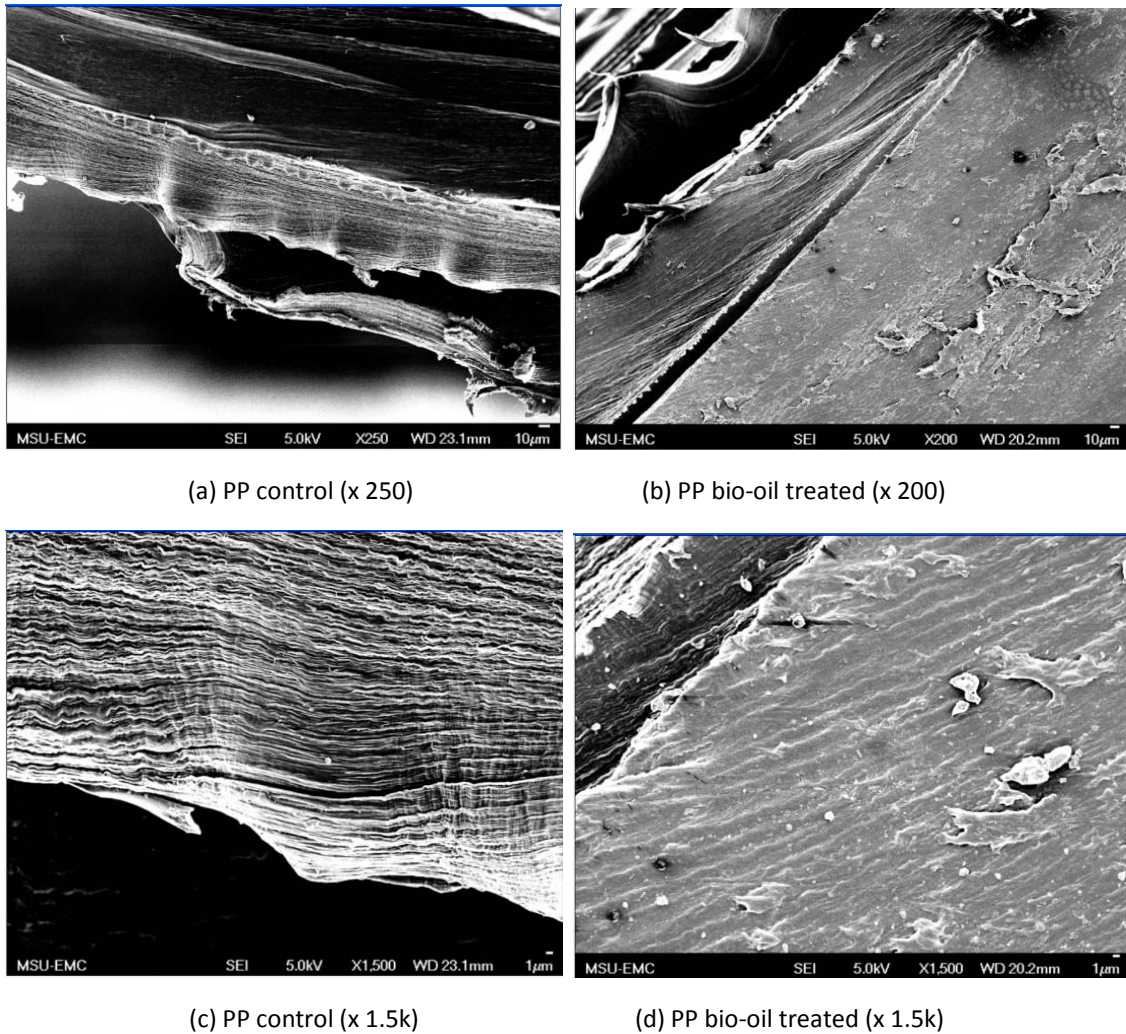
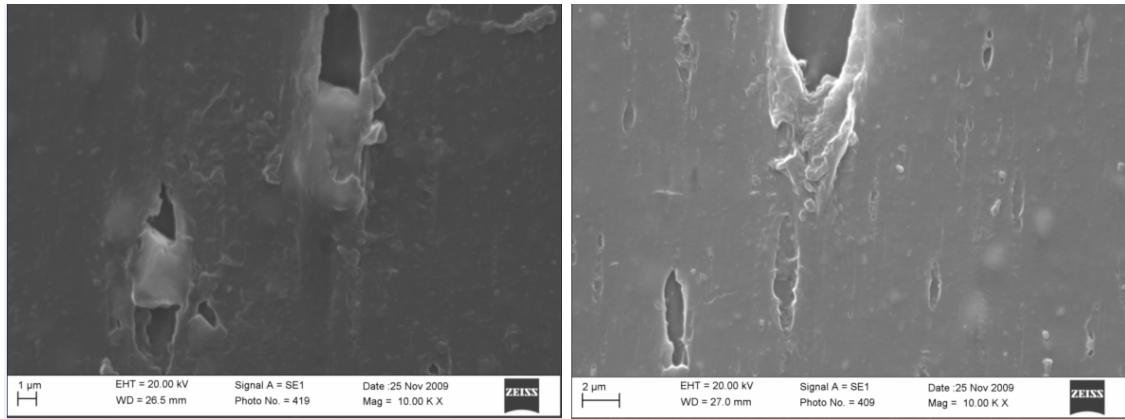


Figure F.12 SEM images for fracture surfaces of PP control and PP bio-oil treated (a) PP control, (x 250), (b) PP bio-oil treated (x 250), (c) PP control (x 1.5k), (d) PP bio-oil treated (x 1.5k)

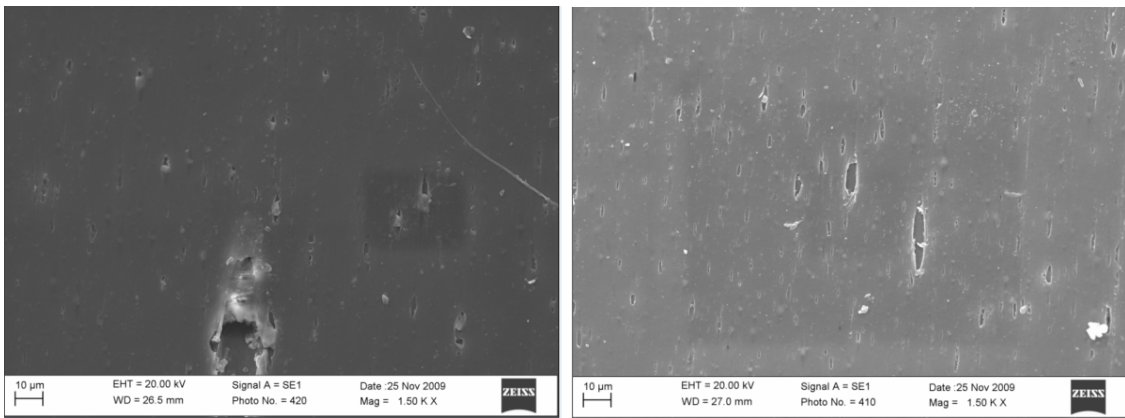
F.4.6 SEM: PVC

Figure F.13 displays the comparison of the control and bio-oil treated PVC at the general surface of the tensile specimens at 10 kx and 1.5 kx. All the images in Figure F.13 display holes that are in the surface of the specimens. These holes are present in both the control and bio-oil treated specimens therefore they may be due to the processing of the material or possible due to the tension testing.



(a) PVC control (x 10k)

(b) PVC bio-oil treated (x 10k)



(c) PVC control (x 1.5k)

(d) PVC bio-oil treated (x 1.5k)

Figure F.13 SEM images for general surfaces on PVC control and PVC bio-oil treated (a) PVC control (x 10k), (b) PVC bio-oil treated (x 10k), (c) PVC control (x 1.5k), (d) PVC bio-oil treated (x 1.5k)

Figure F.14 displays the comparison of the control and bio-oil treated PVC at the fracture surface of the tensile specimens at 200 x and 500 x. At magnifications higher than 500 the electron beam visibly deformed parts of the specimens. When comparing the control images (a) and (c) to the bio-oil treated images (b) and (d) there is a significant difference which indicates a change in the ductility on the PVC specimen. The control images of the PVC (a and c) display a stretched fracture surface characteristic of a ductile fracture while the bio-oil treated PVC images (b and d) display a relatively clean fracture surface which is characteristic of a brittle fracture. This may be an indicator that

the bio-oil treatment altered the PVC to cause a more brittle fracture of the material. When comparing these results to the mechanical properties from the tensile testing there was a decrease in the elongation to failure and the tensile strength at failure. These may be two indications that the material became more brittle after the bio-oil treatment.

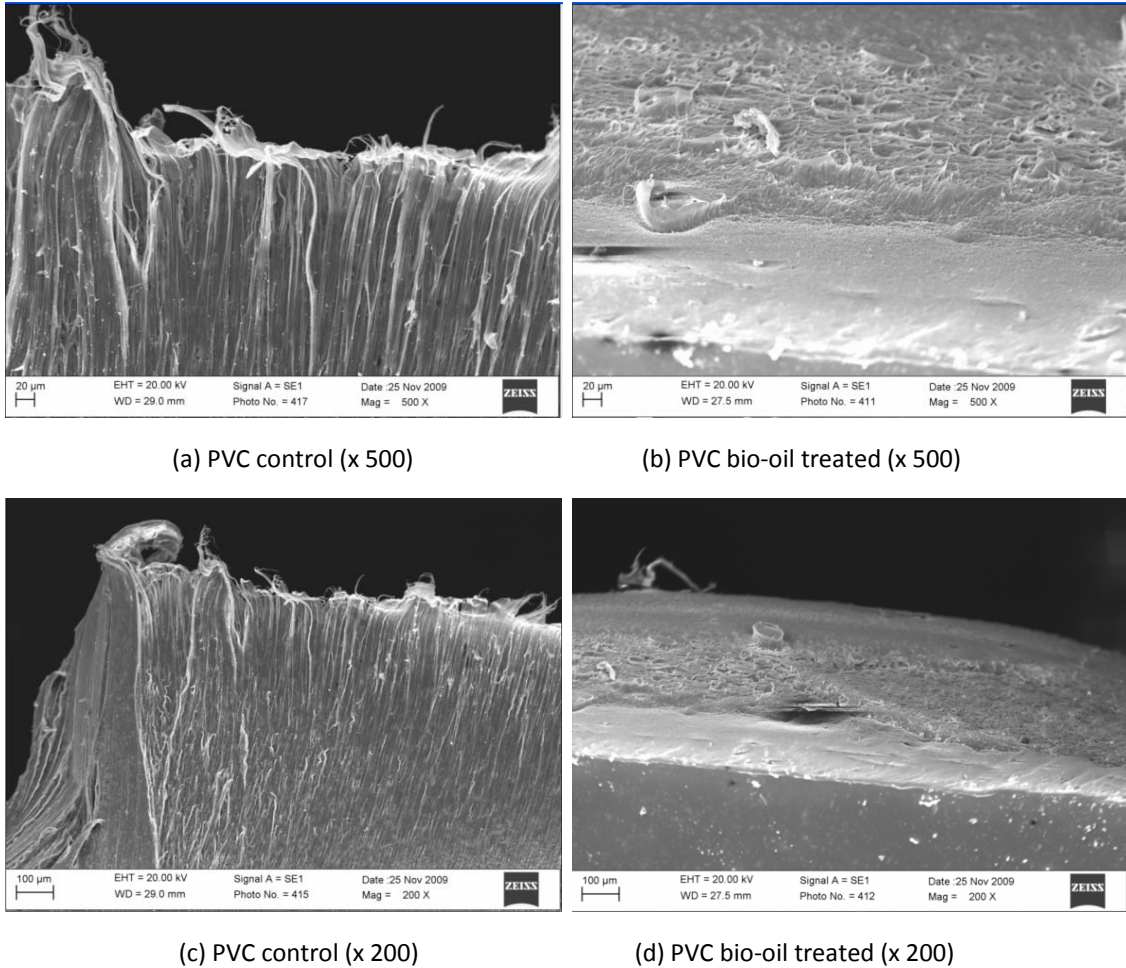


Figure F.14 SEM images for fracture surfaces on PVC control and PVC bio-oil treated (a) PVC control (x 500), (b) PVC bio-oil treated (x 500), (c) PVC control (x 200), (d) PVC bio-oil treated (x 200).

F.4.7 XPS Analysis: PP

Figure F.15 displays the repeating structure of polypropylene demonstrates that the polymer is constructed strictly of carbon and hydrogen. When examining the

elemental composition of the polymer using XPS it would be expected to only find carbon because the instrument cannot detect hydrogen.

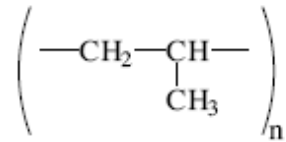


Figure F.15 The structures of polypropylene¹⁶.

Figure F.16 displays the atomic percentages obtained from the analysis of the survey scan of the XPS data. The displayed values are averages of three spots with 95% CI error bars. It was expected that only carbon would be present but there was approximately 3 % oxygen in the control specimen due to possible surface contamination or a polymer additive such as a plasticizer or antioxidant. When comparing the control PP to the bio-oil treated PP there is a statistically significant difference between the atomic percentages of the carbon, oxygen and silicon. Also, in the bio-oil treated specimen there is approximately 17% silicon. The presence of the silicon is due to either the contamination of the bio-oil with silicon or possibly the bio-oil leached silicon from the glass jar used for storage. In addition to the presence of silicon there is an increase of oxygen to 11 % from 3 %. The increase in oxygen is a statistically significant increase because the 95% confidence intervals do not overlap.

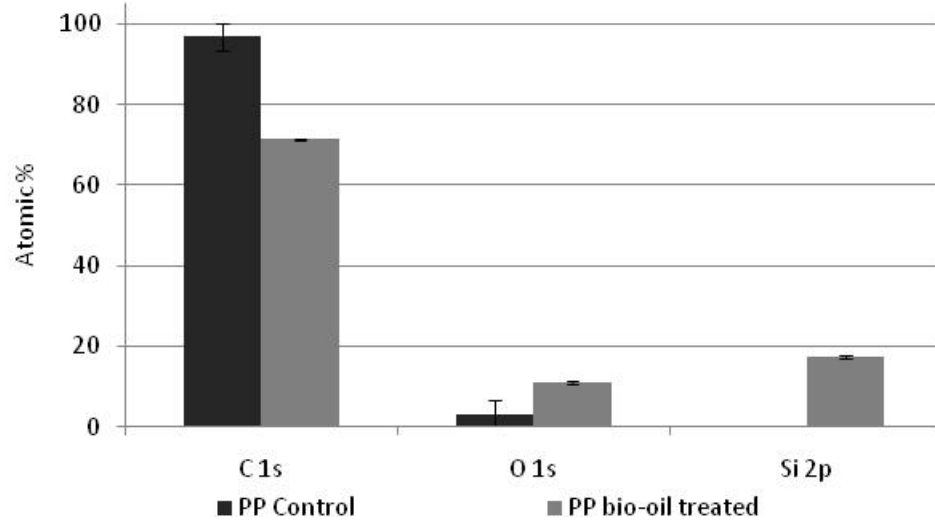


Figure F.16 Atomic percentages obtained by XPS compared for the control and bio-oil treated PP specimens.

Figure F.17 displays an example of the peak fitting results for the C 1s peak of a control PP specimen. It was determined that three peaks were present in the carbon peak. There were shifts in all of the peaks due to charging resulting from the insulating nature of the polymer. A correction was made which set the $-CH_n$ peak bonding energy to 285.0 eV^{15,18}. The largest peak is due to the $-CH_n$ bonding in the center. The peak to the left at 286.6 eV is due to the $-C-OH$ bonding. In addition the small peak to the right of the $-CH_n$ peak is added to account for charge broadening^{15,18}.

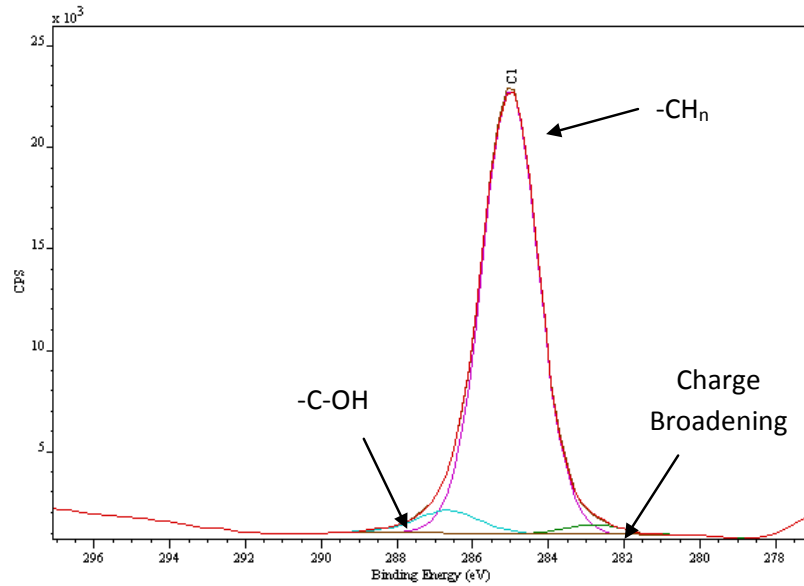


Figure F.17 An Example of the C 1s peak fitting for a control PP specimen.

Figure F.18 displays an example of the peak fitting results for the C 1s peak of a bio-oil treated PP specimen. The same correction was used setting the $-CH_n$ peak bonding energy to 285.0 eV^{15,18} to account for the shift due to charging. The C 1s peak fitting for the bio-oil treated specimen still has three peaks where the largest peak is due to the $-CH_n$ bonding in the center. The peak to the left at 286.6 eV is due to the $-C-OH$ bonding and the small peak to the right of the $-CH_n$ peak is added to account for charge broadening^{15,18}. There is no significant change in the appearance of the peaks and no addition peaks present after the bio-oil treatment.

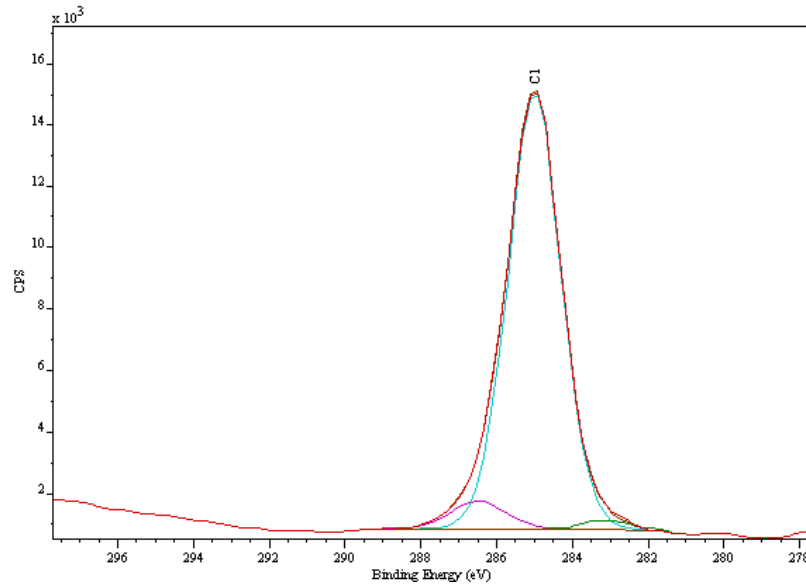


Figure F.18 An Example of the C 1s peak fitting for a bio-oil treated PP specimen.

Table F.7 displays the peak fitting results for the control PP C 1s peak including the position and area % for each of the three peaks. Also included are the total peak area and the chi squared value indicating the goodness of the peak fit. The area % was calculated using the area for the individual peak divided by the total area of the peak and the position is after the charging effect correction. The third spot had a different shaped peak when compared to the other two and the area percentages reflect the difference. This difference could be due to either variation in the surface or possibly a dirty or contaminated surface.

Table F.7 The peak fitting results for the high resolution XPS data of the control PP C 1 s peak.

Spot #	Total peak Area	Charge broadening		-CH _n		-C-OH		Chi Squared
		Position	Area %	Position	Area %	Position	Area %	
1	43969.9	282.77	2.03%	285.00	92.92%	286.66	5.07%	31.3
2	45641.5	282.80	2.03%	285.00	91.66%	286.61	6.21%	43.3
3	40723.6	282.86	9.12%	285.00	85.14%	286.76	5.62%	21.3
	Avg.	282.81	4.40%	285.00	89.91%	286.68	5.64%	
	Std Dev	0.04	4.09%	0.00	4.17%	0.08	0.57%	
	95% CI	0.05	4.63%	0.00	4.72%	0.09	0.64%	

Table F.8 displays the peak fitting results for the bio-oil treated PP C 1s peak including the position and area % for each of the three peaks. The area % was calculated in the same manner as in Table F.7. When comparing the results of the control PP in Table 7 to the bio-oil treated PP in Table 8 there is no statistical difference in the area percentages of the three peaks. This demonstrates that there is no change in the carbon-carbon bonds or the carbon-oxygen bonds. This is unexpected due to the increase in oxygen and silicon in the survey scan. If there was an increase in the amount of carbon-oxygen bonding then the peak area percentage should also increase. This indicates that the oxygen increase indicated in the survey scan is not a carbon-oxygen bond but rather a silicon-oxygen bond.

Table F.8 The peak fitting results for the high resolution XPS data of the bio-oil treated PP C 1 s peak.

Spot #	Total peak Area	Charge broadening		-CH _n		-C-OH		Chi Squared
		Position	Area %	Position	Area %	Position	Area %	
1	26981.3	283.14	1.91%	285.00	91.76%	288.77	6.39%	28.8
2	27127.5	282.93	2.49%	285.00	91.96%	288.90	5.50%	30.8
3	27232.3	282.87	2.05%	285.00	93.15%	289.01	4.69%	24.5
	Avg.	282.98	2.15%	285.00	92.29%	288.89	5.53%	
	Std Dev	0.14	0.30%	0.00	0.75%	0.12	0.85%	
	95% CI	0.16	0.34%	0.00	0.85%	0.14	0.96%	

Figure F.19 displays an example of the peak fitting results for the Si 2p peak of a bio-oil treated PP specimen. There is only one peak present which has a peak position of 102.5 eV. When comparing the peak position after the correction to the reference manual PHI Chemical States²³ the expected position for Si is 99.45 eV and SiO₂ is 103.5 eV. These two values are not close to the peak position determined from the high resolution scan and changing the peak fitting does not change the position of the major peak. The possible silicon compounds that have peak positions in the range of 102 eV are presented in Table F.9²³. When examining Table F.9 it can be observed that all of the possibilities are minerals containing silicon, oxygen and all but one contain aluminum.

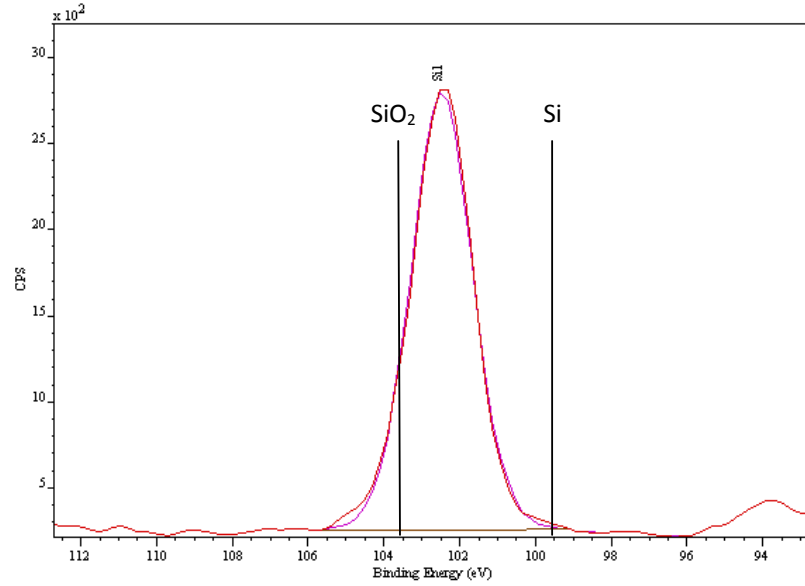


Figure F.19 An Example of the Si 2p peak fitting for a bio-oil treated PP specimen.

Table F.9 The potential minerals responsible for the Si peak in the bio-oil treated PP specimens^{23,24}.

Name	Peak Position (eV)	Chemical Formula
Kaolinite	102.65	$Al_4H_8O_{18}Si_4$
Kaolinite	102.98	$Al_4H_8O_{18}Si_4$
Mica, Muscovite	102.36	$Al_2Fe_2H_2K_2O_{10}Si$
Natrolite	102.22	$Na_2Al_2Si_3O_{10} \cdot 2H_2O$.
Pyrophyllite	102.88	Al_2O_5Si
Sillimanite	102.64	Al_2O_5Si
Spodumene	102.46	$AlLiO_6Si_2$
Kyanite	102.80	Al_2O_5Si
Sillimanite	102.60	Al_2O_5Si
Albite	102.63	$AlNaO_8Si_3$
Wollastonite	102.36	CaO_3Si

After determining that the silicon and oxygen were potentially from a mineral embedded in the polymer the survey scan was then reexamined for aluminum and calcium. Figure F.20 displays a section of the survey scan with lines indicating where the

silicon and aluminum peaks should be present. The lines were generated using the XPS analysis software. The silicon peaks are shifted to the left some and there is no evidence indicating the presence of aluminum. Figure F.21 displays a similar section of the survey scan displaying where the oxygen 1s peak appears where the calcium peaks should appear. In the area where there the calcium 2s and 2p peaks should appear there are also no peaks present. This suggests that none of the minerals listed in Table F.9 are present in the bio-oil treated PP. It may be possible that a different mineral is present or something similar.

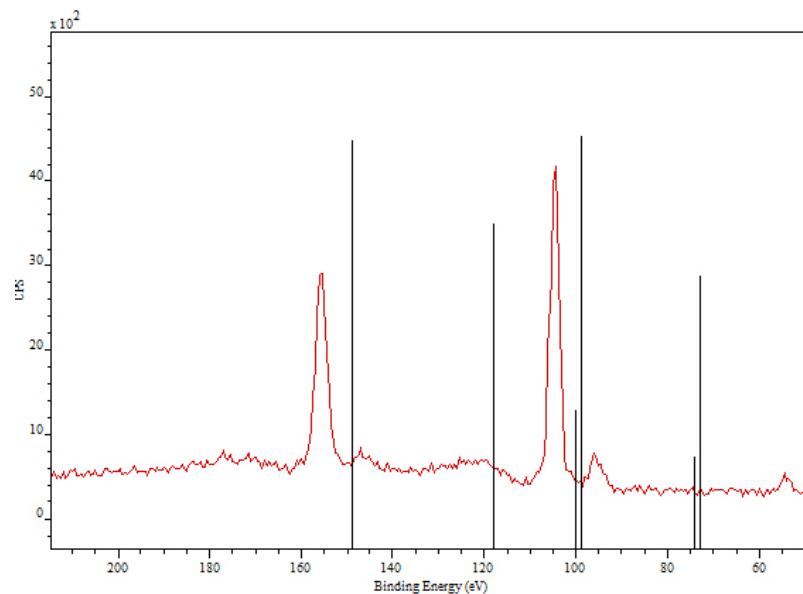


Figure F.20 A section of the survey scan displaying the silicon peaks.

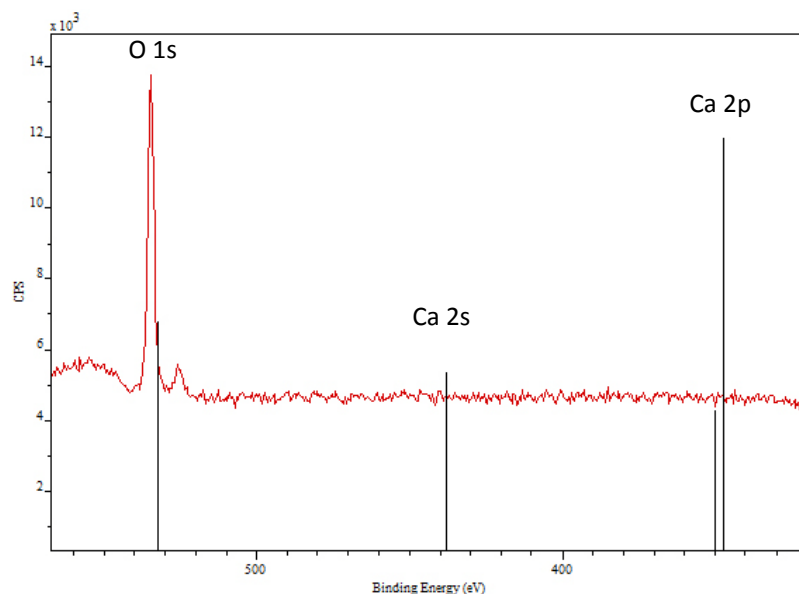


Figure F.21 A section of the survey scan displaying the Oxygen peak.

F.4.8 XPS Analysis: PVC

Figure F.22 displays the repeating structure of polypropylene demonstrates that the polymer is constructed strictly of carbon and hydrogen. When examining the elemental composition of the polymer using XPS it would be expected to only find carbon because the instrument cannot detect hydrogen.

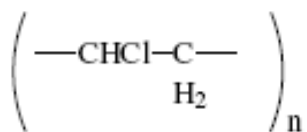


Figure F.22 The structures of polyvinyl chloride¹⁷.

In Figure F.23 the comparison of the atomic percentages for control and bio-oil treated PP and PVC are displayed. The error bars displayed with the data are the 95% confidence intervals. When comparing the atomic percentage of carbon in the PP there is a significant decrease due to the bio-oil treatment. In addition there is also a statistically significant decrease in the carbon atomic percentage in the PVC due the bio-oil treatment.

In both the PP and PVC specimens there was also a statistically significant increase in the oxygen atomic percentages due to the bio-oil treatment. The original oxygen content is most likely due to contamination and the bio-oil provided further contamination of oxygen. This is not an unreasonable assumption due to the high oxygen content of the bio-oil.

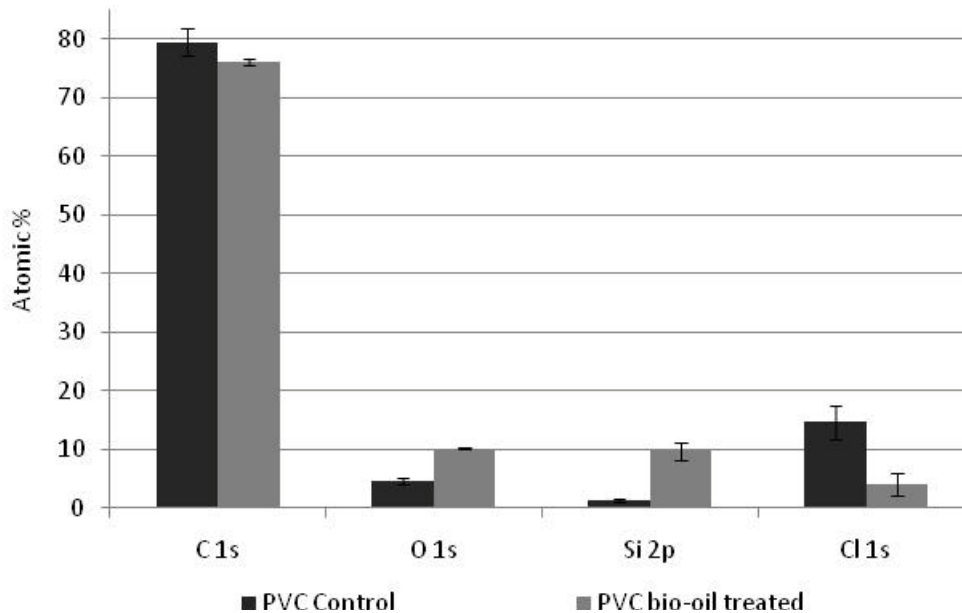


Figure F.23 The atomic percentages obtained by XPS compared for the control and bio-oil treated specimens for PP and PVC.

Figure F.24 displays an example of the peak fitting results for the C 1s peak of a control PVC specimen. It was determined that four peaks were present in the carbon peak. There were shifts in all of the peaks due to charging resulting from the insulating nature of the polymer. A correction was made which set the $-CH_n$ peak bonding energy to 285.0 eV^{15,18}. The largest peak is due to the $-CH_n$ bonding in the center. The peak to the immediate left at ~286 eV is due to the $-C-OH$ bonding. In addition the small peak to the right of the $-CH_n$ peak is added to account for charge broadening^{15,18} and the peak to

the far left is due to the -C-Cl bonding¹⁷. It is not expected that the oxygen peak would be larger than the chlorine peak when the concentration of the oxygen is less than the chlorine as determined in the survey scan. This may indicate a flaw in the peak fitting.

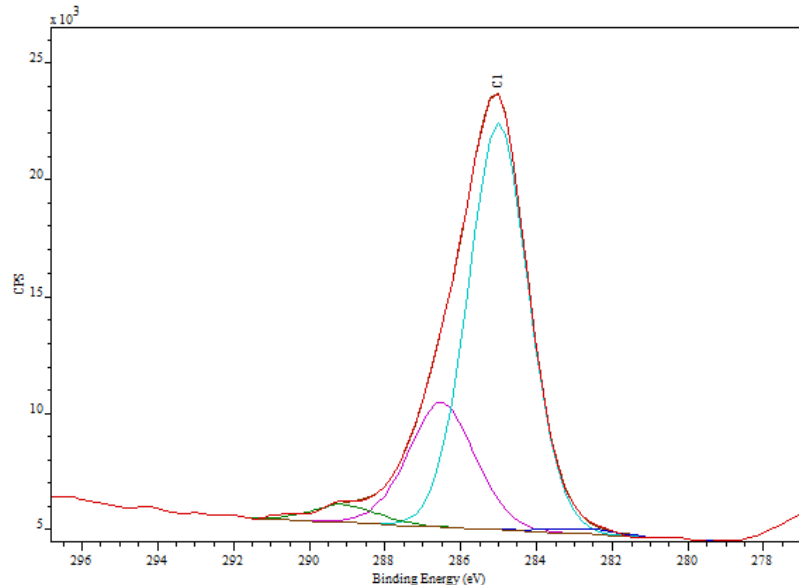


Figure F.24 An Example of the C 1s peak fitting for a control PVC specimen.

Figure F.25 displays an example of the peak fitting results for the C 1s peak of a bio-oil treated PVC specimen. There are also four peaks present in the carbon peak after the bio-oil treatment. There correction was made for the charging effect. There is no significant difference in the appearance of the peak fitting. The oxygen peak in the control specimen appears to be larger when compared to the bio-oil treated specimen. There were no additional peaks present in the peak fitting due to the bio-oil treatment.

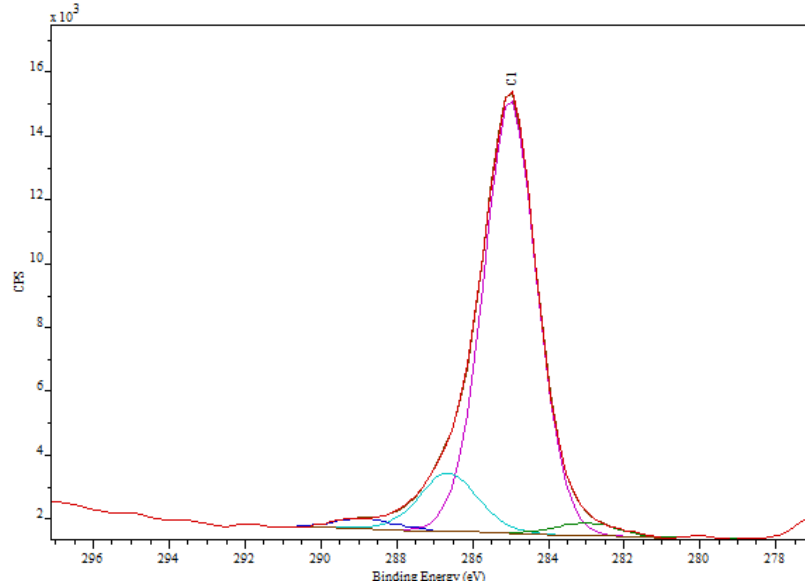


Figure F.25 An Example of the C 1s peak fitting for a bio-oil treated PVC specimen.

Table F.10 displays the peak fitting results for the control PVC C 1s peak including the position and area % for each of the three peaks. Also included are the total peak area and the chi squared value indicating the goodness of the peak fit. The area % was calculated using the area for the individual peak divided by the total area of the peak and the position is after the charging effect correction. The percentage of the oxygen bonding when compared to the chlorine bonding does not match the survey scan percentages as discussed earlier.

Table F.10 Peak fitting results for the high resolution XPS data of the control PVC C 1s peak.

Spot #	Total peak Area	Charge broadening		-CH _n		-C-OH		-C-Cl		Chi Squared
		Position	Area %	Position	Area %	Position	Area %	Position	Area %	
1	48899.4	282.80	0.95%	285.00	71.50 %	286.51	24.15 %	289.06	3.38%	16.45
2	50424.8	282.75	1.54%	285.00	73.08 %	286.47	22.53 %	288.75	2.88%	13.69
3	49670.2	282.62	0.93%	285.00	77.81 %	286.48	17.89 %	288.90	3.30%	23.56
	Avg.	282.72	1.14%	285.00	74.13 %	286.49	21.52 %	288.90	3.19 %	
	Std Dev	0.09	0.35%	0.00	3.28%	0.02	3.25%	0.15	0.27%	
	95% CI	0.11	0.40%	0.00	3.71%	0.02	3.67%	0.17	0.30%	

Table F.11 displays the peak fitting results for the bio-oil treated PVC C 1s peak including the position and area % for each of the three peaks. The area % was calculated in the same manner as in Table F.10. There is a statically significant difference in the area percentages of -CH_n bonding and the -C-OH bonding where the -CH_n bonding increased after the bio-oil treatment and the -C-OH bonding decreases after the treatment. This suggests that the oxygen increase is not due to the oxygen bonding with carbon but rather the oxygen is bonded with another element such as silicon as observed in the PP specimen. In addition the decrease in the carbon-oxygen content may be due to the interaction of the bio-oil with the PVC specimen. The oxygen could be bonding with the silicon separately or with compounds in the bio-oil.

Table F.11 The peak fitting results for the high resolution XPS data of the bio-oil treated PVC C 1 s peak.

Spot #	Total peak Area	Charge broadening		-CH _n		-C-OH		-C-Cl		Chi Squared
		Position	Area %	Position	Area %	Position	Area %	Position	Area %	
1	28931.9	282.98	2.78%	285.00	82.65 %	286.63	12.36 %	288.87	2.23%	23.46
2	29114.3	282.97	2.54%	285.00	80.37 %	286.67	15.53 %	288.75	2.54%	15.13
3	28929.7	282.91	1.51%	285.00	81.00 %	286.64	15.46 %	288.79	2.08%	10.08
	Avg.	282.95	2.28%	285.00	81.34 %	286.65	14.45 %	288.80	2.28 %	
	Std Dev	0.04	0.67%	0.00	1.18%	0.02	1.81%	0.06	0.23%	
	95% CI	0.04	0.76%	0.00	1.33%	0.02	2.05%	0.07	0.26%	

Figure F.26 displays the peak fitting results for the silicon 2p peak in a bio-oil treated PVC specimen XPS data. As observed in the PP specimens the silicon peak fitting resulted in one peak. The position of the Si 2p peak is at 102.4 eV which is relatively the same position observed for the PP specimens. This suggests that the silicon is bonded to oxygen in a mineral that is absorbed in the polymer. This may account for the increase in oxygen in the survey scan when there was a decrease in the carbon-oxygen bonding. On the other hand it does not explain what is causing the decrease in carbon-oxygen bonding.

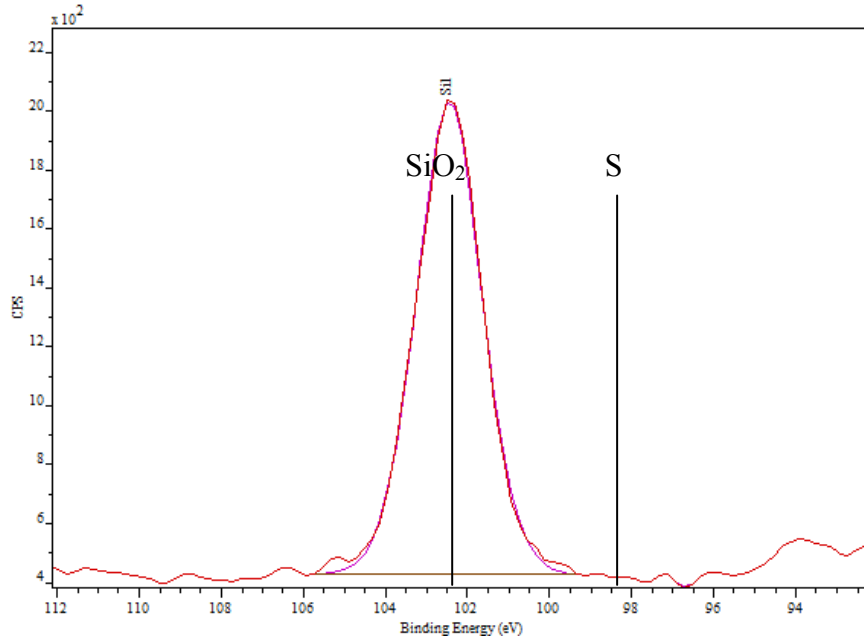


Figure F.26 An Example of the Si 2p peak fitting for a bio-oil treated PVC specimen.

F.5 Conclusions

There was no statistically significant change in the pH of the bio-oil after storage of the polymer specimens nor was there a statistically significant change in the weights of the polymer specimens after storage of bio-oil for three weeks. The tensile test results do not demonstrate a change in the mechanical properties of polypropylene due to storage in bio-oil for three weeks.

There were some changes observed in the SEM analysis including a roughness of the bio-oil treated PP as well as cracking in the surface of the PP. Also the fracture surface of the PVC appeared to become more brittle after the bio-oil treatment.

The XPS survey scan analysis displayed an increase in oxygen and silicon concentrations after the bio-oil treatment for both the PP and PVC specimens. The XPS high resolution peak fitting displayed no significant change in the peak positions or areas of the carbon 1s peaks for both the PP specimens. The lack of change in the carbon 1s

peak indicates that there is not additional oxygen bonding due to the bio-oil treatment. The PVC carbon 1s peak fitting indicated a decrease in the carbon-oxygen bonding due to the bio-oil treatment. The decrease in carbon-oxygen bonding may be due to an alteration of the chemical structure due to the bio-oil. The silicon peaks for both the PP and PVC after bio-oil treatment displayed a peak position unique to minerals and the polymers absorbed a mineral from the bio-oil.

In general the bio-oil had no significant effect on the mechanical properties of the polymers. The acidic nature of the bio-oil may have roughened the surface the materials to some degree and it is most likely the polymer absorbed a mineral containing silicon and oxygen from the bio-oil.

F.6 Future Work

Many of the analysis methods were inconclusive due to the variation in the samples. An increase in the number of samples examined could help reduce the variance and therefore help determine if there is any effect of the bio-oil treatment. In addition the three week treatment time may also be increased in length and elevated temperatures could be examined.

In addition to repeating the experiment additional analysis including ATR-FTIR could be conducted on the current samples. The FTIR analysis may provide more information about the functional groups that are present in the control and bio-oil treated specimens. In addition the bio-oil could be analyzed to determine what chemical compounds it contains. In addition it would be of interest to determine if there are any changes in the chemical composition of the bio-oil due to contact with the polymers.

This may provide more information about the decrease in carbon-oxygen bonding in the PVC specimens.

F.7 References

- Oasmaa, A.; Leppamaki, E.; Koponen, P.; Levander, J.; Tapola, E. Physical Characterization of Biomass-Based Pyrolysis Liquids. Application of Standard Fuel Oil Analyses; VTT Publications 306.
- Technical Research Centre of Finland: Espoo, Finland, 1997
- Wikipedia “Polvinyl Chloride” 10/04/09 <http://en.wikipedia.org/wiki/Pvc>
- ASTM E 18 - 02; Standard Test Methods for Rockwell Hardness and Rockwell Superficial Hardness of Metallic Materials, p.123 – 138
- ASTM D 638 – 03; Standard Test Methods for Tensile Properties of Plastics, p. 1 – 15
- ASTM E 8- 04; Standard Test Methods for Tension Testing of Metallic Materials, p. 1-24
- Mat Web: Material Property Data, Polypropylene, polyvinyl chloride, 304LL Stainless Steel <http://www.matweb.com>
- A. Mousa, G. Heinrich, U. Gohs, R. Hässler, and U. Wagenknecht, 2009, Polymer-Plastic Technology and Engineering, 48, 1030 – 1040
- Ali M, Alian and Nidal H. Abu-Zahra, 2009, Polymer-Plastic Technology and Engineering, 48, 1014 – 1019
- Lingyan Z., Tingting W., Huijie C., Weigiang L., Junfen B., 2009, Journal of Wuhan University of Technology-Master. Sci. Ed, 24, 581- 587
- F. Velasco *, G. Blanco, A. Bautista, M.A. Martinez, 2009, Construction and Building Materials, 23, 1883–1891
- Substances and Technology,
http://www.substech.com/dokuwiki/doku.php?id=stainless_steel_aisi_304L
- Nguyen, T., Sheng, X., Ting, Y.,* and Pehkonen, S., Ind. Eng. Chem. Res. 2008, 47, 4703–4711
- Wang, R., Applied Surface Science 227 (2004) 399–409
- Brandon, D., and Kaplan, W., “Microstructural Characterization of Materials, Second Edition” John Wiley & Sons, Ltd., 2008, New Jersey.
- Massey, S., Adnot, A., Roy, D., Journal of Applied Polymer Science, Vol. 92, 3830–3838 (2004)
- Louette, P., Bodino, F., Pireaux, J., Surface Science Spectra, 2005, Vol. 12, 80-83.

Louette, P., Bodino, F., Pireaux, J., Surface Science Spectra, 2005, Vol. 12, 111-115.

Rjeba, A., Letarteb, S., Tajountea, L., Chafik El Idrissia, M., Adnotb, A., Roy. D., Claire, Y., Kaloustian, J., Journal of Electron Spectroscopy and Related Phenomena 107 (2000) 221–230.

Darmsradt, H., Garcia-Perez, M., Adnot, A., Chaala, A., Kretschmer, D., Roy, C., Energy & Fuels 2004, 18, 1291-1301.

Hu, P., Jiang, M., Chen, M., Yang, B., Li, H.P., Surface Engineering, 2006, 22 (5), 327-330.

Exp Methods Class Lecture Notes, 18. SEM (Scanning Electron Microscopy), Instructor: Schneider, Fall 2009.

Outlier calculator, Quick Calcs: Online calculators for Scientists, GraphPad Software, <http://www.graphpad.com/quickcalcs/Grubbs1.cfm>, 11/28/09.

PHI Chemical states, Perkin-Elmer Physical Electronics Division (PHI)

NIST Chemistry WebBook, National Institute of Standards and Technology, <http://webbook.nist.gov/chemistry/>, 11/30/09.